Bose-Einstein Condensation, Superfluidity and Superconductivity

Prof.dr. Jacques Tempere

Universiteit Antwerpen
Faculteit Wetenschappen
Departement Fysica

ii

Contents

Preface

In these course notes I attempt to give an overview of the physics of (i) Bose-Einstein condensates in dilute atomic gases, (ii) superfluid helium, and (iii) superconductivity. While the choice of material and presentation is my own, I like to acknowledge hand-picking nice ideas for presentations from a score of excellent textbooks, that I list in the biography. I would encourage you to also consult these textbooks – they can in particular give additional clues to solving the problem sets.

Introduction

The world around us, observed and experienced on the human scale, is very well described by classical theories (and a bit of Pauli exclusion). While quantum mechanics is (at the moment) the fundamental theory on which we build our insight into the world, its counterintuitive predictions usually remain hidden deep into the microscopic world of atoms. At the macroscopic scale quantum effects usually only appear in the form of subtle refinements of classical theories, brought about by intricate experiments. To bring out the quantum nature of matter these experiments peer at the microscopic scale. This course discusses another way to probe quantum mechanics, namely by transfering the quantum aspect of the microscopic world on to macroscopic objects, making those objects behave in the same manner as the quantum particles they are built up from. This is, condensed in one sentence, what superfluids and superconductors are – in this state of matter, the appropriate description is a macroscopic wave function.

Until 1995 there were only two macroscopic quantum states available: superfluid helium and superconducting solids. Since then, a third realization appeared: ultracold dilute atomic gases. The latter offers an unexpected level of experimental control: it is a very pure state whose geometry, interaction strength, and composition can be very accurately tuned by experimentalists. It has since then been used to build systems that correspond to specific model Hamiltonians. These Hamiltonians can now be studied and manipulated not only by analytical calculation or by computer simulation, but "in vivo", and they can be brought in conditions hitherto unavailable. So, not only fundamental tests of quantum mechanics are made possible, but also new territory has been opened up for exploration, in particular regarding the many-body aspects of quantum mechanics. That is why in this course we will spend a lot of attention to this new and exciting system – the first chapter focuses entirely on it. In that chapter we introduce and discuss the concept of Bose-Einstein condensation. While this concept and the properties engendered by it are most clearly learnt from the quantum gases, they are also at the basis of superfluidity in liquid helium and of superconductivity. The difference lies in the nature of the interactions and the building blocks. In superfluid helium-4, the system is no longer dilute, and the role of interactions is more prominent. We discuss this system in the second chapter. Finally, in superconductors, electrons exhibit macroscopic quantum behavior – but in order to do so they have to form pairs first. Here, the interactions are crucial. We investigate superconductivity in the third chapter.

Chapter 1

Bose-Einstein Condensation

Classical physics started out as a study of the familiar world around us, on human length scales. But as our ability to probe larger or smaller scales got better, it became clear that classical physics had to be extended and corrected. Better telescopes shifted the boundary of the largest possible scale, and better microscopes or particle accelators reduced the smallest scales available. At the largest scale, Newtonian physics could not explain the precession of Mercury, and at the smallest scale, black-body radiation did not fit in with classical mechanics. The former required general relativity to be developed, and the latter led to quantum mechanics. Here, we focus on another boundary that physicists have been working on: the record of the coldest temperature. It is by moving that boundary ever closer to absolute zero that first superconductivity and then superfluidity were discovered. For these phenomena, the laws of classical physics do not apply, and it was found that quantum mechanics –under normal circumstances of temperature and pressure confined to the microscopic world– governs the behaviour of superconductors and superfluids on a macroscopic scale.

To understand how low temperatures can bring out the quantum nature of matter, we start from Boltzmann's classical description of a gas of atoms. The atoms are described as mass points with definite positions and momenta, drawn
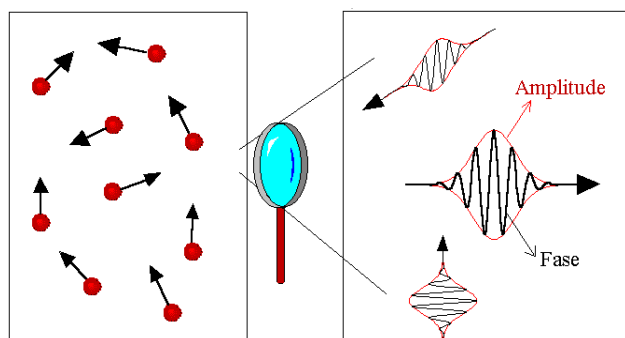

Figure 1.1: A gas of atoms, from Boltzmann to De Broglie, from classical to quantum mechanics.
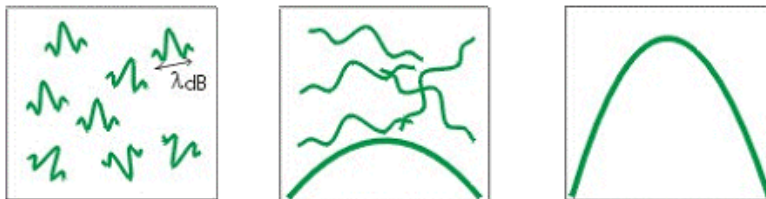
Figure 1.2: Upon cooling, the wave packets spread out, until they overlap and -in the case of bosonic atoms- result in a macroscopic wave function shared by all atoms.

from a statistical distribution. They jiggle and bump into eachother. As the gas cools down, the average velocity (and hence momentum $\mathbf{p}$) of these mass points is reduced, the jiggling motion becomes less agitated. The average kinetic energy of the atoms is given by $(3/2)k_BT = \langle p^2 \rangle /(2m)$, where $\langle .. \rangle$ represents and averaging over Boltzmann's statistical distribution.

Since Louis de Broglie, we know that the atoms should not be thought of as little balls with definite position and momentum, but they must be represented by wave packets. These wavepackets necessarily result in a certain spread in the momentum Δp and a spread in the position Δx of every single atom, illustrated in figure 1.1. The average kinetic energy can still be written as $(3/2)k_BT = \langle p^2 \rangle /(2m)$, but now $\langle .. \rangle$ must represent an averaging over *both* the classical ensemble and over the quantum mechanical uncertainty. It remains true that a colder gas will have, on average, slower atoms than a hot gas.

The spread or uncertainty in the position is linked to the uncertainty in the momentum through the Heisenberg relation $\Delta x \Delta p < h/(4\pi)$. When the gas cools down, the average momentum of the atoms is reduced, and hence the uncertainty on the momentum must decrease as well, since obviously $\Delta p < \sqrt{\langle p^2 \rangle}$ so $\Delta p < \sqrt{3mk_BT}$. Heisenberg's uncertainty relation then states that Δx must start to grow when the temperature is reduced. The relation between the spread on the atom's position and the temperature is given by the wavelength of de Broglie:

$$\lambda_{\mathrm{dB}} = \sqrt{\frac{2\pi\hbar^2}{mk_BT}}.$$

For a gas of nitrogen molecules N_2 ($m_{\mathrm{nitrogen}} = 4.65 \times 10^{-26}$ kg) at room temperature ($T = 293$ K) the de Broglie wavelength equals $\lambda_{\mathrm{dB}} = 0.019$ nm. The distance between the molecules is a lot larger. At a typical gas density of $\rho = 1.25$ kg/m^3 the density of molecules is $n = 2.7 \times 10^{25}$ N_2 molecules/m^3, from which we derive an intermolecular distance of 3.3 nm. A good measure of the ratio between the quantum mechanical uncertainty in the position (i.e. the spread of the wave packet) and the distance between the atoms or molecules is the "gas parameter" $n\lambda_{\mathrm{dB}}^3$. For air at room temperature we have $n\lambda_{\mathrm{dB}}^3 \approx 10^{-7}$.

We've argued that as the gas cools, the momentum decreases, so also the uncertainty on the momentum decreases, which implies that the uncertainty on the position increases. This goes un until $n\lambda_{\mathrm{dB}} \approx 1$, when the spread on the atom's position is as large as the distance between the atoms. Then we can no longer consider the atoms as separate classical mass points: their wave

functions start to overlap. Two cases must be distinguised: either the particles are **fermions**, in which case they cannot share the same wave function, either they are **bosons** and they can be in the same quantum state. In the latter case the individual wave functions will get in phase, just as people, in an audience that starts to appload, will end up clapping their hands simultaneously. If this were not the case, the spreading wave functions would destructively interfere. All the bosonic atoms acquire the same wave function that oscillates in phase. This phenomenon, described here qualitatively, is called **Bose-Einstein condensation** or **BEC** : a macroscopic occupation of a single-particle state, together with phase coherence. Don't worry if these words sound alien now, we'll delve into their meaning soon enough. The idea is that cooling the gas has resulting in overlap of the atomic wave functions, so that the individual atoms "lose their identity" and start acting collectively and on the macroscopic scale. That is why Bose-Einstein condensation is said to be an expression of quantum mechanical behavior on a macroscopic scale. This behavior differs from that of usual gases, fluids or solids; BEC is a new phase of matter.

1.1 The experimental search for the new phase

A gas at room temperature is very far from this quantum phase of matter: its gas parameter $n\lambda_{\mathrm{dB}}^3 \approx 10^{-7}$ is much smaller than one. Cooling down the gas will increase λ_{dB}^3 and also reduce the distance between the atoms, so that is what you'll want to do to get closer to BEC. The story about the experimental detection of BEC in atomic gases is basically the story of our quest to make things colder and colder. Just as it is interesting to build telescopes that look farther and farther into the university (in the hope that we'll see something new just beyond the current horizon), it is interesting to develop techniques that bring us closer and closer to absolute zero, even though thermodynamics tells us we can never get to absolute zero itself. Let's have a look at this long journey into the cold.

The proverbial man in the street has a simple technique to cool things down: bring them in contact with something colder. Drop an ice cube in your drink. Or drop some liquid nitrogen in your drink, for even better cooling. Liquid nitrogen is called a "cryogen", from Greek *cryos* (cold) and *genesis* (to produce). So it's quite literaly something you can use to produce cold. The liquid nitrogen is produced itself by expanding nitrogen gas (the Joule–Thomson effect says it will cool down when expanding adiabatically!), which is also the principle behind a fridge. The best croygenic fluid is liquid helium, which boils at 4.2 K. If you pump on the helium vapor that boils off, you can reduce the vapor pressure and bring down the boiling temperature to about 1 K without too much trouble. Physicists can do much better, and pump out helium-3 from a helium-4 and helium-3 mix in a so-called "dilution refrigerator", bringing the edge of cold to about 10 millikelvin. Since $\lambda_{\mathrm{dB}} \propto T^{-3/2}$ and $n \propto T^{-1}$ for pV constant, such a drop in temperature by a factor 1000 would bring us close to the holy frontier of $n\lambda_{\mathrm{dB}}^3 = 1$.

But that's too easy. At such low temperatures, the aggregation of atoms is no longer gaseous, but it has long become solid (helium itself is the only material that would remain liquid, as we'll discuss later). In a solid we can no
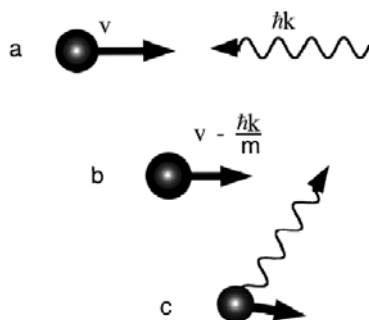
Figure 1.3: The principle of laser cooling: (a) after frontal collision and absorption of a photon with momentum $\hbar k$, (b) the atom has been slowed by the recoil $\hbar k/m$. (c) After spontaneous re-emission of the -now redshifted- photon the atom will remain slower.

longer think of the movement of atoms as free wave packets cruising through space, because the atoms are anchored to their lattice sites. That means that by definition their center-of-mass wavefunctions shouldn't overlap (the orbitals are a different thing!): the lattice potential localizes the atom wavefunctions to well within one unit cell so that the distance between the atoms remains always larger than the uncertainty on their position. If that were not the case, we couldn't claim to have atoms on a lattice! Solids cannot undergo Bose-Einstein condensation[1]. So we need to avoid solidification as we cool down, and this can be done by keeping the gas dilute and pure. Then crystallization does not start and we keep the system in a metastable gaseous state. The price to pay is of course that the density has to be kept low and that is bad news when we want to increase $n\lambda_{\mathrm{dB}}$.

In the eighties, Cohen-Tannoudji, Chu and Phillips developed laser cooling to slow down a beam of atoms and cool them down. Their spectacular results were rewarded by the 1996 Nobel prize. The idea behind laser cooling is a frontal collision between the atomic beam and a laser beam (see figure 1.3). The atoms absorb the photon, along with its momentum $\hbar k = \hbar\omega/c$. The collision has reduced atom's velocity in its direction motion by $\hbar k/m$, and excited the atom. After spontaneous de-excitation the atoms re-emit the photon in an arbitrary direction, not necessarily the beam direction, so the velocity along the beam remains reduced on average. There is also a reduction in the overall kinetic energy: the doppler shift causes the atoms to emit photons that have higher energy than the photons absorbed. Let's see how this works, and suppose the atoms are resonant with blue light. We, in our lab, shine red light at them. The atoms are fast when seen in our lab reference frame, so they will experience our red light as blueshifted and accept our red photons for absoption. But once they've absorbed them, the atoms are slow, and have joined us in the lab frame of reference. When they re-emit light to the lab, it will be blue. There has been a net transfer from kinetic (thermal) energy of the atoms to the energy in the

---

[1] Never say never... there is still ongoing discussion about "supersolids": solids that act like superfluids.
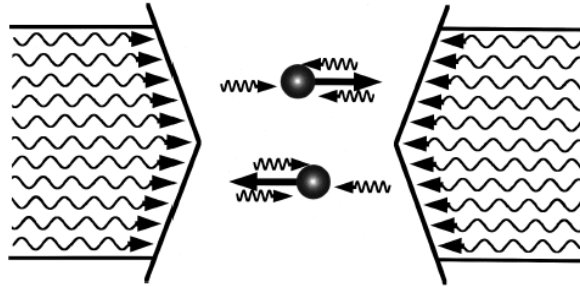
Figure 1.4: Doppler cooling in 1 dimension using 2 laser beams. If the atoms are moving in a particular direction, they will preferentially absorb photons from the beam that pushes them back.

photons. But we even have better news: now that the atoms are slow, they are no longer influenced by our red light! They won't collide with the red photons any more and won't be pushed back by our laser beam. The doppler effect is a crucial element in laser cooling, and hence lasers are because we need to be able to carefully tune the frequency of the light that we want to use.

Doppler cooling is also used to trap atoms. This uses two counterpropagating beams. If an atom is moving towards the right, it will get in better resonance with the photons from the beam that comes from the right and pushes it back, and it will go out of resonance with the left beam. It will therefore absorb more photons from the right beam and be pushed back to the center of the trap, as shown in figure 1.4. This setup is called "optical molasses". Since the resonant frequency of a hyperfine transition in an atom is also influenced by the Zeemann splitting in a magnetic field, we can also use spatially varying magnetic fields to get resonance in one place and not in another place. This will further help the trapping : outside the trap region we bring atoms into even better resonance with the push-back beam. By having counterpropagating beams in all three orthogonal directions, we get a 3D trap for atoms called a **magneto-optical trap** or MOT, illustrated in figures 1.5 and 1.6. If there are enough atoms captured in the MOT, the laser beams can be switched off: for atoms with a strong magnetic moment and intrinsic angular momentum the magnetic trap suffices. Alternatively, the magnetic trap can be switched off once the gas is cold enough, and then we can rely on the optical trapping alone to keep the blob of atoms trapped.

This cooled and trapped collection of about a billion atoms is the starting point of any experiment on atomic Bose-Einstein condensates. At this stage, the cloud has a temperature of a few tens of microkelvins, a thousand times colder than what can be achieved with a dilution refrigerator. No bulk material can be made that cold! The walls of the cell that contains the trapped cloud are much warmer than the cloud itself, and it is important that the cloud does not come into contact with the walls of the cell. That is why a magnetic (or optical) trap is needed. The purely optical trap is only a strong trap is the cloud is even colder, so at this stage in the experiment usually a magnetic trap is used. As a consequence, you can only trap atoms or molecules with a magnetic moment

Figure 1.5: A magneto-optical trap with a cloud of trapped atoms (indicated by the arrow). The glass cell is vacuum-pumped, and has protrusions where the cooling laser beams enter. A coil for the magnetic quadrupole trapping is also visible on top and at the bottom of the cell.
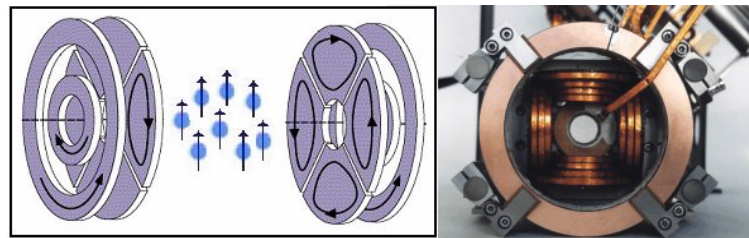
Figure 1.6: By correctly positioning external magnets a cloud of atoms with a magnetic moment can be trapped.

different from zero. Alkali atoms, with a single electron in the outer s-orbital are particularly well suited.

But a few tens of microkelvins is still too hot for our purpose: to reach the regime where $n\lambda_{\mathrm{dB}}^3 \approx 1$ the cloud needs to be cooled down to about hundred nanokelvins. This can no longer be done with laser cooling, since to reach the nanokelvin regime, the velocity of the atoms should be made smaller than the recoil they get from re-emitting the photon. So we need another method: the last cooling stage is evaporative cooling. Using a radiofrequency electromagnetic field, spin flips can be induced in the atoms. This alters the magnetic moment of the atom with respect to the magnetic trapping field, so that the spin-flipped atoms are expelled from the cloud. The most energetic atoms are those that can travel into the regions farthest from the center of the trap, regions where the magnetic trapping field is higher. If we choose the radiofrequent field resonant only in these regions (using again the Zeeman effect), we can actively select which atoms will be expelled from the trap, as illustrated in figure 1.7. Choosing the most energetic atoms for banishment, the remainder of the cloud will have a smaller average energy, and hence the remaining cloud has a smaller temperature. This is the principle of evaporative cooling, which is also at work when you blow on
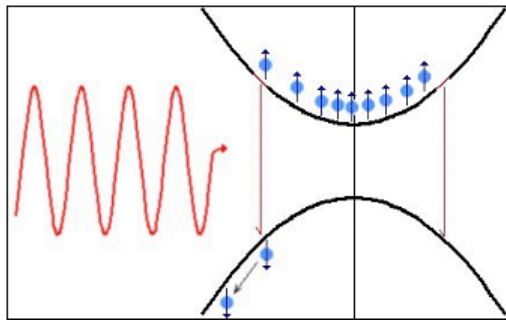
Figure 1.7: Evaporative cooling with a radiofrequent field, chosen in resonance for atoms that have the most energy and climb the highest in the trapping potential.

hot soup. The most energetic soup molecules can reach the vapour, and bounce back between vapour and liquid. By blowing on the soup, you remove these more energetic molecules, and cool down the whole.

With this technique, we can reach well within the nanokelvin regime with still about a million atoms remaining in the cloud. This is amazingly cold: even in the cosmic voids between galaxy clusters, far away from any star, the universe with its background radiation of 2.7 K is scorchingly hot in comparison to what we need. The current record in cold, the coldest spot in the known universe, is at a lab in Finland, where experimenters reach 100 picokelvin... Evaporative cooling imposes another constraint on what atoms we can use: we need 'good' elastic collisions that rethermalise the cloud and make new 'most energetic atoms' that we can remove, and we need to avoid 'bad' inelastic collisions that could flip spins of atoms with small energy in the center of the trap. One of the very best atoms to use for evaporative cooling turns out to be ^{87}Rb. Also ^{23}Na and ^{7}Li are good, although lithium presents an added difficulty since it has attraction between the atoms and this could lead to clustering and bad losses.

We don't need to go down to 100 picokelvin to witness a change occurring in the cloud. At about 100 nanokelvin, a density anomaly appears in the central region of the cloud, a small region of higher density. Also in the velocity distribution something happens, as shown in the top row of figure 1.8: the height represents how many atoms, and the x-and y-axis are the velocities in x-and y-direction, respectively. These velocity distributions are measured by a time-of-flight measurement: switch off the trap and let the cloud expand. The fastest atoms will travel farther and after a while the density represents the velocity distribution. The tails of the velocity distribution (far away from the central anomaly) are used to estimate the temperature (by fitting a Maxwell distribution to them): remember that we cannot stick a thermometer into the cloud! The shape of the central anomaly is remarkable: it is the quantum mechanical ground state wavefunction, modulus squared. Typical magnetic traps give rise to harmonic potentials – you have already solved the Schrödinger equation for a harmonic potential and know what the ground state wave function looks like. We'll later calculate what effect the interactions have on this wave function, but it is always remarkable to see quantum mechanical wave functions
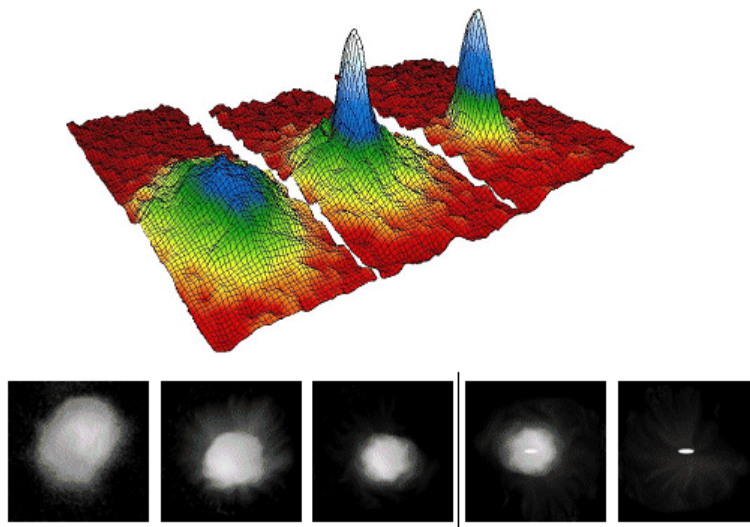
Figure 1.8: As the cloud cools down (lower row of figures) the cloud shrinks. Below a certain temperature a droplet of condensate appears, and the velocity distribution (upper panel) gets peaked around zero. As the temperature is reduced further, all atoms collect in the condensate. Figure source: Ketterle lab, MIT.

with the naked eye. All the atoms have the same wave function, and so measuring the density is like doing many repeated measurements of this single, macroscopic wavefunction.

As the atoms are cooled to below the transition temperature, there are less and less atoms in the 'normal' tails of the distribution, and they all collect in the central region. This is the Bose-Einstein condensate. The BEC is then only a few tens of microns large (up to a hundred microns but this is still a a macroscopic object, the size of a speck of dust just visible with the naked eye), and contains typically hundred thousand up to a million atoms. So it is not only very cold, but also very dilute. In the previous section we mentioned that in the BEC, not only do we have all atoms sharing the same single-particle wave function (we'll be more precise later), but also there should be phase coherence. The central anomaly in figure 1.8 only reflects the modulus square of the macroscopic wave function, not the phase. To check that there is also a well defined phase throughout the entire BEC, we can try to mix two BEC's: their phases will interfere, and this will show up in the resulting density as interference fringes, as shown in figure 1.9.

Bose-Einstein condensates were predicted by the Indian physicist S.N. Bose[2,3] in collaboration with Einstein in 1924. But it was only in 1995 that

---

[2]S.N. Bose, Zeitschrift für Physik **26**, 178 (1924).
[3]A. Einstein, Sitzungsberichte der Preussischen Akademie der Wissenschaften **1**, 3 (1925).
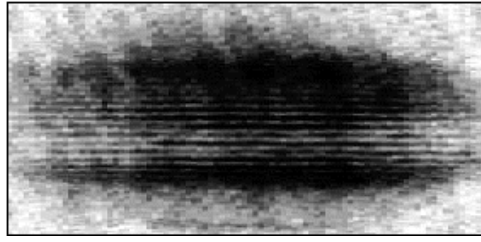
Figure 1.9: When two condensates overlap, they make a matter interference pattern. Image source: M.R. Andrews, C.G. Townsend, H.-J. Miesner, D.S. Durfee, D.M. Kurn, and W. Ketterle, Science **275**, 637-641 (1997).

BECs were first observed in trapped atomic gases[4,5,6]. For this feat Ketterle, Cornell and Wiemann received the 2001 Nobel prize. Since then, many more labs have created condensates and exotic atoms as ytterbium have been Bose condensed. Condensates also grew larger, up to about a centimeter in size for a sigar-shaped hydrogen condensate. A new challenge is to Bose condense molecules: we want to use ever larger objects with more internal degrees of freedom and bring their quantum nature to the macroscopic scale.

SUMMARY: A DILUTE ATOMIC GAS CAN BE TRAPPED AND COOLED DOWN TO THE NANOKELVIN REGIME, WHERE THE DE BROGLIE WAVELENGTH BECOMES LARGER THAN THE DISTANCE BETWEEN THE ATOMS AND A PHASE TRANSITION TAKES PLACE TO THE BOSE-EINSTEIN CONDENSED PHASE. IN THE BEC, ALL ATOMS CAN BE SAID TO BE IN THE SAME SINGLE-PARTICLE QUANTUM STATE, LEADING TO A MACROSCOPIC WAVE FUNCTION AND PHASE COHERENCE.

1.2 The ideal Bose gas

1.2.1 The idea behind BEC

The cloud of atoms in the magnetic trap is still very dilute: 10^{13} atoms/cm^3. To start, we can treat the atoms as if they are not interacting, and write the Hamiltonian of the many-body system as a sum over single-particle Hamiltonians. These can be solved to find, for every particle, the energy levels ε_v in the trap. For example, for free particles in a square box, the states are labeled by the wave numbers ($\nu \to k_x, k_y, k_z$) and the corresponding energy level is $(\hbar k)^2/(2m)$. Most magnetic traps are better described by a harmonic potential rather than a square box, and in that case the single-particle states are labeled by the harmonic oscillator quantum numbers ($v \to n_x, n_y, n_z$) and the

---

[4]M.H. Anderson, J.R. Ensher, M.R. Matthews, C.E. Wieman, and E.A. Cornell, Science **269**, 5221 (1995).

[5]K.B. Davis, M.-O. Mewes, M.R. Andrews, N.J. van Druten, D.S. Durfee, D.M. Kurn, and W. Ketterle, Physical Review Letters **75**, 3969 (1995).

[6]C. C. Bradley, C. A. Sackett, J. J. Tollett, and R. G. Hulet, Physical Review Letters **75**, 1687 (1995).

corresponding energy is $\hbar\omega(n_x + n_y + n_z + 3/2)$. In thermodynamic equilibrium at temperature T, the occupation of the single-particle state labeled by v is given by the Bose-Einstein distribution:

$$f(\varepsilon_\nu) = \frac{1}{\exp\{(\varepsilon_\nu - \mu)/(k_B T)\} - 1}, \tag{1.1}$$

since we work with bosonic atoms. These are all the isotopes that contain an even number of fermionic building blocks – for example ^{7}Li contains 3 electrons, 3 protons and 4 neutrons $\rightarrow$ 10 fermion compound $\rightarrow$ this isotope acts like a boson when treated as a point particle itself. In the Bose-Einstein distribution, μ is the chemical potential. This indicates that we work in the grand-canonical description. Granted, for a trap the canonical ensemble seems more suitable, since we have a fixed number of particles. But the grand-canonical ensemble is easier to use. The price to pay is that we always need to find the correct chemical potential, so that the total number of particles is correct:

$$N = \sum_v f(\varepsilon_v). \tag{1.2}$$

The chemical potential will thus depend on the temperature and on the total number of particles. At high temperature, the chemical potential is large and negative, meaning that it lies well below the lowest energy level $\varepsilon_{\min}$. The occupation of the any level is much smaller than one, and the gas can be treated classically (with the Boltzmann distribution). As the temperature goes down, we need to increase the chemical potential to satisfy (1.2), and with it the occupation of the lower levels. Indeed, for any ε_v, $f(\varepsilon_\nu)$ increases monotonically with increasing μ. However, the chemical can never become larger than $\varepsilon_{\min}$, otherwise $f(\varepsilon_{\min})$ would be negative and we cannot have a negative number of atoms in a certain energy level. This means that there is a maximum occupation, a maximum to any $f(\varepsilon_\nu)$, that is reached when $\mu \rightarrow \varepsilon_{\min}$:

$$f^{\max}(\varepsilon_v) = \frac{1}{\exp\{(\varepsilon_\nu - \varepsilon_{\min})/(k_B T)\} - 1} \tag{1.3}$$

The crucial insight is that for any ε_v, *except for* $\varepsilon_{\min}$, the maximal occupation $f^{\max}(\varepsilon_v)$ is finite. Only $f(\varepsilon_{\min})$ can grow indefinitely. As we keep increasing the number of atoms, at some point the occupation of any energy level will be maxed out and the only energy level left over to put additional atoms is $\varepsilon_{\min}$. The special role of the lowest energy level is made explicit in

$$N = \underbrace{f(\varepsilon_{\min})}_{N_0} + \underbrace{\sum_{v \neq \min} f(\varepsilon_v)}_{N_{exc}}. \tag{1.4}$$

Here, we denote the number of atoms in the lowest energy level N_0, and this number can be infinite. The number of atoms in higher energy levels, called excited energy levels, is N_{exc}. Since all the $f(\varepsilon_{v \neq \min})$ are bounded from above, it is certainly possible that also N_{exc} is bounded from above by some number $N_{exc}^{\max}$. This depends on how many excited levels there are, in a sense that we make more clear in the next subsection. At any given temperature, if N strongly exceeds $N_{exc}^{\max}$, then we need to put a macroscopically large number of atoms in
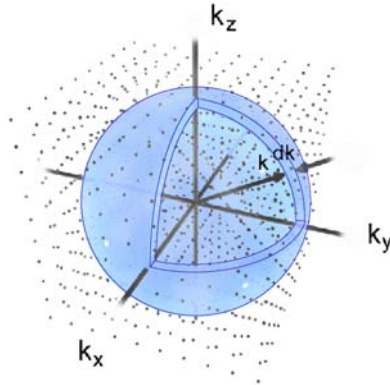
Figure 1.10: The space of states

N_0, and we have a condensate. It is also clear that $f^{\max}(\varepsilon_v)$ and hence $N_{exc}^{\max}$ are decreasing functions of temperature. So, for any number of particles N, we can drop the temperature to a point where $N_{exc}^{\max}(T)$ becomes smaller than N. Below that temperature, we again have to place a large number of atoms in N_0, and have a condensate. The temperature where this happens is the critical temperature for Bose-Einstein condensation, T_c.

1.2.2 Density of states

The sums over single-particle that appear in the previous subsection can in general not be performed analytically. In order to calculate these, the sums are replaced by integrals, where a density of terms should be included to do the conversion. That is, we replace the sum over single-particle states by an integral over the energy $\int d\varepsilon$, and to do that we need to include a factor $g(\varepsilon)$ that counts how many single-particle states (terms in the sum) there were between ε and $\varepsilon + d\varepsilon$. This is the density of states. It allows to smoothen out the sum into an integral,

$$\sum_v F(\varepsilon_v) \rightarrow \int d\varepsilon \ g(\varepsilon) F(\varepsilon) \tag{1.5}$$

where F can be any function of energy, and will work whenever there are many states in the domain over which we want to integrate and over which $F(\varepsilon)$ varies smoothly. Some examples will clarify this.

First, the particles in a 3D box of size L and periodic boundary conditions. There we have quantum numbers $\{k_x, k_y, k_z\} = \{n_x, n_y, n_z\} \, 2\pi/L$, where the n are integers (both positive and negative[7]). The triplet $\{k_x, k_y, k_z\}$ can be viewed as cartesian coordinates of a cubic grid of lattice points as illustrated in figure 1.10, and there is one point per $(2\pi/L)^3$ of **k**-space volume. The surface

---

[7]Alternatively, we can use dirichlet boundary conditions on the box and find $\{k_x, k_y, k_z\} = \{n_x, n_y, n_z\} \, \pi/L$. Note the factor 2 difference in the scale factor π/L that gives the separation between the points. This lattice of points is $2 \times 2 \times 2 = 8$ times as dense, but now n is restricted to the positive integers – one eight of the sphere – so you'll get the same result for the density of states.

of constant energy is a sphere with radius $R(\varepsilon) = \sqrt{2m\varepsilon}/\hbar$ in the $\{k_x, k_y, k_z\}$, so that the total number of states with energy less than ε is the number of points within a sphere with radius $R(\varepsilon)$, i.e.

$$G(\varepsilon) = \frac{4\pi}{3}\left(\frac{\sqrt{2m\varepsilon}}{\hbar}\right)^3 \times \frac{L^3}{(2\pi)^3} = V\frac{2}{3\pi^2}\frac{(2m\varepsilon)^{3/2}}{\hbar^3}. \tag{1.6}$$

with $V = L^3$. We defined the density of states as the number of states with energy between ε and $\varepsilon + d\varepsilon$, so that

$$g(\varepsilon) = V\frac{1}{\pi^2}\frac{(2m)^{3/2}}{\hbar^3}\varepsilon^{1/2}. \tag{1.7}$$

The next example is the harmonic trapping potential, given by

$$V_1(\mathbf{r}) = \frac{m}{2}(\omega_x^2 x^2 + \omega_x^2 y^2 + \omega_x^2 z^2). \tag{1.8}$$

This is the usual case when magnetic trapping potentials are used. Often, there will still be axial symmetry eg. $\omega_x = \omega_y$ and the trap can now be prolate (cigar shaped) for $\omega_z < \omega_{x,y}$ or oblate (pancake shaped) for $\omega_z > \omega_{x,y}$. The quantum numbers are $\{n_x, n_y, n_z\}$, triplets of positive integers, and the corresponding energy is

$$\varepsilon = \hbar\omega_x n_x + \hbar\omega_y n_y + \hbar\omega_z n_z \tag{1.9}$$

where we put the zero of energy at the ground state energy. For fixed ε, this equation defines a plane in $\{n_x, n_y, n_z\}$-space, going through $\varepsilon/(\hbar\omega_x)$ at the x-axis, $\varepsilon/(\hbar\omega_y)$ at the y-axis and $\varepsilon/(\hbar\omega_z)$ at the z-axis. The points with less energy than ε are contained in a tetrahedron with with these points as corners and the origin as the fourth corner. The volume of this tetrahedron also equals the number of states with energy less than ε,

$$G(\varepsilon) = \frac{1}{\prod_{i=1}^{3}(\hbar\omega_i)}\int_0^\varepsilon d\varepsilon_1 \int_0^{\varepsilon-\varepsilon_1} d\varepsilon_2 \int_0^{\varepsilon-\varepsilon_1-\varepsilon_2} d\varepsilon_3 = \frac{\varepsilon^3}{6\hbar^3\omega_1\omega_2\omega_3} \tag{1.10}$$

from which we find the density of states

$$g(\varepsilon) = \frac{\varepsilon^2}{2\hbar^3\omega_1\omega_2\omega_3}. \tag{1.11}$$

In both cases we find that the density of single-particle quantum states increases with a the energy as a power law. This is a conclusion that holds for many cases: the ways to distribute the energy over the excitations related to the different quantum numbers grows as some power of the energy. So, we will proceed with a general formula

$$g(\varepsilon) = C_\alpha \varepsilon^{\alpha-1} \tag{1.12}$$

where C_α is some constant. Once we obtain the results for this general density of states, we can plug in the specifics. For our atoms in a 3D box, $\alpha = 3/2$ and the coefficient is

$$C_{3/2} = \frac{Vm^{3/2}}{\sqrt{2}\pi^2\hbar^3}. \tag{1.13}$$

For atoms in a 3D harmonic trap, $\alpha = 3$ and the coefficient is

$$C_3 = \frac{1}{3\hbar^3\omega_1\omega_2\omega_3}. \tag{1.14}$$

1.2.3 Transition temperature

The BEC transition temperature is defined as the temperature below which we have to start populating the lowest energy state N_0 by a macroscopic amount of atoms. By macroscopic, we mean something large as compared to 1. Yes, we'll have difficulties defining this temperature when we only have a few atoms... Let's get back to expression 1.4 and rewrite the sum in N_{exc} by an integral:

$$N_{exc} = \int\limits_0^\infty g(\varepsilon)f(\varepsilon)d\varepsilon. \tag{1.15}$$

Here $f(\varepsilon)$ is the Bose-Einstein distribution (1.1). Firstly, note that we have set the zero of the energy at $\varepsilon_{\min}$. That is why the integral has as its lowest boundary 0 and not $\varepsilon_{\min}$. Next, you could be worried that the sum was over states $v \neq \min$, i.e. in the sum we have excluded the single-particle ground state. But that is not a problem in moving from the summation to the integration. Switching to the integral is an approximation, and it turns out that this approximation throws away the lowest energy level anyway. Indeed, $g(\varepsilon \to 0) = 0$, so we could just as well have written δ, an infinitesimal positive number, as lower boundary in the integral.

Remember that the occupations $f(\varepsilon)$, and hence N_{exc}, increase as the chemical potential is increased. However, we cannot increase the chemical potential beyond $\mu = \varepsilon_{\min}$ $(= 0$ in our case). Thus, the upper bound for N_{exc} is found by setting $\mu = 0$ in Bose-Einstein distribution:

$$N_{exc}^{\max}(T) = \int\limits_0^\infty g(\varepsilon)\frac{1}{e^{\varepsilon/(k_BT)} - 1}d\varepsilon$$

We see that as the temperature drops, $N_{exc}^{\max}$ becomes smaller, and we'll reach a temperature where $N = N_{exc}^{\max}(T_c)$. If we still decrease the temperature $T < T_c$ we find that $N > N_{exc}^{\max}(T)$, and we cannot put all the atoms in excited states. We are forced to put $N_0(T) = N - N_{exc}^{\max}(T)$ atoms in the condensate. Hence, the equation that defines T_c is

$$\begin{aligned} N &= N_{exc}^{\max}(T_c) \\ &\Leftrightarrow N = \int\limits_0^\infty g(\varepsilon)\frac{1}{e^{\varepsilon/(k_BT_c)} - 1}d\varepsilon \end{aligned}$$

Now we can plug in $g(\varepsilon) = C_\alpha\varepsilon^{\alpha-1}$,

$$N = C_\alpha\int\limits_0^\infty \frac{\varepsilon^{\alpha-1}}{e^{\varepsilon/(k_BT_c)} - 1}d\varepsilon$$

and use the following formula from the calculus books

$$\int_0^\infty \frac{x^{\alpha-1}}{e^x - 1} dx = \Gamma(\alpha)\zeta(\alpha). \tag{1.16}$$

where $\Gamma(\alpha)$ is the gamma function (defined by $\Gamma(\alpha) = (\alpha - 1)\Gamma(\alpha - 1)$) and $\zeta(\alpha) = \sum_{n=1}^\infty 1/n^\alpha$ is the Riemann zeta function. In the table below we list some value for common α's :

α	1	3/2	2	5/2	3
$\Gamma(\alpha)$	1	$\sqrt{\pi}/2$	1	$3\sqrt{\pi}/4$	2
$\zeta(\alpha)$	∞	$2.612\ldots$	$\pi^2/6$	$1.341\ldots$	$1.202\ldots$

Using our formula (1.16) we can now find the critical temperature (note the substitution $x = \varepsilon/(k_B T)$):

$$N = C_\alpha(k_B T_c)^\alpha \int_0^\infty \frac{x^{\alpha-1}}{e^x - 1} dx = C_\alpha(k_B T_c)^\alpha \Gamma(\alpha)\zeta(\alpha). \tag{1.17}$$

from which

$$\boxed{k_B T_c = \frac{N^{1/\alpha}}{[C_\alpha \Gamma(\alpha)\zeta(\alpha)]^{1/\alpha}}.} \tag{1.18}$$

So, for a three dimensional harmonic trap we have

$$k_B T_c = \hbar\bar{\omega} \sqrt[3]{\frac{N}{\zeta(3)}} \approx 0.94\, \hbar\bar{\omega} N^{1/3}, \tag{1.19}$$

with $\bar{\omega} = (\omega_1\omega_2\omega_3)^{1/3}$ the geometric average of the confinement frequencies. These confinement frequencies are typically $100 - 1000$ Hz, and the number of atoms can range $N = 10^3 - 10^7$. Let's choose $\bar{\omega} = 100$ Hz and $N = 10^6$, then the typical transition temperature from this formula is indeed of the order of 100 nK. Note that $k_B T_c \gg \hbar\bar{\omega}$ (in our example even by a factor 100). That is good, since it means we can safely replace the sums by integrals as we did. The discrete nature of the lattice of states doesn't matter when we look from afar, from an energy scale much larger than the energy differences between the individual states.

For a uniform Bose gas in a 3D box with volume V, we find

$$k_B T_c = \frac{2\pi}{[\zeta(3/2)]^{2/3}} \frac{\hbar^2 (N/V)^{2/3}}{m} \approx 3.31 \frac{\hbar^2 n^{2/3}}{m}. \tag{1.20}$$

The critical temperature grows as the 2/3 power of the density. Note that for the uniform Bose gas in two dimensions you would have $\alpha = 1$, and since $\zeta(1) = \infty$ the transition temperature $T_c = 0$. Indeed, the density of states is such that at any nonzero temperature we can accomodate all the particles safely in excited states, $N_{exc}(T) > N$ for all $T > 0$. This means that Bose-Einstein condensation cannot occur in a uniform, two-dimensional Bose gas. However, if we go to a harmonically trapped two dimensional Bose gas, $\alpha = 2$ and once again BEC is possible.
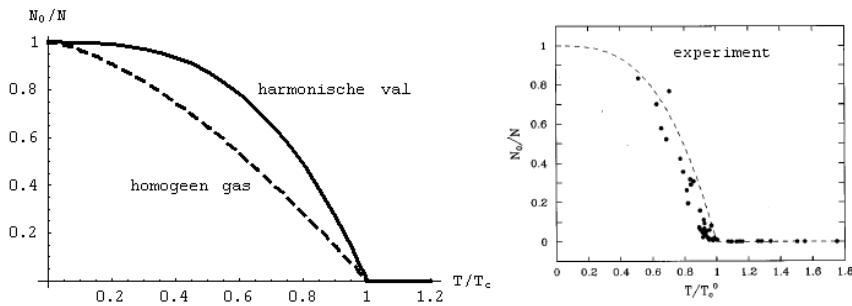
Figure 1.11: Fraction of the total number of atoms in the condensate, N_0/N, as a function of the temperature, plotted for a uniform Bose gas (dashed curve) and for the harmonically trapped Bose gas (full curve).

1.2.4 Condensate fraction

For temperatures smaller than the critical temperature, the number of atoms is excited states is still given by (1.15) with $\mu = 0$. We keep the chemical potential "maxed out" in the BEC phase, and find

$$
\begin{aligned}
N_{exc}(T \;\; < \;\; T_c) &= C_\alpha \int_0^\infty \frac{\varepsilon^{\alpha-1}}{e^{\varepsilon/(k_B T)} - 1} d\varepsilon \\
&= C_\alpha \Gamma(\alpha)\zeta(\alpha)(k_B T)^\alpha.
\end{aligned} \tag{1.21}
$$

Of course this result only holds for $\alpha > 1$. We see that it doesn't depend on the total amount of particles, only on the temperature and the exponent α. Using our result (1.18) for the critical temperature, we can divide this by $N = C_\alpha(k_B T_c)^\alpha \Gamma(\alpha)\zeta(\alpha)$ to find

$$
\frac{N_{exc}(T < T_c)}{N} = \left(\frac{T}{T_c}\right)^\alpha \tag{1.22}
$$

since the common factor $C_\alpha \Gamma(\alpha)\zeta(\alpha)k_B^\alpha$ drops out. From this we can find the fraction of particles in the condensate,

$$
\frac{N_0}{N} \;\; = \;\; 1 - \frac{N_{exc}(T < T_c)}{N} = 1 - \left(\frac{T}{T_c}\right)^\alpha \quad \text{for } T < T_c \tag{1.23}
$$

$$
\text{(and 0 for } T > T_c). \tag{1.24}
$$

This result, for atoms in a box and in a harmonic trap, is shown in figure 1.11. The right hand side also shows the comparison with the experiment[8]. Our theory matches the experimental dots well, but there seems to be a systematic shift to the left, the experimental critical temperature is a bit lower. This is due to the interactions – remember that we are restricting ourselves in this section to the ideal Bose gas. The effect of interactions may be small sometimes, but it is not completely absent.

---

[8] The experiment is reported in "Bose-Einstein Condensation in a Dilute Gas: Measurement of Energy and Ground-State Occupation", J.R. Ensher, D.S. Jin, M.R. Matthews, C.E. Wieman, and E.A. Cornell, Phys. Rev. Lett. **77**, 4984 (1996).
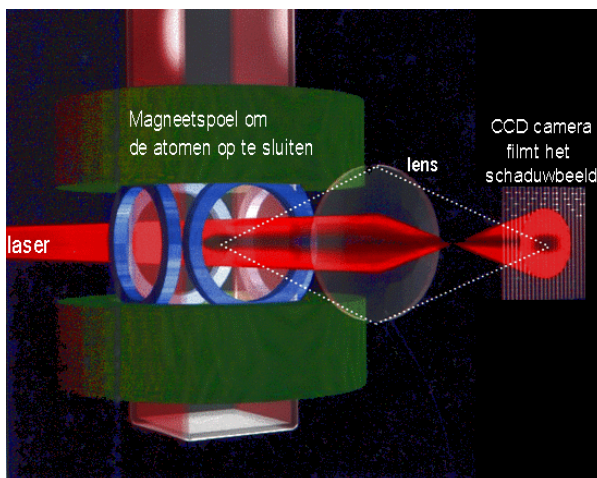
Figure 1.12: The condensate is observed by shining in light and capturing the shadow image on a CCD camera (after some magnifying optics). This is how the images in figure 1.8 were obtained. Image source: Eric Cornell lab, JILA.

1.2.5   Condensate density and velocity distribution

The magnetically trapped cloud of atoms is observed by simply taking a picture! Laser light is focused on the condensate, and some of that light gets absorbed so that the cloud casts a shadow. Some lenses are needed to zoom in on the 10-micron sized object, but basically the image of this shadow is the measurement result (see figure 1.12). As mentioned, you can use a time of flight method to convert the density into the velocity distribution (and then you won't need to zoom in that much any more, but you lose some contrast). Taking the picture destroys the condensate: the flash of light heats it up too much. Techniques have been developed to do non-destructive imaging: by looking basically at the refraction of light that does not get absorbed, we can reconstruct the density. Also, the images in the basic set-up project the 3D density profile onto a plane, summing all the density along the line of sight. Also here there are work-arounds: you can do tomographic imaging, or rely on the symmetry of the cloud to reconstruct the full 3D image.

The ground state of the atoms in the harmonic trap is a Gaussian as a wave function

$$\phi_0(\mathbf{r}) = \frac{1}{\pi^{3/4}(a_1 a_2 a_3)^{1/2}} \exp\left\{ -\frac{x^2}{2a_1^2} - \frac{y^2}{2a_2^2} - \frac{z^2}{2a_3^2} \right\}$$

where the a_i are the oscillator lengths in the three directions, $a_i = \sqrt{\hbar/(m\omega_i)}$. Each of the $N_0 \gg 1$ atoms is in the state described by this wave function. Experimenters usually rewrite this as

$$a_i = 10.1 \left(\frac{100 \text{ Hz}}{\omega_i} \frac{1}{A} \right)^{1/2} \mu\text{m}. \tag{1.25}$$

Here A is the mass number of the isotope that is being Bose condensed (i.e. it's 87 for ^{87}Rb). This expression is basically telling you that the typical oscillator

length of the trap is on the order of 10 micron. The ground state wave function in momentum space (in momentum representation) is the Fourier transform of $\phi_0(\mathbf{r})$:

$$\tilde{\phi}_0(\mathbf{p}) = \frac{1}{\pi^{3/4}(c_1 c_2 c_3)^{1/2}} \exp\left\{ -\frac{p_x^2}{2c_1^2} - \frac{p_y^2}{2c_2^2} - \frac{p_z^2}{2c_3^2} \right\}, \tag{1.26}$$

with $c_i = \hbar/a_i$. The velocity distribution $n(\mathbf{p}) = N \left| \tilde{\phi}_0(\mathbf{p}) \right|^2$ will be anistropic, in contrast to the Maxwell-Boltzmann velocity distribution of the thermal atoms $n(\mathbf{p}) \propto \exp\{-p^2/(2mk_BT)\}$. The anisotropy of the central condensate bump in figure 1.8 is therefore due to the anistropy in the ground state wave function, and a sign that the object in the center is not an ideal gas in the normal state.

1.2.6 Thermodynamic quantities

The energy of the condensate is $E = 0$. Indeed, we have put our zero of the energy at $\varepsilon_{\min}$, and all N_0 atoms in the condensate are in this energy level, so obviously $N_0\varepsilon_{\min} = 0$. Only the excited states contribute to the energy,

$$E = \sum_{v \neq \min} \varepsilon_v f(\varepsilon_v) \tag{1.27}$$

and again we rewrite this as an integral

$$E = \int_0^\infty \varepsilon g(\varepsilon) f(\varepsilon) d\varepsilon \tag{1.28}$$

For $T < T_c$ we know that $\mu \to 0$, so we can substitute $f(\varepsilon) = 1/(e^{-\varepsilon/k_BT} - 1)$. Also we use our general power law for the density of states, $g(\varepsilon) = C_\alpha \varepsilon^{\alpha-1}$, and get

$$E(T < T_c) = C_\alpha \int_0^\infty \frac{\varepsilon^\alpha}{e^{\varepsilon/(k_BT)} - 1} d\varepsilon \tag{1.29}$$

$$= C_\alpha \Gamma(\alpha + 1)\zeta(\alpha + 1)(k_BT)^{\alpha+1} \tag{1.30}$$

We have used the integration formula (1.16) again, with now an extra energy factor so we have $\alpha + 1$ in stead of α.

The specific heat (still for $T < T_c$) is

$$C = \frac{\partial E}{\partial T} = (\alpha + 1)\frac{E}{T} \tag{1.31}$$

The specific heat can be used to calculate the entropy via $C = T\partial S/\partial T$, leading to

$$S = \frac{\alpha + 1}{\alpha}\frac{E}{T}. \tag{1.32}$$

The condensate also does not contribute to the entropy (regardless of where we place the zero of the energy). So, below T_c, the specific heat, the energy and the entropy are independent of the number of particles, just like the number
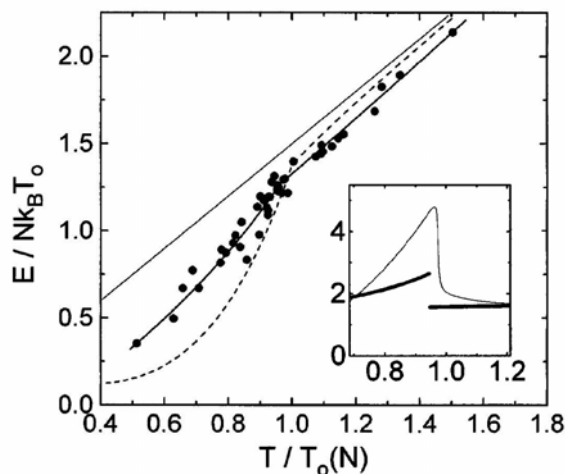
Figure 1.13: Measurement of the energy and the specific heat (inset) as a function of temperature (here the critical temperature is T_0). This graph comes from the publication mentioned earlier (Phys. Rev. Lett. **77**, 4984 (1996)).

of atoms in excited states. In fact, these thermodynamic quantities grow as the number of excited particles! Dividing the energy by the number of atoms $N = C_\alpha (k_B T_c)^\alpha \Gamma(\alpha)\zeta(\alpha)$ we get

$$\frac{E(T < T_c)}{N} = \frac{\Gamma(\alpha+1)\zeta(\alpha+1)}{\Gamma(\alpha)\zeta(\alpha)} \left(\frac{T}{T_c}\right)^\alpha k_B T \tag{1.33}$$

we can simplify this since $\Gamma(\alpha + 1) = \alpha\Gamma(\alpha)$ and since $(T/T_c)^\alpha = (N_{exc}/N)$, and find

$$E(T < T_c) = \alpha \frac{\zeta(\alpha+1)}{\zeta(\alpha)} \times N_{exc} k_B T \tag{1.34}$$

A comparison with experiment as can be seen from figure 1.13. The main figure shows the energy. The full straight line is the value for a classical ideal Maxwell-Boltzmann gas, $E/(Nk_B T_c) = \alpha T/T_c$, it is what we expect above T_c. We see that below T_c the energy falls short of this classical result. We still more or less have $(1/2)\, k_B T$ per degree of freedom (equipartition), but the degrees of freedom are related to the atoms in excited states, not the total number of atoms, and N_{exc} drops well below N. The dashed line represents the result for the ideal gas. Again the dots are not perfectly corresponding to the ideal gas result: interactions change the results somewhat. From the energy we can now also extract

$$C = \alpha(\alpha+1)\frac{\zeta(\alpha+1)}{\zeta(\alpha)} \times N_{exc} k_B, \tag{1.35}$$

$$S = (\alpha+1)\frac{\zeta(\alpha+1)}{\zeta(\alpha)} \times N_{exc} k_B. \tag{1.36}$$

In the classical limit the specific heat of a homogeneous ideal gas is $C = \alpha N k_B$ and $E = \alpha N k_B T$. What happens near T_c ? As we approach T_c from above,

$C/Nk_B = \alpha$. As we approach T_c from the BEC side however, we find

$$\frac{C}{Nk_B} = \alpha(\alpha + 1)\frac{\zeta(\alpha + 1)}{\zeta(\alpha)} \qquad (1.37)$$

There is a jump: below T_c the specific heat is a factor $(\alpha + 1)\zeta(\alpha + 1)/\zeta(\alpha)$ larger. For the uniform Bose gas this factor equals $1.28\ldots$, for the harmonically trapped Bose gas it is larger, $3.60\ldots$This jump is generally smoothed out into a peak, that has a typical "lambda" shape: rising with some power law below T_c, and then rapidly dropping to some constant above T_c. Keep this in mind as we start studying liquid helium: the superfluid transition there is also known as the "lambda transition" because of the shape of the specific heat. This is shown in the inset of figure 1.13: the predicted ideal Bose gase result is the thin curve, the measurement result is the thick curve. The jump is not so large as predicted, again due to interactions.

It seems we should no longer delay taking a close look at interactions.

And that is precisely what we'll do in the next sections.

SUMMARY: AN IDEAL BOSE GAS CAN BE DESCRIBED AS A COLLECTION OF INDEPENDENT ATOMS TO BE PLACED ON A SET OF SINGLE-PARTICLE ENERGY LEVELS. USING THE TECHNIQUES OF STATISTICAL MECHANICS WE SEE THAT DEPENDING ON THE DENSITY OF STATES WE SHOULD START PLACING A MACROSCOPIC NUMBER OF ATOMS IN THE GROUND STATE LEVEL AS WE LOWER THE TEMPERATURE BELOW A CRITICAL TEMPERATURE. ALL RELEVANT THERMODYNAMIC QUANTITIES CAN BE CALCULATED EXACTLY, ONCE THE DENSITY OF STATES IS GIVEN.

1.3 The Penrose-Onsager criterion for BEC

We need to generalize our definition of Bose-Einstein condensation to the case of the interacting Bose gas. The main difficulty is that we can no longer assign atoms to different energy levels of the trapping potential. The Hamiltonian is no longer a sum of single-particle Hamiltonians but contains two-body interaction potentials. To define BEC in this case, we following the reasoning of Penrose and Onsager[9]:

1. The non-interacting Bose gas that we have discussed up till now is only an idealisation, and we have seen that interactions still play a role. It will be even more important in liquid helium. For an interacting system, the concept of single-particle levels, derived from solving the single-particle Schrödinger equation for the trapping porential, should be modified.

2. The solution is to turn to density matrices to describe the interacting Bose system. In a 'pure state' the system of N atoms is described by a single many-body wave function $\Psi(\mathbf{r}_1, ..., \mathbf{r}_N)$, just like we have single-particle wave functions $\Psi(\mathbf{r})$ for $N = 1$. The many-body wave function describes the

---

[9]O. Penrose en L. Onsager, Phys. Rev. **104**, 576 (1956).

amplitude for a certain configuration of atoms (with an atom at position $\mathbf{r}_1$, one at position $\mathbf{r}_2$, etc...)   The corresponding **density matrix** is defined by

$$
\begin{aligned}
\hat{\rho} &= |\Psi\rangle\langle\Psi| \\
&\Leftrightarrow \rho(\mathbf{r}_1,..,\mathbf{r}_N;\mathbf{r}_1',..,\mathbf{r}_N') = \Psi^*(\mathbf{r}_1,...,\mathbf{r}_N)\Psi(\mathbf{r}_1',...,\mathbf{r}_N').
\end{aligned}
\qquad (1.38)
$$

The many-body wave function contains all the information we need to calculate the expectation value of any observable. Similary, the many-body density matrix contains all the necessary information about our system. Indeed,

$$
\begin{aligned}
\left\langle \hat{A} \right\rangle &= \int d\mathbf{r}_1 \ldots \int d\mathbf{r}_N \Psi^*(\mathbf{r}_1,...,\mathbf{r}_N)A(\mathbf{r}_1,...,\mathbf{r}_N)\Psi(\mathbf{r}_1,...,\mathbf{r}_N) \\
&= \mathrm{Tr}[\hat{\rho}\hat{A}]
\end{aligned}
\qquad (1.39)
$$

You can choose whether you describe physics through the wave function or through the density matrix. We can construct so-called **reduced density matrices** by tracing out some of the N variables. The single-particle reduced density matrix or first order reduced density matrix is defined by taking the trace over all but one position variable:

$$
\rho_1(\mathbf{r};\mathbf{r}') = N \int d\mathbf{r}_2...d\mathbf{r}_N \ \rho(\mathbf{r},\mathbf{r}_2,..,\mathbf{r}_N;\mathbf{r}',\mathbf{r}_2,..,\mathbf{r}_N).
\qquad (1.40)
$$

This is a very general definition, usable for both interacting and non-interacting systems. The one-particle density matrix can also be written as a function of the field operators $\hat{\psi}^+(\mathbf{r}),\hat{\psi}(\mathbf{r})$ that respectively create and annihilate a boson on position $\mathbf{r}$, and obey bosonic commutation relations:

$$
\rho_1(\mathbf{r};\mathbf{r}') = \left\langle \hat{\psi}^+(\mathbf{r})\hat{\psi}(\mathbf{r}') \right\rangle.
\qquad (1.41)
$$

The idea is that for many expectation values we don't need the full information contained in the many-body density matrix, but we have enough information in the reduced density matrix. Indeed, if an observable $\hat{A}_1$ acts only on a single particle, or if it can be written as a sum of operators acting on individual particles, then $N-1$ integrations do not contain $\hat{A}$ and $\left\langle \hat{A}_1 \right\rangle = \int d\mathbf{r}$ $A_1(\mathbf{r})\rho_1(\mathbf{r},\mathbf{r}) = \mathrm{Tr}[\hat{\rho}_1\hat{A}_1]$. These operators are called single-particle operators. The potential energy of the trap, and the kinetic energy are examples. Also the density is an example, and a particularly simple one since

$$
n(\mathbf{r}) = \rho_1(\mathbf{r};\mathbf{r}).
\qquad (1.42)
$$

Hence the name "density matrix".

3.   Starting from an ideal gas we can work with single-particle states determined solely by the external trapping potential. Then the many-body wave function can be written as a product of single-particle wavefunctions:

$$
\Psi(\mathbf{r}_1,...,\mathbf{r}_N) = \prod_{j=1}^{N} \varphi_{\ell_j}(\mathbf{r}_j).
\qquad (1.43)
$$

This describes a system of N particles where particle number j is in the single-particle quantum state labeled by ℓ_j, with corresponding single-particle state φ_{ℓ_j} (and energy level ε_j). For bosons, we need to symmetrize this wave function. The atoms are identical, and swapping two atoms should not change the many-body wave function. So, we need to write:

$$\Psi(\mathbf{r}_1, ..., \mathbf{r}_N) = \sum_P \left[\prod_{j=1}^N \varphi_{\ell_j}(P[\mathbf{r}_j]) \right]. \tag{1.44}$$

where P are the permutations of the N coordinates $\mathbf{r}_1, ..., \mathbf{r}_N$. The single-particle reduced density matrix can then easily be found:

$$\rho_1(\mathbf{r}; \mathbf{r}') = \sum_{\ell=0}^{\infty} n_\ell \varphi_\ell^*(\mathbf{r}) \varphi_\ell(\mathbf{r}') \tag{1.45}$$

Here n_ℓ is the occupation of the single-particle state ℓ. From the previous discussion, we know that below the transition temperature the single-particle ground state φ_0 will become macroscopically occupied, meaning that $n_0 \to N$ while all other $n_{\ell > 0}$ remain small (since the sum over all occupations is also N). The macroscopically occupied ground state is the hallmark of a BEC.

4. The preceding analysis shows the way to generalize the results to interacting Bose gases. Even for strongly interacting systems, we can always define the density matrix and trace it out until we get to the first order reduced density matrix. This is a hermitean (linear) operator by definition, $\rho_1^*(\mathbf{r}, \mathbf{r}') = \rho_1(\mathbf{r}', \mathbf{r})$. The spectral decomposition theorem tells us that every hermitean linear operator can be decomposed in its (orthonormal) eigenfunctions and (real) eigenvalues

$$\int \rho_1(\mathbf{r}, \mathbf{r}') \phi_\ell(\mathbf{r}) d\mathbf{r} = \lambda_\ell \phi_\ell(\mathbf{r}'), \tag{1.46}$$

as follows:

$$\rho_1(\mathbf{r}, \mathbf{r}') = \sum_{\ell=1}^{\infty} \lambda_\ell \phi_\ell^*(\mathbf{r}) \phi_\ell(\mathbf{r}'). \tag{1.47}$$

Note the analogy between (1.47) and (1.45). In the present case the ϕ_ℓ's are no longer single-particle wave functions relating to the trapping potential. And yet they play the same role as single-particle states that get occupied by λ_ℓ particles. So we can define BEC using these "effective" best single-particle wavefunctions:

5. The Penrose-Onsager criterionstates: **BEC occurs if and only if the single-particle reduced density matrix has an eigenvalue λ_0 that is of order N.** The function $\Psi(\mathbf{r}) = \sqrt{\lambda_0} \phi_0(\mathbf{r})$, proportional to the eigenfunction with the largest eigenvalue and normalized to λ_0, is the **order parameter** for the Bose-Einstein condensed phase. The eigenvalue itself is interpreted as the number of particles in the condensate, $\lambda_0 = N_0$. So, the order parameter $\Psi(\mathbf{r})$ is zero (or negligibly small, $1/N \to 0$) in the normal phase, and becomes macroscopically large in the Bose-Einstein condensed phase. The order parameter determines the phase transition from the normal to the Bose-Einstein condensed phase.

6. The fact that $\lambda_0 = N_0 \approx N$ implies that all other eigenvalues are small, so that

$$\rho_1(\mathbf{r}, \mathbf{r}') \approx \Psi^*(\mathbf{r})\Psi(\mathbf{r}'). \qquad (1.48)$$

The remaining terms are called (thermal) **fluctuations**, and vanish as $T \to 0$. We'll get back to them when we study temperature effects. However, for the temperature zero result it is clear that the expectation values that we now calculate will be equal to the single-particle expectation values calculated for a single-particle wave function $\Psi(\mathbf{r})$. We again have that all the atoms act as if they have the same wave function, this time not related only to the trap, but also including effects of interactions. That is why the order parameter of the BEC is also called the "wave function of the condensate" or the '**macroscopic wave function**': it is a wave function depending on a single position variable, describing the global behavior of the system. Note that this macroscopic wave function is normalized to N_0, the number of particles in the condensate. We have $\int |\Psi(\mathbf{r})|^2 \, d\mathbf{r} = N_0$ in stead of $= 1$. From the density matrix, it is clear that $|\Psi(\mathbf{r})|^2 = \rho_1(\mathbf{r}, \mathbf{r})$: the modulus square of the order parameter can be interpreted as the **density of the condensate**. Only in the limit of vanishingly small interactions, the condensate wave function $\Psi(\mathbf{r})$ becomes proportional to the ground state single-particle wave function of the trap.

SUMMARY: INTERACTING BOSE GASES CANNOT BE DESCRIBED AS A SET OF INDEPENDENT ATOMS TO BE PLACED ON SINGLE-PARTICLE LEVELS. BUT WE CAN WORK WITH THE FIRST ORDER REDUCED DENSITY MATRIX ANDE DEFINE THAT BEC OCCURS WHEN THIS OBJECT HAS AN EIGENVALUE THAT BECOMES MACROSCOPICALLY LARGE. THEN WE CAN TREAT THE CORRESPONDING EIGENFUNCTION AS THE WAVE FUNCTION OF THE CONDENSATE, AND THE ORDER PARAMETER OF THE BEC PHASE.

1.4   The Gross-Pitaevskii equation

From Penrose and Onsager's definition of Bose-Einstein condensation, we learn that the order parameter $\Psi(\mathbf{r})$ is the central quantity from which to derive the properties of an interacting BEC. We have argued that it should exist, since the density matrix can always in principe be written in spectral decomposition. But how should we find $\Psi(\mathbf{r})$? In this section we derive an equation that $\Psi(\mathbf{r})$ has to satisfy (just as ordinary wave functions have to satisfy Schrödinger's equation). This equation for the order parameter is called the Gross-Pitaevskii equation after the two theorists who derived it[10].

---

[10] E. P. Gross, Nuovo Cimento **20**, 454 (1961) and L. P. Pitaevskii, Zh. Eksp. Teor. Fiz. **60**, 646 (1961).

1.4.1 Derivation

We start from the general Hamiltonian of an interacting Bose gas, written in second quantization:

$$
\begin{aligned}
\hat{H} &= \int d\mathbf{r} \; \hat{\psi}^\dagger(\mathbf{r}) \left[-\frac{\hbar^2 \nabla^2}{2m} + V_1(\mathbf{r}) \right] \hat{\psi}(\mathbf{r}) \\
&+ \frac{1}{2} \int d\mathbf{r} \int d\mathbf{r}' \; \hat{\psi}^\dagger(\mathbf{r}) \hat{\psi}^\dagger(\mathbf{r}') V_2(\mathbf{r} - \mathbf{r}') \hat{\psi}(\mathbf{r}') \hat{\psi}(\mathbf{r}).
\end{aligned}
\tag{1.49}
$$

Here $V_1(\mathbf{r})$ is an external potential (for example the magnetic trapping potential (??)). The interatomic interaction potential is given by $V_2(\mathbf{r} - \mathbf{r}')$, and depends on the distance between the interacting atoms. The operators $\hat{\psi}^+(\mathbf{r}), \hat{\psi}(\mathbf{r})$ respectively create and annihilate an atom with mass m at position $\mathbf{r}$. The fact that the first order reduced density matrix satisfies the Penrose-Onsager criterion for BEC,

$$
\rho_1(\mathbf{r}; \mathbf{r}') = \left\langle \hat{\psi}^\dagger(\mathbf{r}) \hat{\psi}(\mathbf{r}') \right\rangle \approx \Psi^*(\mathbf{r}) \Psi(\mathbf{r}'),
\tag{1.50}
$$

allows to replace the operators effectively by macroscopic wave functions,

$$
\hat{\psi}(\mathbf{r}) \approx \Psi(\mathbf{r}).
\tag{1.51}
$$

Let's first focus a bit deeper on this remarkable step, and look at a familiar example, the non-interacting uniform gas, to understand its meaning. The ground state $|\Phi_0\rangle$ is the zero-momentum state, $\mathbf{p} = 0$. This ground state is macroscopically occupied. If we let the (bosonic) creation operator $\hat{a}_0^+$ act on the ground state, we have by definition

$$
\hat{a}_0^+ |\Phi_0\rangle = \sqrt{N+1} \, |\Phi_0\rangle \approx \sqrt{N} \, |\Phi_0\rangle.
\tag{1.52}
$$

The last step is a physical approximation based on $N \gg 1$. In this way, $\hat{a}_0^+ \approx \sqrt{N}$ (multiplied by the identity operator). Mathematically this replacement makes no sense, but physically we expect all relevant expectation values to be approximately the same. For a homogeneous Bose gas the ground state is uniform, so the Penrose-Onsager order parameter is $\Psi(\mathbf{r}) = \sqrt{N}.1$. Here we see that dat $\hat{a}_0^+ \approx \Psi(\mathbf{r})$ (again multiply with the identity operator if you're worried about keeping the operator character), which is what we described above. This concept of shifting the operator $\hat{\psi}(\mathbf{r}) \approx \Psi(\mathbf{r})\hat{1} + fluctuation\ operator$ was first introduced by Bogoliubov[11] in the description of liquid helium where alas it is also necessary to look at the fluctuations. In quantum gases, the effect of interactions and of the fluctuations is much smaller (at least for temperatures well below the transition temperature), and we can therefore get a good estimate of the energy by dropping all fluctuation terms:

$$
\begin{aligned}
E &= \int d\mathbf{r} \; \Psi^*(\mathbf{r}) \left[-\frac{\hbar^2 \nabla^2}{2m} + V_1(\mathbf{r}) \right] \Psi(\mathbf{r}) \\
&+ \frac{1}{2} \int d\mathbf{r} \int d\mathbf{r}' \; \Psi^*(\mathbf{r}) \Psi^*(\mathbf{r}') V_2(\mathbf{r} - \mathbf{r}') \Psi(\mathbf{r}') \Psi(\mathbf{r}).
\end{aligned}
\tag{1.53}
$$

---

[11] N. N. Bogoliubov, J. Phys. Moscow **11**, 23 (1947).

Now we can treat the macroscopic wave function as if it is a variational trial wave function, and use variational calculus to obtain an equation for the best $\Psi(\mathbf{r})$. When varying $\Psi(\mathbf{r})$, we need to keep the norm $N = \int |\Psi(\mathbf{r})|^2 \, d\mathbf{r}$ fixed. This constraint can be taken into account with the method of Lagrange multipliers. The Lagrange multiplier associated with fixing the number of particles is interpreted as the chemical potential μ. So we get:

$$\frac{\delta E}{\delta \Psi(\mathbf{r})} - \mu \frac{\delta N}{\delta \Psi(\mathbf{r})} = 0. \tag{1.54}$$

In order to perform the minimization, we still need to specify the form of the interatomic potential. When working with a very dilute, cold gas (so that both the de Broglie wave length and the distance between the atoms is much larger than the range of the potential), we can use a contact potential:

$$V_2(\mathbf{r} - \mathbf{r}') = \frac{4\pi\hbar^2 a}{m} \delta(\mathbf{r} - \mathbf{r}') \tag{1.55}$$

Indeed, for a dilute cold gas the range of the potential is very small compared to the other relevant length scales, and when zooming out the potential looks as if it only acts when atoms are at the same position. The prefactor takes care of the correct units and contains the parameter a which denotes the strength of the potential. So, the entire effect of the interatomic interactions in the cold, dilute regime can be characterized by a single number a, the s-wave scattering length. This is a remarkable result, and if you want to learn more about this you can check out books on interatomic scattering[12]. The scattering length tells us how much the plane-wave wave function will shift due to the presence of another atom. Far away from that atom, the solution remains a plane wave, only its phase can be shifted: pulled in ($a < 0$) for attraction, or pushed out ($a > 0$) for repulsion. The scattering length depends on the type of atoms interacting and on the hyperfine state of the two interacting atoms. Some values are given in the table below, in units of the Bohr radius ($a_B = 0.0529$ nm), and for the triplet potential:

atomic species	a/a_B
^{7}Li	-27.6 ± 0.5
^{23}Na	65.3 ± 0.9
^{41}K	65 ± 13
^{87}Rb	106 ± 4

(1.56)

Note that lithium has a negative scattering length, so these atoms attract each other.

Substituting the contact potential (1.55) in the expression for the energy (1.53), and performing the minimization (1.54), we obtain the Gross-Pitaevskii equation for the order parameter:

$$\boxed{-\frac{\hbar}{2m}\nabla^2\Psi(\mathbf{r}) + V_1(\mathbf{r})\Psi(\mathbf{r}) + \frac{4\pi\hbar^2 a}{m}|\Psi(\mathbf{r})|^2\Psi(\mathbf{r}) = \mu\Psi(\mathbf{r})} \tag{1.57}$$

This equation describes the condensate at zero temperature, assuming that all particles are in the condensate $\lambda_0 = N$. It is a **non-linear Schrödinger**

---

[12]Landau and Lifschitz, volume 3, *Quantum Mechanics – non-relativistic theory*, section 132 "scattering of slow particles" is a good source of information.

equation, which looks like an ordinary Schrödinger equation where the potential is the sum of the external potential $V_1(\mathbf{r})$ and a mean-field potential $(4\pi\hbar^2 a/m)\,|\Psi(\mathbf{r})|^2$. The non-linear character has important consequences: it is no longer true that the sum of two solutions is still a solution of the equation. Another difference with the usual Schrödinger equation is that we have the chemical potential occuring where we expect to find the energy eigenvalue. Only in the case of non-interacting gases, the chemical potential will be equal to the energy per particle, in general it is different. Finally, note that we also have a time-dependent version of the Gross-Pitaevskii equation,

$$-\frac{\hbar}{2m}\nabla^2\Psi(\mathbf{r},t) + V_1(\mathbf{r})\Psi(\mathbf{r},t) + \frac{4\pi\hbar^2 a}{m}\,|\Psi(\mathbf{r},t)|^2\,\Psi(\mathbf{r},t) = i\hbar\frac{\partial}{\partial t}\Psi(\mathbf{r},t) \quad (1.58)$$

From which we see that solutions of the time-independent Gross-Pitaevskii equation have a trivial time dependence $\Psi(\mathbf{r},t) = \exp\{-i\mu t/\hbar\}\Psi(\mathbf{r})$. Of course, this is no longer true if we start from any other initial value $\Psi(\mathbf{r},t_0)$ for the order parameter. We'll get back to the condensate dynamics in section 1.5.

1.4.2 Solution for the ideal Bose gas

Let's look at the simplest example first, and consider an ideal Bose gas in a harmonic trap. Then the Gross-Pitaevskii equation reduces to the linear Schrödinger equation for the harmonic oscillator:

$$-\frac{\hbar}{2m}\nabla^2\Psi(\mathbf{r}) + \frac{m\omega^2}{2}r^2\Psi(\mathbf{r}) = \mu\Psi(\mathbf{r}), \quad (1.59)$$

The solution is well known to those who know it. It is the Gaussian wave function

$$\Psi_{a=0}(\mathbf{r}) = A\exp\{-r^2/(2a_{HO}^2)\}. \quad (1.60)$$

with $a_{HO} = \sqrt{\hbar/(m\omega)}$ the oscillator length of the trapping potential. The norm A has to be fixed through the total number of condensed atoms

$$
\begin{aligned}
N &= \int |\Psi_{a=0}(\mathbf{r})|^2\,d\mathbf{r} = |A|^2\int e^{-r^2/a_{HO}^2}\,d\mathbf{r} \\
&= |A|^2\left(\frac{\pi}{a_{HO}^2}\right)^{3/2},
\end{aligned}
\quad (1.61)
$$

from which

$$|A| = N^{1/2}a_{HO}^{3/2}/\pi^{3/4}. \quad (1.62)$$

The chemical potential is $\mu = 3\hbar\omega/2$. Note that this is just the ground state energy of the 3D harmonic oscillator, so we get $\mu \to \varepsilon_{\min}$ as discussed in the very beginning of this course.

1.4.3 The Thomas-Fermi approximation

Expression (1.53) for the Gross-Pitaevskii energy can be split up in a kinetic energy term E_{kin}, a term representing the confinement energy E_{HO}, and a term representing the interaction energy E_{int} :

$$E_{kin} = -\frac{\hbar^2}{2m}\int d\mathbf{r}\ \Psi^*(\mathbf{r})\nabla^2\Psi(\mathbf{r}) \quad (1.63)$$

$$E_{HO} = \frac{m\omega^2}{2} \int d\mathbf{r} \; r^2 \left|\Psi(\mathbf{r})\right|^2 \tag{1.64}$$

$$E_{int} = \frac{2\pi\hbar^2 a}{m} \int d\mathbf{r} \; \left|\Psi(\mathbf{r})\right|^4 \tag{1.65}$$

Here we consider an isotropic trapping potential so that $\omega = \omega_x = \omega_y = \omega_z$, and we have also used the contact potential (1.55) to describe interactions. The use of the contact potential is, as mentioned before, linked to the diluteness parameter $n|a|^3$ where n is the density of atoms and a the scattering length. This diluteness parameter tells us how many atoms are contained in a volume detemined by the effective range a of the potential. For at typical experiment $n = 10^{13} - 10^{15}$ cm^{-3}, so that $n|a|^3$ is smaller than 10^{-3}, and we can safely replace the real interatomic potential by a contact potential.

This doen not mean that the effects of interactions are necessarily small. We have to compare the interaction energy with the kinetic energy, for atoms trapped within a region of typical size a_{HO}. This means that the density of atoms is $N/(a_{HO}^3)$, and we have

$$\int d\mathbf{r} \; \left|\Psi(\mathbf{r})\right|^4 \;\;\approx\;\; \int d\mathbf{r} \left(\frac{N}{a_{HO}^3}\right)^2 \approx \frac{N^2}{a_{HO}^3} \tag{1.66}$$

$$\Rightarrow \;\; E_{int} \propto \frac{N^2 a}{a_{HO}^3} \tag{1.67}$$

The kinetic energy of a particle in a box of size L scales as $1/L^2$, so that for a trap with size a_{HO} and N paticles,

$$E_{int} \propto \frac{N}{a_{HO}^2} \tag{1.68}$$

Hence, the ratio of interaction energy to kinetic energy scales as

$$\frac{E_{int}}{E_{kin}} \propto \frac{Na}{a_{HO}}. \tag{1.69}$$

This is the **Thomas-Fermi parameter.** If $N|a|/a_{HO}$ is much larger than one, the interaction energy is much larger than the kinetic energy, and the latter can be neglected. Doing this is called the **Thomas-Fermi approximation**. How many atoms do we typically need to be in the Thomas-Fermi (TF) regime ? Since the scattering length is of order nanometers and the oscillator length of the trap is of order microns, we'll be in the Thomas-Fermi regime already for more than a few thousand atoms. Most experiments work with hundreds of thousands of atoms, and are well within the TF regime.

In the Thomas-Fermi regime we don't need any additional approximation to solve the Gross-Pitaevskii equation! Indeed, without the kinetic energy term the GP equation becomes

$$V_1(\mathbf{r})\Psi_{TF}(\mathbf{r}) + \frac{4\pi\hbar^2 a}{m} \left|\Psi_{TF}(\mathbf{r})\right|^2 \Psi_{TF}(\mathbf{r}) = \mu\Psi_{TF}(\mathbf{r}) \tag{1.70}$$

$$\Leftrightarrow \left|\Psi_{TF}(\mathbf{r})\right|^2 = \frac{m}{4\pi\hbar^2 a}[\mu - V_1(\mathbf{r})]. \tag{1.71}$$
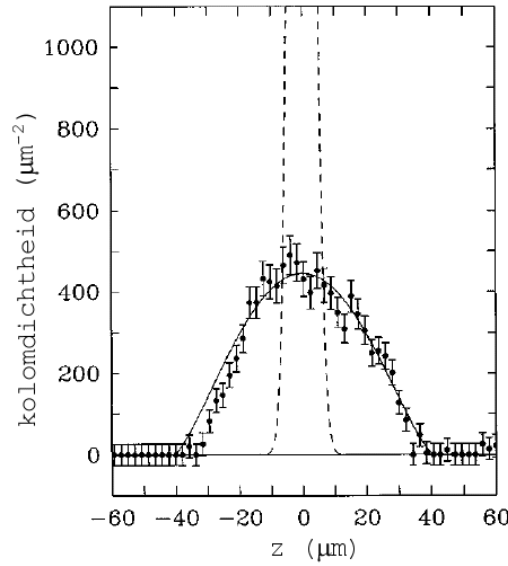
Figure 1.14: Column density of the condensate (this is the density integrated along the line of sight), as a function of the distance to the center of the trap. The dashed curve is the result for the ground state of the trap (and for the ideal Bose gas). The full curve represents the Thomas-Fermi result, which agrees well with the experimental measurement (the points). Image source: Pethick and Smith's book (see bibliography).

The density of the condensate is the modulus square of the order parameter (cf. expression (1.42)) so that $n_{TF}(\mathbf{r}) = |\Psi_{TF}(\mathbf{r})|^2$. For a harmonic trap, $V_1 = m\omega^2 r^2/2$, and the density profile is an inverted parabola:

$$n_{TF}(\mathbf{r}) = \begin{cases} \dfrac{m}{4\pi\hbar^2 a}\left[\mu - \dfrac{m\omega^2}{2}r^2\right] & \text{for } m\omega^2 r^2/2 < \mu \\ 0 \text{ elsewhere} \end{cases} . \qquad (1.72)$$

The height (and hence extent) of the inverted parabola is set by the chemical potential μ, it's curvature is set by the scattering length. The chemical potential in turn is fixed by the total number of atoms:

$$N = \int n_{TF}(\mathbf{r})d\mathbf{r} \qquad (1.73)$$

$$= \frac{m}{\hbar^2 a}\int_0^{\sqrt{2\mu/(m\omega^2)}} r^2\left[\mu - m\omega^2 r^2/2\right]dr \qquad (1.74)$$

$$\Rightarrow \mu = \frac{\hbar\omega}{2}\left(\frac{15Na}{a_{HO}}\right)^{2/5} . \qquad (1.75)$$

With this, we can rewrite the density of the condensate as

$$n_{TF}(\mathbf{r}) = \begin{cases} n_{TF}(0)\left[1 - \left(\dfrac{r}{R_{TF}}\right)^2\right] & \text{for } r < R_{TF} \\ 0 \text{ for } r > R_{TF} \end{cases} , \qquad (1.76)$$

with R_{TF} the Thomas-Fermi radius given by

$$R_{TF} = a_{HO} \left(\frac{15Na}{a_{HO}} \right)^{1/5} \tag{1.77}$$

and the central density

$$n_{TF}(0) = \frac{R_{TF}^2/(aa_{HO})}{16\pi a_{HO}^3}$$

Outside the Thomas-Fermi radius there are no more condensate atoms. Without interactions the atoms would all be in the (Gaussian) ground state of the trap. Interactions modify this result strongly: we now get an inverted parabola, less dense in the center but extending further out – the repulsive interactions push out the atoms. Figure 1.14 compares the two theoretical curves with the experimental result for a ^{87}Rb condensate of 100000 atoms, well in the TF regime. It is clear that the TF approximation describes the measurements best. Note that at the edge of the cloud (near the TF radius), the experimental points deviate a little from the Thomas-Fermi solution. Indeed, where the density becomes low, the interaction energy again becomes (locally) less important than the kinetic energy and we have a tiny region near the edge of the condensate where in principle the TF approximation doesn't hold. There, we expect the kinetic energy to smoothen then sharp kink between the parabola and the zero-density line.

1.4.4   Coherence length

What will be the typical length scale over which the kinetic energy smoothens the TF profile? This should also be the smallest length scale over which the order parameter can change. Let's consider a scale ξ over which the order parameter changes. So, for distances smaller than ξ we take the order parameter constant and the kinetic energy is $\hbar^2/(2m\xi)$. The interaction energy is $(4\pi\hbar^2 an/m)$ with n the density. Equating these two energies gives us a qualitative estimate of ξ, namely

$$\xi = \frac{1}{\sqrt{8\pi an}}. \tag{1.78}$$

The TF approximation works when the length scales over which the order parameter varies is much larger than ξ.

Let's rephrase this to get a better insight into ξ, and as the following question: what is the smallest length scale over which the order parameter can grow from zero to its bulk value? To find this, we'll use the Gross-Pitaevskii equation in one dimension, and place a hard wall at $x = 0$. The condensate is restricted to the half-space $x > 0$. It is zero for $x \leqslant 0$. So our boundary conditions are that (1) far away from the wall $x \to +\infty$ the condensate is homogeneous and the density has reached its bulk value $n_\infty = |\Psi_\infty|^2 = |\Psi(x \to \infty)|^2$; and (2) at the wall $\Psi(x = 0) = 0$. Let's solve the Gross-Pitaevskii equation

$$-\frac{\hbar^2}{2m} \frac{d^2\Psi(x)}{dx^2} + \frac{4\pi\hbar^2 a}{m} |\Psi(x)|^2 \Psi(x) = \mu\Psi(x).$$

for these boundary conditions. Firstly, let's look far away from the wall. In this region, the second derivative vanishes, and we must have our **bulk solution**:

$$\frac{4\pi\hbar^2 a}{m} \left|\Psi_\infty\right|^2 \Psi_\infty = \mu\Psi_\infty$$

$$\rightarrow \quad \mu = \frac{4\pi\hbar^2 a}{m} n_\infty = g n_\infty \tag{1.79}$$

Interpreting the chemical potential as usual as a cost to remove a particle from the condensate, we see that to remove all N particles from a volume V, we need to pay an energy $(\mu N) = g N^2/V = g n V$. Having fixed μ, we can substitute it in the Gross-Pitaevskii equation:

$$-\frac{\hbar^2}{2m}\frac{d^2\Psi(x)}{dx^2} + \frac{4\pi\hbar^2 a}{m}\left|\Psi(x)\right|^2 \Psi(x) = \frac{4\pi\hbar^2 a}{m}n_\infty\Psi(x) \tag{1.80}$$

We can simplify this by writing

$$\Psi(x) = \left|\Psi_\infty\right| f(x) = \sqrt{n_\infty} f(x) \tag{1.81}$$

so that our boundary condition for $x \rightarrow \infty$ now simply becomes $f(x \rightarrow \infty) = 1$. Then we have, after division by $\sqrt{n_\infty}$:

$$-\frac{\hbar^2}{2m}\frac{d^2 f(x)}{dx^2} + \frac{4\pi\hbar^2 a}{m}n_\infty\left[f(x)^2 - 1\right]f(x) = 0 \tag{1.82}$$

Dividing by $4\pi\hbar^2 a n_\infty/m$, we get

$$-\xi^2\frac{d^2 f(x)}{dx^2} + \left[f(x)^2 - 1\right]f(x) = 0 \tag{1.83}$$

where again our length scale $\xi = 1/\sqrt{8\pi a n_\infty}$ pops up. To find the solution, we substitute a trial form $f(x) = \tanh(ax)$. The hyperbolic tangent starts at 0 in $x = 0$ and goes to 1 for $x \rightarrow \infty$, so it satisfies the boundary conditions. Since

$$\frac{d^2}{dx^2}\tanh(ax) = 2a^2\tanh(ax)\left[\tanh^2(ax) - 1\right] \tag{1.84}$$

we find that $a = \xi/\sqrt{2}$ and

$$\Psi(x) = \sqrt{n_\infty}\tanh\left(\frac{a}{\sqrt{2}\xi}\right) \tag{1.85}$$

The hyperbolic tangent rises from zero to 1 over a length ξ ! This length is also known as the **healing length** (healing a condensate back from zero to its bulk value) or the **coherence length** (the shortest length scale over which the order parameter can appreciably vary). Indeed, it costs energy to bend the wave function, and it is energetically unfavorable to bend it over a shorter distance than ξ. If you do that, the wavefunction "breaks" and you excite atoms out of your condensate. So, the coherence length is a very important length scale for the study of condensates! It's typical size in the experiments that we have considered is of the order of 100 nm.

SUMMARY: THE ORDER PARAMETER OF THE BEC SATISFIES A NON-LINEAR SCHRODINGER EQUATION KNOWN AS THE GROSS-PITAEVSKII

EQUATION. FOR A DILUTE GAS THE INTERACTION IS FULLY DESCRIBED BY A SINGLE PARAMETER, THE SCATTERING LENGTH, WHICH TOGETHER WITH THE DENSITY GIVES RISE TO THE COHERENCE LENGTH, THE SHORTEST LENGTH OVER WHICH THE ORDER PARAMETER CAN CHANGE. WHEN $N|a|/a_{HO} >> 1$, THE ORDER PARAMETER VARIES MUCH MORE SLOWLY THAN THE COHERENCE LENGTH, AND WE CAN APPLY THE THOMAS-FERMI APPROXIMATION, NEGLECTING KINETIC ENERGY.

1.5 Condensate dynamics

1.5.1 Time dependent Gross-Pitaevskii equation

The second-quantized Bose gas Hamiltonian (1.49) is

$$
\begin{aligned}
\hat{H} &= \int d\mathbf{r}\ \hat{\psi}^\dagger(\mathbf{r}) \left[-\frac{\hbar^2 \nabla^2}{2m} + V_1(\mathbf{r}) \right] \hat{\psi}(\mathbf{r}) \\
&\quad + \frac{1}{2} \int d\mathbf{r} \int d\mathbf{r}'\ \hat{\psi}^\dagger(\mathbf{r}) \hat{\psi}^\dagger(\mathbf{r}') V_2(\mathbf{r} - \mathbf{r}') \hat{\psi}(\mathbf{r}') \hat{\psi}(\mathbf{r}).
\end{aligned} \tag{1.86}
$$

This also allows to investigate the time dependence of the operator $\hat{\psi}(\mathbf{r}, t)$ in the Heisenberg picture. For bosonic operators the following commutation rules hold:

$$
\left[\hat{\psi}^\dagger(\mathbf{r}, t), \hat{\psi}(\mathbf{r}', t) \right] = \delta(\mathbf{r} - \mathbf{r}') \tag{1.87}
$$

$$
\left[\hat{\psi}(\mathbf{r}, t), \hat{\psi}(\mathbf{r}', t) \right] = 0 \tag{1.88}
$$

With these rules, we can work out Heisenberg's equation of motion for $\hat{\psi}(\mathbf{r}, t)$:

$$
\begin{aligned}
i\hbar \frac{\partial \hat{\psi}(\mathbf{r}, t)}{\partial t} &= \left[\hat{\psi}(\mathbf{r}, t), \hat{H} \right] \\
&= \left[-\frac{\hbar^2 \nabla^2}{2m} + V_1(\mathbf{r}) \right] \hat{\psi}(\mathbf{r}, t) \\
&\quad + \left[\frac{1}{2} \int d\mathbf{r}'\ \hat{\psi}^\dagger(\mathbf{r}', t) V_2(\mathbf{r} - \mathbf{r}') \hat{\psi}(\mathbf{r}', t) \right] \hat{\psi}(\mathbf{r}, t).
\end{aligned} \tag{1.89}
$$
$$\tag{1.90}$$

Now we can proceed by again making using Bogoliubov's assumption that the Bose-Einstein condensed state is characterized by $\hat{\psi}(\mathbf{r}, t) \approx \Psi(\mathbf{r}, t)$: we can replace the field operator by the order parameter (times the identity operator). From this we find the **time dependent Gross-Pitaevskii equation** already mentioned in the previous section:

$$
i\hbar \frac{\partial \Psi(\mathbf{r}, t)}{\partial t} = \left[-\frac{\hbar}{2m} \nabla^2 + V_1(\mathbf{r}) + \frac{4\pi \hbar^2 a}{m} |\Psi(\mathbf{r}, t)|^2 \right] \Psi(\mathbf{r}, t) \tag{1.91}
$$

We re-iterate that in the ground state –and only in the ground state– the right hand side is equal to $\mu \Psi(\mathbf{r}, t)$ and hence

$$
\Psi(\mathbf{r}, t) = \Psi(\mathbf{r}) \exp\{i\mu t/\hbar\}. \tag{1.92}
$$

Note that for the usual Schrödinger equation, eigenstates behave just like the ground state here: as a function of time all that happens is that they acquire a uniform phase factor $\exp\{iEt/\hbar\}$ where E is the energy-eigenvalue. Here, the chemical potential takes the role of the ground state energy, and we no longer have a simple time dependence for excited states. The appearance of the chemical potential here is not surprising, since Ψ corresponds to the matrix element of an annihilation operator $\hat{\psi}$ between the ground state with N atoms and the ground state with $N-1$ atoms:

$$\Psi(\mathbf{r},t) = \langle N-1 | \hat{\psi}(\mathbf{r}) | N \rangle \propto \exp\{-i(E_N - E_{N-1})t/\hbar\}. \qquad (1.93)$$

Here E_N and E_{N-1} are the energies of the ground state with N and $N-1$ atoms, respectively. For large N this difference is equal to $\partial E/\partial N$, the chemical potential.

1.5.2 Velocity as a phase gradient

We have already seen that the modulus squared of the order parameter corresponds to the particle density of the condensate, $|\Psi(\mathbf{r},t)|^2 = n(\mathbf{r},t)$. But what is the meaning of the phase? To find out, let's multiply the time dependent Gross-Pitaevskii equation (1.91) with $\Psi^*(\mathbf{r},t)$,

$$i\hbar\Psi^*(\mathbf{r},t)\frac{\partial\Psi(\mathbf{r},t)}{\partial t} = -\frac{\hbar}{2m}\Psi^*(\mathbf{r},t)\nabla^2\Psi(\mathbf{r},t) + V_1(\mathbf{r})\,|\Psi(\mathbf{r},t)|^2 + \frac{4\pi\hbar^2 a}{m}\,|\Psi(\mathbf{r},t)|^4, \qquad (1.94)$$

and subtract from this equation its complex conjugate. We then obtain

$$\frac{\partial\,|\Psi(\mathbf{r},t)|^2}{\partial t} + \nabla\cdot\left\{\frac{\hbar}{2mi}\left[\Psi^*(\mathbf{r},t)\nabla\Psi(\mathbf{r},t) - \Psi(\mathbf{r},t)\nabla\Psi^*(\mathbf{r},t)\right]\right\} = 0. \qquad (1.95)$$

This looks like the continuity equation for the probability density in the Schrödinger equation. For the Gross-Pitaevskii equation this becomes the continuity equation for the particle density:

$$\boxed{\frac{\partial n}{\partial t} + \nabla\cdot(n\mathbf{v}) = 0}, \qquad (1.96)$$

where we have identified the velocity field of the condensate as:

$$\mathbf{v} = \frac{\hbar}{2mi}\frac{\Psi^*\nabla\Psi - \Psi\nabla\Psi^*}{|\Psi|^2}. \qquad (1.97)$$

In the usual Schrödinger equation this continuity equation describes the conservation of the probability density of the wave function. For the Gross-Pitaevskii equation it becomes more tangible: we now have conservation of the condensate density. This means that if the condensate density decreases somewhere and increases somewhere else, there must have been a flow of atoms between these two spots. Writing the order parameter with modulus and phase,

$$\Psi = \sqrt{n}e^{iS}, \qquad (1.98)$$

we now find that the velocity is given by

$$\boxed{\mathbf{v} = \frac{\hbar}{m}\nabla S}. \qquad (1.99)$$

This is an important result: **the velocity field of the condensate is given by the gradient of the phase of the order parameter.** An equally important consequence of this is that the velocity field of a condensate is **irrotational**,

$$\boldsymbol{\nabla} \times \mathbf{v} = \mathbf{0}.$$

Indeed, the curl of a gradient is always zero.

We end this subsection by defining another useful hydroynamic variable, the condensate current density:

$$\mathbf{j} = mn\mathbf{v} = \hbar \left|\psi\right|^2 \boldsymbol{\nabla}S. \tag{1.100}$$

This is of course not an electrical current, but a mass current indicating the flow of mass. So in SI units is is expressed in kg passing per second through a square meter window, set in a plane perpendicular to $\mathbf{j}$. These big units are quite unsuited for the atomic condensates, where often we use the healing length as a length scale at the atomic mass as mass unit, and set also planck's constant to one. For the moment, let's not specify the units. Note furthermore that the density we have used till now, $n(\mathbf{r}, t)$ is an atom density (#atoms per volume), different from the mass density $\rho(\mathbf{r}, t) = mn(\mathbf{r}, t)$ in kg per volume. Using this mass density and the current density, we can write the continuity equation in its usual form $\dot{\rho} + \boldsymbol{\nabla} \cdot \mathbf{j} = 0$.

1.5.3 Hydrodynamic equations

Rather that using an equation for the order parameter (the Gross-Pitaevskii equation), we could look for equations for the condensate density and velocity. Such equations, in analogy with the theory of fluids and continuous media, are called hydrodynamic equations[13]. The density and velocity of the condensate contain essentially the same information as the order parameter, since they are related to modulus and phase (gradients), respectively. Substituting (1.98) in the Gross-Pitaevskii equation, we get

$$i\hbar \frac{\partial \sqrt{n}}{\partial t} e^{iS} - \hbar\sqrt{n}\frac{\partial S}{\partial t}e^{iS}$$
$$= -\frac{\hbar^2}{2m}\left[\left(\nabla^2 \sqrt{n}\right) + 2i\left(\nabla\sqrt{n}\right)\cdot(\nabla S) + i\sqrt{n}\left(\nabla^2 S\right) - \sqrt{n}\left(\nabla S\right)^2\right]e^{iS}$$
$$+ V_1(\mathbf{r})\sqrt{n}e^{iS} + \frac{4\pi\hbar^2 a}{m}n\sqrt{n}e^{iS} \tag{1.101}$$

Both the real part and the imaginary part of this equation should hold. Collect the imaginary parts and multiply by divide by $2\sqrt{n}e^{-iS}$ to find

$$2\hbar\sqrt{n}\frac{\partial \sqrt{n}}{\partial t} = -\frac{\hbar^2}{m}\left[2\sqrt{n}\left(\nabla\sqrt{n}\right)\cdot(\nabla S) + n\left(\nabla^2 S\right)\right]. \tag{1.102}$$

Since $2\sqrt{n}\left(\nabla\sqrt{n}\right) = \nabla n$ this can be rewritten as

$$\frac{\partial n}{\partial t} = -\boldsymbol{\nabla}\cdot\left[\frac{\hbar}{m}\left(n\boldsymbol{\nabla}S\right)\right]. \tag{1.103}$$

---

[13]In the context of the Schrödinger equation these would be called the Madelung equations for the probability density.

The imaginary parts correspond to the continuity equation, nothing new. Next, collect the real parts of (1.101), and divide by $\sqrt{n}e^{iS}$. You obtain:

$$\hbar\frac{\partial S}{\partial t} + \left(\frac{\hbar^2}{2m}\left(\nabla S\right)^2 + V_1 + \frac{4\pi\hbar^2 a}{m}n - \frac{\hbar^2}{2m\sqrt{n}}\nabla^2\sqrt{n}\right) = 0 \qquad (1.104)$$

Now take the gradient of this equation, and write the phase gradients as velocities using (1.99). This yields

$$\boxed{m\frac{\partial \mathbf{v}}{\partial t} = -\boldsymbol{\nabla}\left(\tilde{\mu} + \frac{1}{2}m\mathbf{v}^2\right),} \qquad (1.105)$$

with

$$\tilde{\mu} = V_1 + \frac{4\pi\hbar^2 a}{m}n - \frac{\hbar^2}{2m\sqrt{n}}\nabla^2\sqrt{n}. \qquad (1.106)$$

This equation for the velocity field (1.105), taken together with the continuity equation (1.96), form a closed set of differential equations for density and velocity field. The equation for the velocity field can be rewritten (using $\boldsymbol{\nabla}\times\mathbf{v} = \mathbf{0}$) as

$$\frac{\partial \mathbf{v}}{\partial t} + (\mathbf{v}\cdot\boldsymbol{\nabla})\mathbf{v} = -\frac{1}{m}\boldsymbol{\nabla}\tilde{\mu} \qquad (1.107)$$

This is known from classical hydrodynamics as the Euler equation for a perfect (frictionless, non-viscous) fluid. In classical hydrodynamics, that is just an approximation, not too bad for water and very bad for marmelade. But here we get the Euler equation without approximation, directly from the Gross-Pitaevskii equation. We must conclude that the **condensate behaves as a perfect fluid**, and **flows without friction**. Hence we can call it a **superfluid**, in analogy with a superconductor where we also have (electrical) flow without resistance.

Let's take a closer look at the notation $\tilde{\mu}$ that we have introduced. In the Euler equation it represents a pressure. Here, it contains three terms:

$$\boldsymbol{\nabla}\tilde{\mu} = \boldsymbol{\nabla}V_1 + \frac{1}{n}\left[\boldsymbol{\nabla}p + n\boldsymbol{\nabla}p_q\right] \qquad (1.108)$$

The first term, represents the mechanical pressure. If we have a container or trap with potential V_1, and we compress it, the mechanical pressure increases. Next,

$$p = (4\pi\hbar^2 a/m)n^2 \qquad (1.109)$$

is the interaction pressure. This is the additional pressure on the "walls" of the container due to the repulsive interactions between the atoms, that strive to expand the container. Finally,

$$p_q = \frac{\hbar^2}{2m\sqrt{n}}\nabla^2\sqrt{n}. \qquad (1.110)$$

is a purely quantum mechanical effect – it represents the aversion of the wavefunction to be deformed, i.e. to change from place to place. The more we deform the wave function locally, the larger it is. In particular, if we have to squeeze the wavefunction into a small box, it grows inversely proportional to the square of the size of the box.

tijdsinterval per prent: 5 msec
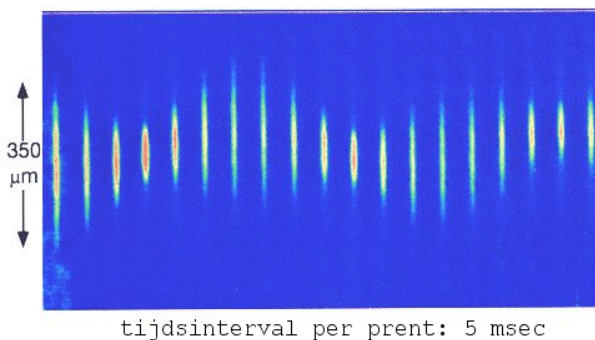
Figure 1.15: This sequence of frames (with 5 msec time interval between each frame) shows the condensate in motion. Blue is low density and red is high density. This motion was initiated by a sudden translation in the confinement potential. After the translation, the condensate sloshes back and forth.

This is called **quantum pressure**. It comes from the quantum kinetic energy $-\hbar^2\nabla^2/(2m)$ and tells us that if the modulus of the order parameter is not constant throughout space, this will cost kinetic energy. Of course, the place-dependent changes in the phase also cost energy, but we already have those in $m\mathbf{v}^2/2$ where $\mathbf{v}$ now contains the gradient of the phase. In the Thomas-Fermi approximation we have learned that the kinetic energy due to the deformation of the wavefunction can be neglected in the regime $N\left|a\right|/a_{HO} >> 1$. So, in this regime we can neglect the quantum pressure p_q.

Collective modes and sound

The Euler equation is a nonlinear equation, just like the Gross-Pitaevskii equation, and hence it is hard to solve. What one usually does is look at perturbations around equilibrium, and then *linearize* the equations by expanding them in the small perturbation and neglecting higher order terms in the small perturbation. Let's take n_{eq} to be the equilibrium density, and $\mathbf{v}_{eq} = \mathbf{0}$ to be our equilibrium velocity field (i.e. no flow). We'll also assume that we are in the Thomas-Fermi regime so we're not bothered by the quantum pressure. To look at the dynamics of such modes[14] we write

$$n = n_{eq} + \delta n \qquad (1.111)$$

and assume that $\delta n \ll n_{eq}$ and that moreover δn and $\mathbf{v}$ vary slowly in space (so the gradients can also be treated as small parameters). Now we can plug in this expression for n, and linearize the hydrodynamic equations (1.96) and (1.105):

$$m\frac{\partial \mathbf{v}}{\partial t} = -\boldsymbol{\nabla}\left(\delta\tilde{\mu}\right), \qquad (1.112)$$

$$\frac{\partial(\delta n)}{\partial t} + \boldsymbol{\nabla}\cdot\left(n_{eq}\mathbf{v}\right) = 0. \qquad (1.113)$$

---

[14] They're called collective modes since all the atoms in the condensate share the energy of the mode and participate in the motion. This contrasts with single-particle excitations, where we kick a single atom out of a condensate.
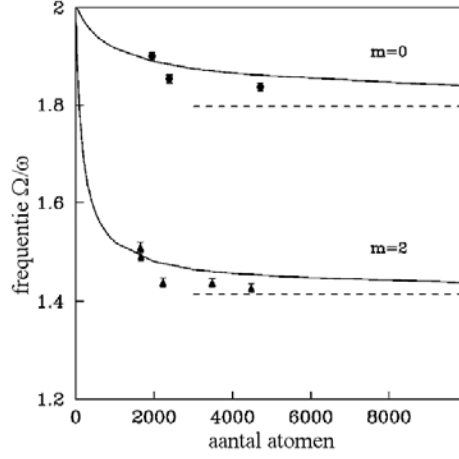
Figure 1.16: Oscillation frequencies for two modes. The dots are the experiment, the dashed line is the result neglecting the quantum pressure, obtained via (1.119). The full line is the numerical result taking quantum pressure into account.

We can combine both equations into one by taking the time derivative of the second equtaion and substituting the first equation into the result:

$$m\frac{\partial^2}{\partial t^2}(\delta n) = \boldsymbol{\nabla} \cdot [n_{eq} \boldsymbol{\nabla}(\delta \tilde{\mu})]. \tag{1.114}$$

We have used that n_{eq} does not depend on time. When the quantum pressure is neglected in (1.106), the effective potential $\tilde{\mu}$ reduces to $V_1 + \dfrac{4\pi\hbar^2 a}{m}n$, so the change in $\tilde{\mu}$ is given by

$$\delta\tilde{\mu} = \frac{4\pi\hbar^2 a}{m}\delta n, \tag{1.115}$$

Now we obtain a second order differential equation for the density disturbance δn:

$$m\frac{\partial^2}{\partial t^2}(\delta n) = \frac{4\pi\hbar^2 a}{m}\boldsymbol{\nabla} \cdot [n_{eq}\boldsymbol{\nabla}(\delta n)]. \tag{1.116}$$

When we're looking for small amplitude *oscillations*, we mean by that that the time dependence of the density disturbance is of the form $\delta n \propto e^{i\Omega t}$. This simplifies the result to

$$-\Omega^2 \delta n = \frac{4\pi\hbar^2 a}{m^2}\left[\boldsymbol{\nabla} n_{eq}\cdot\boldsymbol{\nabla}(\delta n) + n_{eq}\nabla^2(\delta n)\right]. \tag{1.117}$$

Now we can the Thomas-Fermi result for the equilibrium density, expression (1.72),

$$n_{eq} = \frac{m}{4\pi\hbar^2 a}(\mu - V_1), \tag{1.118}$$

where μ is the chemical potential, not to be confused with $\tilde{\mu}$. After substitution we get

$$-\Omega^2 \delta n = \frac{1}{m}\left[\boldsymbol{\nabla} V_1 \cdot \boldsymbol{\nabla}(\delta n) + n_{eq}\nabla^2(\delta n)\right] \tag{1.119}$$
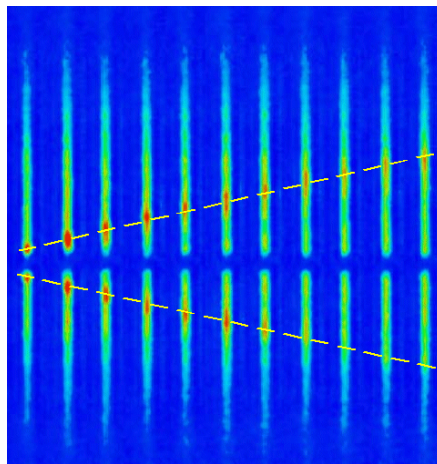
Figure 1.17: Measuring the speed of sound in a condensate: a bump in the density travels with constant speed through the cloud. This is seen in this sequence of frames, showing a condensate cut in half so that the central atoms show up as bumps just above and below the cut.

Solving this equation allows us to find the frequencies of the small amplitude oscillation modes of the condensate. In figure 1.16 we see that the results of this equation match the experimental measurements well. Below $N = 2000$ atoms (x-axis), the deviation between experiment and theory grows, signalling that the number of particles has become too small for the Thomas-Fermi approximation to be applicable.

An important collective mode is **sound**. Sound modes are density waves, and hence we get $\delta n \propto e^{i\mathbf{k}\cdot\mathbf{r}-i\omega t}$. Looking at a homogeneous condensate ($\boldsymbol{\nabla}V_1$ negligible), equation (1.116) becomes

$$\frac{\partial^2}{\partial t^2}(\delta n) - \frac{4\pi\hbar^2 a n_{eq}}{m^2}\boldsymbol{\nabla}^2\left(\delta n\right) = 0. \tag{1.120}$$

This is indeed the wave equation, with wave velocity

$$c = \frac{\hbar}{m}\sqrt{4\pi a n_{eq}} = \frac{1}{\sqrt{2}}\frac{\hbar}{m\xi}. \tag{1.121}$$

Once again the healing length pops up: it determines the speed of sound in a condensate. We'll get back to this special role of the healing length when we look closer at the difference between collective modes and single-particle modes, in the section on finite temperatures. For now, we can note that the sound velocity calculated here also matches experimental results well. The experiment is done as follows: with a blue detuned laser beam, atoms are repelled from the center of the condensate. These atoms heap up in the condensate just next to the region where the beam is, as is seen in the leftmost frame of figure 1.17. The bumps start travelling up (resp. down) the condensate, and go equal distances in equal time (i.e. at constant speed), as indicated by the yellow dashed line in figure 1.17. This constant speed is the sound velocity.

1.5.4 Superfluidity

We have seen that the dynamics of the condensate is governed by the equations for a frictionless, irrotational fluid. Untill before the discovery of the macroscopic quantum mechanical phases of matter, it was assumed that every fluid experiences some friction, just as it was thought that every electrical conductor, no matter how good, has a little bit of resistance. Here we see that condensates are really completely frictionless, just as superconductors really have no electrical resistance, at least below a critical current or velocity. This frictionless, irrotational behavior of a fluid is called **superfluidity**. Another property is that superfluids carry no entropy. Remember our discussion for the ideal Bose gas: Bose condensed atoms do not contribute to the entropy, only the atoms in excited states. Another way to see this is that there is only one microscopic state that gives energy zero, namely the state with all particles in the same single-particle state. From Boltzmann's formula we then know that $S = k_B \log(1) = 0$.

Note that superfluidity is not a concept which is rigourously defined in the same way as Penrose and Onsager define Bose-Einstein condensation. Superfluidity is an "umbrella" concept covering a number of properties that in superfluid helium all occur together, but that do not necessarily have to occur together. For each of these properties you can find criteria, but it is the collection of these properties that earn a fluid the title of superfluid, as will become clear when we proceed in our study of macroscopic quantum systems. Frictionless flow is just one of these properties. Another important property is the occurrence of quantized vortices, and this phenomena is the subject of the next section.

THE TIME DEPENDENT GROSS-PITAEVSKII EQUATION IS EQUIVALENT TO A SET OF HYDRODYNAMIC EQUATIONS FOR THE DENSITY (MODULUS SQUARED OF THE ORDER PARAMETER) AND THE VELOCITY FIELD (GRADIENT OF THE PHASE OF THE ORDER PARAMETER). THESE EQUATIONS SHOW THAT CONDENSATE FLOWS ARE INHERENTLY IRROTATIONAL AND FRICTIONLESS. A SYSTEM WITH THESE PROPERTIES IS CALLED A SUPERFLUID.

1.6 Vortices

1.6.1 Quantization of the circulation

Laser light that is blue detuned from an atomic resonance will not be absorbed (since it is off resonance), but it will still repel the atoms from regions of high laser intensity due to the optical stark effect. Red detuned laser light in a similar manner attracts atoms to regions of high light intensity. These detuned light sources are therefore routinely used to engineer potentials for the atomic condensates. In particular, if we shine a blue laser beam right through the center of a condensate, the atoms will be pushed away from the laser beam and the condensate will become toroidal in shape, as in figure 1.18.

To find the possible patterns of flow in such a toroidal condensate, we calculate the circulation κ defined by a line integral of the velocity along a
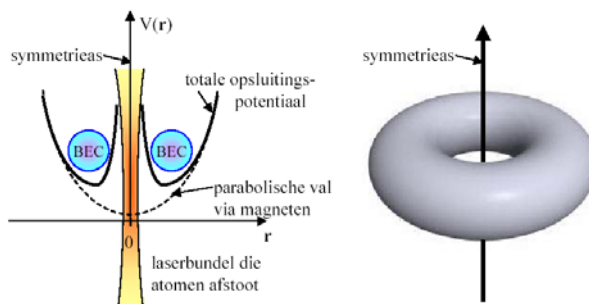
Figure 1.18: With a blue detuned laser beam and a harmonic potential from the magnetic trap, a toroidal condensate can be prepared.

closed contour C:

$$\kappa = \oint_C \mathbf{v} \cdot d\mathbf{x}. \tag{1.122}$$

We take the contour to be completely in the condensate and to go around the torus, circling the axis of symmetry. Since the velocity can be written as the gradient of the phase, we find

$$\kappa = \frac{\hbar}{m} \oint_C \boldsymbol{\nabla} S \cdot d\mathbf{x}. \tag{1.123}$$

It is tempting to use Stokes' theorem and relate the line integral to a surface integral over a surface bounded by the contour. In general we must distinguish two cases:

1. the surface A bounded by the contour lies completely in the condensate $\Rightarrow$ Stokes' theorem holds

2. a piece of the surface lies outside the condensate, i.e. there are holes in the condensate and the contour circles one of these holes

In the first case, the phase is well defined everywhere on the surface A and Stokes' theorem can be applied:

$$\kappa = \frac{\hbar}{m} \int_A \left(\boldsymbol{\nabla} \times (\boldsymbol{\nabla} S) \right) \cdot \mathbf{n} \; d^2 r. \tag{1.124}$$

But the curl of a gradient is always zero! We have already noted the irrotational nature of superfluid flow in the previous section. Here we see that it is equivalent with stating that the circulation in the condensate is zero $\kappa = 0$. In the second case however, we cannot apply Stokes' theorem since there in part of the surface over which we want to integrate the integrand is ill-defined. This is be the case is we take a contour in the toroidal condensate circling the hole of the torus – along such a contour the circulation can be different from zero.

However, we can still calculate the circulation exactly, using the fact that the order parameter should be single-valued. This means that if we go round the contour and we end up back where we started, the phase of the order parameter
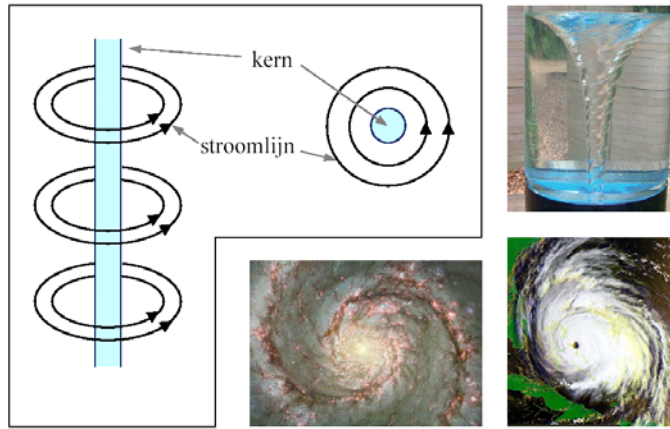
Figure 1.19: Some examples of classical vortices

can only have changed an integer times 2π. The line integral (1.123) adds up all the changes in the phase along the contour, so it is equal to the phase after 1 loop around the contour minus the phase we started with – and we just stated that this difference should be an integer times 2π. Hence we have

$$\kappa = \frac{\hbar}{m}(n \times 2\pi) = n\frac{h}{m},\qquad(1.125)$$

with $n \in \mathbb{Z}$. This means that h/m can be interpreted as a '**quantum of circulation**' (equal to 9.98×10^{-8} m^2/s). The quantization of circulation –sometimes called **Onsager-Feynman quantization**– means that not just any velocity is possible as the condensate flows around the torus, but only discrete velocities are allowed. This is truly quantum behavior, expressed on a macroscopic scale.

The presence of non-zero circulation in the condensate has important implications for the topology of the condensate. Suppose that we find that a condensate contains circulation, i.e. that $\kappa \neq 0$ along some loop C. This means that there should be a 'hole' in the condensate. In fact, there should be a hole in any surface A bound by the loop C. No matter how we distort the surface bound by the loop, going for example from A to A', the hole should be there. The simplest way to achieve this is to let the condensate density go to zero along some line. Then, any loop around the line may have non-zero circulation.

The line along which the density is zero could be created by an external potential, for example the blue-detuned laser beam described above, giving rise to the toroidal condensate of figure 1.18. But the line of zero density can also appear spontaneously in the condensate, in which case the resulting flow pattern is called a **vortex** (the line itself is referred to as the **vortex line**). We know that the condensate takes a little distance ξ to heal from zero back to its bulk value, so in fact the line is a tubular region going through the condensate, where the condensate density is suppressed, reaching zero at the center of the tube. The tube is called the **vortex core**. This should not be completely unfamiliar from the world of classical fluids as is shown in figure 1.19. Whirling around

a fluid can create a vortex, as can be seen in water draining from a sink, or in hurricanes with the eye of the hurricane as the vortex core. The difference between classical and quantum vortices is that the circulation of the latter is quantized.

Let's investigate the superfluid flow pattern around a straight vortex line. We can place the vortex line along the z-axis, and choose for our loops C a circle with radius r. Cylindrical symmetry tells us that the velocity field can only depend on r and our experience with tornado's tells us that the velocity will be parallel to the circle, so $\mathbf{v}(\mathbf{r}) = v(r)\mathbf{e}_\theta$ where $\{r, \theta, z\}$ are cylindrical coordinates. With this we can easily calculate the circulation, and the velocity:

$$
\begin{aligned}
\kappa &= \oint_C \mathbf{v} \cdot d\mathbf{x} \\
&\Leftrightarrow \quad \kappa = \int_0^{2\pi} rv(r)d\theta \\
&\Leftrightarrow \quad v(r) = \frac{\kappa}{2\pi r} = \frac{\hbar}{mr}.
\end{aligned}
\tag{1.126}
$$

Solid body rotation has a velocity field $v(r) = r\Omega\mathbf{e}_\theta$ where Ω is the angular velocity. Take a long stick, hold from one end, and point horizontal. Then whirl around your vertical axis until you get dizzy. The outer end of the stick goes faster than the inner end, following the solid body rotation law. *A quantum fluid does something very different*: $v(r) = (\kappa/(2\pi r))\mathbf{e}_\theta$. The velocity increases as you go closer to the vortex line – just like the wind gets more strong as you go towards the center of the hurricane. In the middle, in the eye of the hurricane, there is no wind – that is the vortex core. The edge of the core is where the wind speed is strong enough to tear the clouds apart. For our quantum hurricanes, if we take ξ to be the typical size of the core, the velocity there is $\hbar/(m\xi)$, compareable to the sound velocity from the previous section. This is no coincidence: as we shall see, this sound velocity is also the critical velocity above which the superfluid flow breaks down and becomes normal flow again.

1.6.2 Vortices

Vortices appear when a condensate is rotated, because rotation induces circulation, and there can be no circulation without a vortex line. One way to rotate the condensate is by using an anisotropic confinement potential, and rotating this confinement potential. This is similar to rotating a bucket of water, except that the bucket cannot be symmetrical in the case of condensates: condensates have no viscosity and would not be dragged along. So you need an anisotropic bucket, and a wall to push the condensate around. Below a critical rotation frequency however, the condensate is seen not to turn around, only some shape oscillations may appear. But when the critical rotation frequency is reached, a hole is seen to come into the order parameter, swiftly moving in from the edge of the cloud and settling in the middle. The appearance of the hole can be seen in figure 1.20. The density of the condensate shown in this figure was measured by the Dalibard group at the ENS in Paris, and the phase of the condensate shown in the bottom row was measured by the Cornell and Wieman group at JILA in Boulder, Colorado. As you move around the vortex core, the phase of the condensate changes by 2π, so we have 1 quantum of circulation.
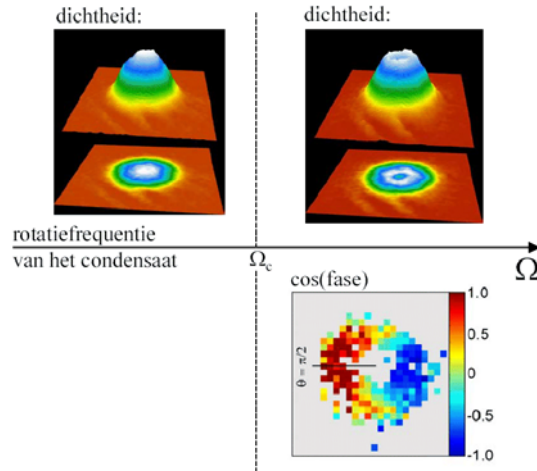
Figure 1.20: The density of the condensate (top row with red=low, wit=high) and the phase of the condensate (bottom row), are shown both above (right column) and below (left column) the critical rotation frequency for vortex nucleation.

The density can be measured by shining light onto the condensate and taking a shadow image with a CCD camera, but the phase is harder to measure. One way to map the phase is by making an interferogram. When two condensates overlap, regions where the complex order parameters are in phase will constructively interfere and obtain a higher density. In regions where the interference is destructive, the density is suppressed. This was how phase coherence was shown for a regular condensate, cf. figure 1.9. However, the phase of a condensate with a vortex is obviously different from the phase of a condensate without vortex! This is due to the defining property of a vortex that in a loop around a (singly quantized) vortex line the phase should increase by 2π. The number of 2π increases along a single loop (the "**winding number**") is equal to the number of circulation quanta within the loop. Because the specific phase field of a vortex condensate being is from that of a condensate without a vortex, the interference pattern will also be different. Our Antwerpen lab has shown that the presence of an edge dislocation in the pattern of parallel fringes is a fingerprint of vorticity, and that can be used to detect the number of vortices and their quantization level in the condensate. This method has been subsequently used by the Paris team of Dalibard and co-workers, and by the MIT team of Ketterle, and is also used in so-called polariton condensates.

The onset of circulation above a critical rotation frequency leads to a jump in the angular momentum of the cloud. If we look at a small volume of condensate at position $\mathbf{r}$, the angular momentum at that spot is

$$L_z(r) = m\mathbf{v}(\mathbf{r}) \times \mathbf{r} = mv(r).r = m\frac{\kappa}{2\pi r}r = n\hbar,$$

where we used cylindrical coordinates again, $\mathbf{r} = r\mathbf{e}_r$ and $\mathbf{v}(\mathbf{r}) = v(r)\mathbf{e}_\theta$, and we look at a singly quantized vortex $\kappa = h/m$. The angular momentum can be measured by looking at the quadrupole mode, a mode of oscillation with $\ell = 2$
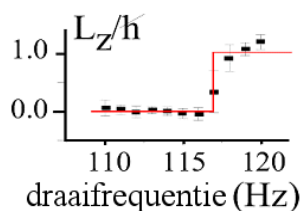
Figure 1.21: Jump in the angular momentum per particle at the critical rotation frequency (117 Hz) where the condensate also transits from zero vortices to one vortex.

and $m = \pm 2$, visible in figure 1.15. Without circulation, the $+2$ and -2 modes are degenerate, but when circulation occurs, the shape oscillation in one sense of rotation is different from that in the other sense of rotation, and the degeneracy is lifted. The difference in oscillation frequencies can be measured by imaging the dynamics of the cloud, and related to the angular momentum by a formula derived by Stringari and co-workers at the BEC center in Trento, Italy:

$$\Delta\nu = 2L_z/(MR^2).$$

Here M is the total mass of the condensate and R is its size. Using this formula, the Paris team was able to detect experimentally the jump in the angular momentum at the critical rotation frequency, as seen in figure 1.21.

1.6.3　Gross-Pitaevskii in a rotating frame

Now let's turn to the theoretical description of the vortex. This will be a nice textbook exercise on using Gross-Pitaevskii theory, so we'll go into detail. The Gross-Pitaevskii energy functional

$$\tilde{E}\left[\Psi\right] = \int d\mathbf{r}\ \left\{\Psi^*(\mathbf{r})\left[-\frac{\hbar^2\nabla^2}{2m} + V_1(\mathbf{r}) - \mu\right]\Psi(\mathbf{r}) + \frac{1}{2}g\left|\Psi(\mathbf{r})\right|^4\right\} \qquad (1.127)$$

is minimized for the ground state, and obviously a vortex condensate is not the ground state in a stationary trapping potential. I write a tilde on $\tilde{E}$ to emphasize that we minimize $E - \mu N$, using the method of Lagrange multipliers to ensure the normalization constraint, and forcing us to find μ from $\int |\Psi(\mathbf{r})|^2\, d\mathbf{r} = N$. That should be clear if you have understood the section where we derive the GP equation, but it is not bad to keep it in mind.

But we know from experiment that it is the ground state in a *rotating* trap. We could simply write out $V_1(\mathbf{r}, t)$, the time-dependent trapping potential, but that would only make matters more complicated to solve: indeed how do we deal with the resulting energy functional? It's better to transform the time-dependence away by going to a *rotating frame of reference*. From your classical mechanics, you know that in a rotating frame of reference, you should not mimize $\tilde{E}\left[\Psi\right]$ but

$$\tilde{E}\left[\Psi\right] - \mathbf{L}\left[\Psi\right]\cdot\mathbf{\Omega} \qquad (1.128)$$

where $\mathbf{L}\left[\Psi\right]$ is the angular momentum and $\mathbf{\Omega}$ is a vector with length equal to Ω, the rotation frequency, and pointing along the axis of rotation. Placing our

vortex line along the z-axis, we find that the functional to be minimized is

$$\tilde{E}\left[\Psi\right] - \Omega L_z\left[\Psi\right] \tag{1.129}$$

Remember from your quantum mechanics course the position representation of the z-component of the angular momentum: $\hat{L}_z = -i\hbar\partial/\partial\theta$. Here θ is the angle of the cilyndrical coordinates $\{r, \theta, z\}$. So, we obtain

$$L_z\left[\Psi\right] = \int d\mathbf{r}\ \Psi^*(\mathbf{r})\left(-i\hbar\frac{\partial}{\partial\theta}\right)\Psi(\mathbf{r}) \tag{1.130}$$

and from this

$$\tilde{E}\left[\Psi\right] = \int d\mathbf{r}\ \left\{\Psi^*(\mathbf{r})\left[-\frac{\hbar^2\nabla^2}{2m} + V_1(\mathbf{r}) - i\hbar\Omega\frac{\partial}{\partial\theta} - \mu\right]\Psi(\mathbf{r}) + \frac{1}{2}g\left|\Psi(\mathbf{r})\right|^4\right\}. \tag{1.131}$$

The different terms allow to write this expression also as

$$\tilde{E}\left[\Psi\right] = (E_{kin} + E_{trap} + E_{int}) - \Omega L_z[\Psi] - \mu N[\Psi] \tag{1.132}$$

where $N[\Psi] = \int|\Psi(\mathbf{r})|^2\, d\mathbf{r}$ and

$$E_{kin} = \int \Psi^*(\mathbf{r})\left(-\frac{\hbar^2\nabla^2}{2m}\right)\Psi(\mathbf{r})d\mathbf{r}, \tag{1.133}$$

$$E_{trap} = \int V_1(\mathbf{r})\left|\Psi(\mathbf{r})\right|^2 d\mathbf{r}, \tag{1.134}$$

$$E_{int} = \frac{1}{2}g\int|\Psi(\mathbf{r})|^4\, d\mathbf{r}, \tag{1.135}$$

are the kinetic energy, the potential energy from the trap, and the interaction energy, respectively.

How would the order parameter for a vortex look like? The density will be a function of the distance r to the vortex line. And, certainly, far away from the vortex line the density should go back to n, whereas on the vortex line the density should go to zero. So we set $|\Psi_v(\mathbf{r})| = f(r)\sqrt{n}$ with $f(r)$ going from zero to one over a 'healing distance' of the order of ξ. How about the phase? We know that as we loop around the z axis, it should increase by 2π. What also does that? The polar angle of the cylindrical coordinates! If we want to have ℓ quanta of circulation, just multiply θ by ℓ. The phase $S(\mathbf{r})$ is just equal to $S(\mathbf{r}) = \ell\theta$. Hence, the order parameter for a condensate with a vortex along the z-axis should look like this:

$$\Psi_{\text{vortex}}(\mathbf{r}) = \sqrt{n}f(r)e^{i\ell\theta} \tag{1.136}$$

It's not too hard to plug this into expression (1.131). The potential energy from a cylindrically symmetric trap and the interaction energy are given by

$$E_{kin} = n2\pi H\int_0^\infty V_1(r)f^2(r)rdr, \tag{1.137}$$

$$E_{trap} = n2\pi H\int_0^\infty f^4(r)rdr, \tag{1.138}$$

Since the vortex line lies along the z-axis, the system is translationally invariant in the z-direction, and the z-integral evaluates to H, the height of the system. Rather than dragging along this H in all the formula's, we will work with the energy per unit height, and set $H = 1$. Moreover, these energies do not depend on the phase any more so the θ integral just gives 2π. The kinetic energy,

$$E_{kin} = Hn \int\limits_0^{2\pi} d\theta \int\limits_0^\infty dr \; r \left\{ f(r)e^{-i\ell\theta} \left(-\frac{\hbar^2}{2m} \right) \nabla^2 \left[f(r)e^{-i\ell\theta} \right] \right\}, \qquad (1.139)$$

still depends on the phase. The Laplacian evaluates to

$$\begin{aligned}
\nabla^2 \left[\sqrt{n} f(r)e^{i\theta} \right] &= \frac{1}{r} \frac{\partial}{\partial r} \left(r \frac{\partial f}{\partial r} \right) \sqrt{n} e^{i\theta} + \sqrt{n} f(r) \frac{1}{r^2} \frac{\partial^2 \left(e^{i\ell\theta} \right)}{\partial \theta^2} \\
&= \sqrt{n} e^{i\theta} \left[\frac{1}{r} \frac{\partial}{\partial r} \left(r \frac{\partial f}{\partial r} \right) - \frac{\ell^2}{r^2} f(r) \right], \qquad (1.140)
\end{aligned}$$

from which we see that the kinetic energy splits up in a quantum pressure part and a part related to gradients of the phase:

$$E_{kin} = E_{qp} + E_{sf} \qquad (1.141)$$

with for the quantum pressure

$$E_{qp} = -\frac{\hbar^2}{2m} 2\pi n \int\limits_0^\infty \frac{\partial}{\partial r} \left(r \frac{\partial f}{\partial r} \right) dr = -\frac{2\pi\hbar^2}{2m} n \; r \frac{\partial f}{\partial r} \bigg|_0^\infty, \qquad (1.142)$$

and for **the kinetic energy of the superflow**:

$$E_{sf} = \frac{\hbar^2}{2m} 2\pi n \int\limits_0^\infty \frac{\ell^2}{r} f(r) dr \qquad (1.143)$$

Why do we call this the kinetic energy associated with the superflow ? Because if we substitue $\rho(\mathbf{r}) = mn f^2(r)$ and $\mathbf{v}(\mathbf{r}) = \hbar/(mr)$ in

$$E_{sf} = \int \frac{1}{2} \rho(\mathbf{r}) \mathbf{v}^2(\mathbf{r}) d\mathbf{r} \qquad (1.144)$$

we get precisely (1.143). So, this corresponds to the kinetic energy of a fluid of mass density $\rho(\mathbf{r})$ flowing with velocity field $\mathbf{v}(\mathbf{r})$.

Finally, let's evaluate $L_z[\Psi_{\text{vortex}}]$:

$$\begin{aligned}
L_z \left[\Psi_{\text{vortex}} \right] &= n \int d\mathbf{r} \; f(r) e^{-i\ell\theta} \left(-i\hbar \frac{\partial}{\partial \theta} \right) f(r) e^{i\ell\theta} \\
&= (-i\hbar)(i\ell) \int d\mathbf{r} \; n f^2(r) \qquad (1.145)
\end{aligned}$$

The derivative just brings a factor $i\ell$ down, that we have put in front of the integral. The integration is $N[\Psi] = \int |\Psi(\mathbf{r})|^2 \, d\mathbf{r}$, so that

$$L_z \left[\Psi_{\text{vortex}} \right] = \hbar\ell \times N[\Psi_{\text{vortex}}] \qquad (1.146)$$

This says that in a (cylindrically symmetric) condensate that contains a vortex with ℓ quanta of circulation (along the axis of symmetry), the angular momentum per particle equals $\hbar\ell$. Hence, if a singly quantized vortex appears, the angular momentum per particle will jump up by $\hbar$, as seen in the experiment and in figure **??**. Another way to see that we have the right expression for the angular momentum is to compute the hydrodynamic equivalent expression:

$$L_z = \int [\mathbf{r} \times \rho(\mathbf{r})\mathbf{v}(\mathbf{r})]\, d\mathbf{r}, \qquad (1.147)$$

i.e. the integrand is the local angular momentum $\mathbf{r} \times m\mathbf{v}$ of a volume elements. Again, if we plug in $\rho(\mathbf{r}) = mnf^2(r)$ and $\mathbf{v}(\mathbf{r}) = \hbar/(mr)$, we obtain the correct result. This shows that we can indeed use the hydrodynamic interpretation effectively, and see the condensate as a fluid with mass density $m\rho(\mathbf{r})$ and superfluid velocity field $\mathbf{v}(\mathbf{r})$.

1.6.4 Critical rotation frequency in a big bucket

Now it's time to specify the trapping potential. We could use a harmonic trap, but in stead I will keep a hard-wall bucket:

$$V_1(\mathbf{r}) = \begin{cases} 0 \text{ for } r < R \\ \infty \text{ for } r > R \end{cases}, \qquad (1.148)$$

so no condensate can live outside $r > R$. We know that also near this wall, the condensate will heal to its bulk value over a distance ξ, but we'll keep $\xi \ll R$, i.e. we use a large bucket and don't care what happens at the wall. That is, we'll assume we are in the Thomas-Fermi regime! Indeed

$$(R/\xi)^2 = 8\pi n a_s R^2 \propto \frac{N a_s}{H} \qquad (1.149)$$

So, provided our scattering length is still smaller than the height of the cylinder, $(R/\xi)^2$ is a good proxy for the Thomas-Fermi parameter. Choosing a large bucket helps a lot! The TF approximation does the following for us:

- Since $V_1 = 0$ inside the bucket, $E_{trap} = 0$.

- The total number of particles won't be affected much by drilling the hole for the vortex core. So, also the chemical won't be affected and we can use the bulk result $\mu = gn$.

- In the TF regime the quantum pressure energy can be safely neglected $E_{qp} \approx 0$.

- This in turn means that is it not important how (i.e. with which slope) $f(r)$ grows from 0 to 1, it is only important to know that it does so over a distance ξ. Hence, we can choose $f(r)$ such that it punches a hole of size ξ, i.e. we set $f(r) = 0$ for $r < \xi$. Since there is no condensate outside the bucket, we also have $f(r) = 0$ for $r > R$. In between, we set $f(r) = 1$. So, in summary, for a cylindrical bucket large compared to ξ, we have

$$\Psi_{\text{vortex}}(r, \theta) = \begin{cases} \sqrt{n}e^{i\ell\theta} \text{ for } \xi < r < R \\ 0 \text{ elsewhere} \end{cases}, \qquad (1.150)$$

With these simplifications, we can calculate the energy of the vortex condensate:

$$\tilde{E}\left[\Psi_{\text{vortex}}\right] \underset{\xi/R \ll 1}{=} E_{sf} + E_{int} - \Omega L_z - \mu N \tag{1.151}$$

with E_{sf} given by expression (1.143), for the vortex

$$E_{sf,\,\text{vortex}} = \frac{\hbar^2}{2m} 2\pi n \int_{\xi}^{R} \frac{\ell^2}{r}\, dr = \pi n \frac{\hbar^2}{m}\ell^2 \log(R/\xi) \tag{1.152}$$

Similarly, we get for the interaction energy

$$E_{int,\,\text{vortex}} = \frac{gn^2}{2} \times 2\pi \left(R^2 - \xi^2\right) \underset{\xi/R \ll 1}{\approx} \frac{gn^2}{2} 2\pi R^2 \tag{1.153}$$

where we neglect ξ^2 with respect to R^2. Note that $N = 2\pi R^2 n$ (remember we set $H = 1$, and $2\pi R^2 H$ is the volume). So, using $\mu = gn$ we can write

$$E_{int,\,\text{vortex}} \underset{\xi/R \ll 1}{\approx} \frac{1}{2}\mu N \tag{1.154}$$

Finally, for the angular momentum we get

$$L_{z,\,\text{vortex}} = \hbar\ell \times 2\pi n \left(R^2 - \xi^2\right) \underset{\xi/R \ll 1}{\approx} \hbar\ell \times 2\pi n R^2 \tag{1.155}$$

Adding up all these terms gives us

$$\tilde{E}\left[\Psi_{\text{vortex}}\right] \underset{\xi/R \ll 1}{=} \pi n \frac{\hbar^2}{m}\ell^2 \log(R/\xi) - \Omega\hbar\ell\, 2\pi n R^2 - \frac{1}{2}\mu N \tag{1.156}$$

The last term, $-\mu N/2$, is the result we'd get for a condensate without a vortex. So, the difference in energy between a condensate with and without a vortex is

$$\begin{aligned} \Delta E \quad &= \quad \tilde{E}\left[\Psi_{\text{vortex}}\right] - \tilde{E}\left[\Psi_{\text{no vortex}}\right] \\ &\underset{\xi/R \ll 1}{=} \quad \pi n \frac{\hbar^2}{m}\ell^2 \log(R/\xi) - \Omega\hbar\ell\, 2\pi n R^2 \end{aligned} \tag{1.157}$$

If this is positive, it costs energy to have a vortex, and the condensate will prefer to remain without vorticity. If ΔE becomes negative, it is energetically advantageous to bring in a vortex. Increasing the rotation frequency Ω tilts the balance in favour of vortices. The rotation frequency at which ΔE becomes negative is the critical rotation frequency

$$\Omega_c = \ell \frac{\hbar}{2m} \frac{\log(R/\xi)}{R^2} \tag{1.158}$$

If you plug in the size of the cloud for R, and set $\ell = 1$ to obtain the critical rotation frequency.
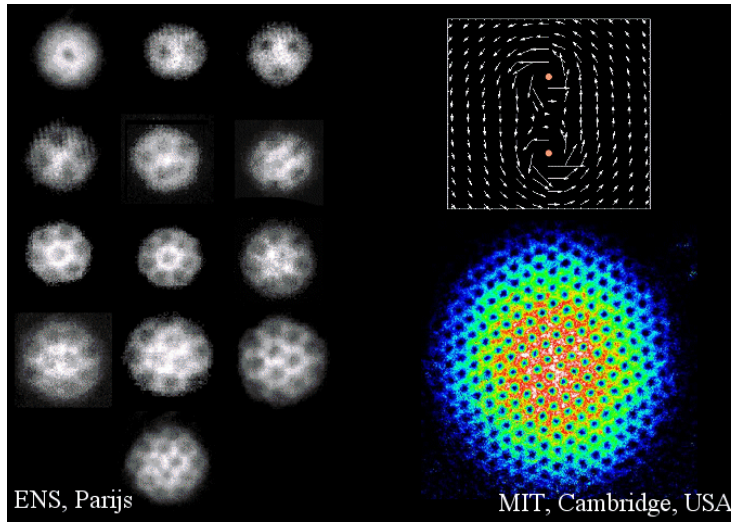
Figure 1.22: When the condensate is stirred faster and faster, a second, third, fourth,... vortex appear, each carrying one quantum of circulation. The vortices repel eachother and form the "Abrikosov lattice".

1.6.5 Abrikosov lattice

How about stirring the condensate faster? Will you obtain an $\ell = 2$ vortex? No! The kinetic energy of the superflow grows with ℓ^2, so it is energetically favourable to have two singly quantized vortices in stead of one doubly quantized vortex. Indeed, $2E_{sf,\,\ell=1} < E_{sf,\,\ell=2}$ because $2 \times 1^2 < 2^2$. For the angular momentum in a homogeneous condensate, it doesn't matter whether $\ell = 1$ or $\ell = 2$. So what happens as you stir faster? The experimental result is shown in figure 1.22: more and more singly quantized vortices appear. The better student may be worried that our formalism will find that the critical rotation frequency for 2 vortices is equal to that of 1 vortex if we use $2E_{sf,\,\ell=1}$ for the kinetic energy of the superflow. And he would be correct. Actually, the kinetic energy of the superflow in the case of two vortices depends on the distance between these vortices: when the two vortices are on top of eachother, the situation is indistinguishable from a doubly quantized vortex and the kinetic energy of the superflow is $E_{sf,\,\ell=2}$. So, the kinetic energy of superflow grows from $2E_{sf,\,\ell=1}$ for vortices far away from eachother to $E_{sf,\,\ell=2}$ when they are close. Vortices repel eachother! This repulsion between the vortices result in an increase in the critical rotation frequency as the number of vortices becomes bigger.

You can intuitively understand this repulsion from the fact that if you have two nearby vortices, their individual velocity fields in the region between the vortices are opposite in sign, as shown in the upper left hand corner of figure 1.22. So, they subtract from each other and in between vortices the superfluid velocity field is supressed. To lower the energy, it is advantageous to make the region between the vortices as large as possible: hence the vortex lines are pushed apart. What happens if we switch the sense of rotation of the superflow around on of the vortices? Then we get an **antivortex**,with $\ell = -1$. In the

region between the vortex and the antivortex, their velocities add up leading to a higher kinetic energy. Now it is energetically favourable to bring the vortex and the antivortex close to eachother. Vortices and antivortices in condensates attract eachother, and annihilate (when they are exactly on top of eachother, the resulting velocity field is zero everywhere).

The repulsion between vortices also means that the vortices want to sit as far away from eachother as possible, and hence they will organise themselves in a lattice, called the **Abrikosov lattice**. When we rotate the condensate fast enough to have a dense Abrikosov lattice, the system will start to act more and more like a solid body. Let's take the axis of rotation to be the z-axis as usual, and have all vortex lines parallel to $\mathbf{e}_z$. Then we compute the circulation for a contour running along the edge of the condensate: we choose a circle with radius R (where R is the radius of the condensate), placed in the xy-plane (perpendicular to the vortex lines). For the superfluid we know that the total circulation along this contour equals

$$\text{superfluid:} \quad \oint_C \mathbf{v} \cdot d\mathbf{x} = N_v \kappa, \tag{1.159}$$

if there are N_v vortices, each carrying a single quantum of circulation $\kappa = h/m$, piercing the disk bounded by our circular contour. For solid body rotation at angular frequency Ω, we know that the velocity at a distance R from the center equals $R\Omega$, so the total circulation is

$$\text{solid body:} \quad \oint_C \mathbf{v} \cdot d\mathbf{x} = 2\pi R \times R\Omega. \tag{1.160}$$

That's what you have when you spin a solid disk like a CD. For our superfluid to mimic solid-body rotation, the surface density of vortices should be

$$\frac{N_v}{\pi R^2} = \frac{2\Omega}{\kappa} \tag{1.161}$$

Rotating faster and faster (increasing Ω) will generate more and more vortices (increasing N_v), and when the above condition is met, the system acts like a regular piece of material rather than as a superfluid.

Remark – Running ahead to the third part, we can say that this is very similar to type II superconductors, where the role of rotation frequency is played by the magnetic field. Think of the superconductor as a charged superfluid – in a magnetic field charges want to run around in cyclotron orbits. At first, there is no running around, but as you increase the magnetic field above the "first critical field", a first vortex enters the superconductor. Increasing the field further brings in more and more vortices, until at the "second critical field" superconductivity breaks down and the system acts like a normal piece of material again. Remark within the remark: vortices in superconductors correspond to charged superflow around a vortex line – but now this current loop generates it own magnetic field! There is magnetic flux going through the vortex core, following the vortex line. This is different from the case of uncharged superflow, and one way the difference is manifested is that there is a "magnetic energy" term that complicates the interaction between the vortices.

1.6.6   Hess-Fairbank effect and field cooling

In the preceding discussion, we always assume that we start from a condensate which we set in motion by beginning to stir it. The "rotation field" is added after we have cooled the gas down to form a condensate. But what happens if we switch the two manipulations. What if we start with a rotating, warm gas, and then cool down below T_c? This protocol is called "**field cooling**": you cool down while the rotation field (or magnetic field, for a superconductor) is already in place.

Above T_c, we can have any angular momentum in the gas – any wind speed is possible in a hurricane. But once we hit T_c and form a condensate, only quantized values of L_z are allowed: $N\hbar$, $2N\hbar$, $3N\hbar$, ... where N is the number of atoms, cf. figure 1.21. What happens is that as we reach T_c, the unquantized angular momentum of the normal gas will snap to the nearest quantum level for L_z. Consider the hot gas rotating at an angular velocity Ω just below Ω_c, with wind speeds in the gas below $v(r) < \hbar/(mr)$. As the gas cools down to form a condensate the system will suddenly speed up right at T_c and reach one full quantum of angular momentum, and form a vortex condensate! This wonderful effect was named after **Hess and Fairbank**[15] who proposed it for the case of liquid helium.

How about cooling down a gas that is spinning at $\Omega > \Omega_c$ and has too much angular momentum? Indeed, that will slow down to the nearest quantized velocity field as it forms a condensate. Field cooling reveals quantum weirdness at the macroscopic scale. And how about conservation of angular momentum? This will have to be absorbed by the rotating bucket – the trap and the non-condensed atoms that are still present near T_c. This brings us seamlessly to the next section where we investigate what happens at non-zero temperatures when not all the atoms are in the condensate.

SUMMARY: THE VELOCITY FIELD OF A CONDENSATE IS PROPORTIONAL TO THE GRADIENT OF THE PHASE OF THE ORDER PARAMETER, AND THIS IMPLIES THAT THE VELOCITY FIELD IRROTATIONAL AND THAT CIRCULATION IS QUANTIZED. CIRCULATION CAN ONLY APPEAR IN THE CONDENSATE IN THE FORM OF VORTICES: LINES WHERE THE CONDENSATE DENSITY IS ZERO AND AROUND WHICH THE PHASE OF THE ORDER PARAMETER CHANGES BY AN NONZERO INTEGER TIMES 2π. VORTICES CARRY QUANTA OF CIRCULATION, AND APPEAR AS YOU ROTATE THE CONDENSATE ABOVE A CRITICAL ROTATION FREQUENCY.

1.7   Condensates at non-zero temperatures

1.7.1   Thermal cloud versus condensate

The Gross-Pitaevskii equation describes a pure Bose-Einstein condensate. There are no thermal atoms in the description. This situation is only realized at temperature zero. In this section we are going to extend the Gross-Pitaevskii equation to the case of non-zero temperature, following Bogoliubov's approach.

---

[15] G.W. Hess and W.M. Fairbank, Physical Review Letters **19**, 216 (1967).

The central idea that we have already encountered in our discussion of the Penrose-Onsager criterion is that, in the Hamiltonian of the interacting Bose gas,

$$
\begin{aligned}
\hat{H} &= \int d\mathbf{r}\ \hat{\psi}^\dagger(\mathbf{r})\left[-\frac{\hbar^2\nabla^2}{2m} + V_1(\mathbf{r})\right]\hat{\psi}(\mathbf{r}) \\
&\quad + \frac{1}{2}\int d\mathbf{r}\int d\mathbf{r}'\ \hat{\psi}^\dagger(\mathbf{r})\hat{\psi}^\dagger(\mathbf{r}')V_2(\mathbf{r}-\mathbf{r}')\hat{\psi}(\mathbf{r}')\hat{\psi}(\mathbf{r}), \qquad (1.162)
\end{aligned}
$$

the operator for the boson field is shifted by a complex number $\Psi(\mathbf{r})$ equal to the order parameter,

$$
\hat{\psi}(\mathbf{r}) = \Psi(\mathbf{r}) + \hat{\phi}(\mathbf{r}). \qquad (1.163)
$$

When Bose-Einstein condensation is present, by definition $\rho_1(\mathbf{r}, \mathbf{r}') = \left\langle \hat{\psi}^\dagger(\mathbf{r}')\hat{\psi}(\mathbf{r})\right\rangle \approx \Psi^*(\mathbf{r})\Psi(\mathbf{r})$ so that the shifted operators $\hat{\phi}^\dagger(\mathbf{r})$ and $\hat{\phi}(\mathbf{r})$ must be in a sense "small". They are called fluctuation operators, indicating that they implement small fluctuations around the order parameter. This was the idea used to derive the GP equation, where we completely neglect $\hat{\phi}(\mathbf{r}) \to 0$ so that we can simply replace $\hat{\psi}(\mathbf{r}) \approx \Psi(\mathbf{r})$. At non-zero temperatures, we must keep $\hat{\phi}(\mathbf{r})$, and look for correction terms. Note that $\hat{\phi}(\mathbf{r})$ is a bosonic operator (it is just a shifted version of $\hat{\psi}(\mathbf{r})$).

Another way to look at this is to remember that the first order reduced density matrix always has a spectral decomposition,

$$
\rho_1(\mathbf{r}, \mathbf{r}') = \sum_{\ell=0}^\infty \lambda_\ell \varphi_\ell^*(\mathbf{r})\varphi_\ell(\mathbf{r}'). \qquad (1.164)
$$

The Penrose-Onsager criterion states that there is BEC if and only if one of the eigenvalues becomes macroscopically large (of order N), forcing the other eigenvalues to be small, since they have to sum to N). With $\Psi(\mathbf{r}) = \sqrt{\lambda_0}\varphi_0(\mathbf{r})$ the reduced density matrix can also be written as

$$
\rho_1(\mathbf{r}, \mathbf{r}') = \underbrace{\Psi^*(\mathbf{r})\Psi(\mathbf{r})}_{\text{condensate}} + \underbrace{\sum_{\ell=1}^\infty \lambda_\ell \varphi_\ell^*(\mathbf{r})\varphi_\ell(\mathbf{r}')}_{\text{fluctuations}} \qquad (1.165)
$$

The fluctuation part is generated by the fluctuation operators defined earlier, $\left\langle \hat{\phi}^\dagger(\mathbf{r}')\hat{\phi}(\mathbf{r})\right\rangle$. This contribution comes entirely from atoms that are not in the condensate. Again: at non-zero temperatures we need to take these fluctuations into account, at least perturbatively, as the thermal energy (and temperature[16]) is linked to excitations. Treating fluctuation with perturbation theory becomes more tenuous as $T \to T_c$, and one can only hope that the higher order terms will only become important very close to T_c.

---

[16] Indeed, you'll recall that the way temperature is measured in the experiments is by fitting to the outer part of the cloud, i.e. the thermal atoms that are not in the condensate.

The perturbation treatment is most easily done by substituting $\hat{\psi}(\mathbf{r}) = \Psi(\mathbf{r}) + \hat{\phi}(\mathbf{r})$ in the Hamiltonian. This substitution results in

$$
\begin{aligned}
\hat{H} - \mu\hat{N} \;=\; & \int d\mathbf{r} \; \left[\Psi^*(\mathbf{r}) + \hat{\phi}^\dagger(\mathbf{r})\right] \left[-\frac{\hbar^2\nabla^2}{2m} - \mu + V_1(\mathbf{r})\right] \\
& \times \left[\Psi(\mathbf{r}) + \hat{\phi}(\mathbf{r})\right] + \frac{4\pi\hbar^2 a}{m}\int d\mathbf{r} \; \left|\Psi(\mathbf{r}) + \hat{\phi}(\mathbf{r})\right|^4 \quad (1.166)
\end{aligned}
$$

Here we have again used the contact pseudopotential as the interatomic interaction. Now we expand this Hamiltonian up to second order in the fluctuation operator, that is, we drop all terms with three or four $\hat{\phi}$'s. If we only keep terms without any $\hat{\phi}$, we get the Gross-Pitaevskii energy functional $E_{GP}[\Psi]$. There are no terms with only one $\hat{\phi}$ operator to be kept, since terms with an odd number of atom creation and annihilation operators do not contibute to the energy: we assume that the system has a well-defined number of atoms. Finally, the terms with two $\hat{\phi}$'s yield the so-called **Gross-Pitaevskii-Bogoliubov** Hamiltonian (also called Bogoliubov-De Gennes Hamiltonian in the context of superconductivity):

$$
\begin{aligned}
\hat{H} - \mu\hat{N} \;=\; & E_{GP}[\Psi] - \mu N[\Psi] \\
& + \int d\mathbf{r} \; \hat{\phi}^\dagger(\mathbf{r})\left[-\frac{\hbar^2\nabla^2}{2m} - \mu + V_1(\mathbf{r}) + \frac{8\pi\hbar^2 a}{m}\left|\Psi(\mathbf{r})\right|^2\right]\hat{\phi}(\mathbf{r}) \\
& + \frac{2\pi\hbar^2 a}{m}\int d\mathbf{r} \; \left\{[\Psi^*(\mathbf{r})]^2\hat{\phi}(\mathbf{r})^2 + \Psi(\mathbf{r})^2[\hat{\phi}^\dagger(\mathbf{r})]^2\right\}. \quad (1.167)
\end{aligned}
$$

The second line is a conventional Hamiltonian for the thermal atoms. Taking the expectation value to obtain the energy, it is clear that the interaction term describes the interaction between between the

$$
N_c = \int d\mathbf{r} \left|\Psi(\mathbf{r})\right|^2
$$

condensate atoms and the

$$
N - N_c = \int d\mathbf{r} \left\langle \hat{\phi}^\dagger(\mathbf{r})\hat{\phi}(\mathbf{r})\right\rangle
$$

thermal atoms, in a mean-field type of description. There is no term describing the interactions between thermal atoms (such a term would have four fluctuation operators). This means that we work in a regime where the density of thermal atoms is still low compared to the density of the condensate. Note that there is a difference (of a factor 2) with the interaction term in the condensate:

$$
\text{condensate-condensate:} \qquad \frac{4\pi\hbar^2 a}{m}\left|\Psi(\mathbf{r})\right|^2\left|\Psi(\mathbf{r})\right|^2 \qquad (1.168)
$$

$$
\text{condensate-thermal atom:} \qquad 2\times\frac{4\pi\hbar^2 a}{m}\left|\Psi(\mathbf{r})\right|^2\left|\hat{\phi}(\mathbf{r})\right|^2 \qquad (1.169)
$$

Where does that factor 2 come from? This is an effect of the Bose symmetry. If two atoms scatter and they are in a different quantum state, we need to symmetrize the two-body wave function that describes the scattering process.

This leads to two terms: besides the direct (Hartree) term there is also an exchange (Fock) term:

$$
\begin{aligned}
E_{int} &= \int \varphi_a(\mathbf{r})\varphi_b(\mathbf{r}')V_2(\mathbf{r}-\mathbf{r}')\varphi_b(\mathbf{r}')\varphi_a(\mathbf{r}) \\
&+ \int \varphi_a(\mathbf{r})\varphi_b(\mathbf{r}')V_2(\mathbf{r}-\mathbf{r}')\varphi_a(\mathbf{r}')\varphi_b(\mathbf{r}).
\end{aligned}
\tag{1.170}
$$

For fermions we get the well-known minus sign. For bosons this becomes a plus sign, and moreover for a contact potential $V_2 \propto \delta(\mathbf{r}-\mathbf{r}')$ both terms are equal, and the total is effectively twice the Hartree contribution. For atoms in the same state, this symmetrization is not needed, and we do not have an exchange term, only the Hartree contribution. Hence, the interaction energy for two bosons in different states is twice as high as for two bosons in the same state. In general, the bosonic exchange contribution for repulsive interaction will increase the energy if bosons are in different states, so it will help to form a condensate and put the bosons in the same state. That is why a 'fractional state', with two large eigenvalues each $N/2$ (i.e. condensation in two different single-particle states with half the total number of particles) does not arise even if the single-particle ground state energies are degenerate: the exchange energy prohibits it.

The last line in the Gross-Pitaevskii Hamiltonian (1.167) doesn't look like a "normal" Hamiltonian at all: it contains the "anomalous" products of two creation operators (and two annihilation operators). Since we can make superpositions of states with different amounts of thermal atoms (even for a fixed total number of atoms), it may be possible that this term also contributes to the energy. The expectation values $\left\langle \hat{\phi}(\mathbf{r})^2 \right\rangle$ and $\left\langle \hat{\phi}^\dagger(\mathbf{r}) \right\rangle$ with respect to such a number-superposition wavefunction need not be zero. Indeed, what this term describes is the transformation of condensate atoms to thermal atoms and vice versa, i.e fluctuations of the number of condensate atoms[17].

1.7.2 Bogoliubov excitations

The Heisenberg equations of motion for the fluctuation operators are:

$$
i\hbar \frac{\partial \hat{\phi}(\mathbf{r})}{\partial t} = \left[\hat{\phi}(\mathbf{r}), \hat{H} - \mu\hat{N} \right],
\tag{1.171}
$$

$$
i\hbar \frac{\partial \hat{\phi}^\dagger(\mathbf{r})}{\partial t} = \left[\hat{\phi}^\dagger(\mathbf{r}), \hat{H} - \mu\hat{N} \right].
\tag{1.172}
$$

Using the bosonic commutation relations for the field operators we find

$$
\begin{aligned}
i\hbar \frac{\partial \hat{\phi}(\mathbf{r},t)}{\partial t} &= \left(-\frac{\hbar^2 \nabla^2}{2m} - \mu + V_1(\mathbf{r}) + \frac{4\pi\hbar^2 a}{m} 2n_c(\mathbf{r}) \right) \hat{\phi}(\mathbf{r},t) \\
&+ \frac{4\pi\hbar^2 a}{m} \Psi(\mathbf{r})^2 \hat{\phi}^\dagger(\mathbf{r},t),
\end{aligned}
\tag{1.173}
$$

---

[17] There is now an additional difficulty in setting the chemical potential μ: in principle, we want to have the total number of particle N fixed by μ, rather than the condensate number N_c as we did before. We'll ignore this complication here, but be aware that by doing this, we treat the termal atoms in a non-number conserving way.

and

$$i\hbar\frac{\partial\hat{\phi}^\dagger(\mathbf{r},t)}{\partial t} = \left(-\frac{\hbar^2\nabla^2}{2m} - \mu + V_1(\mathbf{r}) + \frac{4\pi\hbar^2 a}{m}2n_c(\mathbf{r})\right)\hat{\phi}^\dagger(\mathbf{r},t)$$
$$+\frac{4\pi\hbar^2 a}{m}\Psi^*(\mathbf{r})^2\hat{\phi}(\mathbf{r},t), \tag{1.174}$$

where we write $n_c(\mathbf{r}) = |\Psi(\mathbf{r})|^2$ for the condensate atom density. In the ground state we can choose $\Psi(\mathbf{r})$ to be a real function (as will be discussed in more detail in the chapter on superfluid helium), so we have $\Psi(\mathbf{r})^2 = n_c(\mathbf{r})$. Equations (1.173) and (1.174) form a set of coupled linear partial differential equations. The advantage of the series expansion up to second order in the fluctuation operator, performed in the previous paragraphs, that that a Hamiltonian that is quadratic in the field operators can always be diagonalized by an appropriate unitary transformation. To solve the set of equations, we will perform the following transformation on the Hamiltonian:

$$\hat{\phi}(\mathbf{r},t) = \sum_j\left(u_j(\mathbf{r})\hat{\alpha}_je^{-i\epsilon_jt} - v_j^*(\mathbf{r})\hat{\alpha}_j^\dagger e^{-i\epsilon_jt}\right), \tag{1.175}$$

$$\hat{\phi}^\dagger(\mathbf{r},t) = \sum_j\left(u_j^*(\mathbf{r})\hat{\alpha}_j^\dagger e^{i\epsilon_jt} - v_j(\mathbf{r})\hat{\alpha}_je^{i\epsilon_jt}\right). \tag{1.176}$$

This is some sort of 'fourier' expansion in the energies ϵ_j – nothing prohibits us from writing the fluctuation fields in such a form. The coefficients u_i and v_i are to be determined so that the transformed Hamiltonian is diagonal in the new operators $\hat{\alpha}_i$ and $\hat{\alpha}_i^\dagger$. That is, we substitute (1.175),(1.176) in the Hamiltonian, look at the terms with $(\hat{\alpha}_i)^2$ and $(\hat{\alpha}_i^\dagger)^2$ and then choose u_i and v_i so that these terms disappear. This is called the Bogoliubov(-Valatin-de Gennes) transformation. Demanding that the new operators $\hat{\alpha}_i$ and $\hat{\alpha}_i^\dagger$ satisfy commutation relations is related to requiring unitarity of the transformation and comes down to

$$\left[\hat{\alpha}_i,\hat{\alpha}_j^\dagger\right] = \delta_{ij}$$
$$\Leftrightarrow \int d\mathbf{r}\left[|u_i(\mathbf{r})|^2 - |v_i(\mathbf{r})|^2\right] = 1 \tag{1.177}$$

We'll always be able to find suitable values for u_i and v_i so that the coefficients of $(\hat{\alpha}_i)^2$ and $(\hat{\alpha}_i^\dagger)^2$ disappear (two variables for two requirements). In other words, the diagonalisation of the Hamiltonian will always work and we get

$$\hat{H}_{diag} = \sum_j\epsilon_j\hat{\alpha}_j^\dagger\hat{\alpha}_j + \text{constant}. \tag{1.178}$$

The coefficient of the $\hat{\alpha}_j^\dagger\hat{\alpha}_j$ term should be the energy ϵ_j that we had before, and this results in self-consistent equations to determine the set of energy levels ϵ_j. This diagonalized Hamiltonian tells us that the excitations of the system are bosonic, have energies ϵ_j and are created by the operators $\hat{\alpha}_j^\dagger$. The elementary excitations are not just thermal atoms, since $\hat{\alpha}_j^\dagger$ is not the same as $\hat{\phi}^\dagger(\mathbf{r})$. Indeed, at low temperatures there are other ways to excite the condensate than kicking

individual atoms out of the condensate and into higher excited trap levels. This "kicking out individual atoms" are the single-particle excitations that we talked about in the section on condensate dynamics. In that same section, we saw that the low-lying energy excitations were sound waves, phonons. These are collective excitations: the $\hat{\alpha}_j^\dagger$ envolve a sum over all the particles, distributing the energy over the collective.

OK, let's proceed and find the energies ϵ_j. Rather than substituting (1.175),(1.176) in the Hamiltonian, we'll substitute these formulae into the Heisenberg equations of motions for the fields. This gives a nice shortcut to finding $u_j(\mathbf{r})$,$v_j(\mathbf{r})$, and ϵ_j. We get

$$\begin{cases} \left(-\dfrac{\hbar^2 \nabla^2}{2m} + V_1(\mathbf{r}) + \dfrac{4\pi\hbar^2 a}{m} 2n_c(\mathbf{r}) - \mu - \epsilon_j \right) u_j(\mathbf{r}) = \dfrac{4\pi\hbar^2 a}{m} n_c(\mathbf{r}) v_j(\mathbf{r}), \\ \left(-\dfrac{\hbar^2 \nabla^2}{2m} + V_1(\mathbf{r}) + \dfrac{4\pi\hbar^2 a}{m} 2n_c(\mathbf{r}) - \mu + \epsilon_j \right) v_j(\mathbf{r}) = \dfrac{4\pi\hbar^2 a}{m} n_c(\mathbf{r}) u_j(\mathbf{r}). \end{cases}$$
(1.179)

These look like Schrödinger equations for a coupled two-component system. From this setting, the fact that eigenstates at different energies are orthonormal leads to

$$\int d\mathbf{r} \left[u_i(\mathbf{r}) u_j^*(\mathbf{r}) - v_i^*(\mathbf{r}) v_j(\mathbf{r}) \right] = \delta_{ij}.$$
(1.180)

The equations (BdGequations) are called the Bogoliubov(-de Gennes) equations. Dr. de Gennes' name is usually added when we look at this formalism in the context of superconductivity, i.e. for a charged Bose gas.

1.7.3 Excitation spectrum for the homogeneous Bose gas

Let's look at the homogeneous Bose gas: setting $V_1(\mathbf{r}) = 0$ simplifies the system as we now have translational invariance. This means that wave numbers are good quantum numbers, and that we can write the solutions of the Bogoliubov equations (1.179) as

$$u_j(\mathbf{r}) = u_q \frac{e^{i\mathbf{q}\cdot\mathbf{r}}}{\sqrt{V}} \text{ and } v_j(\mathbf{r}) = v_q \frac{e^{i\mathbf{q}\cdot\mathbf{r}}}{\sqrt{V}},$$
(1.181)

where V is the volume of the system. We already found (cf. expression (1.79)) that, for a uniform system with condensate density n_c, the order parameter satisfies the following Gross-Pitaevskii equation:

$$\frac{4\pi\hbar^2 a}{m} n_c \Psi(\mathbf{r}) = \mu \Psi(\mathbf{r}),$$
(1.182)

from which we obtained $\mu = 4\pi\hbar^2 a n_c/m$. In keeping this solution, we make an approximation: in fact we should use the chemical potential to fix the total number of particles, not only the condensate, as mentioned in footnote 17. In this (non-number-conserving) approximation, the Bogoliubov equations become

$$\begin{cases} \left(-\dfrac{\hbar^2 q^2}{2m} + \dfrac{4\pi\hbar^2 a}{m} n_c - \epsilon_q \right) u_q = \dfrac{4\pi\hbar^2 a}{m} n_c v_q, \\ \left(-\dfrac{\hbar^2 q^2}{2m} + \dfrac{4\pi\hbar^2 a}{m} n_c + \epsilon_q \right) v_q = \dfrac{4\pi\hbar^2 a}{m} n_c u_q. \end{cases}$$
(1.183)

This set of linear equations has a nontrivial solution if and only if the determinant of the coefficients is zero, so if

$$\left(-\frac{\hbar^2 q^2}{2m} + \frac{4\pi\hbar^2 a}{m}n_c - \epsilon_q\right)\left(-\frac{\hbar^2 q^2}{2m} + \frac{4\pi\hbar^2 a}{m}n_c + \epsilon_q\right) = \left(\frac{4\pi\hbar^2 a}{m}n_c\right)^2,$$
(1.184)

is satisfied. It is easy to solve this with respect to ϵ_q :

$$\epsilon_q = \sqrt{\epsilon_q^0\left(\epsilon_q^0 + 2\frac{4\pi\hbar^2 a}{m}n_c\right)}.$$
(1.185)

Here $\epsilon_q^0 = (\hbar q)^2/(2m)$ is the excitation spectrum of the non-interacting system, and ϵ_q is the excitation spectrum of the interacting (uniform) Bose gas. In the non-interacting system, all atoms condense in the $\mathbf{q} = 0$ state. The excitations then consist of bumping a single atom out of the $\mathbf{q} = 0$ condensate and into a higher $\mathbf{q}$ plane wave state, gaining energy ϵ_q^0. Interactions change this picture. Not only should we now recalculate the condensate wavefunction Ψ, but now the excitations are bosonic quasiparticles, created and annihilated by the Bogoliubov operators $\hat{\alpha}_{\mathbf{q}}^\dagger$, and with excitation energy ϵ_q different from the free-particle dispersion, and given by (1.185). We call ϵ_q the Bogoliubov spectrum.

In the last chapter we'll see that the Bogoliubov transformation also allows to find the excitation energy spectrum of a superconductor, and in that case the energy spectrum has a band gap Δ. However, for condensates of atomic Bose gases, the behavior of the Bogoliubov spectrum at small q is given by

$$\lim_{q\to 0} \epsilon_q = \sqrt{\frac{4\pi\hbar^2 a}{m^2}n_c} \times \hbar q.$$
(1.186)

These low-lying energy modes are sound waves: the energy grows linearly with the wave number. These are clearly collective modes, you cannot build a density wave in the condensate from a single atom. In stead, all the atoms need to shift small amounts away from their equilibrium density (like phonons in a lattice). We've already seen in figure () that a bump in density moves through the condensate with a constant sound velocity c. We can also extract this sound velocity from the dispersion relation: for sound waves we always have $\omega = cq$, so in our case we get

$$c = \sqrt{\frac{4\pi\hbar^2 a}{m^2}n_c}.$$
(1.187)

This is exactly the same result as what we had before.

The high-energy excitations correspond to large q, and are again free particles, with dispersion $(\hbar q)^2/(2m)$, since

$$\lim_{q\to\infty} \epsilon_q = \epsilon_q^0$$
(1.188)

The transition between "sound wave" type collective excitations and single-particle like excitations happens when

$$\frac{\hbar^2 q_c^2}{2m} \approx \frac{4\pi\hbar^2 a}{m}n_c$$
(1.189)
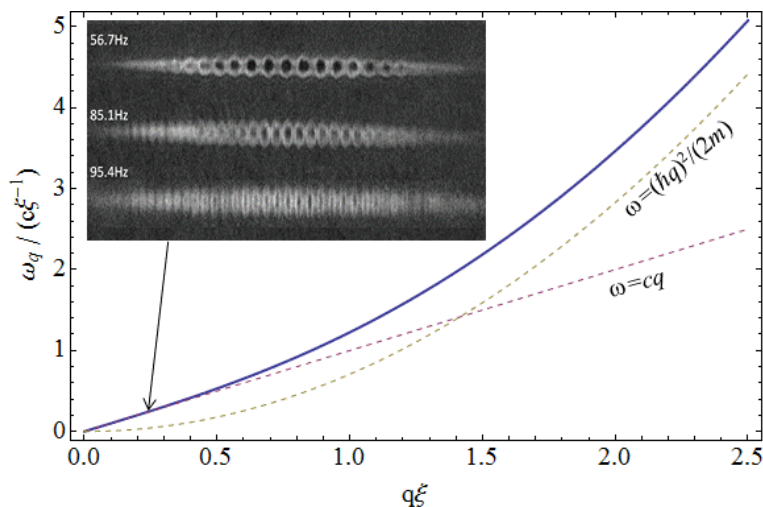
Figure 1.23: The Bogoliubov dispersion is shown as a function of the wave number. For small wave numbers $q \ll \xi^{-1}$ we have sound waves, visible as standing density waves in the condensate images, and for which $\omega = cq$. For $q \gg \xi^{-1}$ the excitations would be thermal atoms kicked out of the condensate, and near $q \approx \xi^{-1}$ there is a continuous transition in the nature of the excitation mode. [reference: Engels et al., Phys. Rev. Lett. **98**, 095301 (2007)]

from which we get

$$q_c = \sqrt{8\pi a n_c} = 1/\xi. \tag{1.190}$$

This is a very intuitive result! It says that when the wave number is larger than the coherence length ξ, the atoms can act in a collective way to form a density wiggle on top of the condensate. But we know that the condensate wave function can be distorted only over distances larger than the healing length! If we try to make the wave length smaller than the coherence length, the individual nature of the atoms reappears, and all we can do is deposit the excitation energy in an atom to kick it out of the condensate. Finally, note that we can rewrite the Bogoliubov spectrum compactly using the healing length as follows:

$$
\begin{aligned}
\epsilon_q &= \sqrt{\epsilon_q^0 \left(\epsilon_q^0 + \frac{\hbar^2}{m\xi^2} \right)} \\
\Rightarrow \quad \omega_q &= \frac{\epsilon_q}{\hbar} = cq\sqrt{(q\xi)^2/2 + 1}
\end{aligned}
\tag{1.191}
$$

where we used $c = \hbar^2/(\sqrt{2}m\xi)$. Now the dimensionless correction factor $\sqrt{(q\xi)^2/2 + 1}$ due to the interactions is evident. The Bogoliubov spectrum is plotted in figure (1.23), where the low-lying modes are visualized. The sound modes here appear as standing waves in the density, with frequency linearly related to the wave number.

1.7.4 Thermodynamics of the interacting Bose gas

In the second section of this chapter we have calculated the thermodynamical quantities for the *ideal* Bose gas. We used the density of states derived from the energy spectrum of free atoms, $\epsilon_q^0 = (\hbar q)^2/(2m)$. In the current section we have seen that the Bogoliubov formalism allows to interpret the *interacting* Bose gas at non-zero temperature as a condensate which does not contribute energy nor entropy, plus an *ideal* gas of (bosonic) Bogoliubov quasiparticles with energy spectrum ϵ_q in stead of ϵ_q^0. The big advantage of this quasiparticle picture of an interacting system is that we can easily extend all the results of the ideal Bose gas – all we need to do is change the dispersion relation (and hence the density of states). The disadvantage of the Bogoliubov treatment is that is becomes less and less accurate when the temperature approaches the critical temperature. In that limit, fluctuations are no longer small with respect to the condensate density, and interactions between quasiparticles becomes important again (the third and fourth order terms in the fluctuation Hamiltonian (1.166) can no longer be neglected). Beliaev worked hard to take into account the third order term, and showed that it leads to damping of the collective modes – also this is seen experimentally. As the temperature gets lower and lower, the damping becomes weaker and weaker and the oscillations of the condensate keep going, and the Bogoliubov treatment works.

From the Bogoliubov spectrum, we can for example get the number of quasiparticles:

$$N = N - N_c = \sum_q \frac{1}{\exp(\epsilon_q/k_B T) - 1}, \tag{1.192}$$

and the internal energy

$$E = \sum_q \frac{\epsilon_q}{\exp(\epsilon_q/k_B T) - 1} \tag{1.193}$$

$$= \frac{V}{(2\pi)^3} \int d^3\mathbf{q} \frac{\epsilon_\mathbf{q}}{\exp(\epsilon_\mathbf{q}/k_B T) - 1}, \tag{1.194}$$

etc... We see that at the lowest temperatures, only the low-lying energy modes contributes, and these have a phonon character. So, at low but nonzero temperatures the condensate acts thermodynamically just like a gas of phonons. An example: for phonons you'll remember from other courses that the specific heat grows as the cube of the temperature. Now you know this is also true for a Bose gas, and if you use the correct sound velocity you get the correct proportionality factor. As the temperature grows, also single-particle excitations become important, and the specific heat with temperature will eventually go as $T^{3/2}$ if we don't reach T_c before.

SUMMARY: AT FINITE TEMPERATURES NOT TOO CLOSE TO T_c WE CAN TREAT THE INTERACTING DILUTE BOSE GAS AS A CONDENSATE PLUS AN IDEAL GAS OF BOGOLIUBOV EXCITATIONS. THESE EXCITATIONS HAVE A PHONON-LIKE DISPERSION RELATION FOR WAVE LENGTHS LONGER THAN THE HEALING LENGTH AND ARE THERMAL ATOMS WHEN THE WAVE LENGTH IS MUCH SMALLER THAN THE HEALING LENGTH.

Chapter 2

Superfluid helium

2.1 The discovery of superfluidity

2.1.1 Helium-II

One of the unique properties of helium is that it cannot be frozen solid at ambient (vapour) pressure. It remains a liquid down to temperature zero. In order to solidify helium, you need to compress it under a pressure of 25 atmospheres. Of course, also helium atoms have a minimum in their interatomic potential: the atoms would like to sit 2.8 Å apart. This minimum is very shallow: a normal chemical bond has an energy of the order of electron volts (thousands of degrees kelvin), but helium as a noble gas is quasi inert – the Van der Waals binding energy is only of the order of ten kelvin, as can be seen in figure 2.1.Still that does not mean helium will indeed become solid below ten kelvin! To determine whether a material is a crystalline solid or a liquid, the Lindemann criterion can be used as a rule of thumb. This criterion states that there can only be crystalline order if the atoms move on average less than 10-20% of the lattice distance. The atoms jiggle around their equilibrium lattice position due to thermal energy: if you heat the solid atoms will oscillate harder and when they their kinetic energy is large enough to displace them 10-20% away from their minimum in the lattice potential, then they are no longer stuck to their lattice site and the material melts. But even when you could cool down to absolute zero, the atoms will not be standing perfectly still due to the Heisenberg uncertainty principle. The uncertainty principle requires a zero point energy larger than the minimum of the classical potential well and a corresponding zero-point motion. The jiggling around due to zero point motion is larger for lighter atoms (smaller mass means more "quantumness"). Helium combines small mass with a weak potential, leading to a zero-point motion larger than 20% of the lattice distance. Thus, helium stays liquid.

The pioneers of cryogenics tried hard to test this by cooling down liquid helium to as low a temperature as they can achieve. The cooling is performed by strong pumps that remove the vapour above the liquid. This lowers the vapour pressure, and brings down the boiling temperature, allowing to reach temperatures down to about 1 kelvin. Heike Kamerlingh Onnes, the son of a rooftile manufacturer, was the first to liquify helium (at 4.2 K) in 1908, and this made him the front-runner in cooling all sorts of things, including helium itself.
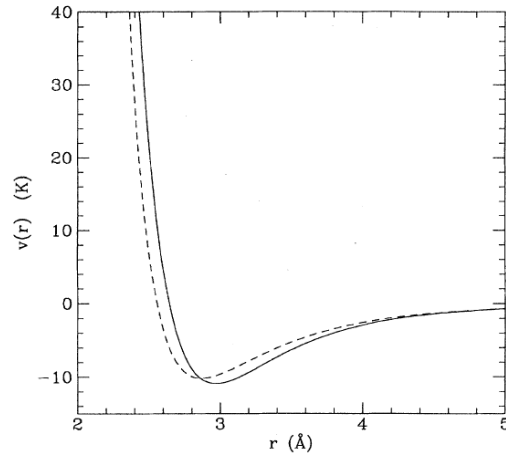
Figure 2.1: The interatomic potential between two helium atoms. The dashed curve is the experimentally determined potential, and the full line is the best fitting Lennard-Jones potential $V(r) = 4\epsilon \left[(\sigma/r)^{12} - (\sigma/r)^6 \right]$ with $\epsilon = 10.22$ K and $\sigma = 2.556$ Å.
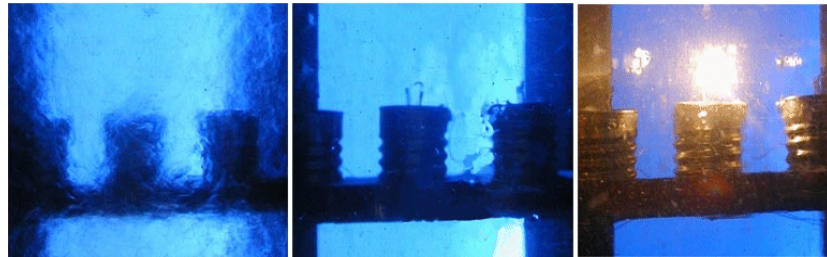
Figure 2.2: Above 2.18 K (left photo) helium boils with bubbles of vapour churning the liquid. But as the temperature is lowered, at 2.18 the boiling stops abruptly (middle photo). There is still evaporation, but no bubbling. Even when a light bulb is switched on, the heat from the bulb does not cause boiling (right photo).
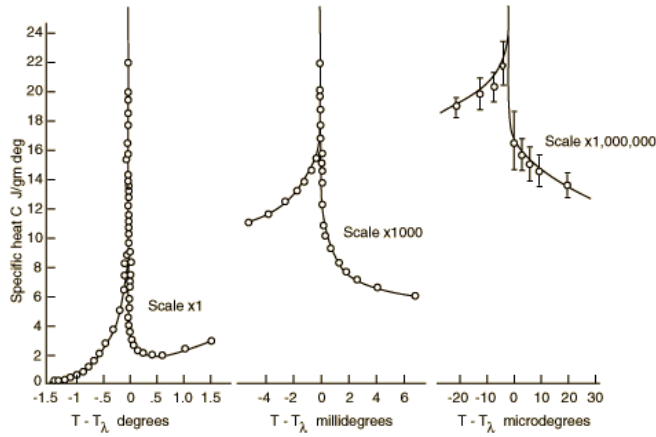
Figure 2.3: The lambda transition is the phase transition between He-II and He-I, and gets its name from the shape of the peak in the specific heat. The peak remains sharp even at the highest temperature resolution achievable (microdegrees), obtained in experiments in space, to avoid chemical potential gradients due to the gravitation potential [source: M. J. Buckingham, W.M. Fairbank, Progress in Low Temperature Physics III, 1961].

He noticed a remarkable phenomenon in 1910: below 2.17 kelvin the violent boiling process of the liquid suddenly stops completely. The liquid becomes still, as can be seen in the middle panel of figure 2.2. The liquid still evaporates and gets colder as you keep pumping away the vapour, but this goes smoothly and is only apparent through the gradual lowering of the level of the helium in the cryostat. Normally, bubbles appear when because some areas in the liquid are hotter and already make the transition to vapour (rising up in the form of a bubble). The disappearance of bubbling means that there are no such thermal gradients. As can be seen in the right panel of figure 2.2, it is possible to switch on a lamp generating a lot of excess heat: helium cooled to well below 2.17 K will still evacuate the heat efficiently enough so no bubbling occurs. This state of helium, below 2.18, became known as "Helium-II", to distinguish it from the normal phase, "Helium-I". Willem Hendrik Keesom (a student of Onnes who later succeeded him as head of the laboratory) found that Helium-II has by far the best heat conduction of any known material, and flattens out any thermal gradients.

For liquid helium-I, the normal state, each gram of vapour extracted removes about 21 J in latent heat of evaporation. Moreover, the specific heat is about 3 Joules per gram per degree. So, to cool 7 grammes of helium-I down by 1 degree requires 21 J, achieved by the evaporation of 1 gram of liquid. Kamerlingh Onnes and Leo Dana notice that the cooling becomes harder near the transition: they had much less helium-II liquid left over than expected, as they had to evaporate more. The culprit is the specific heat: it rises sharply near the transition temperature. Dana and Onnes first measure it in 1923, noting that the curve has a "lambda" shape. The shape of the specific heat peak gave a name to the phase transition between He-II and He-I: it became known as
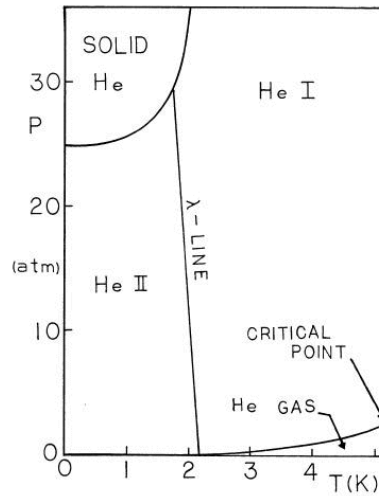
Figure 2.4: The phase diagram of liquid helium, showing the λ-line demarkating the He-II phase.

the "lambda transition". This is the sharpest phase transition that we know: experiments in weightlessness (to eliminate potential gradients) show that the lambda transition is sharp down to the best experimental resolution, on the microkelvin scale, as can be seen in figure 2.3. A lambda-ish peak in the specific heat should ring a bell: we found similar shapes studying the specific heat of Bose gases near the Bose-Einstein condensation temperature: just flip back to figure 1.13 and look at the inset. Gradually, the lambda-transition line was mapped throughout the temperature-pressure phase diagram, shown in figure 2.4: the transition temperature goes down a bit as pressure increases up to the solidification pressure.

2.1.2   Superflow

It was only in 1938 that the most remarkable property of He-II was discovered: it can flow without any viscosity. Two papers appeared back to back in Nature (volume 141): one by Jack Allen and Donald Misener, and one by Pjotr Kapitza. They had independently performed experiments on the flow of helium through narrow channels. If you drill a hole of about a millimeter diameter in the bottom of an (open) pot of mayonnaise, the mayonnaise will not flow out – it is viscous. If you replace the mayonnaise with water, it will flow through the millimeter hole. But it will remain stuck at some point if you make the hole smaller, micron sized. This would also block helium-I, the normal state. But amazingly, as the temperature drops below the lambda temperature, helium-II seems to have no problems and leaks out. Nowadays, capillary channels can be made even smaller, down to the nanometer scale using porous plugs from tightly packed fine powder such as jewellers rouge. Still that forms no unsurmountable obstacle for helium-II, it can flow through such a plug as can be seen in figure
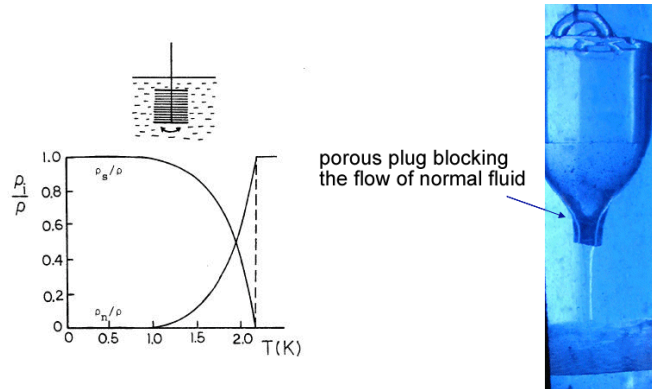
Figure 2.5: A photo of He-II flowing without problems through a porous plug that would definite stop He-I is shown to the right. On the left the result of Andronikashvili's experiment is shown: the superfluid and normal fractions of He-II as a function of temperature.

2.5. This phenomenon –the capacity to flow through the tiniest capillaries– was dubbed **superfluidity**. In 1938 this behaviour was a complete mystery, but to you it is already familiar from the previous chapter. Already two elements are in place to support the hypothesis that helium-II has a Bose condensate of helium atoms: the lambda peak and the ideal fluid behavior.

It would be easy to claim that the capacity to flow through porous plugs is due to the complete vanishing of viscosity, but the story is more complicated than that. The viscosity can be measured directly by an oscillating wire experiment. A tiny loop ℓ of wire is placed in a magnetic field $\mathbf{B}$: when an oscillating current $\mathbf{I}(t)$ is sent through the wire, a driving force $\mathbf{F}(t) = \ell\mathbf{I} \times \mathbf{B}$ swings the wire back and forth. It starts to oscillate, with an amplitude that is maximal if the frequency of the drive is equal to the mechanical resonance frequency of the wire. But it is a damped harmonic oscillator: the width of the resonance is related to the damping caused by the viscosity of the liquid in which the wire is submerged. Thus, our little vibrating wire device is actually a viscosimeter, and one that is able to measure very small viscosities. What the vibrating wire viscosimeter shows is that the viscosity of He-II does not drop to zero right at the transition temperature T_λ. It does decrease, and gradually falls away as the temperature is reduced further and further below T_λ.

2.1.3 Andronikashvili torsional oscillator experiment

So what is going on ? All the liquid can drain through nanometer small capillaries, but aparently there is still viscosity near T_λ ? This baffling behaviour led the theorist Lev Landau to hypothesize that there is a viscous component and a superfluid component, the former leading to the viscosity picked up by the vibrating wire. However, these components are somehow not separate fluids: you are not left over with the viscous component after you strain the liquid through a porous plug. These components can morph into eachother, as if each atom has both viscous and superfluid nature. That definitely sounds like

something quantum mechaniccy – the Helium-II phase is a quantum state of matter.

Elepter Andronikashvili set out to study this duality in a remarkable experiment in 1946. He constructed a stack of disks with only a very small spacing between the disks. This pile of disks was mounted on to a central pillar, a rigid metal rod, that itself was fixed firmly to the ceiling of the experimental cell. This forms a torsional oscillator: as you try to twist the stack with the rod as axis of rotation, it will resist this torsion, and if you let go it will rotate back and forth, oscillating. The frequency of oscillation is $\omega = \sqrt{\kappa/I}$ where κ is the stiffness coefficient of the rod and I is the moment of inertia of the rod+disks (this is similar to $\sqrt{k/m}$ for a spring where k is the spring constant and m is the inertial mass). A sketch of the setup, with the pile of disks immersed in liquid helium, is shown in figure 2.5.

By measuring the frequency of the torsional oscillation you can find the moment of inertia. The moment of inertia is determined by the oscillating mass of both the disks and any fluid dragged along with them. Any viscous fluid between the closely packed disks is certainly dragged along and contributes to the moment of inertia. But any component of the fluid with zero viscosity is not dragged along by the disks. As He-II is cooled down and its viscosity drops, it develops a larger and larger superfluid component, and Andronikashvili could now determine what fraction of the total helium density was superfluid (not dragged along) and what fraction was still viscous. The result is shown, as a function of temperature, in figure 2.5.

The experiment shows that the total mass density ρ can indeed be seen as a sum of a superfluid component ρ_s, that has no viscosity and does not allow temperature gradients, and a normal component ρ_n that carries viscosity. At T_λ, the superfluid component appears. More and more of the total density becomes superfluid density as the temperature is lowered, until below about 1 K the normal component is negligibly small. The total viscosity is the sum of both components, and that is why also the viscosity gradually decreases as the temperature is lowered below T_λ. The normal component may have some thermal resistance, but it always acts in parallel with the superfluid component that has zero thermal resistance: that is why the thermal gradients vanish abruptly at T_λ. The ratio between superfluid and normal component is fixed for a given temperature, and that, in combination with the absence of thermal gradients, means that it is not possible to separate the two components, for example by straining the liquid through a porous plug. Indeed, if you would have more superfluid on one side, it would mean that this side is colder (as you can read off the graph in 2.5), but thermal gradients are not allowed: the superfluid component would immediately rush back to the hotter side and restore a uniform temperature.

2.1.4   Are there supersolids?

We have already argued that there can be no Bose-Einstein condensation of atoms when they are localized in lattice points (to within 10-20% of the lattice site, as per the Lindeman criterion). Indeed, to obtain Bose-Einstein condensation, we need the wavefunctions to spread out (their de Broglie wavelength) over distances larger than the distance between the atoms. Accordingly nobody expected superfluid behaviour in solid helium. The lambda
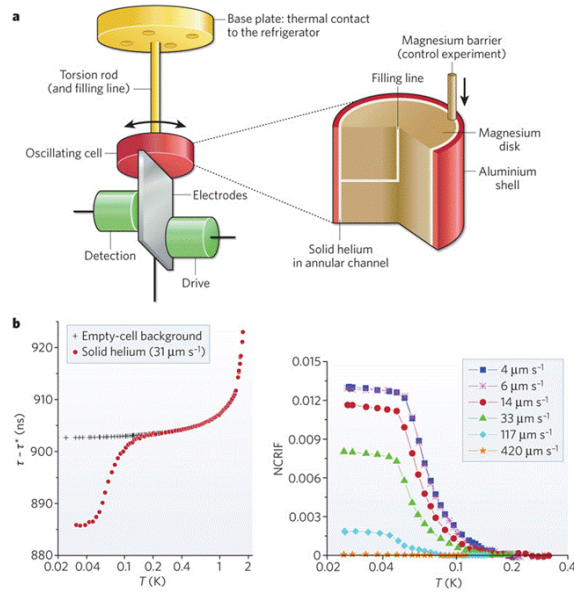
Figure 2.6: Recently, the torsional oscillator experiment was performed for *solid* helium, and strangely enough also there a drop in the moment of inertia was found below a critical temperature [E. Kim and M. H. W. Chan, Nature **427**, 225 (2004)].

line stops at the solidification line in figure 2.4. This doesn't stop good physicists from looking for it anyway: the torsional oscillator experiment was repeated in 2004 but now with solid, pressurized helium in the oscillating bob, as shown in figure 2.6, top. And, to everyones big surprise, below about 100-150 millikelvin, a part of the solid helium seems to avoid oscillating along, and the moment of inertia drops, leading to a decrease in the period of the oscillation (left lower panel in figure 2.6). Moreover, there is also a critical velocity[1]: if the velocity of the solid is increased, the superflowing component is decreased, becoming zero at the critical velocity. This is shown in the right lower panel of figure 2.6, where "NCRIF" stands for Non-Classical Rotational Inertia Fraction and corresponds to our ρ_s/ρ – note that this is at most about 1-2%.

The phase with this anomalous moment of inertia was named a "**supersolid**", in analogy with superfluids, and caused quite a stir, and a lot of follow-up experiments. The supersolid phase, and what underpins it microscopically, is still a mystery today. And there has been a big setback: it was also discovered that the shear modulus of solid helium changes very strongly at about 100-150 millikelvin. As there is also some solid helium in the filling line inside the torsion rod, this influences the rod stiffness κ. So, the small change in rotational frequency $\omega = \sqrt{\kappa/I}$ could be due not to a change in the moment of inertia, as originally claimed, but to a change in the stiffness κ, a far more mundane explanation. The devil is in the details: this is not something

---

[1] I'm running ahead on the course: we'll introduce the critical velocity for superfluid helium later in this chapter.

that affects Andronikashvili's experiments, since the rod stiffness in his case stays constant as the rod is made completely from a material with a well-known behavior and only the disks are submerged in helium! In 2012, Chan and his team diligently repeated the original experiments with a new apparatus that was designed to eliminate any contribution from elasticity of the helium, and with the new setup they found no evidence of supersolidity. But other experimenters still do find phenomena that they cannot explain purely by a change in solid helium elastic moduli, and the issue is not yet settled as researchers continue to seek hard evidence for supersolidity.

2.2   The two-fluid model

Andronikashvili's experiment mapped the superfluid and normal components and gave such a strong corroborating evidence for Lev Landau's hypothesis that Eleptor was awarded the Stalin medal in 1952 (Kapitza got the "western" Nobel prize, he had some trouble with the KGB). Lev Landau and Laszlo Tisza captured the essence of Helium-II in 1940-1941 in their "**two-fluid model**". According to this model, Helium-II is considered an unseparable mix of a viscous and an ideal component, so that $\rho = \rho_n + \rho_s$. Each component also has its own velocity field, the normal component velocity $\mathbf{v}_n$ and the superfluid velocity $\mathbf{v}_s$. The total current density is given by

$$\mathbf{j} = \rho_s \mathbf{v}_s + \rho_n \mathbf{v}_n. \tag{2.1}$$

The model aims to set up a hydrodynamic theory for these two fluids. Let's summarize their properties as we encountered them in the previous section:

	density	current	viscosity	entropy
total	$\rho = \rho_n + \rho_s$	$\mathbf{j} = \mathbf{j}_s + \mathbf{j}_n$	η_n	S
superfluid	ρ_s	$\mathbf{j}_s = \rho_s \mathbf{v}_s$	0	0
normal	ρ_n	$\mathbf{j}_n = \rho_n \mathbf{v}_n$	η_n	S

$$\tag{2.2}$$

We know that ρ_s/ρ is fixed by temperature: lower temperature means more superfluid fraction and less normal fraction. So, if we have a spot where there is excess superfluid, then the temperature there is lower. Similarly, if we have a shortfall of superfluid in a spot, this corresponds to a hotspot. The superfluid component will quickly flow away from the spot with too much superfluid and towards the spot with too few superfluid to restore the correct fraction ρ_s/ρ and iron out the temperature gradient. The thermodynamist in you should be shocked: superfluid flows from cold spot to hot spot! This must mean that the superfluid component carries zero entropy: that there can be no heat flow from cold to hot.

How should we interpret these two components? All the pieces of the puzzle have been set in place in the chapter on Bose gases. The superfluid component has everything in common with a Bose-Einstein condensate: a lambda peak in the specific heat, frictionless flow, zero entropy. Also the fraction of condensed particles increases as you lower the temperature below the critical temperature, just as ρ_s/ρ does (compare figure 1.11 to the ρ_s/ρ curve in figure 2.5). It comes as no surprise that the superfluid component is indeed underpinned by a

Bose-Einstein condensate of helium atoms! How about the normal component? It appears as the temperature rises, and we've also seen that aspect before. The normal component can be interpreted as the gas of *Bogoliubov excitations on top of the condensate*. We still have to figure out the nature of these excitations, as the Bogoliubov dispersion will certainly be different than that of a gas of atoms interacting with a contact potential. That's the programme for the next section. But first, in this section, we want to figure out the correct hydrodynamic equations for superfluid and normal components.

For the superfluid component this easy – we have already derived the hydrodynamic equation for a condensate. It is the Euler equation, expression (1.107):

$$\frac{\partial \mathbf{v}_s}{\partial t} + (\mathbf{v}_s \cdot \boldsymbol{\nabla}) \mathbf{v}_s = -\frac{1}{m} \boldsymbol{\nabla} \mu. \tag{2.3}$$

The chemical potential is no longer that of a dilute Bose gas (at a finite temperature). In order to get the correct chemical potential, we won't try to calculate it from the microscopics, but we will derive it from thermodynamics. The chemical potential as a function of pressure and temperature (the relevant parameters for liquid helium experiments) is connected to the Gibbs free energy[2]:

$$G(N, p, T) = N\mu(p, T). \tag{2.4}$$

From this we find that

$$
\begin{aligned}
N \, d\mu(p, T) &= \left.\frac{\partial G}{\partial p}\right|_T dp + \left.\frac{\partial G}{\partial T}\right|_p dT \\
&= V \, dp - S \, dT
\end{aligned}
\tag{2.5}
$$

Hence, gradients of the chemical potential are connected to gradients in pressure or temperature by

$$\nabla \mu = \frac{V}{N} \nabla p - \frac{S}{N} \nabla T. \tag{2.6}$$

Note that if there is an external potential $V(\mathbf{r})$, such as a gravitational potential, the chemical potential also depends on position and we have to add ∇V to the right hand side. We need the mass density ρ, related to the density of atoms by

$$\rho = (Nm)/V. \tag{2.7}$$

where m is the mass of a helium atom. We can rewrite the entropy S (in Joule per kelvin) to an entropy σ in units of Joule per kelvin per gram,

$$\sigma = \frac{S}{mN}. \tag{2.8}$$

With these notations expression (2.6) becomes

$$\nabla \mu = \frac{m}{\rho} \nabla p - m\sigma \nabla T. \tag{2.9}$$

---

[2]Reminder: The Gibbs free energy is defined from the internal energy U as $G = U + pV - TS = \mu N$, so that $dG = V \, dp - S \, dT + \mu \, dN$ and G is a function of pressure, temperature and number of particles.

leading to the following equation for the superfluid component:

$$\frac{\partial \mathbf{v}_s}{\partial t} + (\mathbf{v}_s \cdot \boldsymbol{\nabla}) \, \mathbf{v}_s = -\frac{1}{\rho} \nabla p + \sigma \nabla T. \tag{2.10}$$

The total fluid, He-II, can't be described by an Euler equation since it can have viscosity – and viscous fluids are described by the Navier-Stokes equation:

$$\rho_s \left[\frac{\partial \mathbf{v}_s}{\partial t} + (\mathbf{v}_s \cdot \boldsymbol{\nabla}) \, \mathbf{v}_s \right] + \rho_n \left[\frac{\partial \mathbf{v}_n}{\partial t} + (\mathbf{v}_n \cdot \boldsymbol{\nabla}) \, \mathbf{v}_n \right] = -\boldsymbol{\nabla} p + \eta_n \nabla^2 \mathbf{v}_n \quad (2.11)$$

To isolate the hydrodynamic equation of the normal component of He-II, we need to subtract the equation for the superfluid component (2.10) from the equation of the entire fluid (2.11):

$$\rho_n \left[\frac{\partial \mathbf{v}_n}{\partial t} + (\mathbf{v}_n \cdot \boldsymbol{\nabla}) \, \mathbf{v}_n \right] = \left(\frac{\rho_s}{\rho} - 1 \right) \boldsymbol{\nabla} p - \rho_s \sigma \nabla T + \eta_n \nabla^2 \mathbf{v}_n \tag{2.12}$$

This equation (2.12) for the normal component, and equation (2.10) for the superfluid component have to be solved with respect to ρ_s, ρ_n, $\mathbf{v}_s$ and $\mathbf{v}_n$. To close this set of equations we need two more equations. The first is the continuity equation $\partial \rho / \partial t = -\boldsymbol{\nabla} \cdot \mathbf{j}$. We only have a continuity equation for the *total* mass density, not for the separate components as you can transform normal into superfluid component and vice versa by changing the temperature. The total mass is conserved, and so it the total entropy. The second equation to be added is the continuity equation for entropy transport $\partial (\rho \sigma) / \partial t = -\boldsymbol{\nabla} \cdot (\rho \sigma \mathbf{v}_n)$.

This gives us a closed set of hydrodynamic equations for He-II, known as the two-fluid model:

$$\rho_s \left[\frac{\partial \mathbf{v}_s}{\partial t} + (\mathbf{v}_s \cdot \boldsymbol{\nabla}) \, \mathbf{v}_s \right] = -\frac{\rho_s}{\rho} \nabla p + \rho_s \sigma \nabla T, \tag{2.13}$$

$$\rho_n \left[\frac{\partial \mathbf{v}_n}{\partial t} + (\mathbf{v}_n \cdot \boldsymbol{\nabla}) \, \mathbf{v}_n \right] = -\frac{\rho_n}{\rho} \boldsymbol{\nabla} p - \rho_s \sigma \nabla T + \eta_n \nabla^2 \mathbf{v}_n, \tag{2.14}$$

$$\frac{\partial (\rho_s + \rho_n)}{\partial t} = -\boldsymbol{\nabla} \cdot (\rho_s \mathbf{v}_s + \rho_n \mathbf{v}_n), \tag{2.15}$$

$$\frac{\partial (\rho \sigma)}{\partial t} = -\boldsymbol{\nabla} \cdot (\rho \sigma \mathbf{v}_n). \tag{2.16}$$

In conjunction with the right boundary conditions, this allows to explain all the strange properties of helium-II. We can add external potentials (gravity,...) easily by adding the corresponding potential energy per unit volume to the pressure. The theory is considered phenomenological: the microscopic interpretation that we will get to in the next section was not worked out by Landau and Tisza.

2.2.1   Fountain effect

As a first application of the two-fluid model, we turn to a curious phenomenon known as the fountain effect. A flask, with a porous plug at the bottom, is half submerged in helium-II. The superfluid component can flow through the plug and enter or leave the bottle, but the normal liquid cannot. A heating wire, or
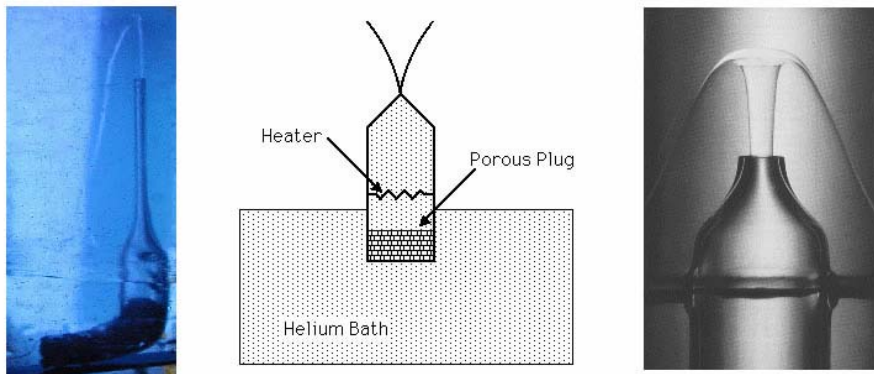
Figure 2.7: The fountain effect: when the bottle is heated inside, superfluid component flows in but normal component is prevented to flow out by a porous plug. As a result, the helium-II level quickly rises and makes a fountain.

even a piece of black carbon absorbing light from a flashlight, is inside the flask and acts as a source of heating. This warms up the helium in the flask, and very quickly (at the speed of second sound!) superfluid helium flows towards the hot spot in an attempt to neutralize the thermal gradient. However, the normal fluid cannot flow away from the hot spot, so that the overall level of helium-II in the bottle will rise. By supplying heat continously, the level may even rise to above the top of the bottle, so that helium-II comes spouting out of the top, forming a fountain. This thermo-mechanical phenomenon is called the **fountain effect**: imposing a temperature gradient (over a porous plug) leads to a pressure head. Figure 2.7 illustrates this effect.

The pressure gradient can be easily computed from equation (2.13), solved in the steady-state regime (so that the time derivative vanishes). If we don't have a fountain but just want to know how high the level in the bottle will rise above the level outside the bottle, we moreover have that $\mathbf{v}_s = 0$ once equilibrium has set in . Then the left-hand side of (2.13) vanishes, and we get $\Delta p = \rho \sigma \Delta T$, the fountain formula of Fritz London. The pressure difference will translate in a level difference through $\Delta p = mg\Delta h$, and this rise can be large enough to bring the helium over the top of the bottle. Indeed, for a ΔT of the same order as T_λ, the pressure head is somewhat over half an atmosphere, corresponding to a Δh of... more than 50 meter. So, even a relatively small temperature gradient needs to be sustained by pumping heat in the bottle to already have a vigorous fountain.

2.2.2 Superfluid creep

Superfluid creep is a related effect, not a person. This strange phenomenon is best seen when a cup is dipped into He-II and then lifted out of the liquid. The helium will start crawling up the cup's inner surface, and then back down the outer surface, making a film that covers the entire surface. Then the helium in the cup crawls along that surface to the bottom on the outside, where it forms droplets and drips back to the liquid below. After a while, the cup is empty
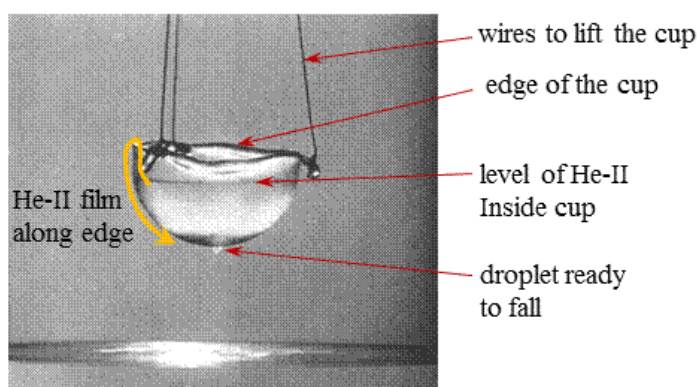
Figure 2.8: Superfluid creep: He-II crawls up the cup's inner surface and back down along the outer surface and then drips back down, emptying the cup.

(but it's surfaces remain covered with a thin helium film). This propensity of helium-II to cover all the surface that it is in contact with, is called superfluid creep. Once the surfaces are covered, it can transport itself along the surface to go to the lowest part of the apparatus.

Superfluid creep is the result of the capacity of helium to organise capillary flow along even the thinnest channels. When you have water in a cup you can also see a meniscus at the cup's surface, where the water crawls up the walls due to the adhesion between the liquid and the wall. But the film thickness quickly reduces to a range in which it is impossible for the "viscous" water to flow. Moreover, the film is fragile: temperature hotspots heat it up and evaporate the film easily. In helium the ease of capillary flow and the good thermal conductivity overcome the restrictions experienced by water.

2.2.3   Second sound

We have already encountered a lot of phenomena related to the fact that heat propagation in helium-II is very different from heat propagation in normal fluids: the absence of boiling, the fountain effect, superfluid creep,... In normal fluids, the heat equation is a diffusion equation, and we get a dissipative proces: a heat pulse will dissipate away, transporting the excess heat over a distance that grows as the square root of elapsed time. But in helium-II, **heat is propagated as a wave**! This means that the excess heat can be transported over a distance that grows linearly in time, i.e. at constant velocity. The temperature "wave" is called **second sound**, and the **second sound velocity** gives the typical speed at which helium-II can iron out temperature gradients.

Superfluid component flows towards a hot spot, and normal component flows away from a hot spot, in an attempt to restore the correct ρ_s/ρ_n ratio. In second sound this is woven into a periodic pattern, as shown in the lower left panel of figure 2.9: velocities of superfluid an normal fluid are exactly opposite and oscillate. The density and pressure remain the same in second sound, but the temperature and entropy density oscillate at a frequency $\omega = c_2 k$. This can be derived in the framework of the two-fluid model, with the result for the second

first sound: pressure wave in bulk

third sound: temperature wave in a film

second sound: temperature wave in bulk

fourth sound: pressure wave in capillary
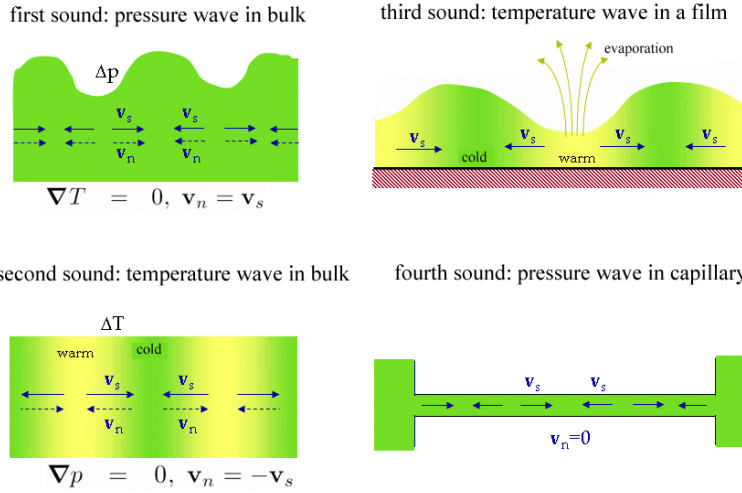
Figure 2.9: Different types of propagating wave-like disturbances in He-II. First sound is the usual density wave. Second sound is the wave-like propagation of heat, peculiar to He-II. Third and fourth sound result from restricting the normal component flow in resp. a film and a capillary.

sound velocity being

$$c_2 = \sqrt{\frac{\rho_s}{\rho_n}} \left(-\left.\frac{\partial S}{\partial T}\right|_p \right)^{-1/2} = \sqrt{\frac{\rho_s}{\rho_n} \frac{TS^2}{C_p}}, \qquad (2.17)$$

where C_p is the specific heat (at constant pressure). The speed of second sound is close to zero near the lambda point, and increases to approximately 20 m/s around 1.8 K, below which it remains about constant (decreasing a little bit towards lower temperatures). This is typically ten times slower than first sound, but still pretty fast in order to remove heat efficiently.

What would happen if the second sound wave encounters a capillary or takes place in a thin film, so that the normal component is pinned? Then $\mathbf{v}_n = 0$, and only $\mathbf{v}_s$ can oscillate. In a film, both ρ_n and the vapour pressure above the film remain constant but we'll heap up superfluid in some areas and deplete it in other areas. This leads to a wave in ρ_s/ρ_n, or a temperature wave, known as **third sound**. In a capillary the heaping up of superfluid density leads to an increased pressure since we have no free surface like for a film – the resulting density wave is known as **fourth sound**. Their velocities can again be derived from (2.13)-(2.16), using suitable boundary conditions. Figure 2.9 shows an overview of the different sounds of superfluid helium.

SUMMARY: LIQUID HELIUM BELOW THE LAMBDA POINT CAN BE DESCRIBED USING THE TWO-FLUID MODEL, EQUATIONS (2.13)-(2.16), COMBINING A FRICTIONLESS SUPERFLUID COMPONENT AND A NORMAL VISCOUS COMPONENT CARRYING ENTROPY. ONE OF THE REMARKABLE CONSEQUENCES IS THAT TEMPERATURE IS TRANSPORTED AS A WAVE.

2.3   Microscopic theory of helium

From the phenomenology of helium-II we already have obtained a good intuition to hypothesize what is going on a the microscopic level. Indeed, the superfluid component is compatible with a condensate of helium atoms, and the normal component corresponds to the thermal excitations, the Bogoliubov modes. We've already outlined Bogoliubov's approach in the chapter on ultracold atoms, but here we will go through it in more detail, and in a way adapted to the uniform helium liquid. The contact potential is no longer a useful pseudopotential, so we'll need to keep the helium interatomic potential in all its generality when we do the Bogoliubov fluctuation expansion.

2.3.1   Fluctuation expansion

The Hamiltonian of the Bose liquid in second quantization, using plane wave states, is given by

$$\hat{H} = \sum_{\mathbf{k}} \epsilon_k^0 \hat{a}_{\mathbf{k}}^\dagger \hat{a}_{\mathbf{k}} + \frac{1}{2} \sum_{\mathbf{k},\mathbf{k}'} \sum_{\mathbf{q}} V_q \hat{a}_{\mathbf{k}+\mathbf{q}}^\dagger \hat{a}_{\mathbf{k}'-\mathbf{q}}^\dagger \hat{a}_{\mathbf{k}'} \hat{a}_{\mathbf{k}} \qquad (2.18)$$

Here ϵ_k^0 is the (kinetic) energy of the plane wave. The operator $\hat{a}_{\mathbf{k}}^\dagger$ creates a helium atom in a plane wave single-particle state, and the operator $\hat{a}_{\mathbf{k}}$ annihilates a helium atom in this state. We use plane waves since they are a suitable basis for a uniform (translation-invariant) system. In contrast to the parabolically trapped gases, the density of the helium liquid in equilibrium is indeed uniform. The operators satisfy bosonic commutation relations $[\hat{a}_{\mathbf{k}}^\dagger, \hat{a}_{\mathbf{k}'}] = \delta_{\mathbf{k}-\mathbf{k}'}$. Note that $\hat{a}_{\mathbf{k}}^\dagger \hat{a}_{\mathbf{k}}$ is the counting operator: its expectation value tells you how many helium atoms are expected to have momentum $\hbar\mathbf{k}$. So, the first term in the Hamiltonian writes the kinetic energy as a sum over all single-particle states, of the kinetic energy that a particle contributes in this state, times the number of particles in this state.

The second term describes collisions between atoms: two atoms with incoming momenta $\hbar\mathbf{k}$ and $\hbar\mathbf{k}'$ scatter off eachoter and obtain final momenta $\hbar(\mathbf{k}+\mathbf{q})$ and $\hbar(\mathbf{k}-\mathbf{q})$. Conservation of momentum is expressed through the fact that in a collision, the only thing atoms can do is exchange a certain momentum $\hbar\mathbf{q}$. The quantum mechanical amplitude to exchange a momentum $\hbar\mathbf{q}$ is given by V_q. This interaction amplitude only depends on the size $\hbar q$ of the exchanged momentum and is given by the Fourier transform of the interatomic helium-helium potential $V(r)$. Now, the range of the potential is compareable to the distance between the helium atoms – a point of difference with the dilute gases where the distance between atoms is typically much larger than the range of the interatomic potential.

Bogoliubov assumes that a Bose-Einstein condensate has formed in the $\mathbf{k}=0$ state. From the Penrose-Onsager criterion we know that this means that the $\mathbf{k}=0$ state is macroscopically occupied:

$$N_0 = \hat{a}_{\mathbf{0}}^+ \hat{a}_{\mathbf{0}} \qquad (2.19)$$

Now since N_0 is a very large number (typically 10^{23} atoms for just a mole, or four grams of liquid helium), we get $N_0 + 1 \approx N_0$. The Bogoliubov shift from

the previous chapter amounts to

$$
\begin{aligned}
\hat{a}_{\mathbf{0}}^{\dagger} \left| N_0 \right\rangle &= \sqrt{N_0 + 1} \left| N_0 + 1 \right\rangle \\
&\approx \sqrt{N_0} \left| N_0 \right\rangle
\end{aligned} \tag{2.20}
$$

where the $\approx$ sign in the second line is to be understood to mean that the expectation values (the physics) calculated with $\left| N_0 \right\rangle$ is not too different from that calculated with $\left| N_0 + 1 \right\rangle$. From this we get that the equivalent of $\hat{\psi}(\mathbf{r}) \approx \Psi(\mathbf{r})$ (used in the previous chapter) is here

$$
\hat{a}_{\mathbf{0}}^{\dagger} \approx \sqrt{N_0}, \tag{2.21}
$$

$$
\hat{a}_{\mathbf{0}} \approx \sqrt{N_0}. \tag{2.22}
$$

Mathematically fussy people will insist that the right hand side should be multiplied with the identity operator. If we now say that only the $\hat{a}_{\mathbf{0}}^{\dagger}, \hat{a}_{\mathbf{0}}$ operators matter, and we neglect all other "thermal" states, this corresponds to our procedure to obtain the temperature zero Gross-Pitaevskii equation from the previous chapter. Let's look at the terms in the Hamiltonian (2.18) that have only $\hat{a}_{\mathbf{0}}^{\dagger}, \hat{a}_{\mathbf{0}}$'s in them. We can collect those and call the result $\hat{H}_0$:

$$
\hat{H}_0 = E_{GP} = \epsilon_{k=0}^0 N_0 + \frac{1}{2} V_0 N_0^2 \tag{2.23}
$$

Since $\mathbf{k}, \mathbf{k}', \mathbf{k}+\mathbf{q}$ and $\mathbf{k}'-\mathbf{q}$ are all set to zero, also $\mathbf{q} = 0$ and we have V_0 appear in this result. This is not too surprising: putting the zero of energy in $\epsilon_{k=0}^0 = 0$, we get $\frac{1}{2} V_0 N_0^2$, or $\frac{1}{2} g n^2$ for the Gross-Pitaevskii energy! That is indeed the result we previously found for Gross-Pitaevskii energy of the homogeneous Bose gas[3].

Next, we can collect all terms that have only one operator that is not $\hat{a}_{\mathbf{0}}^{\dagger}$ or $\hat{a}_{\mathbf{0}}$. We'll refer to these $\hat{a}_{\mathbf{k}}^{\dagger}, \hat{a}_{\mathbf{k}}$ with $\mathbf{k} \neq 0$ as fluctuation operators. But... there are no such terms! That's clear for the first term, and also for the interaction term we find that if you set three of the momenta in the collision event zero, the fourth is also zero. The smallest non-vanishing fluctuation effect is found by collecting terms with precisely two fluctuation operators. The kinetic energy is again easy, there we have just the summation without the $\mathbf{k} = 0$ term. For the interaction part, we make a table to find all the ways to set two operators to momentum zero while keeping two others nonzero:

$\mathbf{k}+\mathbf{q}$	$\mathbf{k}'-\mathbf{q}$	$\mathbf{k}'$	$\mathbf{k}$	$\rightarrow$	terms remaining:
$\neq 0$	$\neq 0$	0	0		$\frac{1}{2} N_0 \sum_{\mathbf{q} \neq \mathbf{0}} V_q \hat{a}_{\mathbf{q}}^{\dagger} \hat{a}_{-\mathbf{q}}^{\dagger}$
$\neq 0$	0	$\neq 0$	0		$\frac{1}{2} N_0 \sum_{\mathbf{q} \neq \mathbf{0}} V_q \hat{a}_{\mathbf{q}}^{\dagger} \hat{a}_{\mathbf{q}}$
$\neq 0$	0	0	$\neq 0$		$\frac{1}{2} N_0 V_0 \sum_{\mathbf{k} \neq \mathbf{0}} \hat{a}_{\mathbf{k}}^{\dagger} \hat{a}_{\mathbf{k}}$
0	$\neq 0$	$\neq 0$	0		$\frac{1}{2} N_0 V_0 \sum_{\mathbf{k} \neq \mathbf{0}} \hat{a}_{\mathbf{k}'}^{\dagger} \hat{a}_{\mathbf{k}'}$
0	$\neq 0$	0	$\neq 0$		$\frac{1}{2} N_0 \sum_{\mathbf{q} \neq \mathbf{0}} V_q \hat{a}_{\mathbf{q}}^{\dagger} \hat{a}_{\mathbf{q}}$
0	0	$\neq 0$	$\neq 0$		$\frac{1}{2} N_0 \sum_{\mathbf{q} \neq \mathbf{0}} V_q \hat{a}_{-\mathbf{q}} \hat{a}_{\mathbf{q}}$

$$ \tag{2.24} $$

All these terms from the interaction also contain two $\hat{a}_{\mathbf{0}}^{\dagger}, \hat{a}_{\mathbf{0}}$ factors, hence the factor N_0 appears everywhere. In the last two rows we've used that V_q is

---

[3] The Fourier transform of $g\delta(r)$ is a constant, $V_q = g/V$, so the energy is $E = \frac{1}{2}(g/V)N_0^2$. The result for the energy per volume E/V is indeed $\frac{1}{2} g n^2$ with $n = N_0/V$ the number density.

insensitive to changing $\mathbf{q} \rightarrow -\mathbf{q}$. Let's place all these terms back together and obtain the Hamiltonian up to second order in the fluctuation expansion:

$$\hat{H} = E_{GP} + \sum_{\mathbf{k} \neq \mathbf{0}} \epsilon_k^0 \hat{a}_{\mathbf{k}}^\dagger \hat{a}_{\mathbf{k}} + N_0 V_0 \sum_{\mathbf{k} \neq \mathbf{0}} \hat{a}_{\mathbf{k}}^\dagger \hat{a}_{\mathbf{k}}$$
$$+ \frac{1}{2} \sum_{\mathbf{q} \neq \mathbf{0}} N_0 V_q \left(\hat{a}_{\mathbf{q}}^\dagger \hat{a}_{-\mathbf{q}}^\dagger + \hat{a}_{\mathbf{q}}^\dagger \hat{a}_{\mathbf{q}} + \hat{a}_{\mathbf{q}}^\dagger \hat{a}_{\mathbf{q}} + \hat{a}_{-\mathbf{q}} \hat{a}_{\mathbf{q}} \right) \qquad (2.25)$$

The strange terms with $\hat{a}_{\mathbf{q}}^\dagger \hat{a}_{-\mathbf{q}}^\dagger N_0$ and $N_0 \hat{a}_{-\mathbf{q}} \hat{a}_{\mathbf{q}}$ represent an event in which two condensate atoms are converted into two thermal atoms, or vice versa. We can rewrite this a bit, since

$$N_{th} = \sum_{\mathbf{k} \neq \mathbf{0}} \hat{a}_{\mathbf{k}}^\dagger \hat{a}_{\mathbf{k}} \qquad (2.26)$$

just counts the number of thermal excitations. This can be included in the Gross-Pitaevskii-Bogoliubov energy

$$E_{GPB} = \frac{1}{2} V_0 N_0^2 + V_0 N_0 N_{th}. \qquad (2.27)$$

This is the simplest correction to the Gross-Pitaevskii energy that we had before (with $\epsilon_k^0 = 0$). That only contained interaction of the condensate atoms amongst themselves, with a factor $1/2$ to avoid double counting. Now we include a term describing the interaction of condensate atoms with thermal atoms (with no risk of double counting, so no $1/2$). The remaining piece of the interaction contribution can be factorized, using

$$\left(\hat{a}_{\mathbf{q}}^\dagger \hat{a}_{-\mathbf{q}}^\dagger + \hat{a}_{\mathbf{q}}^\dagger \hat{a}_{\mathbf{q}} + \hat{a}_{-\mathbf{q}}^\dagger \hat{a}_{-\mathbf{q}} + \hat{a}_{\mathbf{q}} \hat{a}_{-\mathbf{q}} \right) = \left(\hat{a}_{\mathbf{q}}^\dagger + \hat{a}_{-\mathbf{q}} \right) \left(\hat{a}_{-\mathbf{q}}^\dagger + \hat{a}_{\mathbf{q}} \right). \qquad (2.28)$$

We get

$$\hat{H} = E_{GPB} + \sum_{\mathbf{q} \neq \mathbf{0}} \left[\epsilon_q^0 \hat{a}_{\mathbf{q}}^\dagger \hat{a}_{\mathbf{q}} + \frac{N_0 V_q}{2} \left(\hat{a}_{\mathbf{q}}^\dagger + \hat{a}_{-\mathbf{q}} \right) \left(\hat{a}_{-\mathbf{q}}^\dagger + \hat{a}_{\mathbf{q}} \right) \right] \qquad (2.29)$$

The goal is now to diagonalize this Hamiltonian. In general, for any Hamiltonian that is at most quadratic in creation and annihilation operators, we can always find a unitary transformation (from operators $\hat{a}$ to $\hat{\alpha}$) that will diagonalise it, i.e. that will bring it in the form

$$\hat{H} = \text{const.} + \sum_{\mathbf{q} \neq \mathbf{0}} \epsilon_q \hat{\alpha}_{\mathbf{q}}^\dagger \hat{\alpha}_{\mathbf{q}}. \qquad (2.30)$$

This can be done by a suitable choice of the operators $\hat{b}_{\mathbf{q}}$ so that cross-terms vanish. The resulting operators $\hat{\alpha}_{\mathbf{q}}^\dagger$ and $\hat{\alpha}_{\mathbf{q}}$ no longer create atoms in excited plane wave states, but they create Bogoliubov excitations that may have a different nature. The thermodynamics of the system of Bogoliubov excitations can then be found easily through standard statistical physics methods by occupied these Bogoliubov modes through a Bose-Einstein distribution,

$$\left\langle \hat{\alpha}_{\mathbf{q}}^\dagger \hat{\alpha}_{\mathbf{q}} \right\rangle = \frac{1}{e^{-\epsilon_q/(k_B T)} - 1} \qquad (2.31)$$

$$\Rightarrow U = \sum_{\mathbf{q} \neq \mathbf{0}} \frac{\epsilon_q}{e^{-\epsilon_q/(k_B T)} - 1} \qquad (2.32)$$

This should all be very familiar to you if you have studied the first chapter well. You will already have realized that the main thing to do now is to find the Bogoliubov dispersion relation ϵ_q for liquid helium!

2.3.2 Equivalence between bosons and oscillators

There is a nice analogy between bosonic particles on the one hand, and a set of harmonic oscillators on the other hand. Populating an energy level $E_k = \hbar\omega_k$ with N_k bosonic particles is equivalent to exciting a harmonic oscillator with frequency ω_k to the N_k'th level. To see this, remember your very first encounter with creation and annihilation operators, when you have been studing the harmonic oscillator in your first quantum physics classes. Suppose we have a great number of harmonic oscillators (all decoupled), that we index by the label $\mathbf{k}$. The Hamiltonian of this set of oscillators is

$$\hat{H}_{osc} = \sum_{\mathbf{k}} \left(\frac{1}{2} \left| \hat{P}_{\mathbf{k}} \right|^2 + \frac{1}{2}\omega_k^2 \left| \hat{Q}_{\mathbf{k}} \right|^2 \right). \tag{2.33}$$

The convention[4] of labeling of the oscillators implies $\hat{Q}_{\mathbf{k}} = \hat{Q}^\dagger_{-\mathbf{k}}$ and $\hat{P}_{\mathbf{k}} = \hat{P}^\dagger_{-\mathbf{k}}$ We keep notations simple, with m and $\hbar$ set to one. You introduced creation and annihilation operators through

$$\hat{b}_{\mathbf{k}} = \sqrt{\frac{\omega_k}{2}}\hat{Q}_{\mathbf{k}} + i\frac{1}{\sqrt{2\omega_k}}\hat{P}_{-\mathbf{k}} \tag{2.34}$$

$$\Rightarrow \hat{b}^\dagger_{\mathbf{k}} = \sqrt{\frac{\omega_k}{2}}\hat{Q}_{-\mathbf{k}} - i\frac{1}{\sqrt{2\omega_k}}\hat{P}_{\mathbf{k}} \tag{2.35}$$

The labeling with $\mathbf{k}$'s was not in your single oscillator problem, now it complicates matter a little. That's why we go through this part in more detail... We've again used that taking the hermitean conjugate of $\hat{Q}$'s and $\hat{P}$'s is the same as changing the sign of $\mathbf{k}$. The inverse transformation is given by

$$\hat{Q}_{\mathbf{k}} = \frac{1}{\sqrt{2\omega_k}}(\hat{b}^\dagger_{-\mathbf{k}} + \hat{b}_{\mathbf{k}}), \tag{2.36}$$

$$\hat{P}_{\mathbf{k}} = i\sqrt{\frac{\omega_k}{2}}(\hat{b}^\dagger_{\mathbf{k}} - \hat{b}_{-\mathbf{k}}). \tag{2.37}$$

With this convention we get the nice property that if the position and momentum operators satisfy the canonical commutation relation, then the $\hat{b}$'s satisfy bosonic commutation relations:

$$[\hat{Q}_{\mathbf{k}}, \hat{P}_{\mathbf{k}'}] = i\delta_{\mathbf{k},\mathbf{k}'} \Leftrightarrow [\hat{b}^\dagger_{\mathbf{k}}, \hat{b}_{\mathbf{k}'}] = \delta_{\mathbf{k},\mathbf{k}'} \tag{2.38}$$

This is easy to prove by substitution. The direction $\Leftarrow$ is shown by

$$[\hat{Q}_{\mathbf{k}}, \hat{P}_{\mathbf{k}'}] = i\frac{1}{2}[\hat{b}^\dagger_{-\mathbf{k}} + \hat{b}_{\mathbf{k}}, \hat{b}^\dagger_{\mathbf{k}'} - \hat{b}_{-\mathbf{k}'}]$$

$$= i\frac{1}{2}\left([\hat{b}^\dagger_{-\mathbf{k}}, \hat{b}_{-\mathbf{k}'}] - [\hat{b}_{\mathbf{k}}, \hat{b}^\dagger_{\mathbf{k}'}]\right) = i\delta_{\mathbf{k},\mathbf{k}'}. \tag{2.39}$$

---

[4]There are other choices possible, but this particular one will link $\mathbf{k}$ to the wave number. If you think of phonons, you'd like the Fourier transform of $\hat{Q}_{\mathbf{k}}$ with respect to $\mathbf{k}$ to be such that $\hat{Q}_{\mathbf{r}}$ gives the displacement of the oscillating atom located at $\mathbf{r}$ for a the phonon with wave length $\mathbf{k}$. More gory details can be found in J.M. Ziman's old book "Electrons and Phonons".

and the direction $\Rightarrow$ is

$$
\begin{aligned}
[\hat{b}_{\mathbf{k}}^{\dagger}, \hat{b}_{\mathbf{k}'}] &= \left[\sqrt{\frac{\omega_k}{2}}\hat{Q}_{-\mathbf{k}} - i\frac{1}{\sqrt{2\omega_k}}\hat{P}_{\mathbf{k}}, \sqrt{\frac{\omega_k}{2}}\hat{Q}_{\mathbf{k}'} + i\frac{1}{\sqrt{2\omega_k}}\hat{P}_{-\mathbf{k}'}\right] \\
&= \frac{i}{2}\left[\hat{Q}_{-\mathbf{k}}, \hat{P}_{-\mathbf{k}'}\right] - \frac{i}{2}\left[\hat{P}_{\mathbf{k}}, \hat{Q}_{\mathbf{k}'}\right] = i\delta_{\mathbf{k},\mathbf{k}'}.
\end{aligned} \tag{2.40}
$$

The harmonic oscillator Hamiltonians are rewritten in the second quantized operators as

$$
\hat{H}_{osc} = \sum_{\mathbf{k}} \omega_k \left(\hat{b}_{\mathbf{k}}^{\dagger}\hat{b}_{\mathbf{k}} + 1/2\right) \tag{2.41}
$$

Indeed, a simple substitutions shows that

$$
\begin{aligned}
\hat{H}_{osc} &= \sum_{\mathbf{k}} \omega_k \left[\left(\sqrt{\frac{\omega_k}{2}}\hat{Q}_{\mathbf{k}}^{\dagger} - i\frac{1}{\sqrt{2\omega_k}}\hat{P}_{\mathbf{k}}\right)\left(\sqrt{\frac{\omega_k}{2}}\hat{Q}_{\mathbf{k}} + i\frac{1}{\sqrt{2\omega_k}}\hat{P}_{\mathbf{k}}^{\dagger}\right) + \frac{1}{2}\right] \\
&= \sum_{\mathbf{k}} \omega_k \left[\hat{P}_{\mathbf{k}}\hat{P}_{\mathbf{k}}^{\dagger} + \omega_k\hat{Q}_{\mathbf{k}}^{\dagger}\hat{Q}_{\mathbf{k}} - \frac{1}{2}i\left(\hat{Q}_{-\mathbf{k}}\hat{P}_{-\mathbf{k}} - \hat{P}_{\mathbf{k}}\hat{Q}_{\mathbf{k}}\right) + \frac{1}{2}\right] \\
&= \frac{1}{2}\left(\left|\hat{P}_{\mathbf{k}}\right|^2 + \omega_k^2\left|\hat{Q}_{\mathbf{k}}\right|^2\right)
\end{aligned} \tag{2.42}
$$

This wonderful result shows that

> THE HAMILTONIAN FOR A SET OF HARMONIC OSCILLATORS IS EQUIVALENT TO THE HAMILTONIAN OF A BOSE FIELD. VICE VERSA, QUANTIZED OSCILLATIONS (SUCH AS PHONONS OR PHOTONS OR GRAVITONS) THEREFORE ALWAYS CORRESPOND TO BOSONIC PARTICLES.

2.3.3 Bogoliubov excitations in helium

We can use this to diagonalise the fluctuation part of our Hamiltonian (2.29),

$$
\hat{H}_{fluct} = \sum_{\mathbf{q}\neq\mathbf{0}} \left[\epsilon_q^0 \hat{a}_{\mathbf{q}}^{\dagger}\hat{a}_{\mathbf{q}} + \frac{N_0 V_q}{2}\left(\hat{a}_{\mathbf{q}}^{\dagger} + \hat{a}_{-\mathbf{q}}\right)\left(\hat{a}_{-\mathbf{q}}^{\dagger} + \hat{a}_{\mathbf{q}}\right)\right] \tag{2.43}
$$

explicitly (note that we dropped out the zero-point energy, the $1/2$ term in the first term between square brackets). In our case

$$
\hat{Q}_{\mathbf{q}} = \frac{1}{\sqrt{2\epsilon_q^0}}(\hat{a}_{\mathbf{q}}^{\dagger} + \hat{a}_{-\mathbf{q}}), \tag{2.44}
$$

$$
\hat{P}_{\mathbf{q}} = i\sqrt{\frac{\epsilon_q^0}{2}}(\hat{a}_{\mathbf{q}}^{\dagger} - \hat{a}_{-\mathbf{q}}). \tag{2.45}
$$

It is here that the convention (or mess, if you prefer to see it that way) with $\mathbf{q}$'s and $-\mathbf{q}$'s pays off: in the interaction term we get

$$
\left(\hat{a}_{\mathbf{q}}^{\dagger} + \hat{a}_{-\mathbf{q}}\right)\left(\hat{a}_{-\mathbf{q}}^{\dagger} + \hat{a}_{\mathbf{q}}\right) = 2\epsilon_q^0\hat{Q}_{\mathbf{q}}\hat{Q}_{-\mathbf{q}} = 2\epsilon_q^0\hat{Q}_{\mathbf{q}}\hat{Q}_{\mathbf{q}}^{\dagger}. \tag{2.46}
$$

This makes the fluctuation Hamiltonian particularly simple, since we can combine the first term

$$\sum_{\mathbf{q}\neq\mathbf{0}} \epsilon_q^0 \hat{a}_{\mathbf{q}}^\dagger \hat{a}_{\mathbf{q}} \rightarrow \sum_{\mathbf{q}\neq\mathbf{0}} \frac{1}{2}\left(\hat{P}_{\mathbf{q}}\hat{P}_{\mathbf{q}}^\dagger + \epsilon_q^0 \hat{Q}_{\mathbf{q}}\hat{Q}_{\mathbf{q}}^\dagger\right), \tag{2.47}$$

with the interaction to get

$$\hat{H}_{fluct} = \sum_{\mathbf{q}\neq\mathbf{0}} \frac{1}{2}\left[\hat{P}_{\mathbf{q}}\hat{P}_{\mathbf{q}}^\dagger + \left(\left(\epsilon_q^0\right)^2 + 2\epsilon_q^0 N_0 V_q\right)\hat{Q}_{\mathbf{q}}\hat{Q}_{\mathbf{q}}^\dagger\right]. \tag{2.48}$$

We see that the (only) effect of the interaction is to shift the frequencies of the oscillators to a new value,

$$\epsilon_q = \sqrt{\epsilon_q^0 \left(\epsilon_q^0 + 2N_0 V_q\right)}. \tag{2.49}$$

This is the Bogoliubov dispersion for a general interaction potential ! Do we still get the same result as before if we specify the interaction potential to be a delta function $V(r) = g\delta(r)$? Well, the Fourier transform of the delta function is just a constant, independent of q: we get $V_q = g/V$ with V the volume. Plugging this into our general formula yields $\sqrt{\epsilon_q^0 \left(\epsilon_q^0 + 2gn_c\right)}$, exactly the result that we found in the previous chapter. Physicists who are familiar with the equivalence between Bose fields and harmonic oscillators can derive the Bogoliubov dispersion in a few lines on the back of an envelope. We also get the Bogoliubov operators for free, by re-introducing second quantization operators for the *frequency-shifted* harmonic oscillators:

$$\hat{\alpha}_{\mathbf{q}} = \sqrt{\frac{\epsilon_q}{2}}\hat{Q}_{\mathbf{q}} + i\frac{1}{\sqrt{2\epsilon_q}}\hat{P}_{-\mathbf{q}} \tag{2.50}$$

$$\hat{\alpha}_{\mathbf{q}}^\dagger = \sqrt{\frac{\epsilon_q}{2}}\hat{Q}_{-\mathbf{q}} - i\frac{1}{\sqrt{2\epsilon_q}}\hat{P}_{\mathbf{q}} \tag{2.51}$$

With this, we can rewrite the fluctuation Hamiltonian as

$$\hat{H}_{fluct} = \sum_{\mathbf{q}\neq\mathbf{0}} \epsilon_q \hat{\alpha}_{\mathbf{q}}^\dagger \hat{\alpha}_{\mathbf{q}} \tag{2.52}$$

(again we leave out the zero-point energy, or if you feel better about it, we place the zero of energy at the $q = 0$ energy level). The full Hamiltonian also includes the condensate part, so we get

$$\hat{H} = E_{GPB} + \sum_{\mathbf{q}\neq\mathbf{0}} \epsilon_q \hat{\alpha}_{\mathbf{q}}^\dagger \hat{\alpha}_{\mathbf{q}}. \tag{2.53}$$

We have completed our program of rewriting the interacting, non-condensed (thermal) atoms as an ideal gas of Bogoliubov quasiparticles, created by $\hat{\alpha}_{\mathbf{q}}^\dagger$, and with dispersion relation ϵ_q. As mentioned in the chapter on dilute gases, we can now calculate all thermodynamic quantities (specific heat, internal energy,...) from ϵ_q using basic statistical mechanics tools. The Bogoliubov excitations form

the normal component of the superfluid, whereas the superfluid component is linked to the condensate. It is now easy to calculate the number of excitations:

$$\rho_n = mN_{exc}/V \text{ with} \tag{2.54}$$

$$N_{exc} = \sum_{\mathbf{q} \neq \mathbf{0}} \frac{1}{e^{-\epsilon_q/(k_B T)} - 1} \tag{2.55}$$

This grows as temperature increases. In a number-conserving theory, $\rho_s = \rho - \rho_n$ will then decrease. However, the Bogoliubov theory as set up here assumes that ρ_n is small: we dropped all terms in the Hamiltonian with more than two fluctuation operators. We can extend the region of validity to temperatures closer to T_λ if we include also the terms with three fluctuation operators. These terms are called Beliaev terms, after the physicist who first studied them. They represent interactions in which a thermal atoms kicks an additional atom out of the condensate, and interactions in which two thermal atoms scatter off each other such that one of the two joins the condensate. These terms lead to damping of the condensate modes. Another aspect of the theory that we'd need to worry about when getting closer to T_λ is the conservation of the total number of atoms, i.e. precisely the relation $\rho_s = \rho - \rho_n$ as ρ_s becomes smaller[5]. However, in any theory there is room for improvement, and the Bogoliubov result that we have is already extremely powerful to understand helium-II and to underpin the two-fluid model.

2.3.4   The phonon-roton spectrum

For dilute gases, the Bogoliubov dispersion contained phonons (first sound) and single-particle excitations. What will it be for helium? We no longer have a dilute system, and the atoms are close enough to one another to feel the details of the interaction potential. Typically, an interatomic interaction potential is weakly attractive when atoms are far apart, and strongly repulsive when the atoms are pushed closely together. This means the interatomic interaction potential has a minimum, usually at a distance of a few ångstrom. A (wide/narrow) dip in the real-space potential at position r_0 will lead to a (narrow/wide) dip in V_q near $q_0 = 1/r_0$. From the Bogoliubov formula $\epsilon_q = \sqrt{\epsilon_q^0 \left(\epsilon_q^0 + 2N_0 V_q \right)}$ with $\epsilon_q^0 = (\hbar q)^2/(2m)$ it is clear that this dip will also appear in ϵ_q. Another aspect that is evident is that, if $V_{q \to 0} \neq 0$ the Bogoliubov dispersion will start off $\propto \sqrt{\epsilon_q^0}$, that is $\propto q$. The lowest-q behavior will again be (first) sound.

The dispersion relation, and the condensate fraction, can be measured experimentally with neutron scatting. This envolves shooting a neutron into He-II, and recording how much energy and momentum was transferred from the neutron to the helium. If there is a Bogoliubov excitation with matching q and ϵ_q, the scattering process is resonantly enhanced, and a peak in the neutron scattering is detected. The result of such experiments is shown in figure 2.10.

---

[5] There are lot of contemporary theory papers out there studying these questions, and even for dilute gases where the interaction is "easy" the finite temperature theory closer to T_λ remains not fully solved. Check out the book "*Quantum gases: finite temperature and non-equilibrium dynamics*" (ed. Proukakis *et al.*, Imperial College Press, 2013) for a review.
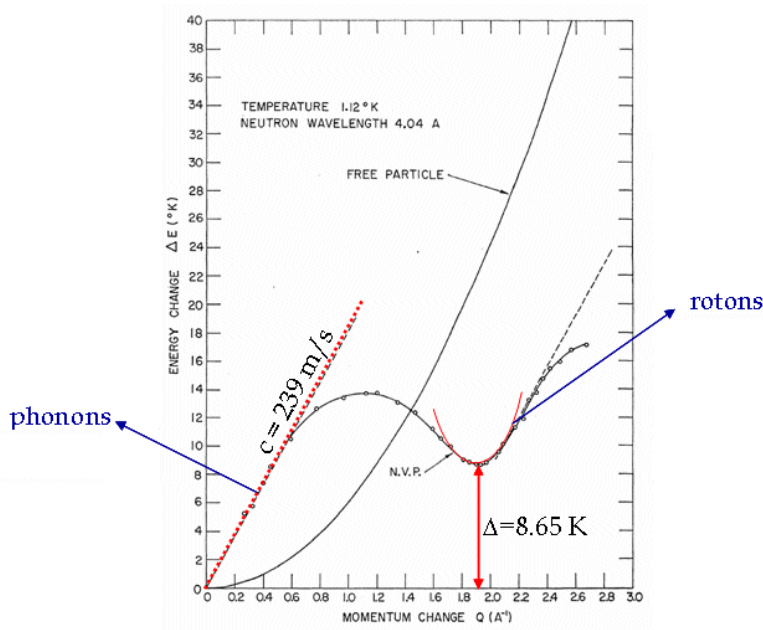
Figure 2.10: The excitation spectrum of He-II, measured with neutron scattering, as reported by Henshaw and Woods (Physical Review, vol. 121).

It is seen that the dispersion indeed starts linearly, with a **phonon** mode,

$$\epsilon_{phonon}(q) = \hbar c q \tag{2.56}$$

and first sound velocity of $c = 239$ m/s. Then it bend back (the excitations at the local maximum are called...maxons), and has a minimum near 2 inverse ångstroms. The Bogoliubov excitations with these wave lengths, i.e. the excitations associated to this minimum, are called **rotons**. Near the minimum, the roton dispersion looks parabolic, i.e.

$$\epsilon_{roton}(q) = \Delta + \frac{\hbar^2(q - q_0)^2}{2m_{rot}}, \tag{2.57}$$

These Bogoliubov quasiparticles are not the single thermal helium atoms! They are still quite different, even if the dispersion looks like that of a particle with mass. The parameters are:

$$\Delta = 8.65 \text{ K}, \tag{2.58}$$
$$q_0 = 19.1 \text{ nm}^{-1}, \tag{2.59}$$
$$m_{rot} = 0.16 \text{ m}_{\text{He}}. \tag{2.60}$$

In fact, rotons are intermediate between truly collective, long-wavelength modes such as phonons, and single-particle excitations that we would have at high wave numbers. The rotons envolve a group of atoms, forming an atomically small "smoke ring" moving through the liquid, as illustrated in figure 2.11
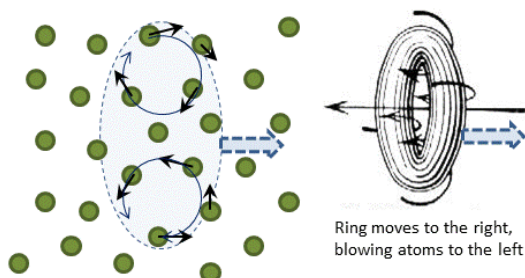
Figure 2.11: Artist's impression of a roton, which is often modeled as an atomically small vortex ring (right figure). This shuffles the atoms about as indicated in the left figure. With this sense of rotation the "smoke ring" moves to the right, displacing atoms to the left.

Starting at temperature zero, we have no phonons or rotons. The lowest energy excitations are phonons. Calculating the specific heat or the internal energy shows that until about 1 K, the thermodynamic properties are dominated by the phonons, and no rotons are present in thermal equilibrium. Indeed, writing down the formula for the number of rotons,

$$N_{roton} = \sum_{\mathbf{q} \neq \mathbf{0}} \frac{1}{\exp\left\{ -\left[\Delta + \frac{\hbar^2(q-q_0)^2}{2m_{rot}}\right]\frac{1}{k_B T}\right\} - 1},$$

it is clear that their number is suppressed by the gap, $e^{-\Delta/(k_B T)}$. This type of excitation has an "activation energy", and starts to kick in in appreciable numbers only at temperatures above 1 K. Above this temperature, the thermodynamics is dominated by rotons, and the phonons matter less, relatively.

The superfluid fraction behaves like a temperature zero condensate. At finite temperatures, Bogoliubov excitations are generated, that act like a free gas of phonons and rotons, from which we can derive the thermodynamic properties. Going to higher temperature can be modeled by including interactions between the rotons and the phonons. We get a remarkable "universe" in which the vacuum is a superfluid through which we can move without dissipation, and this space is populated by "massive" particles called rotons, interacting through "massless" force carriers called phonons. An alien particle physicist living in very cold temperatures in the helium-II filled world might make a "standard model" of his/her universe using just phonons and rotons, oblivious to the condensate that is everywhere. She/he might then apply her standard model to "high-energy physics", meaning for her/him about 10 Kelvin. But at this scale, the theory would break down! Unaware that at 10K, the system is a gas of helium atoms for which a description based on phonons and rotons is meaningless, the high-energy theory would fail dramatically, and strange stuff like extra dimensions and strings would be introduced. This is the topic of an interesting book "*the universe in a helium droplet*" by Grigory Volovik.

2.4 The Landau criterion for frictionless flow

So, are phonons and rotons –or Bogoliubov excitations in general– really unimportant at temperature zero? Not necessarily, most interesting situations do not correspond to the thermal equilibrium. We might consider an object, such as a submarine, to be moving through the liquid helium. Now we need to examine whether it is really true that the submarine can move without friction through the liquid if we include the possibility to create Bogoliubov excitations, even at temperature zero. This would happen by converting some of the kinetic energy of the submarine to make excitations such as rotons that wander off into the helium-II sea. Such a process would take away a bit of the kinetic energy of the submarine, slowing it down.

Let's take the submarine to have a velocity $\mathbf{v}$. We can consider two frames of reference: a frame of reference at rest with respect to the helium-II sea, and the frame of reference of the submarine. From the point of view of the helium-II sea, if there are no excitations, it has the condensate at energy E_{GPB}. The submarine captain sees the condensate in motion: the entire sea (with mass M) seems to be moving with velocity $-\mathbf{v}$, so its energy should be

$$E_{no\ exc}^{submarine} = E_{GPB} + \frac{1}{2}M\mathbf{v}^2 \qquad (2.61)$$

Now, we kick an atom out of the condensate, and give it momentum $\mathbf{p}$. It has excitation energy $\epsilon_{\mathbf{p}}^0 = p^2/(2m)$ from the point of view of the condensate. Again, the captain of the submarine sees it differently (though connected by a galileo transform), for him the thermal atom has a momentum $\mathbf{p} - m\mathbf{v}$, and the helium sea is also still moving $-\mathbf{v}$. Well, the sea is moving with one atom less, so the total mass of the condensate sea is $M - m$. Hence, in the submarine reference frame the total energy becomes

$$E_{total}^{submarine} = E_{GPB} + \frac{1}{2}\left(M - m\right)\mathbf{v}^2 + \frac{\left(\mathbf{p} - m\mathbf{v}\right)^2}{2m} \qquad (2.62)$$

It's easy to work this out,

$$E_{total}^{submarine} = E_{GPB} + \frac{1}{2}M\mathbf{v}^2 + \frac{p^2}{2m} - \mathbf{p} \cdot \mathbf{v} \qquad (2.63)$$

Hence, to the submarine captain the energy of the excitation is

$$
\begin{aligned}
\epsilon_{\mathbf{p}}^{0,submarine} &= E_{total}^{submarine} - E_{no\ exc}^{submarine} \\
&= \frac{p^2}{2m} - \mathbf{p} \cdot \mathbf{v} = \epsilon_{\mathbf{p}}^0 - \mathbf{p} \cdot \mathbf{v}.
\end{aligned}
\qquad (2.64)
$$

This Galilei transform also holds when there is an interaction shift in the excitation energies, i.e. for the Bogoliubov spectrum $\epsilon_{\mathbf{p}}^0 \to \epsilon_q$. Then we get

$$\epsilon_q^{submarine} = \epsilon_q - (\hbar\mathbf{q}) \cdot \mathbf{v}. \qquad (2.65)$$

Under what circumstances will the submarine slow down? When it can make excitations in the He-II sea! And it can only do so if these excitations do not cost any energy, *from the point of view of the submarine*. That is, when $\epsilon_q^{submarine} \leqslant 0$. From expression (2.65) it is clear that it can make $\epsilon_q^{submarine}$
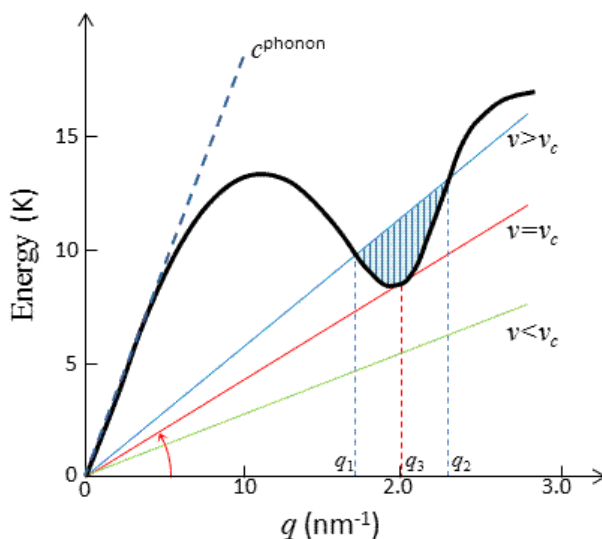
Figure 2.12: An object moving at a velocity larger than v_c, the critical velocity for frictionless flow, can spontaneously create excitations: $\hbar\mathbf{q}\cdot\mathbf{v} > \epsilon_q$ for at least some q. In the example above, this is for $q \in [q_1, q_2]$. Lowering v lowers the slope of the $\hbar\mathbf{q}\cdot\mathbf{v}$ line, and below the critical velocity, the object can no longer transfer its kinetic energy to excitations of the system, and so it no longer experiences friction.

negative if it just goes fast enough, if $\mathbf{v}$ is large enough. There is a critical velocity

$$v_q = \frac{\epsilon_q}{\hbar q} \tag{2.66}$$

needed to be able to emit an excitation with wave length q, it will then be emitted in the direction of $\mathbf{v}$. The smallest value of this,

$$v_c = \min_{q \geqslant 0}\left[\frac{\epsilon_q}{\hbar q}\right] \tag{2.67}$$

gives the **Landau critical velocity**. Any object that moves faster than this through the superfluid, will be able to send out some excitations and hence feel friction. So, our property of frictionless flow that we associate with a superfluid is only valid if the objects move relative to the superfluid at a velocity that is small enough.

If the critical velocity becomes zero, this means there is always friction, no matter how slow the submarine goes. Hence,

$$v_c > 0$$

is the Landau criterion for superfluidity. That's the historical name. By now you should know better and call this more accurately the "**Landau criterion for frictionless flow**". Indeed, this criterion doesn't tell you anything about the quantization of circulation, the irrotational nature of the flow, or the appearance

of singly quantized vortices upon rotation. All these properties are in turn not related to the dispersion relation, but they are derived from the fact that the superfluid velocity can be written as the gradient of the phase of a macroscopic wave function. In helium, frictionless flow and the phenomena related to vorticity appear together, so they were confusingly all brough together under the umbrella concept "superfluidity". They should be distinguished! Indeed, an ideal Bose gas will still have a macroscopic wave function $|\Psi(r)| e^{iS(r)}$ such that $\mathbf{v}_s \propto \nabla S$, but it will have zero critical velocity and objects moving through it will always feel friction. Indeed the Bogoliubov excitations should also be taken into the picture when thinking about friction, and for an ideal gas we get $\epsilon_q = \epsilon_q^0 = (\hbar q)^2/(2m)$, for which

$$v_c^{ideal\ Bose\ gas} = \min_{q \geqslant 0} \left[\frac{(\hbar q)^2/(2m)}{\hbar q} \right] = \frac{\hbar}{2m} \times \min_{q \geqslant 0} [q] = 0 \qquad (2.68)$$

The critical velocity can be found graphically, from a plot of the dispersion relation ϵ_q. Draw a straight line from the origin, representing the line $\hbar q v$. The slope of this line is determined by v, for large velocities the line will be more steep. For example, consider the blue line labeled $v > v_c$ in figure 2.12. In the reference frame of the submarine captain, the energy needed to make an excitation (in the direction of $\mathbf{v}$) is $\epsilon_q - \hbar q v$, so the captain measures the energy with this line as the zero-energy baseline. This means that when the dispersion relation dips below this line, it is energetically advantageous for the submarine to emit Bogoliubov excitations. The shaded region, between q_1 and q_2 in 2.12, indicates which excitations can be emitted. The submarine feels friction as it moves through the liquid. Now reduce v, i.e. reduce the slope of the $\hbar q v$ line. You see that for the phonon-roton spectrum, there is a minimum velocity below which no part of the dispersion relation falls under the $\hbar q v$ line. For the green line, labeled $v < v_c$, there is no possibility to emit excitations, so a submarine cruising at that velocity feels no friction. The critical velocity is the slope of the red line: it touches the dispersion relation at a point where *the tangent line to the dispersion relation goes through the origin*. For the phonon-roton spectrum, this point is $\{q_3, \epsilon_{q_3}\}$ in figure 2.12; in this point the red line is also the tangent to the dispersion relation. Applying our graphical approach to the case of the ideal Bose gas, we see that the only point on the $\epsilon_q^0 = (\hbar q)^2/(2m)$ parabola where the tangent to the curve goes through the origin is $q = 0$. This tangent lies horizontal, so $v_c = 0$.

When interatomic interactions are present,

$$\epsilon_q = \frac{\hbar q}{2m} \sqrt{(\hbar q)^2 + 4m N_0 V_q} \qquad (2.69)$$

and as long as V_q goes to zero slower than q in the limit $q \to 0$ (which is satisfied for interatomic potentials), we find that the long wavelength excitations are always phonons. For phonons,

$$v_c^{phonons} = \min_{q \geqslant 0} \left[\frac{\hbar c q}{\hbar q} \right] = c, \qquad (2.70)$$

the critical velocity is the speed of sound. The critical velocity can be smaller than the speed of sound, for example if we look at rotons

$$
\begin{aligned}
v_c^{rotons} &= \min_{q \geqslant 0} \left[\frac{1}{\hbar q} \left(\Delta + \frac{\hbar^2 (q - q_0)^2}{2m_{rot}} \right) \right] \\
&= \left(\left(\frac{hq_0}{m} \right)^2 + \frac{2\Delta}{m} \right) - \frac{hq_0}{m}.
\end{aligned}
\tag{2.71}
$$

This would go to zero only if the roton gap Δ goes to zero. But this would imply that phonons are not the only low-energy excitations. Feynman was able to show, using another reasoning[6], that phonons are the *only* low(est)-energy excitations of an Bose gas with interatomic interactions. This ensures that there is a range of velocities where frictionless flow exists in an atomic Bose gas or liquid, even if it doesn't say what the critical velocity is. As is the case in helium, v_c could be smaller than the speed of sound[7].

---

[6] This is a very beautiful resoning, reported by Feynman in a paper with nearly no formulae, "Atomic Theory of Liquid Helium Near Absolute Zero", Physical Review **91**, 1301 (1953).

[7] The true critical velocity of He-II is still lower than v_c^{rotons}. It turns out that the submarine will emit large vortex rings when it moves too fast: emitting rotons (atomically small vortex rings) is not the favoured process. The shape of the submarine is also important in determining its ability to emit certain excitations.

Chapter 3

Superconductivity

3.1 Phenomenology of superconductors

3.1.1 Perfect conduction and Meissner effect

Superconductivity was discovered by Kamerlingh Onnes in 1911. The Onnes laboratory in Leiden was the only place where helium could be liquified, and materiaals cooled down to about one degree Kelvin. As metals are cooled down, the resistivity decreases. There was a debate on how the resistivity of materials would behave at the lowest temperatures. One theory claimed that it would saturate to a value determined by the level of impurities. The competing theory claimed that resistivity would go up as the electrons would freeze into a crystal and become immobile. Experiment[1] proved both theories wrong: surprisingly, some materials lost their electrical resistance completely! This was first observed in mercury: there is a sharp transition between the normal resistive state and the "superconducting" state below a critical temperature T_c, as can be seen in Onnes' graph, figure 3.1.

In the superconducting state, the material moreover expells the magnetic flux, as illustrated in figure 3.2. This effect was discovered by Meissner and Ochsenfeld[2] in 1933 and is called the Meisser effect. Poor Ochsenfeld, I don't know what he did wrong. The effect could also be called "perfect diamagnetism": an external field $\mathbf{H}$ results in a magnetization $\mathbf{M} = -\mathbf{H}$ inside the material, giving $\mathbf{B} = \mu(\mathbf{M} + \mathbf{H}) = \mathbf{0}$ However, as the external magnetic field $\mathbf{H}$ is increased, at some *critical magnetic field* eventually the magnetic field will penetrate the superconductor.Then, two possible scenario's are possible[3]. The first possibility is that the piece of material becomes normal again, allowing the magnetic field to penetrate completely. Materials exhibiting this behavior are called "Type I" materials. The second possibility is that the block of superconductor allows magnetic flux to penetrate in thin tubes piercing the material. As the magnetic field is increased further, more and more

---

[1] H. Kamerlingh Onnes, "*Further experiments with liquid helium.*", Comm. Phys. Lab. Univ. Leiden; No. 120b (1911).

[2] W. Meissner, R. Ochsenfeld, "*Ein neuer Effekt bei Eintritt der Supraleitfähigkeit*". Naturwissenschaften **21**, 787–788 (1933).

[3] Recently, a third possibility was found: the magnetisation jumps down at the critical field as in the type I materials, but not completely to zero. After the jump it decreases as in the type II materials. This is sometimes called a type 1.5 material.
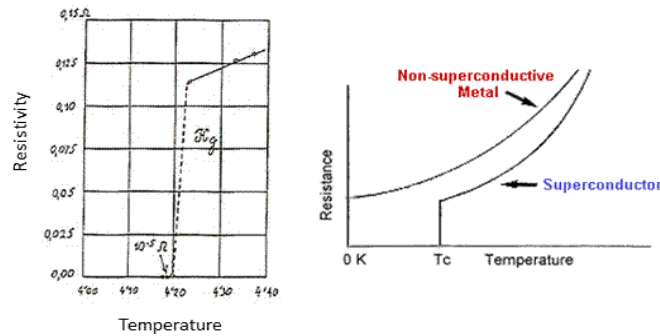
Figure 3.1: Resistivity as a function of temperature. Left: the "historical" figure by Onnes.
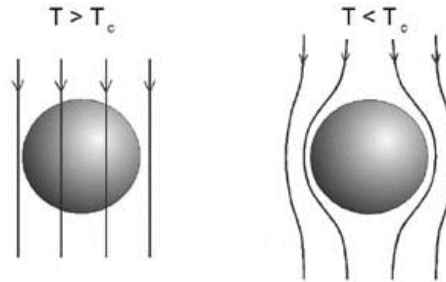

Figure 3.2: Below the critical temperature, the superconductor expells the magnetic flux.

flux tubes pierce the superconductor, untill at a *second critical magnetic field* the material turns normal. These materials are called Type II superconductors. The magnetic response of type I and type II superconductors is illustrated in figure 3.3 and we will come back to this remarkable difference.

Besides the critical temperature and the critical magnetic field, there is still a third critical parameter: there is a maximum current density that can be pushed through a superconductor before it becomes normal. This is connected to the critical magnetic field: currents generate their own magnetic fields. The three parameters, current density $\mathbf{J}$, magnetic field $\mathbf{H}$ and temperature T, set up a phase diagram, as shown in figure 3.4

3.1.2   The non-classical nature of superconductivity

The two defining properties, perfect conductivity and perfect diamagnetism, cannot both be explained by classical (non-quantummechanical) physics! For a perfect conductor, $\rho \to 0$, and Ohm's law dictates that the electric field $\mathbf{E} = \rho \mathbf{J}$ should be zero. Then Maxwell's law $\mathbf{\nabla} \times \mathbf{E} = -\partial \mathbf{B}/\partial t$ in turn implies that $\partial \mathbf{B}/\partial t = \mathbf{0}$. In a perfect conductor, the magnetic flux is "frozen in". Plasma's are pretty good conductors, and they trap magnetic flux. Some of the highest
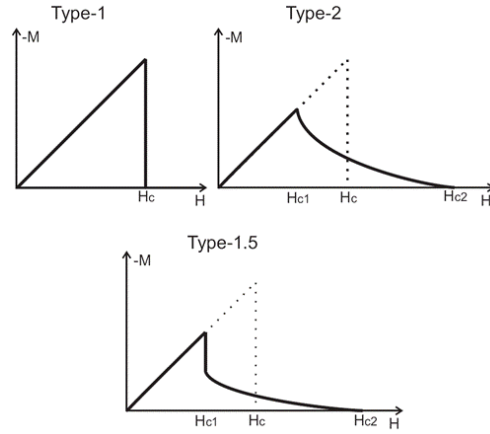
Figure 3.3: Magnetization versus applied external magnetic field, for type I and type II superconductors (top row) and for the intermediate behavior, exemplified in recently discovered "type 1.5 superconductors" [V. Moshchalkov *et al.*, Phys. Rev. Lett. **102**, 2010].
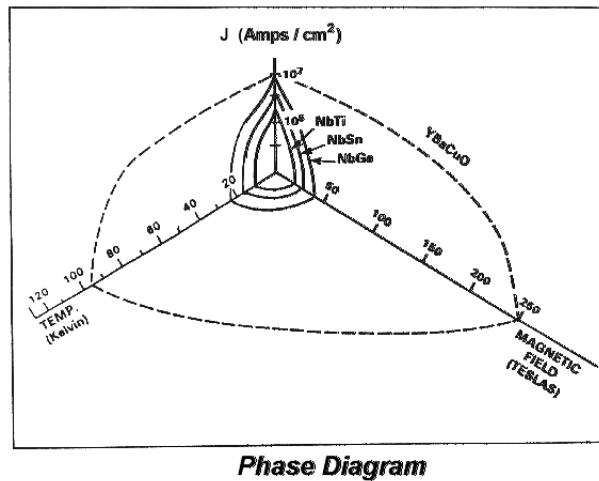
Figure 3.4: Phase diagram for (type II) superconductors, the magnetic field indicated is the second critical field for a ring. The high-temperature superconducting ring, made of YBCO, has much better parameters [figure reproduced from: Michael Tinkham, Introduction to Superconductivity (New York: McGraw-Hill].

magnetic flux densities on earth are created by freezing in flux in a plasma and then compressing the plasma (in the famous "z-pinch" machine).

So, if you start without magnetic field penetrating the material, and then you cool it untill it becomes superconducting, it will keep the magnetic flux out. So far, no problem. But consider the *field-cooling* experiment: first bring the magnetic field in the material, and *then* cool it down until it becomes superconductor. Classical physics dictates that the magnetic flux is frozen in, but Meissner observed that reality is very different: it is expelled from the superconductor. This means $\partial \mathbf{B}/\partial t \neq \mathbf{0}$ and something is wrong.

3.1.3   The London equations and the penetration depth

The brothers Fritz and Heinz London considered how to adapt the laws of electrodynamics so that they would explain the Meissner effect, also in field-cooling. What has to give way is not the Maxwell equations (they remain valid), but Ohm's law. They were looking for a more quantum-mechanical version – and that was quite controversial at the time. The London's posited that charge carriers in the superconducting state behaves like a quantum mechanical wave function, which have $\langle \hat{\mathbf{p}} \rangle = 0$ in the ground state. For charge carriers of mass M and charge Q, the canonical momentum $\mathbf{p}$ is given by

$$\mathbf{p} = M\mathbf{v} + Q\mathbf{A}(\mathbf{r}). \tag{3.1}$$

"Canonical momentum" is the variable conjugate to the position (i.e. the canonical momentum is defined by $\partial \mathcal{L}/\partial \dot{x}$ where $\mathcal{L}$ is the Lagrangian). This is difference from the "kinematic momentum" $M\mathbf{v}$ with $\mathbf{v} = d\mathbf{x}/dt$. Currents are related to the kinematic momentum, not the canonical momentum. Hence, if $\langle \hat{\mathbf{p}} \rangle = 0$ we get

$$M \langle \hat{\mathbf{v}}_s \rangle = -Q\mathbf{A}(\hat{\mathbf{r}}) \tag{3.2}$$

and the current density $\mathbf{J}_s = nQ \langle \hat{\mathbf{v}}_s \rangle$ becomes

$$\mathbf{J}_s = nQ \langle \hat{\mathbf{v}}_s \rangle = -\frac{nQ^2}{M}\mathbf{A} \tag{3.3}$$

where n is the density of charge carriers. This rather handwaving arguments were the inspiration to propose[4] the **London law**:

$$\mathbf{A} = -\frac{M}{nQ^2}\mathbf{J} \tag{3.4}$$

In other words, *it is not the electric field which is proportional to the current (Ohm), but the vector potential*. The Londons did not know about Cooper pairs as the charge carriers, so they did not know M or Q. So why two parameters if they always occur in the same combination? It's better to combine them into a length scale

$$\lambda_L = \sqrt{\frac{M}{\mu_v nQ^2}}, \tag{3.5}$$

---

[4]F. London, H. London, "*The Electromagnetic Equations of the Supraconductor*". Proceedings of the Royal Society **A149**, 866 (March 1935).
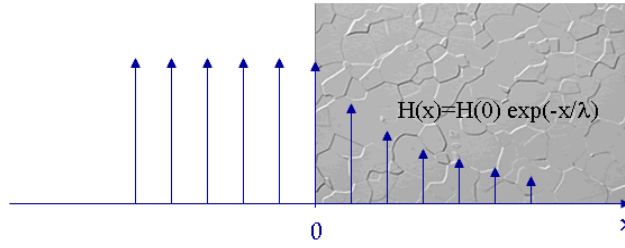
Figure 3.5: A magnetic field $\mathbf{H} = \mathbf{B}/\mu$ applied parallel to the surface of the superconductor cannot penetrate deeply into it: it decays exponentially with a length scale λ_L of 10-100 nm.

called the **London penetration depth**. To get the correct units, we need to include also the permeability (we use the vacuum permeability, $\mu_v = 4\pi \times 10^7$ N/A^2 in SI units). With it, we express the London law as

$$\mu_v \mathbf{J} = -\frac{1}{\lambda_L^2} \mathbf{A} \tag{3.6}$$

This also means

$$\mathbf{E} = -\frac{\partial \mathbf{A}}{\partial t} = \mu_v \lambda_L^2 \frac{\partial \mathbf{J}}{\partial t} \tag{3.7}$$

$$\mathbf{B} = \boldsymbol{\nabla} \times \mathbf{A} = -\mu_v \lambda_L^2 \boldsymbol{\nabla} \times \mathbf{J} \tag{3.8}$$

In hindsight, we now know that the charge carriers are Cooper pairs, and we can estimate $M = 2m_e$ en $Q = -2e$. For the density we take a typical electron density of order $n = 10^{22}$ cm^{-3}. With these values we get $\lambda_L = 10 - 100$ nm, and that is precisely what is found experimentally.

Let's see how the Meissner effect follows from this. Take a half-space of superconducting material, situated at $x > 0$. There's vacuum at $x < 0$. The magnetic flux density $\mathbf{B}$ is directed along the z-axis, as is shown in figure 3.5, so $\mathbf{B} = B(x)\mathbf{e}_z$. We want to find a solution for $B(x)$ in the superconductor. We start from the Maxwell equation (in SI units):

$$\boldsymbol{\nabla} \times \mathbf{B} = \mu_v \mathbf{J} + \mu_v \varepsilon_v \frac{\partial \mathbf{E}}{\partial t} \tag{3.9}$$

We assume that there is no time dependence in the problem (so $\partial \mathbf{E}/\partial t = 0$), as we look for the stationary solution. Taking the curl of this equation gives

$$\boldsymbol{\nabla} \times (\boldsymbol{\nabla} \times \mathbf{B}) = \mu_v \boldsymbol{\nabla} \times \mathbf{J} \tag{3.10}$$

The left hand side can be simplified using the well known identity from vector calculus

$$\boldsymbol{\nabla} \times (\boldsymbol{\nabla} \times \mathbf{B}) = \boldsymbol{\nabla} \underbrace{(\boldsymbol{\nabla} \cdot \mathbf{B})}_{0} - \boldsymbol{\nabla}^2 \mathbf{B} \tag{3.11}$$

where we use another Maxwell equation, $\boldsymbol{\nabla} \cdot \mathbf{B} = 0$. The right hand side can be simplified using equation (3.8), and we find

$$-\boldsymbol{\nabla}^2 \mathbf{B} = -\lambda_L^{-2} \mathbf{B} \tag{3.12}$$

$$\Rightarrow \quad \frac{\partial^2 B(x)}{\partial x^2} = \lambda_L^{-2} B(x) \tag{3.13}$$

What are the appropriate boundary conditions for the case depicted in figure 3.5? We have $B(x = 0) = B_a$ en $B(x \to \infty) = 0$. The solution of (3.13) with these boundary conditions should be obvious to you:

$$B(x) = \begin{cases} B_0 \exp(-x/\lambda_L) \text{ for } x > 0 \\ B_0 \text{ for } x \leqslant 0 \end{cases} \tag{3.14}$$

The magnetic flux density decays exponentially fast inside the material. It cannot penetrate deeper than a layer of typical thickness λ_L (that's why λ_L is called the penetration depth). Remembering that λ_L is typically $10 - 100$ nm, we see that unless the sample is nanoscopically small, the magnetic flux cannot permeate it.

It costs an energy per volume V

$$\frac{E}{V} = \frac{\mu_v H^2}{2} \tag{3.15}$$

in order to expel a magnetic flux density $B_0 = \mu_v H$ fully from a block of material. As the external field is made larger, it costs more energy. The critical field H_c determines how much energy is available per unit volume of superconductor to expel magnetic field. This energy is gained from becoming superconducting; it is the energy difference ΔE_{s-n} between the normal and the superconducting state,

$$\Delta E_{s-n} = \frac{\mu_v H_c^2}{2} V \tag{3.16}$$

3.1.4 Superconducting films

The London penetration depth was determined experimentally using thin superconducting films. Suppose we have a superconducting layer confined in $-d/2 < x < d/2$, and vacuum outside. Again, we apply a magnetic field $\mathbf{B} = B(x)\mathbf{e}_z$ parallel to the surface. We have the same equation (3.13) to solve, but now with boundary conditions $B(-d/2) = B_0 = B(d/2)$. The solution now becomes

$$B(x) = \begin{cases} B_0 \dfrac{\cosh(x/\lambda_L)}{\cosh[d/(2\lambda_L)]} \text{ for } -d/2 < x < d/2 \\ B_0 \text{ elsewhere} \end{cases} \tag{3.17}$$

The magnetization $M(x) = [B(x) - B_0]/\mu_v$ at an externally applied field $H = \mu_v B_0$ is given by

$$M(x, H) = \begin{cases} H\left(\dfrac{\cosh(x/\lambda_L)}{\cosh[d/(2\lambda_L)]} - 1\right) \text{ for } -d/2 < x < d/2 \\ 0 \end{cases} \tag{3.18}$$
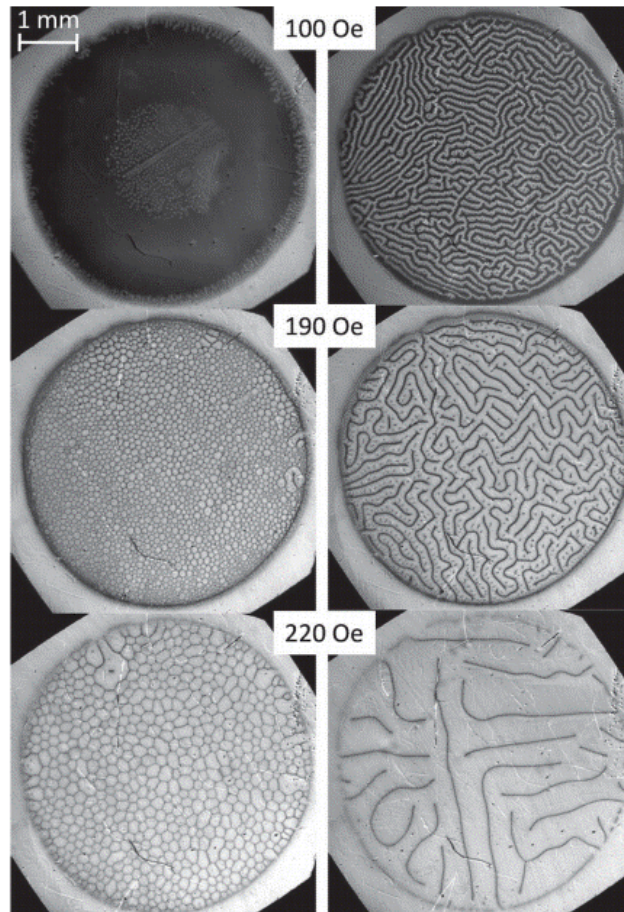
Figure 3.6: Structure of the intermediate state (in between superconducting and normal) in a disc-shaped Pb single crystal at 5 K obtained by magneto-optical imaging. A light color correponds to the normal state, a dark color to the superconducting state. Left column: increasing magnetic field after cooling in zero field. Right column: decreasing field [sources: R. Prozorov, Phys. Rev. Lett. **98**, 257001 (2007); R. Prozorov, A.F. Fidler, J.R. Hoberg et al., Nature Physics **4**, 327 (2008)].

When the film thickness is compareable to the London penetration depth, then the magnetic flux doesn't go all the way to zero in the thin film! It's minimum value in the film is at the center: $B_0/\cosh\left[d/(2\lambda_L)\right]$. Let's calculate the energy required to magnetise the film by ramping up the applied magnetic field from $H = 0$ to $H = H_a$:

$$\frac{E}{V} = -\mu \int\limits_0^{B_a} M(H)dH \tag{3.19}$$

The magnetisation depends also on position, and we need to sum all the pieces of material. The energy per volume V becomes

$$\frac{E}{V} = -\frac{1}{d}\int\limits_{-d/2}^{d/2}dx\int\limits_0^{H_a} M(x,H)dH \tag{3.20}$$

Now we can plug in our result for the magnetization, and get

$$
\begin{aligned}
\frac{E}{V} &= -\frac{1}{\mu_v d}\int\limits_{-d/2}^{d/2}dx\left(\frac{\cosh\left(x/\lambda_L\right)}{\cosh\left[d/(2\lambda_L)\right]} - 1\right)\int\limits_0^{H_a} H dH \\
&= \frac{\mu_v H_a^2}{2}\left(1 - \frac{\tanh\left[d/(2\lambda_L)\right]}{d/(2\lambda_L)}\right)
\end{aligned}
\tag{3.21}
$$

The superconductor still has an energy $\Delta E_{s-n}/V = \mu_v H_c^2/2$ to spend on the expulsion of magnetic flux. For a thin film, it doens't need to expell the magnetic flux as thoroughly as for bulk, so the available energy lasts longer, and the critical magnetic field for a film is larger than for bulk:

$$H_c^{film} = \frac{H_c^{bulk}}{\sqrt{\dfrac{\tanh\left[d/(2\lambda_L)\right]}{d/(2\lambda_L)} - 1}}. \tag{3.22}$$

This result was used to determine the London penetration depth experimentally from measurements of the critical magnetic field for thin films of given thickness d. It also shows that reducing superconductors to the nanoscale can enhance their critical parameters, in this case the critical magnetic field.

The situation is much more complicated when we apply the magnetic field *perpendicular* to the film. It becomes very difficult, even for a type-I material, to push the magnetic flux all the way to the side of the sample when the magnetic field becomes more intense. Rather, magnetic domains can appear, in which the flux penetrates. These domains are interleaved with regions that remain fully superconducting. The domain structure of the so-called "intermediate" state is shown in figure 3.6 for a Pb (type I) disk. This behavior is again very different from the type-II materials: upon increasing the field above the first critical field, magnetic flux starts to enter the sample in the form of superconducting vortices carrying flux quanta, as shown in figure 3.7 We'll explore this in more detail later in the chapter.
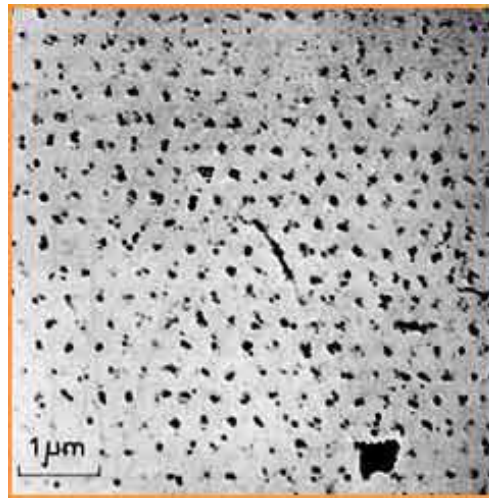
Figure 3.7: In a type-II material, the magnetic field (for strengths above the first critical field) penetrates in thin tubes (visible as black dots) each carrying a flux quantum. The magnetic flux is made visible by a technique similar to sprinkling iron filings on the sample and looking where they stick [U. Essmann H. Trauble, Physics Letters 24A, 526 (1967)].

3.1.5 The Pippard correlation length

Nowadays experimenters have more sophisticated methods to determine the penetration depth: they can map the magnetic flux density inside the material directly! This is done using muon spin resonance. Muons with a given energy are injected into a superconductor. The energy of the muon determines precisely how deep under the surface it will end up. The muon spin will feel the magnetic field at that precise depth inside the superconductor. Measuring the zeeman splitting by spin-resonance allows to determine this magnetic field. The result of such an experiment is a precise profile of the magnetic field as a function of depth beneath the superconducting surface, is shown in figure 3.8. The experimental results (dots and squares) correspond quite well to the exponential decay predicted by the London equations. Note that on the logarithmic scale the exponential law corresponds to a straight line. However, upon closer inspection there is a clear systematic deviation.

The Londons assumed that the charge carriers are point particles, and their theory is **local**, just like Ohm's law. "Local" means that the current density in a point **r** depends only on the vector potential (or electric field, for Ohm) at the same a point **r**. This does not need to be the case, and if the size of the charge carriers is compareable to the penetration depth, deviations from London's laws are to be expected. In that case, the charge carrier will respond to the vector potential over an extended region, and as a result current density in **r** depends on the vector potential in a region around **r**. Such a theory is called **non-local**.

There also exists a non-local extension to good old Ohm's law. This is known
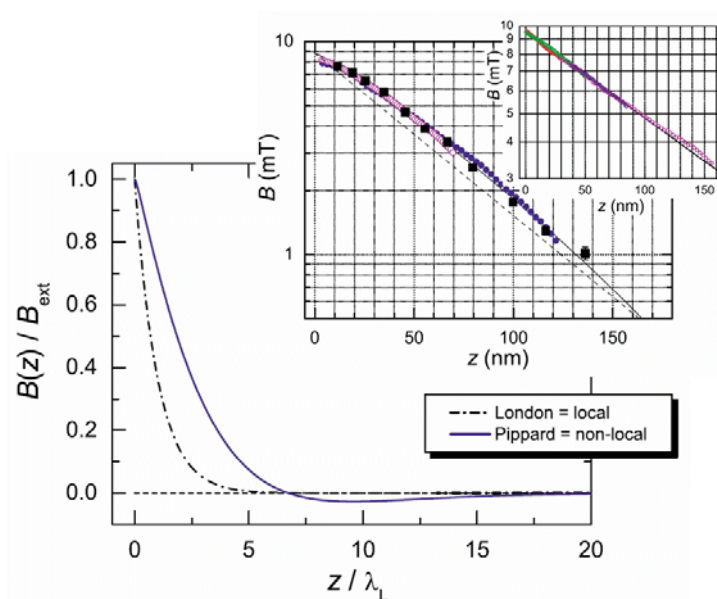
Figure 3.8: Magnetic flux density as a function of the depth under the surface of the superconductor, measured by muon spin resonance [from: Suter *et al.*, Phys.Rev. B **72**, 024506 (2005)]. The dots represent the experimental measurements, the dashed curves are the results from London theory and the full curves are those from Pippard theory.

as Chambers's law:

$$\mathbf{J} = \frac{1}{\rho} \times \frac{3}{4\pi\ell} \int \frac{\mathbf{R}(\mathbf{R}\cdot\mathbf{E}(\mathbf{r}'))}{R^4} e^{-R/\ell} d^3\mathbf{r}'. \tag{3.23}$$

Here $\mathbf{R} = \mathbf{r} - \mathbf{r}'$. The integral averages out the electric field over an area of size ℓ. For Chambers this was the length that an electron could travel before getting scattered. Pippard[5] used the analogy between the London equations and Ohm's law to propose

$$\mathbf{J} = \left(-\frac{1}{\mu_v \lambda_L^2}\right) \times \frac{3}{4\pi\xi_P} \int \frac{\mathbf{R}(\mathbf{R}\cdot\mathbf{A}(\mathbf{r}'))}{R^4} e^{-R/\xi_P} d^3\mathbf{r}'. \tag{3.24}$$

This is known as **Pippard's equation**. It is now the vector potential that is being averaged out over a region ξ_P, called the **Pippard correlation length**. The full curves in figure 3.8 show the result of Pippard's equation, and you can see that it matches the experiment perfectly, removing the (small) deviations that were present when we use just the London equations.

How large is the area over which we need to average out the vector potential? This should correspond to the size of the superconducting charge carrier. Pippard assumed that only electron states within a range $k_B T_c$ around the

---

[5] A.B. Pippard "*Trapped Flux in Superconductors*", Philosophical Transactions of the Royal Society A**248,** 97–129 (1955).

Fermi energy could contribute to the construction of superconducting charge carriers. Since $p = \sqrt{2mE}$, we get that only states with

$$\sqrt{2m\left(E_F + k_B T_c\right)} > p > \sqrt{2m\left(E_F - k_B T_c\right)} \tag{3.25}$$

contribute to the wave function of the superconducting charge carriers. The width of this interval is

$$
\begin{aligned}
\Delta p &= \sqrt{2m\left(E_F + k_B T_c\right)} - \sqrt{2m\left(E_F - k_B T_c\right)} \\
&\approx \sqrt{2mE_F}\frac{k_B T_c}{E_F}
\end{aligned} \tag{3.26}
$$

where we expanded in $k_B T_c / E_F \ll 1$. Since the Fermi velocity $v_F = \sqrt{m/(2E_F)}$ we get that $\Delta p = 2k_B T_c / v_F$. According to Heisenberg's uncertainty relation, the "size" of the wave function of the superconducting charge carrier consequently has to be larger than

$$\Delta x = \frac{\hbar v_F}{k_B T_c} \tag{3.27}$$

which is typically of the order of 100 nm, since $v_F \approx 10^6 - 10^7$ m/s and $T_c \approx 1$ K. This is indeed compareable to the penetration depth, so that we expect non-local effects to be present. Pippard chose his correlation length to be of the similar magnitude as this Δx, and sets

$$\xi_P = a\frac{\hbar v_F}{k_B T_c} \tag{3.28}$$

with a a constant of order 1. This allowed to improve the correspondence between theory and experiment (cf. figure 3.8), and it was also possible to include the effects of impurities in the superconductor. These lead to an effective decrease in the correlation length, determined by

$$\xi_{P,\text{impure}}^{-1} = \xi_{P,\text{pure}}^{-1} + \ell^{-1} \tag{3.29}$$

where ℓ is the free path length (determined by the impurity density and type).

	λ_L (nm)	ξ_P (nm)	$\kappa = \lambda_L/\xi$
Sn	34	230	0.15
Al	16	1600	0.01
Pb	37	83	0.45
Cd	110	760	0.14
Nb	39	38	1.03

$$\tag{3.30}$$

The table above shows the results for several materials, for our *two* fundamental length scales for superconductors. For condensates, we only had one fundamental length scale, ξ, which we will see is related to Pippard's correlation length although it is not completely the same. The presence of charge, and the magnetic response, leads to the second fundamental length scale λ_L. The ratio between the two length scales determines whether a material behaves more as type I (for $\kappa = \lambda_L/\xi \ll 1$) or more as type II (for $\kappa \gg 1$). With Pippard's theory we have completed the phenomenological survey of superconductivity and we
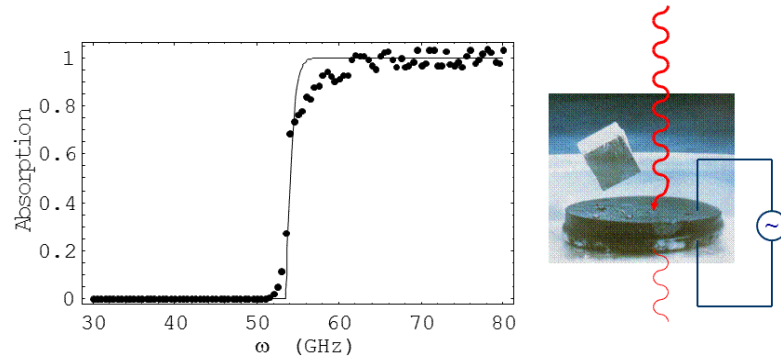
Figure 3.9: The absorption (or AC resistance) remains zero up to a frequency in the microwave domain (10 μeV - 1 meV).

have the most complete phenomenological theory of the electromagnetism of superconductors. It's now time to turn to the microscopic fundaments.

SUMMARY: SUPERCONDUCTIVITY EXISTS BELOW A CRITICAL TEMPERATURE, A CRITICAL EXTERNAL MAGNETIC FIELD, AND A CRITICAL CURRENT DENSITY. THE DEFINING PROPERTY OF SUPERCONDUCTIVITY IS THE JOINT OCCURRENCE OF PERFECT CONDUCTION AND PERFECT DIAMAGNETISM. THIS CAN BE MODELED BY REPLACING OHM'S LAW BY THE LONDON EQUATION SETTING THE VECTOR POTENTIAL PROPORTIONAL TO THE CURRENT DENSITY. THE PROPORTIONALITY CONSTANT DEFINES THE FIRST IMPORTANT LENGTH SCALE, THE PENETRATION DEPTH. A SECOND IMPORTANT LENGTH SCALE WAS INTRODUCED BY PIPPARD, THE CORRELATION LENGTH, AND THIS RELATES TO THE SIZE OF THE SUPERCONDUCTING CHARGE CARRIER.

3.2   Key experiments

In the 1950's a series of experiments revealed new properties of superconducting materials. These experiments also provided the crucial clues to understanding the microscopic mechanism that underpins superconductivity.

3.2.1   Microwave absorption / AC resistivity

The DC resistivity is zero: this is the perfect conductivity observed by Onnes. How about the AC resistivity (as a function of frequency ω?) This is shown in figure 3.9. The AC drive can be generated by an electric circuit, or by shining in light. As soon as the incoming photons have an energy larger than a certain treshold, they will be absorbed. This sounds very similar to what happens in a semiconductor: shine in photons with an energy larger than the bandgap, and they will be absorbed by exciting a charge carrier accross the gap.The difference here is that the bandgap for the superconductor is very small, typically ten
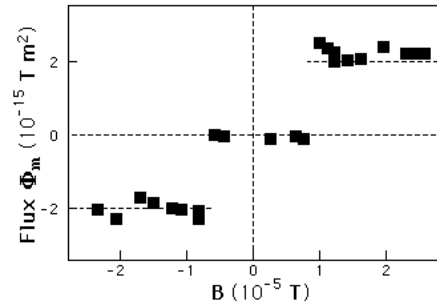
Figure 3.10: Flux quantisation through a superconducting ring [from B.S. Deaver, W.M. Fairbank, Phys. Rev. Lett. **7**, 43 (1961)].

thousand times smaller than that for semiconductors. Remarkably, the bandgap is of similar magnitude as $k_B T_c$.

3.2.2 Flux quantization

When a particle is translated in space over a distance $\Delta \mathbf{r}$, its wave function acquires a phase shift $\exp\{i\mathbf{p}\cdot\Delta\mathbf{r}/\hbar\}$, where $\mathbf{p}$ is the canonical momentum. In group theoretical jargon, one says that the canonical momentum is the generator of the Lie group of translations.

When a particles is moved around in a loop and comes back to its original position, the wave function should go back to its original value (i.e. the total phase shift should be an integer multiple of 2π). This works when you add up all the phase shifts, as in this example for a small square loop:

$$
\begin{array}{ccc}
\psi & \xrightarrow{\text{shift} + \Delta x} & \psi e^{ip_x\Delta x/\hbar} \\
\text{shift } +\Delta y \uparrow & & \downarrow\text{shift} -\Delta y \\
\psi e^{i(-p_y\Delta y)/\hbar} & \xleftarrow{\text{shift} - \Delta x} & \psi e^{i(p_x\Delta x - p_y\Delta y)/\hbar}
\end{array}
\tag{3.31}
$$

For a general loop C, we must tally up all the $\exp\{i\mathbf{p}\cdot d\ell/\hbar\}$ contibutions along the curve, and our previous result generalizes to

$$
\exp\left\{\frac{im}{\hbar}\oint_C \mathbf{v}\cdot d\ell\right\} = 1.
\tag{3.32}
$$

Things become a bit more complicated when a magnetic field is present and the particle has charge q. We know that in that case, the canonical momentum is given by $\mathbf{p} = m\mathbf{v} + q\mathbf{A}$, and we obtain an additional phase shift

$$
\exp\left\{\frac{i}{\hbar}\oint_C (m\mathbf{v} + q\mathbf{A})\cdot d\ell\right\} = \underbrace{\exp\left\{\frac{im}{\hbar}\oint_C \mathbf{v}\cdot d\ell\right\}}_{=1 \text{ as before}} \exp\left\{\frac{iq}{\hbar}\oint_C \mathbf{A}\cdot d\ell\right\}
\tag{3.33}
$$

The additional phase picked up by a charged particle as it moves in a loop in a

magnetic field is called a geometric phase or Berry phase. It is equal to

$$\exp\left\{\frac{iq}{\hbar}\oint_C \mathbf{A}\cdot d\ell\right\} \;\; = \;\; \exp\left\{\frac{iq}{\hbar}\int_S \boldsymbol{\nabla}\times\mathbf{A}\cdot d\mathbf{S}\right\}$$

$$= \;\; \exp\left\{\frac{iq}{\hbar}\int_S \mathbf{B}\cdot d\mathbf{S}\right\} = \exp\left\{\frac{iq}{\hbar}\Phi\right\}. \qquad (3.34)$$

Here Φ is the total magnetic flux going through the loop. We have used Stokes theorem to convert the contour integral into an integral over a surface bounded by the contour. The combination h/q also has units of flux, and is called the flux quantum $\Phi_0 = h/q$. So, when a charged particle goes around in a loop we get

$$\psi \rightarrow \psi e^{2\pi i\Phi/\Phi_0}. \qquad (3.35)$$

Since the wave function should be single-valued in any point (i.e. it has to go back to the same value after we've translated our frame of reference in a loop), the total flux through the loop should be an integer multiple of the flux quantum,

$$\Phi = n\Phi_0. \qquad (3.36)$$

If the London brothers are right, and the superconducting state can only be characterized by a quantum mechanical wavefunction without classical analogue, then this must lead to flux quantization. Experimenters set out to measure this, using superconducting rings placed in external magnetic fields. The result is shown in figure 3.10: there is indeed flux quantization. However, the steps in the flux are consistent with a flux quantum h/Q where the charge is *twice* the electron charge: $Q = -2e$. This suggests that the superconducting charge carriers are built from pairs of electrons.

Moreover, if we combine this insight with the band gap discussed in the previous subsection, we can infer that these electron pairs are bound with a very small energy (equal to the gap, i.e. 10-100 μeV, of something of the order of GHz). Irradiating the pairs with photons that have enough energy can break them up and suppress the superconductivity.

3.2.3   Specific heat anomaly

In a metal, we know that the electronic contribution to the specific heat is linear in temperature, and the phononic contribution is going to zero as T^3 so it is very small below 100 K. Hence, at temperatures below 100 K, the specific heat is usually plotted as C_V/T. This should be a constant (of order Nk_B where N is the number of electrons). For a superconductor, this doesn't look constant at all, as you can see from figure 3.11. As the temperature drops below T_c, there is a jump, after which the specific heat drops faster than T to zero.

Sounds familiar? That is exactly what we discussed for Bose gases below T_c, where now T_c was the temperature for Bose-Einstein condensation. Fermions ought not to do Bose condense! But keeping in mind the previous two key experiments, we know that the electrons are bound up in pairs. These pairs can behave as a boson, and undergo Bose-Einstein condensation, as the specific heat shape seems to suggest. This means that the microscopic picture of a
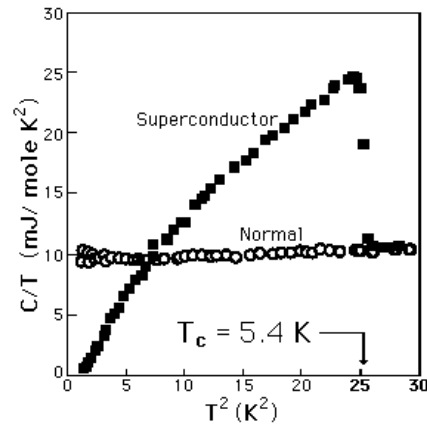
Figure 3.11: Specific heat anomaly in vanadium as a function of temperature [from W. S. Korak, et al., Phys. Rev. **102**, 656 (1956)].

superconductor is that of a charged Bose-Einstein condensate, or rather, a **charged superfluid**. Up till now we've only looked at neutral superfluids, so we'll have to extend our theory.

But first we need to clear up a mystery. Why do electrons pair up? Electrons repel eachother through the Coulomb interaction, so something else should be providing the glue that binds the electrons together

3.2.4 Isotope effect

The final experimental clue came from the isotope effect. Mercury, the element in which superconductivity was first observed, has a large variety of stable isotopes. If the mechansims of superconductivity is purely due to the electrons, or the types of chemical bonds between the atoms and the band structure arising from these, then there should be no difference between isotopes of the same material, such as ^{203}Hg en ^{199}Hg. Isotopes only differ in the number of neutrons per atom and do not change orbital structure or chemical bonds or number of conduction electrons. And yet, there turns out to be a dependence of the critical temperature on isotope mass, as can be seen in figure 3.12.

The particular dependence, $T_c \propto 1/\sqrt{A}$ with A the isotope mass, is a tell-tale sign that phonons are involved. Firstly, phonons are the only other relevant excitation that depends on the isotope mass. Secondly, the phonon frequency, just like a spring frequency, depends on the isotope mass as $\omega \propto 1/\sqrt{A}$ too. This means that the critical temperature is proportional to the phonon frequency, which in turn leads us to hypothesize that the glue that binds the electrons together comes from phonons.

Fröhlich[6] has shown that phonons can indeed constitute a glue that leads to effective attraction between electrons. He was well placed, as he had already developed a theory for the electron-phonon interaction, showing that electrons locally deform the lattice around them. When the electrons move, they trail this

---

[6] H. Fröhlich, Phys. Rev. **79**, 845 (1950).
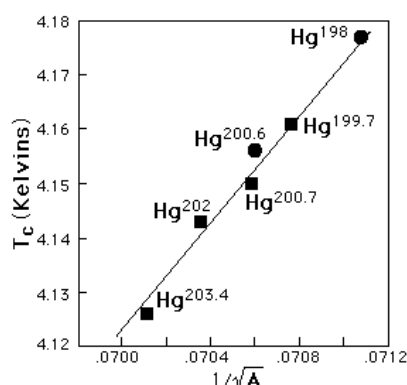
Figure 3.12: The critical temperature of mercury as a function of the isotope mass. Circles: experiment of E. Maxwell, Phys. Rev. **78**, 477 (1950), squares: C.A. Reynolds et al., Phys. Rev. **78**, 487 (1950).

lattice deformation behind them, as the lattice ions are heavier and thus respond more slowly. As a result the moving electron has a comet tail of induced positive charge behind it, that not only holds back the electron (giving it a larger effective mass), but that also attracts other electrons. Bardeen and Pines[7] showed that this attraction is strong enough even to overcome the Coulomb repulsion.

The comet tail of induced positive charge density can attract another electron, and the semi-classical picture emerges of two electrons running around in a circle, each attracted to the polarization left behing by the other electron. Quantum mechanics tells us that this picture needs to be refined, and we will come back to that in great detail further on in this chapter. Nevertheless, the idea survives: as Cooper has shown[8], electron-phonon interaction can leads to the formation of a "molecule" of electrons, called a Cooper pair.

SUMMARY: WHAT WE LEARN FROM THE EXPERIMENTAL CLUES IS THE FOLLOWING: THE ELECTRONS IN A SUPERCONDUCTOR PAIR UP INTO "COOPER PAIRS", THAT ACT LIKE BOSONIC MOLECULES IN THE SENSE THAT THEY CAN UNDERGO BOSE-EINSTEIN CONDENSATION. THIS CHARGED CONDENSATE WILL LEAD TO SUPERFLUIDITY OF THE CHARGE CARRIERS: THEIR FRICTIONLESS FLOW EXPLAINS THE DISAPPEARANCE OF RESISTIVITY, AND THE POSSIBILITY TO HAVE PERSISTENT SHIELDING CURRENTS ALLOWS FOR PERFECT DIAMAGNETISM.

3.3   Penrose-Onsager-Yang criterion

First, we'll look at what "a condensate of pairs" means, irrespective of the particular glue that is used to make pairs. This part of the chapter is rather technical, and in a first reading you can skip to the next section, on the

---

[7] J. Bardeen, D. Pines, Phys. Rev. **99**, 1140 (1955).
[8] L.N. Cooper, Phys. Rev. **104**, 1189 (1956).

Ginzburg-Landau equations. Remember that for bosons we derived a criterion for condensation – the goal here is to extend this criterion to a fermi gas where pairing is possible. This in turn will provide a microscopic justification of the Ginzburg-Landau theory that we'll explore in the next section.

3.3.1 Density matrices

In second quantization, we can write the Hamiltonian of an interacting Fermi gas with field operators as follows:

$$\hat{H} = \int d\mathbf{r}\ \hat{\psi}^\dagger(\mathbf{r})H_0(\mathbf{r})\hat{\psi}(\mathbf{r}) + \frac{1}{2}\int d\mathbf{r}\int d\mathbf{r}'\ \hat{\psi}^\dagger(\mathbf{r})\hat{\psi}^\dagger(\mathbf{r}')V(\mathbf{r}-\mathbf{r}')\hat{\psi}(\mathbf{r}')\hat{\psi}(\mathbf{r}).$$
(3.37)

Here $\hat{\psi}^\dagger(\mathbf{r})$ (and $\hat{\psi}(\mathbf{r})$) create (respectively annihilate) an electron in a localized state $|\mathbf{r}\rangle$. Note that we don't write down the spin degrees of freedom explicitly, we could do that by writing $\hat{\psi}^\dagger(\mathbf{r},\sigma)$ that creates an electron with spin σ in at position $|\mathbf{r}\rangle$. In the above Hamiltonian V is the effective two-particle interaction potential (including any "glue" that is present) and

$$H_0(\mathbf{r}) = -\frac{\hbar^2}{2m}\nabla_\mathbf{r}^2 + V_1(\mathbf{r}) - \mu$$
(3.38)

is the single-particle part of the Hamiltonian – $V_1(\mathbf{r})$ can be a trapping potential or an external field. The chemical potential μ will be used to fix the total number of particles.

The many-body quantum states are described by a many-body wave function $\Psi(\mathbf{r}_1,...,\mathbf{r}_N)$, or alternatively, the density matrix that we have also defined and used in the first chapter:

$$\rho(\mathbf{r}_1,..,\mathbf{r}_N;\mathbf{r}_1',..,\mathbf{r}_N') = \Psi^*(\mathbf{r}_1,...,\mathbf{r}_N)\Psi(\mathbf{r}_1',...,\mathbf{r}_N').$$
(3.39)

We'll need both the first-order and now also the second-order reduced density matrices, and their representation with field operators:

$$\rho_1(\mathbf{r};\mathbf{r}') = \int d\mathbf{r}_2\int d\mathbf{r}_N\ \Psi^*(\mathbf{r},\mathbf{r}_2,...,\mathbf{r}_N)\Psi(\mathbf{r}',\mathbf{r}_2',...,\mathbf{r}_N') = \left\langle\hat{\psi}^+(\mathbf{r})\hat{\psi}(\mathbf{r}')\right\rangle,$$
(3.40)

and

$$\begin{aligned}\rho_2(\mathbf{x},\mathbf{y};\mathbf{y}',\mathbf{x}') &= \int d\mathbf{r}_3\int d\mathbf{r}_N\ \Psi^*(\mathbf{x},\mathbf{y},\mathbf{r}_2,...,\mathbf{r}_N)\Psi(\mathbf{y}',\mathbf{x}',\mathbf{r}_2',...,\mathbf{r}_N')\\ &= \left\langle\hat{\psi}^+(\mathbf{x})\hat{\psi}^+(\mathbf{y})\hat{\psi}(\mathbf{y}')\hat{\psi}(\mathbf{x}')\right\rangle.\end{aligned}$$
(3.41)

The knowledge of these two reduced density matrices suffice to calculate the expectation value of the Hamiltonian,

$$\left\langle\hat{H}\right\rangle = \int d\mathbf{r}\ H_0(\mathbf{r})\rho_1(\mathbf{r};\mathbf{r}')|_{\mathbf{r}'=\mathbf{r}} + \frac{1}{2}\int d\mathbf{r}\int d\mathbf{r}'\ V(\mathbf{r}-\mathbf{r}')\rho_2(\mathbf{r},\mathbf{r}';\mathbf{r}',\mathbf{r}).\ (3.42)$$

That's nice: we don't need to know a function of 10^{23} position coordinates, functions of at most four positions turn out to be enough.

But how would you find these density matrices? What equation must they satisfy? Their time dependence (in the Heisenberg picture) must be given by the Heisenberg equation of motion for $\hat{\psi}^+(\mathbf{r})\hat{\psi}(\mathbf{r}')$:

$$
\begin{aligned}
i\hbar\frac{d\rho_1(\mathbf{r};\mathbf{r}')}{dt} &= \left\langle i\hbar\frac{d}{dt}\left[\hat{\psi}^+(\mathbf{r})\hat{\psi}(\mathbf{r}')\right]\right\rangle \\
&= \left\langle \left[\hat{\psi}^+(\mathbf{r})\hat{\psi}(\mathbf{r}'),\hat{H}\right]\right\rangle
\end{aligned}
\tag{3.43}
$$

Plugging in the Hamiltonian, and using the anticommutation relations between the fermionic field operators, results in:

$$
\begin{aligned}
i\hbar\frac{d\rho_1(\mathbf{r};\mathbf{r}')}{dt} &= \left[H_0(\mathbf{r})-H_0(\mathbf{r}')\right]\rho_1(\mathbf{r};\mathbf{r}') \\
&\quad + \int d\mathbf{x}\ \left[V(\mathbf{x}-\mathbf{r})-V(\mathbf{x}-\mathbf{r}')\right]\rho_2(\mathbf{r},\mathbf{x};\mathbf{x},\mathbf{r}')
\end{aligned}
\tag{3.44}
$$

As you can see, the equation for ρ_1 depends on ρ_2. If you now go and set up the equation for ρ_2, you'll find that this depends on ρ_3, etc. The result is a hierarchy of equations (like the BBGKY hierarchy), that you'll need to break off at some point if you want to close the set of equations. On the other hand, if you have ρ_n you can find all the lower-order reduced density matrices from it. Indeed, if you know ρ_2, you can also simply trace out a variable, and find

$$
\rho_1(\mathbf{x};\mathbf{x}') = \int d\mathbf{y}\ \frac{1}{2}\left[\rho_2(\mathbf{x},\mathbf{y};\mathbf{x}',\mathbf{y}) \pm \rho_2(\mathbf{y},\mathbf{x};\mathbf{y},\mathbf{x}')\right]
\tag{3.45}
$$

The upper sign is for bosons, the lowe sign for fermions (the present case).

3.3.2   Pair condensation of fermions

The Penrose-Onsager criterion for Bose-Einstein condensation (in interacting Bose gases) stated that BEC occurs if and only if one of the eigenvalues of ρ_1 becomes macroscopically large (i.e. compareable to the total number of particles). Since these eigenvalues turn out to be the occupation of the Hartree-Fock states (the best suited single-particle states), and fermions cannot be with more than one in the same single-particle state, it is clear that for fermions all eigenvalues of ρ_1 should be less than or equal to one. So, according to Penrose-Onsager (and common sense) fermions cannot undergo Bose-Einstein condensation.

But many bosons, such as ^{4}He, are composite objects rather than point bosons. They are built up from a bunch of fermions (protons, neutrons, electrons are all fermions). Another example are molecules. Take a fermionic atom such as deuterium D (1 proton+1 neutron+1 electron = an odd number of fermionic building blocks = a fermion). Molecules of D_2 will obey Bose statistics, as long as you work at energy scales that are small compared to the binding energy. Clearly, we need to extend the Penrose-Onsager criterium to allow for the condensation of even clusters of fermions.

This extension was formulated by C.N. Yang[9], who defined it in analogy with the Penrose-Onsager criterion as follows:

---

[9] C. N. Yang, *Concept of Off-Diagonal Long-Range Order and the quantum phases of liquid He and superconductors*, Rev. Mod Phys. **34**, 694-704 (1962).

Pair condensation (in a Fermi system) occurs if and only if the second order reduced density matrix has an eigenvalue that becomes macroscopically large (i.e. compareable to the number of fermions N).

The second-order reduced density matrix is Hermitian, and thus can be diagonalized with real eigenvalues

$$\rho_2(\mathbf{r}_1, \mathbf{r}_2; \mathbf{r}'_1, \mathbf{r}'_2) = \sum_i \nu_i \chi_i(\mathbf{r}_1, \mathbf{r}_2) \chi_k^*(\mathbf{r}'_1, \mathbf{r}'_2). \qquad (3.46)$$

where for fermions the eigenfunctions need to be antisymmetric, $\chi_k(\mathbf{r}_1, \mathbf{r}_2) = -\chi_k(\mathbf{r}_2, \mathbf{r}_1)$. The eigenvalues must satisfy

$$\sum_i \nu_i = N(N-1) \qquad (3.47)$$

where N is the number of particles. Yang showed that for fermions these must satisfy $\nu_i \leqslant N$. Intuitively these eigenvalues v_k can be interpreted as the number of atomic pairs that occupy the two-particle state $\chi_k(\mathbf{r}_1, \mathbf{r}_2)$. This is similar to the interpretion of the eigenvalues of the first-order reduced density matrix as the number of atoms having the corresponding eigenfunction for effective single-particle state. In order to classify the possible two-particle states[10], we introduce the center of mass coordinate and the relative coordinate,

$$
\begin{aligned}
\mathbf{r} &= (\mathbf{r}_1 + \mathbf{r}_2)/2 \\
\mathbf{x} &= \mathbf{r}_2 - \mathbf{r}_1
\end{aligned}
$$

and make the *assumption* that the two-particle wave functions can be factorized in a center-of-mass piece and a wave function for the relative coordinate,

$$\chi_i(\mathbf{r}_1, \mathbf{r}_2) = \Psi_i(\mathbf{r})\phi_i(\mathbf{x}). \qquad (3.48)$$

Certainly, if you look at hydrogen atoms (built out of two fermions: a proton + an electron), this is very familiar. It is in fact the very first thing you do when solving the Schrödinger equation for the hydrogen atom: you factorize out the center of mass coordinate. The wave function of the internal coordinate is then solved and depends on the glue between the proton and the electron (in casu: the Coulomb potential between them). The wave function of the internal coordinate is what you know as all the orbitals of the hydrogen atom, and you tend to forget about the center of mass piece, assuming that it is a plane wave or a free particle.

When the system (and thus ρ_2) have translational invariance, we indeed must have $\Psi_i(\mathbf{r}) = \exp\{i\mathbf{K} \cdot \mathbf{r}\}$ with $\mathbf{K}$ the center of mass momentum. Then we can divide the eigenfunctions χ_i into three classes, depending on the value of $\mathbf{K}$, and on whether or not $\phi_i(\mathbf{x})$ is bounded. By bounded, we mean mathematically that $|\chi_i|^2$ decays faster than $1/x^2$ as $x \to \infty$. When $\phi_i(\mathbf{x})$ is bounded, the relative coordinate wavefunction is localized in space, meaning that the two particles stay closely together. The three classes are:

---

[10]For the classification of the eigenfunctions, I follow *"The BEC–BCS Crossover: Some History and Some General Observations"* by A.J. Leggett and S. Zhang (chapter 2 in the book *"The BCS–BEC Crossover and the Unitary Fermi Gas"* edited by W. Zwerger (publ. Springer-Verlag, 2012)).

- "**scattering state**" pair wavefunctions: ϕ unbound and $\mathbf{K}$ can be anything. We always have of the order of N^2 of these, and they have eigenvalue ≈ 1. For a non-interacting fermi gas, all the eigenfunctions are of this type since we just have plane waves for all electrons, $\chi_i(\mathbf{r}_1, \mathbf{r}_2) = e^{i\mathbf{k}_1 \cdot \mathbf{r}_1} e^{i\mathbf{k}_2 \cdot \mathbf{r}_2}$. It is also clear that we have of order N^2 of these in the limit of tightly bound molecules, simply because if you pick two fermions at random, it is highly likely that these fermions will belong to different molecules and thus be uncorrelated.

- "**preformed pairs**": ϕ bound, $\mathbf{K} \neq \mathbf{0}$.

- "**condensed pairs**": ϕ bound, $\mathbf{K} = \mathbf{0}$.

The classes of preformed pairs and condensed pairs taken together intuitively describe any bound pairs that occur in the system. Such bound pairs are expected to occur when there is an attractive interaction present. The number of relevant (i.e. with non-negligible eigenvalues) eigenfunctions in these two classes can be at most N, because the sum rule (3.47) must hold and we already have N^2 scattering pair states.

The onset of pairing (for example with decreasing temperature) can be thought of as the point at which the sum of eigenvalues for preformed and condensed pair wave functions becomes of order N. These pairs (or molecules, for strong binding) are not necessarily condensed, that is why we refer to most of these states are "preformed pairs". The onset of pair condensation is the point at which the number of condensed pairs becomes of order N, i.e. one gets back to the simple BEC picture and only one relevant bound pair wave function $\chi_0(\mathbf{r}_1, \mathbf{r}_2) = \phi_0(\mathbf{r}_2 - \mathbf{r}_1)$,

$$\rho_2(\mathbf{r}_1, \mathbf{r}_2; \mathbf{r}_1', \mathbf{r}_2') \approx v_0 \chi_0(\mathbf{r}_1, \mathbf{r}_2) \chi_0^*(\mathbf{r}_1', \mathbf{r}_2') + \rho_2^{fluct} \qquad (3.49)$$

We see that ρ_2 only has non-negligible contributions for $\mathbf{r}_1 \approx \mathbf{r}_1', \mathbf{r}_2 \approx \mathbf{r}_2'$, or $\mathbf{r}_1 \approx \mathbf{r}_2', \mathbf{r}_2 \approx \mathbf{r}_1'$ or $\mathbf{r}_1 \approx \mathbf{r}_2, \mathbf{r}_1' \approx \mathbf{r}_2'$, where it is dominated by the first term. Just as we did for the Bose gas, we can then use this to estimate the energy as a function of $\chi_0(\mathbf{r}_1, \mathbf{r}_2)$, in order to try and find an equation that χ_0 has to satisfy. This is our road to generalize the Gross-Pitaevskii equation to the case of fermion pairs.

3.3.3   Energy of the pair condensate

The energy can be written via $\left\langle \hat{H} \right\rangle = \mathrm{Tr}[\hat{\rho}\hat{H}]$ as

$$
\begin{aligned}
E &= \int d\mathbf{r}_1 \int d\mathbf{r}_2 \frac{1}{2m} \left([-i\hbar \boldsymbol{\nabla}_{\mathbf{r}_1} - q\mathbf{A}(\mathbf{r}_1)]^2 \right. \\
&\quad \left. + [-i\hbar \boldsymbol{\nabla}_{\mathbf{r}_2} - q\mathbf{A}(\mathbf{r}_2)]^2 \right) \rho_2(\mathbf{r}_1, \mathbf{r}_2; \mathbf{r}_1', \mathbf{r}_2') \Big|_{\mathbf{r}_1' = \mathbf{r}_1, \mathbf{r}_2' = \mathbf{r}_2} \\
&\quad + \frac{1}{2} \int d\mathbf{r}_1 \int d\mathbf{r}_2 V(\mathbf{r}_2 - \mathbf{r}_1) \rho_2(\mathbf{r}_1, \mathbf{r}_2; \mathbf{r}_2, \mathbf{r}_1) \qquad (3.50)
\end{aligned}
$$

Here we have included the electromagnetic effects, assuming that our fermions have a charge q and there is a vector potential $\mathbf{A}$. It is the canonical momentum

$\mathbf{p} = m\mathbf{v} + q\mathbf{A}$ that gets "quantized" to $-i\hbar\boldsymbol{\nabla}$, rather than the kinematical momentum $m\mathbf{v}$, so that we need to write the kinetic energy as $mv^2/2 = (\mathbf{p} - q\mathbf{A})^2/(2m)$. For ^{6}Li atoms, $q = 0$, for electrons $q = -e = -1.6 \times 10^{-19}$ C.

We'll now plug in our $\rho_2(\mathbf{r}_1, \mathbf{r}_2; \mathbf{r}_1', \mathbf{r}_2')$ for pair condensation. To do this, we decompose the pair wavefunctions in center of mass and relative coordinate as before. For the condensed pair we write

$$\sqrt{v_0}\chi_0(\mathbf{r}_1, \mathbf{r}_2) = \Psi(\mathbf{r})\phi_0(\mathbf{x}) \tag{3.51}$$

This incorporates the $\sqrt{v_0}$ factor into the center of mass wavefunction, renormalizing it like in the ordinary Penrose-Onsager case to $\Psi(\mathbf{r}) = \sqrt{v_0}\Psi_0(\mathbf{r})$. For identical fermions, the antisymmetry condition implies $\phi(-\mathbf{x}) = -\phi(\mathbf{x})$, and $\Psi(-\mathbf{r}) = \Psi(\mathbf{r})$. It is in this sense that we can claim that the pairs condensate wave function $\Psi(\mathbf{r})$ behaves "bosonically". The fermionic nature is relegated to the internal clockwork of the composite particle.

We need to rewrite (3.50) into relative coordinate and center-of-mass coordinate, using

$$\mathbf{r}_{1,2} = \mathbf{r} \pm \mathbf{x}/2, \quad \text{and} \quad \boldsymbol{\nabla}_{\mathbf{r}_{1,2}} = \frac{1}{2}\boldsymbol{\nabla}_{\mathbf{r}} \pm \boldsymbol{\nabla}_{\mathbf{x}} \tag{3.52}$$

from which

$$\boldsymbol{\nabla}_{\mathbf{r}_1}^2 + \boldsymbol{\nabla}_{\mathbf{r}_2}^2 = \frac{1}{2}\boldsymbol{\nabla}_{\mathbf{r}}^2 + 2\boldsymbol{\nabla}_{\mathbf{x}}^2. \tag{3.53}$$

We get (in the transverse gauge):

$$\sum_{j=1}^{2}\left[-\frac{\hbar^2}{2m}\boldsymbol{\nabla}_{r_j}^2 + 2i\hbar q\mathbf{A}(\mathbf{r}_j)\boldsymbol{\nabla}_{\mathbf{r}_j} + q^2\mathbf{A}^2(\mathbf{r}_j)\right] \tag{3.54}$$

$$= -\frac{\hbar^2}{2m}\left(\frac{1}{2}\boldsymbol{\nabla}_{\mathbf{r}}^2 + 2\boldsymbol{\nabla}_{\mathbf{x}}^2\right) + q^2\left[\mathbf{A}^2\left(\mathbf{r} - \frac{\mathbf{x}}{2}\right) + \mathbf{A}^2\left(\mathbf{r} - \frac{\mathbf{x}}{2}\right)\right]$$

$$-i\hbar q\left[\mathbf{A}\left(\mathbf{r} - \frac{\mathbf{x}}{2}\right) + \mathbf{A}\left(\mathbf{r} + \frac{\mathbf{x}}{2}\right)\right]\boldsymbol{\nabla}_{\mathbf{r}} + 2i\hbar q\left[\mathbf{A}\left(\mathbf{r} + \frac{\mathbf{x}}{2}\right) - \mathbf{A}\left(\mathbf{r} - \frac{\mathbf{x}}{2}\right)\right]\boldsymbol{\nabla}_{\mathbf{x}}$$

You see that this simplifies a lot when $\mathbf{A}$ is smooth over the distance of the Cooper pair. If we keep effects up to order $\nabla^2\mathbf{A}$ (as this is related to currents, from the Maxwell equations), we get

$$\sum_{j=1}^{2}\left[-\frac{\hbar^2}{2m}\boldsymbol{\nabla}_{r_j}^2 + 2i\hbar q\mathbf{A}(\mathbf{r}_j)\boldsymbol{\nabla}_{\mathbf{r}_j} + q^2\mathbf{A}^2(\mathbf{r}_j)\right]\chi_0(\mathbf{r}_1, \mathbf{r}_2) \tag{3.55}$$

$$= \frac{[-i\hbar\boldsymbol{\nabla}_{\mathbf{r}} - Q\mathbf{A}(\mathbf{r})]^2}{2M} - \frac{\hbar^2}{2m}\boldsymbol{\nabla}_{\mathbf{x}}^2 - q\left(\nabla^2\mathbf{A}(\mathbf{r})\right)[\mathbf{x} \cdot (i\hbar\boldsymbol{\nabla}_{\mathbf{r}} - q\mathbf{A}(\mathbf{r}))]$$

with $Q = 2q$ and $M = 2m$. With this we can write

$$E = \int d\mathbf{r}\ \Psi^*(\mathbf{r})\left\{\frac{[-i\hbar\boldsymbol{\nabla}_{\mathbf{r}} - Q\mathbf{A}(\mathbf{r})]^2}{2M}\right\}\Psi(\mathbf{r}) + E_\phi[\Psi] \tag{3.56}$$

with

$$
\begin{aligned}
E_\phi[\Psi] &= \int d\mathbf{x}\ \phi_0(\mathbf{x}) \left\{ -\frac{\hbar^2}{2m}\boldsymbol{\nabla}_{\mathbf{x}}^2 + V(\mathbf{x}) \right. \tag{3.57}\\
&\quad \left. -q \int d\mathbf{r}\ \Psi^*(\mathbf{r}) \left(\nabla^2 \mathbf{A}(\mathbf{r}) \right) \left[\mathbf{x} \cdot (i\hbar\boldsymbol{\nabla}_{\mathbf{r}} - q\mathbf{A}(\mathbf{r})) \right] \Psi(\mathbf{r}) \right\} \phi_0^*(\mathbf{x})
\end{aligned}
$$

The contribution $E_\phi[\Psi]$ is *almost* the binding energy that we'd calculate with for the relative coordinate problem. Sometimes, the terms mixing $\Psi(\mathbf{r})$ and $\phi_0(\mathbf{x})$ are small. This occurs when the gradients of $\Psi(\mathbf{r})$ and/or the magnetic field is small over the size of the pair. Then the problem separates nicely into internal degrees of freedom and external degrees of freedom (as for the hydrogen atom). But, as we know from Pippard's result, this is not the case for Cooper pairs. We need to be more careful! The energy of the pair condensate depends on $\Psi(\mathbf{r})$, and we can expand it as a function of $|\Psi(\mathbf{r})|^2$

$$
E_\phi[\Psi(\mathbf{r})] = a + \frac{b}{2}\,|\Psi(\mathbf{r})|^2 + ... \tag{3.58}
$$

Indeed, as long as $\Psi(\mathbf{r})$ does not have a phase oscillating many times over the size of the pair, a reasonable assumption, E_ϕ will be a function of $|\Psi(\mathbf{r})|^2$ as can be seen from (3.57). This is the basis for the Ginzburg-Landau theory, which we will explore in the next subsection.

SUMMARY: THE EIGENFUNCTIONS OF THE SECOND ORDER REDUCED DENSITY MATRIX CAN BE CLASSIFIED AS SCATTERING STATES, PREFORMED PAIRS AND CONDENSED PAIRS. WHEN THE SUMMED EIGENVALUES OF PAIR STATES BECOMES OF ORDER N, WE HAVE PAIR FORMATION IN THE FERMI SYSTEM. WHEN THE EIGENVALUE OF ONE PARTICULAR PAIR STATE BECOMES OF ORDER N, WE HAVE BOSE-EINSTEIN CONDENSATION OF FERMION PAIRS. FACTORING THE CONDENSED PAIR WAVE FUNCTION IN CENTER OF MASS AND RELATIVE COORDINATE, WE OBTAIN THE CENTER OF MASS WAVE FUNCTION THAT TAKES ON THE ROLE OF THE CONDENSATE WAVE FUNCTION.

3.4   Ginzburg-Landau formalism

3.4.1   Ginzburg-Landau energy functional

First, we consider the case without magnetic field. The discussion of the previous section encourage us to claim that there will again be a macroscopic wave function, which we can treat as the order parameter of the superconducting state. This means that near the critical temperature, the free energy F_s of the superconducting state can be expanded as a function of this order parameter since it is small:

$$
F_s(T,V) = F_n(T,V) + V\left(a(T)\,|\Psi|^2 + \frac{b(T)}{2}\,|\Psi|^4 + ...\right) \tag{3.59}
$$

We use the free energy rather than the internal energy since the former is a function of temperature whereas the latter is a function of entropy, and we

prefer calculating properties at a given temperature to calculating them at a fixed entropy. We also define our expansion constants for the free energy per unit volume, which is why the volume appears explicitly and a bit clumsily here.

When the order parameter turns to zero $|\Psi|^2 \to 0$, we recover the free energy of the normal state, $F_n(T)$. From the previous section, we also know that when Ψ is position dependent, there should be a gradient term, expressing the kinetic energy contribution to the total free energy, so let's add this:

$$
F_s(T,V) \;\; = \;\; F_n(T,V) + \int d\mathbf{r} \left\{ \Psi^*(\mathbf{r}) \frac{[-i\hbar\boldsymbol{\nabla}_{\mathbf{r}} - Q\mathbf{A}(\mathbf{r})]^2}{2M} \Psi(\mathbf{r}) \right.
$$
$$
\left. + a(T)\,|\Psi(\mathbf{r})|^2 + \frac{b(T)}{2}\,|\Psi(\mathbf{r})|^4 \right\}. \tag{3.60}
$$

When $\Psi(\mathbf{r}) = |\Psi|$ is constant, this expression reverts to (3.59). In the kinetic energy term, we have included the effects of an external magnetic field (characterized by the corresponding vector potential) on the pair condensate[11]. Placing a superconductor in a magnetic field will induce shielding currents for the Meissner effect. But these in turn affect the magnetic field distribution near the superconductor! That is why we also want to keep track of the change in the energy of the magnetic field itself:

$$
\int d\mathbf{r} \frac{\mu \mathbf{H}^2(\mathbf{r})}{2} = \int d\mathbf{r} \frac{\mathbf{B}^2(\mathbf{r})}{2\mu} = \int d\mathbf{r} \frac{1}{2\mu} \left(\boldsymbol{\nabla}\times\mathbf{A}(\mathbf{r})\right)^2 \tag{3.61}
$$

Including this term in the free energy gives:

$$
F_s(T,V) \;\; = \;\; F_n(T,V) + \int d\mathbf{r} \left\{ \Psi^*(\mathbf{r}) \frac{[-i\hbar\boldsymbol{\nabla}_{\mathbf{r}} - Q\mathbf{A}(\mathbf{r})]^2}{2M} \Psi(\mathbf{r}) \right.
$$
$$
\left. + a(T)\,|\Psi(\mathbf{r})|^2 + \frac{b(T)}{2}\,|\Psi(\mathbf{r})|^4 + \frac{1}{2\mu}\left(\boldsymbol{\nabla}\times\mathbf{A}(\mathbf{r})\right)^2 \right\}. \tag{3.62}
$$

This is known as the **Ginzburg-Landau free energy**[12]. It is derived as an expansion in small $|\Psi(\mathbf{r})|$, so in principle it is only valid near T_c. In practice, its region of validity extends well below T_c. This is different from the Gross-Pitaevskii equation, which is derived at $T = 0$ (and for a neutral superfluid), and becomes less accurate as the temperature is increased.

3.4.2 Ginzburg-Landau equations

The GL free energy can be used as a variational energy functional, minimized by the true pair wave function $\Psi(\mathbf{r})$,

$$
\frac{\delta F_s}{\delta \Psi^*(\mathbf{r})} = 0. \tag{3.63}
$$

---

[11] We don't include effects linked with a scalar potential ϕ in the superconductor, since the perfect conduction nullifies any electric potential differences in the superconductor. Note that in some cases, ϕ might occur (as when we are moving vortices around), and then we'd need to include it. So, in essence, in this chapter we are restricting ourselves to *steady state* situations with magnetic fields only. Check out the books in the bibliography to open up the wider world of Ginzburg-Landau equations.

[12] V.L. Ginzburg and L.D. Landau, Zh. Eksp. Teor. Fiz. **20**, 1064 (1950).

Performing the functional derivative yields the **first Ginzburg-Landau equation**:

$$-\frac{\hbar^2}{2M}\left[\nabla_{\mathbf{r}} - \frac{iQ}{\hbar}\mathbf{A}(\mathbf{r})\right]^2 \Psi(\mathbf{r}) + a(T)\Psi(\mathbf{r}) + b(T)\left|\Psi(\mathbf{r})\right|^2 \Psi(\mathbf{r}) = 0 \qquad (3.64)$$

This looks very similar to the Gross-Pitaevskii equation: again we find a non-linear Schrödinger-type equation. The mass appearing here is now the mass of the Cooper pair (twice the electron mass), and Cooper pair charge Q is $-2e$ with $e = 1.602... \times 10^{-19}$ C the elementary charge. Note that many handbooks give the formula CGS units.

As mentioned above, the vector potential is not just an external parameter, it is also affected by $\Psi(\mathbf{r})$. To find the correct vector potential we use Maxwell's equation in its variational form:

$$\mathbf{J}_s = -\frac{\delta F_s}{\delta \mathbf{A}(\mathbf{r})}. \qquad (3.65)$$

which results in an expression for the supercurrent density:

$$\mathbf{J}_s = \frac{iQ\hbar}{2M}\left[\Psi(\mathbf{r})\boldsymbol{\nabla}_{\mathbf{r}}\Psi^*(\mathbf{r}) - \Psi^*(\mathbf{r})\boldsymbol{\nabla}_{\mathbf{r}}\Psi(\mathbf{r})\right] - \frac{Q^2}{M}\left|\Psi(\mathbf{r})\right|^2 \mathbf{A}(\mathbf{r}). \qquad (3.66)$$

The first term is familiar from our study of superfluid currents: gradients in the order parameter's phase will lead to a flow of Cooper pairs. Indeed, with $\Psi(\mathbf{r}) = |\Psi(\mathbf{r})|\, e^{i\theta(\mathbf{r})}$ we could rewrite the first term as:

$$\mathbf{J}_s = Q\left|\Psi(\mathbf{r})\right|^2 \frac{\hbar}{2M}\boldsymbol{\nabla}\theta - \frac{Q^2}{M}\left|\Psi(\mathbf{r})\right|^2 \mathbf{A}(\mathbf{r}). \qquad (3.67)$$

This can be case in the usual expression for the current, $\mathbf{J}_s = qn\mathbf{v}_s$, where $n = \left|\Psi(\mathbf{r})\right|^2$ is the density of charge carriers, q their charge and

$$\mathbf{v}_s = \frac{\hbar}{2M}\left[\boldsymbol{\nabla}\theta - \frac{Q}{\hbar}\mathbf{A}(\mathbf{r})\right] \qquad (3.68)$$

the superfluid velocity. The second term is the London term. When $\Psi(\mathbf{r}) = |\Psi|$ is constant, this is the only term, and we get the London equation, with

$$\mathbf{J}_s = -\frac{Q^2}{M}\left|\Psi(\mathbf{r})\right|^2 \mathbf{A}(\mathbf{r}) = -\frac{1}{\mu\lambda_L^2}\mathbf{A} \Leftrightarrow \lambda_L = \sqrt{\frac{M}{\mu Q^2 \left|\Psi\right|^2}} \qquad (3.69)$$

Now flip back a few pages to equation (3.5)... These supercurrent adds to any externally applied currents $\mathbf{J}_{ext}$, and generate the total magnetic induction field in accordance with $\boldsymbol{\nabla} \times \mathbf{B} = \mu_v\left(\mathbf{J}_s + \mathbf{J}_{ext}\right)$. This leads us to the **second Ginzburg-Landau equation**:

$$\frac{1}{\mu}\nabla \times (\nabla \times \mathbf{A}) = \frac{iQ\hbar}{2M}\left[\Psi(\mathbf{r})\boldsymbol{\nabla}_{\mathbf{r}}\Psi^*(\mathbf{r}) - \Psi^*(\mathbf{r})\boldsymbol{\nabla}_{\mathbf{r}}\Psi(\mathbf{r})\right] - \frac{Q^2}{M}\left|\Psi(\mathbf{r})\right|^2 \mathbf{A}(\mathbf{r}) + \mathbf{j}_{ext}$$
$$(3.70)$$

The two Ginzburg-Landau ("GL") equations (3.64) and (3.70) are coupled. The first one can be thought of as the equation for the order parameter, influenced

by the vector potential, and the second one can be thought of as the equation for the vector potential, brought about both by external influenced and by the supercurrents. In general, they need to be solved simultaneously. The usual electromagnetic boundary conditions apply for the second equation, and for the first equation we require that there is no current of Cooper pairs going outside the superconductor:

$$\left(-i\hbar\nabla_{\mathbf{r}} - Q\mathbf{A}\right)\Psi(\mathbf{r})\big|_{\text{edge}} = 0.$$

This is suitable when the superconductor is bounded by vacuum or an insulator. De Gennes[13] found that for a metal the boundary condition

$$\left(-i\hbar\nabla_{\mathbf{r}} - Q\mathbf{A}\right)\Psi(\mathbf{r})\big|_{\text{edge}} = i\Psi(\mathbf{r}_{\text{edge}})/\gamma$$

is more appropriate, with a constant γ that depends on the metal ($\gamma \to \infty$ for an insulator, and $\gamma \to 0$ for a magnetic metal).

3.4.3 Empirical determination of the GL parameters

The GL parameters $a(T)$ and $b(T)$ are still undetermined... We could look at the microscopic theory, and derive them from that. However, it is very difficult to do so (although Gor'kov managed[14]). Moreover, for whole classes of superconductors (the cuprates or high-T_c superconductors, we don't even have a microscopic theory of the glue that binds the electrons. So, our best option there is to link these parameters to measurable quantities.

Let's first turn our attention to the case of a uniform bulk piece of superconductor, and no magnetic field. In the ground state for this uniform system, we do not expect any gradients in the order parameter, so $\Psi(\mathbf{r}) = |\Psi|$ is constant. In that case, the free energy

$$F_s(T, V) = F_n(T, V) + V \times \left(a(T)|\Psi|^2 + \frac{b(T)}{2}|\Psi|^4\right) \tag{3.71}$$

is minimized for

$$\frac{\partial F_s}{\partial |\Psi|^2} = 0 \Leftrightarrow |\Psi|^2 = -\frac{a}{b} \tag{3.72}$$

The free energy difference between the normal state and the superconducting state is

$$F_s - F_n = -\frac{a^2}{2b}V \tag{3.73}$$

We have a way to find the free energy difference: turn the magnetic field to its critical value. At the critical field, the energy $\mu H_c^2/2$ spent expelling the magnetic field is precisely equal to the energy gained from becoming superconductor, so we have

$$\frac{\mu H_c^2}{2} - \frac{a^2}{2b} = 0. \tag{3.74}$$

---

[13]P.G. De Gennes, *Superconductivity Of Metals And Alloys* (Westview Press, 1999, ISBN 0813345847).

[14]L.P. Gorkov, *"Microscopic derivation of the Ginzburg-Landau equations in the theory of superconductivity"*, Soviet Physics JETP **36**, 1364 (1959).

We need another equation relating the unknowns a, b to measurable properties. This turns out to be expression (3.69) for the London penetration depth

$$\lambda_L = \sqrt{\frac{M}{\mu Q^2 \left|\Psi\right|^2}} \Rightarrow \frac{M}{\mu \lambda_L^2 Q^2} = -\frac{a}{b} \tag{3.75}$$

Expressions (3.74),(3.75) allow to solve for a, b as a function of H_c and λ_L :

$$a = -\frac{2 \left(\mu e\right)^2}{m_e} \lambda_L^2 H_c^2, \tag{3.76}$$

$$b = \frac{4\mu^3 e^4}{m_e^2} \lambda_L^4 H_c^2. \tag{3.77}$$

Here, we've also used $Q = -2e$ and $M = 2m_e$. For some common superconductors, this gives

	λ_L (nm)	H_c (G)	$-a$ (μeV)	b (μeV·nm^3)	n_s (nm^{-3})
Sn	34	309	0.36	0.22	12
Al	16	105	0.0074	0.013	55
Pb	37	803	2.77	0.61	10
Cd	110	90	0.036	0.19	1.2
Nb	39	1980	13	1.38	9.3

Note that the results are expressed in μeV for energy and nm for lengths – Joules and metres would give tiny numbers. It is no coincidence that a has the same energy scale as the superconducting gap! From our study of Penrose-Onsager-Yang criterion, we obtained that the binding energy of the pairs $E_\phi[\Psi(\mathbf{r})] \approx a$, if we keep only the first term in the expansion (3.58).

From these numbers, we can also get the density of superconducting charge carriers, $n_s = -a/b$, shown in the last column. This shows that the density of superconducting charge carriers is compareable to the density of conduction electrons (also of order 10^{22} cm^{-3}, or 10 nm^{-3}). Keep in mind that the electron band mass in the material may be different from the bare electron mass that was used in computing the numbers for this table. In view of Pippard's insight – that the size of the Cooper pair, the Pippard correlation length – can be as large as one micron, we get a remarkable picture: the Cooper pairs must overlap in real space. In that sense Cooper pair condensates are very different from Bose condensates of molecules, where the size of the *internal (relative-coordinate)* part of the atom's wave function remains much smaller than the distance calculated from the density.

The temperature dependence of the critical magnetic field,

$$H_c(T) = H_c(0) \left[1 - \left(\frac{T}{T_c}\right)^2\right] \tag{3.78}$$

and of the London penetration depth,

$$\frac{1}{\lambda_L^2} \propto 1 - \left(\frac{T}{T_c}\right)^4 \tag{3.79}$$

can be used to determine the temperature dependence of the GL parameters. Near the critical temperature $(T \approx T_c)$ we find

$$a(T) = a(0)\frac{\left[1-\left(\frac{T}{T_c}\right)^2\right]^2}{1-\left(\frac{T}{T_c}\right)^4}$$

$$\Rightarrow \quad a(T) \approx -|a(0)|\left[1-\frac{T}{T_c}\right] \tag{3.80}$$

and

$$b(T) = b(0)\frac{1}{\left[1+\left(\frac{T}{T_c}\right)^2\right]^2}$$

$$\Rightarrow \quad b \approx \text{constant} \tag{3.81}$$

The behavior of a is not altogether unexpected. Indeed, if a can intuitively be related to the pair binding energy, then it should go from negative (bound pairs) below T_c to positive above T_c. The other coefficient, b, also has an intuitive interpretation coming from a comparison of the GL equation and the Gross-Pitaevskii equation. It can be though of as an interaction amplitude for the interaction between Cooper pairs. This is relatively temperature independent. Finally, note that the "small parameter expansion" is based on the order parameter $|\Psi|^2 = -a/b$, which grows proportional to $1 - T/T_c$ as T is lowered away from T_c.

SUMMARY: INDEPENDENTLY OF THE GLUE THAT BINDS THE PAIRS, THE PAIR CONDENSATE CAN ALWAYS BE DESCRIBED BY A MACROSCOPIC WAVE FUNCTION. THIS WAVE FUNCTION OBEYS THE GINZBURG-LANDAU EQUATIONS VALID NEAR T_c, WHICH NOW INCLUDE THE INTERACTION OF THE CHARGED SUPERFLUID WITH MAGNETIC FIELDS. THE TWO PARAMETERS, a AND b, APPEARING IN THIS THEORY CAN BE CALCULATED FROM CRITICAL MAGNETIC FIELD AND PENETRATION DEPTH, AND RELATE TO THE PAIR BINDING ENERGY (a) AND PAIR INTERACTION AMPLITUDE (b).

3.5 Type I and type II superconductivity

3.5.1 Coherence length

First, we look at an interface between a superconductor $(x > 0)$ and vacuum $(x < 0)$, in **the absence of magnetic fields**. Then we only need the first GL equation

$$-\frac{\hbar^2}{2M}\nabla_{\mathbf{r}}^2\Psi(\mathbf{r}) + a(T)\Psi(\mathbf{r}) + b(T)|\Psi(\mathbf{r})|^2\Psi(\mathbf{r}) = 0. \tag{3.82}$$

Since we don't want currents (no magnetic fields), $\Psi(\mathbf{r})$ should have a constant phase, so we can choose $\Psi(\mathbf{r})$ real. The derivation follows closely the derivation of the healing length for neutral condensates. That is, we set $\Psi(\mathbf{r}) = f(x)\Psi_{bulk}$

with $\Psi^2_{bulk} = -a/b = n_s$ the bulk density of cooper pairs. After this substitution, the GL equation becomes

$$-\frac{\hbar^2}{2M}\frac{\partial f}{\partial x} + af + b\left(\frac{-a}{b}f^2\right)f = 0,$$

$$\Leftrightarrow \frac{\hbar^2}{2M\,|a|}\frac{\partial f}{\partial x} + f - f^3 = 0. \qquad (3.83)$$

(keep in mind that $a < 0$). This makes it clear that the characteristic length scale for the variations in f is

$$\xi = \sqrt{\frac{\hbar^2}{2M\,|a|}}, \qquad (3.84)$$

the analogue of the healing length that we saw for Bose condensates. Here it is usually not called a healing length, but a **coherence length**. It is the smallest length scale over which the pair condensate wave function can vary.

There is a link with Pippard's correlation length $\xi_P = \hbar v_F/(k_B T_c)$ that we also denoted with the Greek letter xi. Remember that the Pippard correlation length is the size of the Cooper pair, or the extent of the relative-coordinate part of the pair wave function. If we confine a particle of mass M to an area of size ξ_P then its ground state $(T = 0)$ energy can be estimated as

$$E_\phi \approx \frac{\hbar^2}{2M\xi_P^2}. \qquad (3.85)$$

Since we also identified the GL parameter a with this binding energy, $E_\phi \approx a$, it is clear that $\xi \approx \xi_P$ at temperature zero. However, the coherence length ξ depends strongly on temperature, through $a(T)$. It even diverges at T_c, as

$$\xi(T) \propto |a|^{-1/2} \propto \frac{1}{\sqrt{1 - (T/T_c)}}. \qquad (3.86)$$

The pair condensate becomes very fragile near T_c. By rewriting T_c as a function H_c (using the BCS microscopic theory that we'll see later on), it is possible to express the ratio of the coherence length to the Pippard correlation length as

$$\frac{\xi}{\xi_P} = \frac{\pi}{2\sqrt{3}}\frac{H_c(0)\lambda_L(0)}{H_c(T)\lambda_L(T)} \qquad (3.87)$$

This in turn allows to write the coherence length more precisely as

$$\xi(T) \approx 0.74\frac{\xi_P}{(1 - T/T_c)^{1/2}} \qquad (3.88)$$

The prefactor depends on the purity of the superconductor (as we've seen when discussion the correlation length, this matters).

3.5.2   Superconductivity at interfaces

Again we consider our interface between a superconductor $(x > 0)$ and a vacuum $(x < 0)$. In fact, as far as the magnetic field and the order parameter are

concerned, the vacuum could just as well be the (non-magnetic) normal state. We will again look for solutions of the form $\Psi(\mathbf{r}) = f(x)\Psi_{bulk}$. For the vector potential, we look for solutions of the form $\mathbf{A} = A(x)\mathbf{e_y}$ so that the magnetic field points along the z-axis. Then the first GL equation is

$$-\frac{1}{\xi^2}\frac{\partial^2 f(x)}{\partial x^2} + \frac{Q^2}{\hbar^2\xi^2}A^2(x)f(x) + f(x) - f^3(x) = 0, \qquad (3.89)$$

and the second is

$$\frac{\partial^2 A(x)}{\partial x^2} - \frac{f(x)}{\lambda_L^2}A(x) = 0. \qquad (3.90)$$

Note how ξ, the coherence length, determines the fundamental length scale of the first GL equation, the one for the order parameter. The fundamental length scale of the second equation, the one for the vector potential, is determined by λ_L, the London penetration depth. Both equations have to be solved jointly, and with boundary equations

$$A(x = 0) = A_{ext}, \qquad \left.\frac{\partial f(x)}{\partial x}\right|_{x=0} = 0 \qquad (3.91)$$

These can only be solved numerically, for general ξ and λ_L. However, for $\xi \gg \lambda_L$ or for $\lambda_L \gg \xi$, the equations tend to decouple. In the first case $\xi \gg \lambda_L$, the magnetic field drops very quickly to zero, so we obtain again equation (3.83) for GL1, and since $f(x)$ cannot vary much over a scale much smaller than ξ, we get simple exponential decay for $A(x)$ in GL2. In the other extreme, $\lambda_L \gg \xi$, the condensate heals very rapidly, and we again obtain the ordinary London equation for GL2, whereas we have just a constant A in the first GL equation.

This means that in both cases, $A(x)$ decays roughly from its bulk value to zero on a scale λ_L and $\Psi(x)$ grows roughly on a scale ξ. Numerical solutions show that this general statement always holds. The top row in figure (3.13) shows examples for $\xi \gg \lambda_L$ (left) and $\lambda_L \gg \xi$ (right).

How much energy does it cost to create a superconductor-normal interface? Firstly, near the interface we have to destroy the Cooper pair condensate. We already know that this costs an energy $(F_s - F_n)/V = \mu H_c^2/2$ per unit volume. At a certain depth x, the pair condensate density is a fraction $f^2(x)$ of its bulk value. So the energy per unit surface that we loose from broken up pairs in the layer between x and $x + dx$ is

$$\epsilon_C(x) = -\frac{\mu H_c^2}{2}\left[1 - f^2(x)\right]dx. \qquad (3.92)$$

This is indicated as the grey shaded areas in the bottom row in figure (3.13). We don't know the precise shape of $f(x)$, so we'll approximate by using the fact that the pair condensate is destroyed up to a depth ξ. In that case, the total energy per unit surface lost to breaking up pairs is

$$E_C \approx -\frac{\mu H_c^2}{2}\xi \qquad (3.93)$$

Secondly, near the interface we can allow some magnetic flux to enter the superconductor. The magnetic energy gained per unit surface, at a depth $x, x + dx$ will be $\epsilon_B(x) \propto A^2(x)dx$. Again, we do not know the precise shape
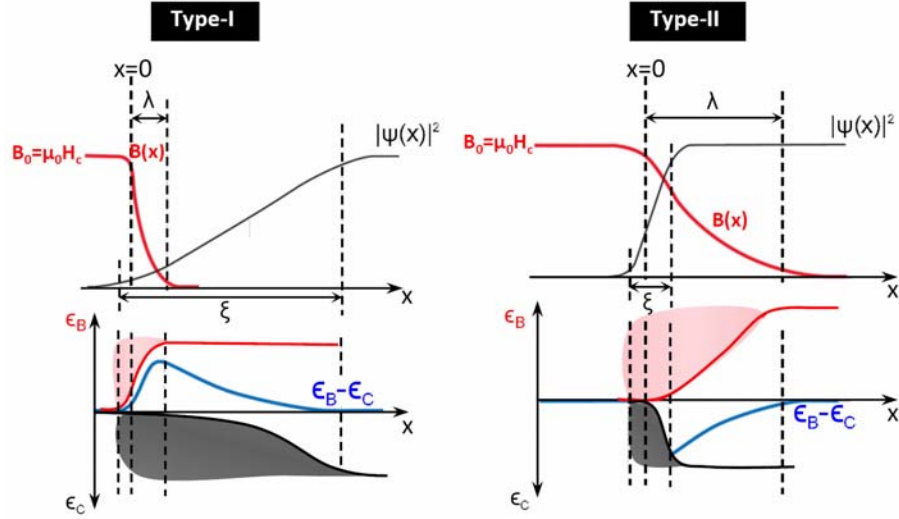
Figure 3.13: The top row shows the magnetic field profile (red) and the order parameter profile (black) as a function of position in a superconductor ($x > 0$) - vacuum ($x < 0$) interface. Left column is for type I, right column is for type II. The bottom row illustrates the balancing between the energy needed to expell the magnetic field (ϵ_B, red), and the energy required to break up cooper pairs (ϵ_C, black) in the interface region [my thanks go to Bart Raes for making this figure].

of $A(x)$, but we know it decays over a length scale λ_L – as illustrated in figure (3.13). So, the total magnetic energy per unit surface that we gain from allowing the flux to seep in is

$$E_B \approx +\frac{\mu H^2}{2}\lambda_L \tag{3.94}$$

The net energy gain per unit surface, from having a normal-superconducting interface, is

$$\gamma \approx \frac{\mu H^2}{2}\lambda_L - \frac{\mu H_c^2}{2}\xi \tag{3.95}$$

Near the critical magnetic field, $H \approx H_c$, this energy gain becomes

$$\gamma \approx \frac{\mu H_c^2}{2}\left(\lambda_L - \xi\right) \tag{3.96}$$

This is negative for $\xi \gg \lambda_L$: in that case the system doesn't like interfaces between normal and superconducting state. It will prefer to be either fully normal or fully superconducting. This is the characteristic behavior of a type I superconductor. However, γ is positive for $\lambda_L \gg \xi$ – so in that case the systems prefers to have a lot of normal-superconducting interfaces, and it will spontaneously generate them. What configuration would guarantee the maximum amount of normal-superconducting interface, keeping in mind that the interface has a "thickness" $\max(\lambda_L, \xi)$?   One could imagine it stacks

interfaces, alternating stripes of normal and superconducting state. That pijama motif sure has a lot of interface length. But you could now also make stripes in the orthogonal direction, having squares, with even more interface length. The true pattern will be a vortex lattice, as shown by Abrikosov. Vortices are the topic of our next section.

The typology of superconductors is often represented using the ratio of penetration depth to coherence length:

$$\kappa = \lambda_L/\xi \tag{3.97}$$

From a more precise calculation with the Ginzburg-Landau equations one finds that $\kappa = 1/\sqrt{2}$ is the dividing point (sometimes called "Bogomolny" point). For $\kappa < 1/\sqrt{2}$ the normal-superconducting interface costs energy, and we get type I behavior, whereas for $\kappa > 1/\sqrt{2}$ making interfaces is energetically advantageous, and we get type II behavior. However, nature is not so tidy, and many compounds with κ close to $1/\sqrt{2}$ show "intermediate" behavior[15] near $H = H_{c_1}$, such as the intricate patterns of superconductor and normal state shown in figure 3.6, leading to magnetizations that look more like the bottom panel of figure 3.3.

SUMMARY: COHERENCE LENGTH AND PENETRATION DEPTH ARE THE TYPICAL LENGTH SCALES OVER WHICH THE SUPERCONDUCTING PAIR CONDENSATE AND THE MAGNETIC FLUX VARY, RESPECTIVELY. THEIR RATIO, $\kappa = \lambda_L/\xi$ DETERMINES WHETHER THE MATERIAL BEHAVES AS TYPE I (FOR κ SMALL) OR TYPE II (FOR κ LARGE).

3.5.3 Superconducting Vortices

The fluxoid

In neutral (Bose-Einstein) condensates, we have encountered vortices. These were lines around which circular superflow took place, such that the phase changed an integer number of times 2π as we go around. The condensate density had to go to zero at the vortex core. We only had a single length scale for all of this to happen, namely the healing length ξ.

In superconductors, vortices will also occur, but now the two length scales ξ and λ_L matter. We will study vortices in a strongly type II material, so $\xi \ll \lambda_L$. We know from the previous section that vortices can become important for those materials. Let's take a closer look at the supercurrent circling the vortex line, using expression (3.67). Substituting $Q = -2e$, $M = 2m_e$, and $\Psi(\mathbf{r}) = \sqrt{n_s}e^{i\theta}$ we get

$$\mathbf{J}_s = -2en_s \times \frac{\hbar}{2m}\left[\boldsymbol{\nabla}_{\mathbf{r}}\theta + \frac{2e}{\hbar}\mathbf{A}(\mathbf{r})\right] \tag{3.98}$$

$$\Rightarrow \mathbf{v}_s = \frac{\hbar}{2m}\left[\boldsymbol{\nabla}_{\mathbf{r}}\theta + \frac{2e}{\hbar}\mathbf{A}(\mathbf{r})\right] \tag{3.99}$$

---

[15] Keep in mind that also type II materials display perfect diamagnetism (Meissner state) below $H < H_{c_1}$ – we assumed $H \approx H_c$ in our estimation of γ, and this corresponds to the first critical field of type II materials.
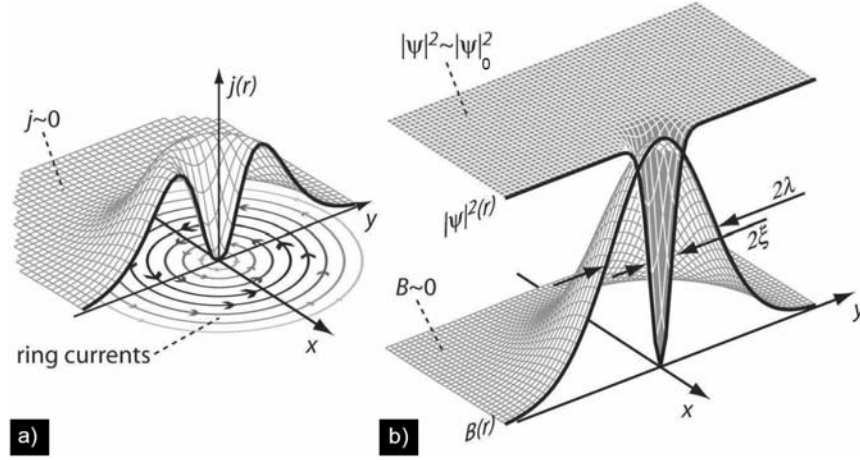
Figure 3.14: The spatial structure of a vortex in a type II material is shown here. On the left, the current density is seen to decay on the same length scale λ_L as the vector potential, with a dip in the middle, of size ξ, due to the fact that the pair condensate is destroyed in the eye of the "hurricane" that the vortex is. The right figure shows the Cooper pair density $|\Psi|^2$ (where $|\Psi_0|^2$ is the bulk value) and the magnetic flux density B. [my thanks go to Bart Raes for making this figure].

The vector potential acts like an additional phase gradient. This is not surprising, since gauge transformations result in a shift of the phase of wave functions. The prefactor $2e/\hbar$ is also $2\pi/\phi_0$ with the superconducting flux quantum,

$$\phi_0 = \frac{h}{2e} = 2.067 \text{ mT } \mu\text{m}^2 = 2.067 \times 10^{-7} \text{ gauss cm}^2. \tag{3.100}$$

The quantization of circulation around a loop C now becomes

$$\oint_C \mathbf{v}_s \cdot d\ell = \frac{\hbar}{2m} \left\{ \oint_C \boldsymbol{\nabla}_\mathbf{r} \theta \cdot d\ell + 2\pi \frac{\phi}{\phi_0} \right\} \tag{3.101}$$

with

$$\phi = \int \mathbf{B} \cdot d\mathbf{S} = \oint_C \mathbf{A}(\mathbf{r}) \cdot d\ell \tag{3.102}$$

the total flux. Using the fact that the macroscopic wave function is single valued, so its phase must have a change $\Delta\theta = 2\pi n$ with $n \in \mathbb{Z}$, we simplify (3.101) to

$$\oint_C \mathbf{v}_s \cdot d\ell = \frac{\hbar}{2m} 2\pi \left(n + \frac{\phi}{\phi_0} \right). \tag{3.103}$$

So, the total flux ϕ going through the loop that encircles the vortex is

$$\phi = n\phi_0 + \frac{2m}{h} \oint_C \mathbf{v}_s \cdot d\ell \qquad \text{with } n \in \mathbb{Z}. \tag{3.104}$$

London referred to the quantity ϕ is referred to as the "**fluxoid**": on top of the flux quanta it contains a contribution from phase gradients in the macroscopic wave function. The fluxoid formula (3.104) has two important consequences:

- If the flux through a superconducting ring is not precisely an integer number times the flux quantum, then a supercurrent must develop in the ring ($\mathbf{v}_s \neq 0 \Rightarrow \mathbf{J}_s = nQ\mathbf{v}_s \neq 0$) to compensate and make equation (3.104) hold.

- For a vortex bulk, we can take a loop with radius much larger than λ_L, and since $\mathbf{J}_s$ (like $\mathbf{A}$) drops down to zero at a typical distance λ_L, we find $\phi = n\phi_0$. **Superconducting vortices carry an integer number of flux quanta.**

Structure of the vortex

Next, we turn to the structure of a superconducting vortex, where the vortex line lies along the z-axis. We use the Ginzburg-Landau equations as we did to study interfaces, only now we will use cylindrical coordinates $\{\mathbf{r}, z\} = \{r, \varphi, z\}$. With (3.98) the second GL equation, $\nabla \times \mathbf{B} = \mu \mathbf{J}_s$, takes the form

$$\nabla \times \mathbf{B} = -2\mu e \left|\Psi(\mathbf{r})\right|^2 \frac{\hbar}{2m}\left[\boldsymbol{\nabla}\theta + \frac{2e}{\hbar}\mathbf{A}(\mathbf{r})\right] \tag{3.105}$$

Substitute $|\Psi(\mathbf{r})| = f(\mathbf{r})|\Psi_{bulk}|$ (with $\mathbf{r}$ the distance vector to the vortex line, in the plane perpendicular to the vortex), and take the curl of equation (3.105):

$$-\nabla^2\mathbf{B} = -\frac{\mu\left(2e\right)^2\left|\Psi_{bulk}\right|^2}{2m}\boldsymbol{\nabla}\times\left[\frac{\hbar}{2e}f^2(\mathbf{r})\boldsymbol{\nabla}\theta + f^2(\mathbf{r})\mathbf{A}(\mathbf{r})\right] \tag{3.106}$$

Now, the assumption $\xi \ll \lambda_L$ means that the pair condensate will have healed to its bulk value at a very short distance from the vortex center, and the variations of the vector potential take place over a much longer scale. Hence, we can set. $f(\mathbf{r}) = 1$ for $\mathbf{r} \neq 0$ and get

$$\begin{aligned}-\nabla^2\mathbf{B} \quad &= -\ \frac{\mu\left(2e\right)^2\left|\Psi_{bulk}\right|^2}{2m}\boldsymbol{\nabla}\times\mathbf{A}(\mathbf{r})\\ \Leftrightarrow \quad &\lambda_L^2\nabla^2\mathbf{B} - \mathbf{B} = 0 \text{ for } \mathbf{r} \neq 0\end{aligned} \tag{3.107}$$

This is just the London equation. We have to be a bit more careful for $\mathbf{r} = 0$. There, the rapid variation in $f(\mathbf{r})$ will result in a delta-function contribution. The strength of the delta function has units of flux density, We know that the vortex carries a flux quantum, so the strength of the delta function cannot be anything else but the flux carried by the vortex,

$$\lambda_L^2\nabla^2\mathbf{B} - \mathbf{B} = \phi\delta(\mathbf{r})\mathbf{e}_z \tag{3.108}$$

Using cylindrical coordinates and substituting $\mathbf{B} = B(r)\mathbf{e}_z$ we find

$$\lambda_L^2\frac{1}{r}\frac{\partial}{\partial r}\left(r\frac{\partial}{\partial r}B(r)\right) - B(r) = \phi\frac{\delta(r)}{2\pi} \tag{3.109}$$

The solution of this equation is

$$B(r) = \frac{\phi}{2\pi\lambda_L^2} K_0(r/\lambda_L) \tag{3.110}$$

with K_0 the (zeroeth order) modified Bessel function of the second kind. For a singly-quantized vortex, $\phi = \phi_0$. The flux density B is of the order of $\phi_0/(\pi\lambda_L)$, confirming that the flux quantum spreads out in space over an area of size λ_L. This analytical solution, valid in the extreme type II limit ($\kappa \gg 1$) is also known as the London vortex. The corresponding supercurrent density is

$$\mathbf{J}_s(\mathbf{r}) = -\frac{1}{\mu}\frac{\partial B}{\partial r}\mathbf{e}_\varphi = \frac{\phi}{2\pi\mu\lambda_L^3} K_1(r/\lambda_L)\mathbf{e}_\varphi \tag{3.111}$$

A more precise result (also valid in the region $r < \xi$) was obtained by Clem[16]:

$$B(r) = \frac{\phi}{2\pi\lambda_L^2} \frac{K_0\left(\sqrt{r^2 + \xi^2}/\lambda_L\right)}{(\xi/\lambda_L)K_1(\xi/\lambda_L)} \tag{3.112}$$

This result, along with the corresponding current profile, is shown in figure 3.14. Outside of the vortex core region ($r < \xi$) the exponential decay –through the modified Bessel function) of both current density and flux density can be seen.

Remark: we looked at vortices in bulk superconductors. For smaller lengths of vortices, in thin films, the boundary conditions are seen to influence the solution, and the flux is not as tightly confined (to a tube of size λ_L) as in bulk. Pearl[17] has shown that one gets a good approximation to the solution by replacing the penetration depth with an effective length scale

$$\Lambda = 2\lambda_L^2/d, \tag{3.113}$$

which of course is only valid for film thicknesses $d < \lambda_L$. This means that as far as vortex properties are concerned, thin films of type I material act like type II materials: indeed $\kappa = \Lambda/\xi$ grows as d becomes smaller.

Intervortex interactions and Abrikosov lattice

In type I superconductors, where $\xi \gg \lambda_L$, the interaction between two vortices is determined by the overlap of their huge cores rather than the small region inside the core where the magnetic field can penetrate. It is energetically advantageous to put the two "holes" in the pair condensate on top of each other, and merge the vortices. That way, less pair condensate is destroyed. Indeed, we know that type I materials prefer to be either completely superconducting or completely normal.

However, in type II superconductors with $\lambda_L \gg \xi$, the region where the pair condensate is depleted is small and the magnetic field reaches much further. There, the interaction is dominated by the magnetic energy, thus by the

---

[16] J.R. Clem, *Simple model for the vortex core in a type II superconductor*, J. Low. Temp. Phys. **18**, 427 (1975).
[17] J. Pearl. *"Current distribution in superconducting films carrying quantized fluxoids"*, Applied Physics Letters **5**, 65 (1964).
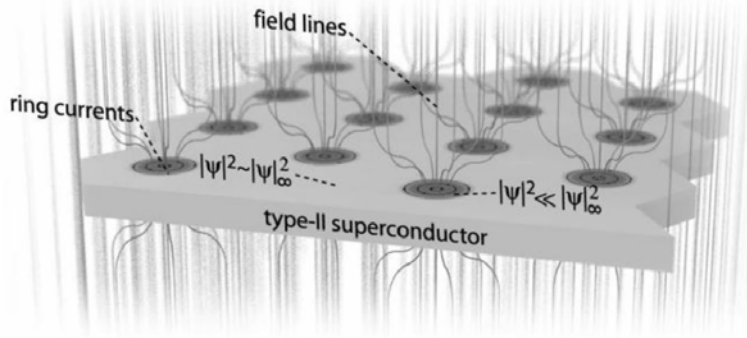
Figure 3.15: An Abrikosov lattice of superconducting vortices [source: V. Moshchalkov and J. Fritzsche, Nanostructured superconductors. World Scientific Publ. Co., Inc., 2011]

supercurrents circling the vortex. In neutral condensates, the superfluid flow pattern around the vortices determined the intervortex interaction, and led to vortex repulsion. Also here, the supercurrents (and the magnetic energy) is reduced in the region between two vortices, so nature strives to make this region as large as possible, and same-circulation vortices experience a mutual repulsion. The repulsion potential is derived from Ginzburg-Landau theory in more detail in the appendix.

The result of this intervortex repulsion in type-II materials is twofold:

- Doubly quantized vortices will prefer to break up into two singly quantized vortices that move as far apart from each other as they can.

- When increasing the magnetic field, as more singly quantized vortices come into the material, they will arrange themselves in a triangular lattice, the Abrikosov lattice, so as to sit as far as possible from eachother.

The Abrikosov lattice is illustrated in figure 3.15. In a type II superconductor placed in an external magnetic flux density B, the intervortex distance in this lattice is

$$a_v = \sqrt{\frac{2}{\sqrt{3}} \frac{\phi_0}{B}},$$

as can be checked with simple geometry. Vortices are pushed closer together as the magnetic flux density is increased. Finally, as a_v becomes of a size compareable to ξ, the vortex core regions will start to overlap, and the entire superconductor will turn to the normal state. Hence, the second critical field is given by

$$\mu H_{c_2} \approx \frac{2}{\sqrt{3}} \frac{\phi_0}{\xi^2}, \tag{3.114}$$

which can become very large as ξ gets very small. Finally, note that when $\kappa \approx 1/\sqrt{2}$ the situation is again much more complex, and the interaction potential between vortices may acquire both attractive and repulsive parts.
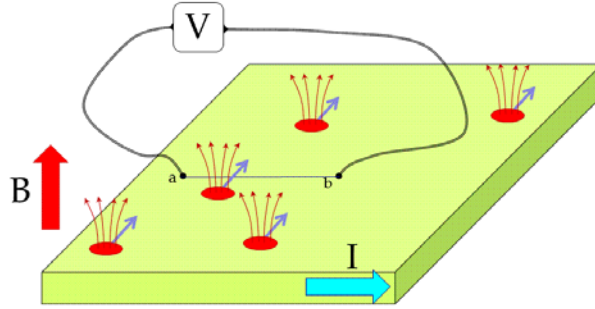
Figure 3.16: Vortices (red circles with flux lines pointing out) subject to a current **I** will move transverse to the current due to the Lorentz force, and generate an electromotive force in the voltmeter circuit.

Pinning and dissipation

Vortices (of length L) carry a quantum of magnetic flux. This means that they will feel the Lorentz force when subject to an electric current desity **J**. The Lorentz Force is given by

$$\mathbf{F} = \int d\mathbf{r} \ (\mathbf{J} \times \mathbf{B}).$$
(3.115)

Each vortex carries a flux ϕ_0, and has a corresponding flux density of the order of ϕ_0/λ_L^2. So, in a current **J**, vortices will be pulled in a direction perpendicular to J and perpendicular to the vortex line, as illustrated in figure **??**. Vortice move transversally to the applied current.

Now consider a voltmeter, whose probes we place in a and b as in figure **??**. In the Meissner state, there should be no voltage drop between these points, because the superconductor has zero resistivity. However, when vortices are present (for $H > H_{c_1}$) the situation is different. Indeed, when a vortex crosses the line ab, this means that a flux ϕ_0 has entered the closed circuit a-b-voltmeter-a. A changing flux leads to an electromotive force according to Faraday's law,

$$V = -\frac{d\phi}{dt}$$
(3.116)

If N vortices cross the line per unit time, the voltage drop will be $V = -N\phi_0$. However, this means we have both a voltage drop along the line ab, and a current along that line. So, there is a nonzero resistivity! Moving vortices lead to energy dissipation, and the reappearance of resistivity.

This is bad news when you want to make a strong electromagnet with a superconductor. When vortices occur and move around, the associated rise in resistivity heats up the material, so it may turn to the normal state, with an even larger resistivity, and the whole electromagnet melts or explodes. In order to avoid this, it is important that the vortices do not move. Luckily there is a trick to achieve this: pinning. The presence of defects or impurities in the superconductor pins vortices. There is no pair condensate density anyway in an impurity, so when threading the vortex line through the impurity, there is no

cost to making the hole in the condensate. It is energetically advantageous to keep the vortex pinned on the impurity. However, as the current is increased, the increased Lorentz force may unpin the vortices, so the maximum current will be limited not by the critical current, but by the unpinning current.

3.6 BCS theory

The Ginzburg-Landau theory describes the pair condensate's order parameter, independently of the glue that binds the fermions into pairs. For the conventional superconductors, we know the glue (indeed we're going to describe the pairing in detail in this chapter). For the cuprates, and more recently the iron pnictides, the nature of the glue is unknown. Nevertheless, Ginzburg-Landau theory works just as well for the conventional superconductors such as tin or mercury, as for the high-temperature classes of superconductors such as cuprates. For the conventional superconductors, we can derive the GL parameters from the microscopic theory, for the other classes we need to pin the GL parameters from experimental measurements.

So, the GL theory doesn't tell us anything about the nature of the pairs, or the nature of the excitations. Certainly, we expect some new excitations such as the breaking up of pairs. Moreover, GL theory is formulated so it is valid near the critical temperature, where an expansion in powers of the order parameter makes sense. If we want to go beyond these inherent limitations of GL theory, we need to set up the microscopic theory that describes pair formation. That is what we will do in the present chapter – to put it colloquially, with GL theory we looked at the center-of-mass factor in the pair wave function, now we'll look at the relative-coordinate factor of the pair wave function.

3.6.1 BCS Hamiltonian

From the key experiments discussed in section 2 of this chapter, we posited that electrons form bound pairs. The isotope effect in particular indicates that it is the electron-phonon interaction that leads to the effective attraction between electrons. Which electrons will feel this attractive interaction the strongest? We have three criteria:

- Firstly, only the electrons in an energy band $\mathcal{D} = [E_F - \hbar\omega_D, E_F + \hbar\omega_D]$ can scatter phonons that have a typical energy $\hbar\omega_D$, the Debye energy. This is because electrons on energy levels deeper than $\hbar\omega_D$ below the Fermi energy do not have unoccupied states to scatter to. Typically E_F is on the order of 10 eV, and $\hbar\omega_D$ is about 10-100 meV, so we have $\hbar\omega_D \ll E_F$.

- Secondly, electrons with opposite momentum will form pairs with the lowest kinetic energy, with total momentum zero. In a homogeneous system, we expect the total momentum-zero state to be the lowest one for the pairs, and the natural state in which to form a pair condensate.

- Thirdly, the glue will be strongest between electrons with opposite spin. The Pauli exclusion principle tells us that two electrons with the same spin cannot be found at the same place. The spatial overlap between

single-electron wave functions of electrons with opposite spin can therefore be made bigger than that for same-spin electrons, leading to a stronger pair binding energy.

These three features are the essence of the model Hamiltonian suggested by Bardeen, Cooper and Schrieffer to describe superconductivity. They were not looking for a complete description of the electron-phonon system, rather they were trying to distill the essence of superconductivity by searching for the simplest type of Hamiltonian that could exhibit superconductivity. Their "minimal model of superconductivity" is given by the BCS Hamiltonian[18]:

$$\hat{H}_{\mathrm{BCS}} = \sum_{\mathbf{k},\sigma} \varepsilon_{\mathbf{k}} \hat{c}^{\dagger}_{\mathbf{k},\sigma} \hat{c}_{\mathbf{k},\sigma} - U \sum_{\mathbf{k}\in\mathcal{D}} \sum_{\mathbf{k}'\in\mathcal{D}} \hat{c}^{\dagger}_{\mathbf{k},\uparrow} \hat{c}^{\dagger}_{-\mathbf{k},\downarrow} \hat{c}_{-\mathbf{k}',\downarrow} \hat{c}_{\mathbf{k}',\uparrow}. \tag{3.117}$$

Here we wrote down the Hamiltonian in second quantization, where $\hat{c}^{\dagger}_{\mathbf{k},\sigma}$ is a fermionic creation operator that creates an electron with spin $\sigma = \uparrow, \downarrow$ in a plane-wave state with wave number $\mathbf{k}$. The operator $\hat{c}_{\mathbf{k},\sigma}$ is the corresponding annihilation operator. A deeper introduction on these operators, and the second quantization formalism, can be found in the UA course on advanced quantum mechanics, and their application to condensed matter systems is described in the UA course on advanced solid state physics. We have already used bosonic creation and annihilation operators in our discussion of the Bogoliubov excitations, the fermionic ones anticommute:

$$\left\{ \hat{c}^{\dagger}_{\mathbf{k},\sigma}, \hat{c}_{\mathbf{k}',\sigma'} \right\} := \hat{c}^{\dagger}_{\mathbf{k},\sigma} \hat{c}_{\mathbf{k}',\sigma'} + \hat{c}_{\mathbf{k}',\sigma'} \hat{c}^{\dagger}_{\mathbf{k},\sigma} = \delta(\mathbf{k} - \mathbf{k}') \delta_{\sigma\sigma'} \tag{3.118}$$

The first term in the BCS Hamiltonian is the energy of the non-interacting Fermi gas where $\varepsilon_{\mathbf{k}} = (\hbar k)^2/(2m) - \mu$ is the single-particle energy corresponding to the plane wave state with momentum $\hbar\mathbf{k}$. Energies are measured from the Fermi level, $\mu = E_F$ (at temperature zero). At finite temperatures we'd need to calculate treat the chemical potential as a Lagrange multiplier fixing the number of particles, but as long as $T_c \ll T_F$ we can keep it fixed at E_F.

The second term describes the interactions. Normally you would find here the Coulomb interaction, to which a phonon-mediated interaction is added. In the BCS model this difficult interaction potential, envolving all electrons, is replaced by a constant-strength attractive potential acting only between electrons of opposite spin and opposite momentum, and within the Debye window $\mathcal{D}$. It describes the scattering of a pair of states with $\mathbf{k}, -\mathbf{k}$ into a pair with $\mathbf{k}', -\mathbf{k}'$, and assigns a constant scattering amplitude U to this process.

STEP 1 – MEAN FIELD ASSUMPTION. With such a strong simplification you would think the model is analytically solvable. But this is not yet the case, and we will look for a mean-field solution. This tinkers with the interaction term by replacing the product of four operators by a product of two operators and the expectation value of the product of the two others. Several different choices are possible for which two operators we keep, but we are not interested in the direct

---

[18]Subsequent researchers have been adding layers of complexity to make the model more realistic, such as $\mathbf{k}$-dependent interactions, or anisotropic Fermi surfaces, phonon density of states,... This can improve quantitatively the result for specific materials, but all of the qualitative results and a fair quantitative agreement is already obtained with the BCS model for all conventional superconductors.

and exchange contributions. The latter is not present by construction (opposite spins) and the former is not expected to change appreciable as we cross into the BCS regime. Indeed we can assume that the direct contribution contributes an interaction shift to the energies $\varepsilon_{\mathbf{k}}$ that does not vary much as we dip below T_c.

There is a third channel for decomposing:

$$\sum_{\mathbf{k}\in\mathcal{D}}\sum_{\mathbf{k}'\in\mathcal{D}}\hat{c}^{\dagger}_{\mathbf{k},\uparrow}\hat{c}^{\dagger}_{-\mathbf{k},\downarrow}\hat{c}_{-\mathbf{k}',\downarrow}\hat{c}_{\mathbf{k}',\uparrow}\approx$$

$$\sum_{\mathbf{k}\in\mathcal{D}}\sum_{\mathbf{k}'\in\mathcal{D}}\left\{\left\langle\hat{c}^{\dagger}_{\mathbf{k},\uparrow}\hat{c}^{\dagger}_{-\mathbf{k},\downarrow}\right\rangle\hat{c}_{-\mathbf{k}',\downarrow}\hat{c}_{\mathbf{k}',\uparrow}+\hat{c}^{\dagger}_{\mathbf{k},\uparrow}\hat{c}^{\dagger}_{-\mathbf{k},\downarrow}\left\langle\hat{c}_{-\mathbf{k}',\downarrow}\hat{c}_{\mathbf{k}',\uparrow}\right\rangle\right.$$

$$\left.-\left\langle\hat{c}^{\dagger}_{\mathbf{k},\uparrow}\hat{c}^{\dagger}_{-\mathbf{k},\downarrow}\right\rangle\left\langle\hat{c}_{-\mathbf{k}',\downarrow}\hat{c}_{\mathbf{k}',\uparrow}\right\rangle\right\} \tag{3.119}$$

This is at first sight a strange way to perform a mean-field approximation. Expectation values of a product of two creation operators, or two annihilation operators are usually zero. "Usually" here means that the wave function with respect to which we take the expectation value tends to be a number state, i.e. it has a fixed, given number of electrons. Only when we have superpositions of different number states expectation values such as $\left\langle\hat{c}^{\dagger}_{\mathbf{k},\uparrow}\hat{c}^{\dagger}_{-\mathbf{k},\downarrow}\right\rangle$ can be different from zero. This is precisely what occurs when Cooper pairing is present. You could think of a Cooper pair being created by an operator

$$\hat{b}^{\dagger}=\sum_{\mathbf{k}\in\mathcal{D}}\hat{c}^{\dagger}_{\mathbf{k},\uparrow}\hat{c}^{\dagger}_{-\mathbf{k},\downarrow} \tag{3.120}$$

When these pairs form a Bose-Einstein condensate, we can use the Bogoliubov shift. Indeed we used in the chapters on BEC that

$$\text{BEC}\Rightarrow\hat{b}^{\dagger}\approx\hat{b}\approx\left\langle\hat{b}^{\dagger}\right\rangle\approx\left\langle\hat{b}\right\rangle\approx\sqrt{N_c} \tag{3.121}$$

where N_c is the number of condensed bosons. This is the motivation to introduce the mean fields $\left\langle\hat{c}^{\dagger}_{-\mathbf{k},\downarrow}\hat{c}_{-\mathbf{k}',\downarrow}\right\rangle$ and $\left\langle\hat{c}_{-\mathbf{k}',\downarrow}\hat{c}_{\mathbf{k}',\uparrow}\right\rangle$! There is of course a big difference to keep in mind with "point" bosons: the operators $\hat{b},\hat{b}^{\dagger}$ introduced by (3.120) do not satisfy Bose commutation relations. So the usefulness of doing the mean-field decomposition as in (3.119) remains to be seen.

STEP 2 – INTRODUCE THE SELF-CONSISTENT GAP VARIABLE. Typically for mean-field treatments, we keep the mean-field as an auxiliary variable, solving the problem for arbitrary vale of the mean-field and then later calculating the value that we need from self-consistency equations. This is the path we will follow here. In fact, we will also absorb the interaction strength constant U in the self-constistent mean field, and introduce

$$\Delta=-U\sum_{\mathbf{k}'\in\mathcal{D}}\left\langle\hat{c}_{-\mathbf{k}',\downarrow}\hat{c}_{\mathbf{k}',\uparrow}\right\rangle \tag{3.122}$$

This allows to write the mean-field approximation (3.119) as

$$-U\sum_{\mathbf{k}\in\mathcal{D}}\sum_{\mathbf{k}'\in\mathcal{D}}\hat{c}^{\dagger}_{\mathbf{k},\uparrow}\hat{c}^{\dagger}_{-\mathbf{k},\downarrow}\hat{c}_{-\mathbf{k}',\downarrow}\hat{c}_{\mathbf{k}',\uparrow}$$

$$\approx\sum_{\mathbf{k}\in\mathcal{D}}\left(\Delta^{*}\hat{c}_{-\mathbf{k},\downarrow}\hat{c}_{\mathbf{k},\uparrow}+\hat{c}^{\dagger}_{\mathbf{k},\uparrow}\hat{c}^{\dagger}_{-\mathbf{k},\downarrow}\Delta\right)+\frac{|\Delta|^{2}}{U}. \tag{3.123}$$

The last term looks a bit odd, but it is necessary to avoid double-counting when we take the expectation value of the product of the four operators $\hat{c}^\dagger_{\mathbf{k},\uparrow}\hat{c}^\dagger_{-\mathbf{k},\downarrow}\hat{c}_{-\mathbf{k}',\downarrow}\hat{c}_{\mathbf{k}',\uparrow}$. This last term is not an operator and will not influence the diagonalisation of the BCS Hamiltonian. However, it is of importance to keep the zero of energy at the same place (E_F) during the calculation of the energy.

Whereas the direct contribution to the interaction energy is not expected to vary much as we dip below T_c, it is clear that Δ will be affected strongly. We expect it to be zero above T_c, where the ground state is a Landau liquid – a Fermi gas with effective energy levels $\xi_\mathbf{k}$ (lying closely to $\varepsilon_\mathbf{k}$ but shifted a bit due to the direct interaction). Below T_c, we hope to find pairs and $\Delta \neq 0$. Therefore we can use Δ as a (complex) order parameter of the BCS superconducting state[19].

This step has brought us to the following mean-field form of the BCS Hamiltonian:

$$\hat{H}^{\mathrm{mf}}_{\mathrm{BCS}} = \sum_{\mathbf{k},\sigma} \xi_\mathbf{k}\hat{c}^\dagger_{\mathbf{k},\sigma}\hat{c}_{\mathbf{k},\sigma} + \sum_{\mathbf{k}\in\mathcal{D}} \left(\Delta^*\hat{c}_{-\mathbf{k},\downarrow}\hat{c}_{\mathbf{k},\uparrow} + \hat{c}^\dagger_{\mathbf{k},\uparrow}\hat{c}^\dagger_{-\mathbf{k},\downarrow}\Delta \right) + \frac{|\Delta|^2}{U} \qquad (3.124)$$

Where I've written $\xi_\mathbf{k}$ rather than $\varepsilon_\mathbf{k}$ to remind us that we have swept direct interactions under the rug and focus in pairs. This Hamiltonian is now quadratic in the creation and annihilation operators and thus it can be diagonalised exactly.

STEP 3 – NAMBU SPINOR NOTATION. To perform the diagonalisation, Nambu rewrites the mean-field BCS Hamiltonian in matrix notation. This is done by introducing the spinors

$$\bar{c}_\mathbf{k} = \begin{pmatrix} \hat{c}_{\mathbf{k},\uparrow} \\ \hat{c}^\dagger_{-\mathbf{k},\downarrow} \end{pmatrix} \qquad (3.125)$$

$$\rightarrow \bar{c}^\dagger_\mathbf{k} = \begin{pmatrix} \hat{c}^\dagger_{\mathbf{k},\uparrow} & \hat{c}_{-\mathbf{k},\downarrow} \end{pmatrix} \qquad (3.126)$$

These allow to write the Hamiltonian (3.124) as

$$\hat{H}^{\mathrm{mf}}_{\mathrm{BCS}} = \sum_{\mathbf{k}\notin\mathcal{D},\sigma} \xi_\mathbf{k}\hat{c}^\dagger_{\mathbf{k},\sigma}\hat{c}_{\mathbf{k},\sigma} + \sum_{\mathbf{k}\in\mathcal{D}} \left(\bar{c}^\dagger_\mathbf{k} \cdot H_\mathbf{k} \cdot \bar{c}_\mathbf{k} + \xi_\mathbf{k} \right) + \frac{|\Delta|^2}{U} \qquad (3.127)$$

It is easy to check that when

$$H_\mathbf{k} = \begin{pmatrix} \xi_\mathbf{k} & \Delta \\ \Delta^* & -\xi_{-\mathbf{k}} \end{pmatrix} \qquad (3.128)$$

is substituted, this expession is identical to (3.124). Indeed the matrix product becomes

$$\begin{pmatrix} \hat{c}^\dagger_{\mathbf{k},\uparrow} & \hat{c}_{-\mathbf{k},\downarrow} \end{pmatrix} \cdot \begin{pmatrix} \xi_\mathbf{k} & \Delta \\ \Delta^* & -\xi_{-\mathbf{k}} \end{pmatrix} \cdot \begin{pmatrix} \hat{c}_{\mathbf{k},\uparrow} \\ \hat{c}^\dagger_{-\mathbf{k},\downarrow} \end{pmatrix}$$

$$= \begin{pmatrix} \hat{c}^\dagger_{\mathbf{k},\uparrow} & \hat{c}_{-\mathbf{k},\downarrow} \end{pmatrix} \cdot \begin{pmatrix} \xi_\mathbf{k}\hat{c}_{\mathbf{k},\uparrow} + \Delta\hat{c}^\dagger_{-\mathbf{k},\downarrow} \\ \Delta^*\hat{c}_{\mathbf{k},\uparrow} - \xi_{-\mathbf{k}}\hat{c}^\dagger_{-\mathbf{k},\downarrow} \end{pmatrix} \qquad (3.129)$$

---

[19] We can relate Δ to the pair condensate wave function that we introduced before, expression (3.51), $\sqrt{v_0}\chi_0(\mathbf{r}_1,\mathbf{r}_2) = \Psi(\mathbf{r})\phi_0(\mathbf{x})$. Now we study a homogeneous gas, with pair momenta $\mathbf{k} + (-\mathbf{k}) = 0$, so $|\chi_0(\mathbf{r}_1,\mathbf{r}_2)| \rightarrow \Delta$ as $|\mathbf{r}_2 - \mathbf{r}_1| \rightarrow \infty$.

so that

$$
\begin{aligned}
\bar{c}_{\mathbf{k}}^{\dagger} \cdot H_{\mathbf{k}} \cdot \bar{c}_{\mathbf{k}} &= \xi_{\mathbf{k}} \hat{c}_{\mathbf{k},\uparrow}^{\dagger} \hat{c}_{\mathbf{k},\uparrow} - \xi_{-\mathbf{k}} \hat{c}_{-\mathbf{k},\downarrow} \hat{c}_{-\mathbf{k},\downarrow}^{\dagger} + \Delta \hat{c}_{\mathbf{k},\uparrow}^{\dagger} \hat{c}_{-\mathbf{k},\downarrow}^{\dagger} + \Delta^{*} \hat{c}_{-\mathbf{k},\downarrow} \hat{c}_{\mathbf{k},\uparrow} \\
&= \xi_{\mathbf{k}} \hat{c}_{\mathbf{k},\uparrow}^{\dagger} \hat{c}_{\mathbf{k},\uparrow} - \xi_{-\mathbf{k}} + \xi_{-\mathbf{k}} \hat{c}_{-\mathbf{k},\downarrow}^{\dagger} \hat{c}_{-\mathbf{k},\downarrow} + \Delta \hat{c}_{\mathbf{k},\uparrow}^{\dagger} \hat{c}_{-\mathbf{k},\downarrow}^{\dagger} + \Delta^{*} \hat{c}_{-\mathbf{k},\downarrow} \hat{c}_{\mathbf{k},\uparrow}.
\end{aligned}
$$

The order of fermionic operators matters, and the minus sign disappears because

$$
\hat{c}_{-\mathbf{k},\downarrow} \hat{c}_{-\mathbf{k},\downarrow}^{\dagger} = 1 - \hat{c}_{-\mathbf{k},\downarrow}^{\dagger} \hat{c}_{-\mathbf{k},\downarrow}
$$

The "1" gives rise to the additional term $\xi_{\mathbf{k}}$ in (3.127). This Hamiltonian contains a lot of jetsam from the transformations, bookkeeping entries without operator character, keeping the zero of energy where it should be:

$$
\hat{H}_{\text{BCS}}^{\text{mf}} = \sum_{\mathbf{k} \notin \mathcal{D}, \sigma} \xi_{\mathbf{k}} \hat{c}_{\mathbf{k},\sigma}^{\dagger} \hat{c}_{\mathbf{k},\sigma} + \sum_{\mathbf{k} \in \mathcal{D}} \bar{c}_{\mathbf{k}}^{\dagger} \cdot H_{\mathbf{k}} \cdot \bar{c}_{\mathbf{k}} + \sum_{\mathbf{k} \in \mathcal{D}} \xi_{\mathbf{k}} + \frac{|\Delta|^{2}}{U} \qquad (3.130)
$$

The first term is the total energy of fermions in the Fermi deap-sea, those electrons that cannot participate in electron-phonon scattering. They must contribute exactly the same energy in the normal state as in the superconducting state, and are unimportant for comparing the energies of those two states. Let's indicate this term with $E_{deap\ sea}$. Only the second term still needs to be diagonalied.

3.6.2   Bogoliubov transformation

Step 4 – Diagonalisation. We look for a unitary transformation $B_{\mathbf{k}}$ that diagonalises the matrix $H_{\mathbf{k}}$. Unitarity means that $B_{\mathbf{k}}^{\dagger} B_{\mathbf{k}} = I$ with I the identity operator (unit matrix). First, we find the eigenvalues of $H_{\mathbf{k}}$:

$$
\begin{aligned}
&\left| \begin{matrix} \xi_{\mathbf{k}} - \lambda & \Delta \\ \Delta^{*} & -\xi_{-\mathbf{k}} - \lambda \end{matrix} \right| = 0 \\
\Leftrightarrow\quad & -(\xi_{k} - \lambda)(\xi_{k} + \lambda) - |\Delta|^{2} = 0 \\
\Leftrightarrow\quad & -\xi_{k}^{2} + \lambda^{2} - |\Delta|^{2} = 0 \\
\Leftrightarrow\quad & \lambda = \pm\sqrt{\xi_{k}^{2} + |\Delta|^{2}} \qquad (3.131)
\end{aligned}
$$

Here we assumed that $\xi_{\mathbf{k}}$ only depends on the magnitude of $\mathbf{k}$, not its direction. Most metals do not have a nice isotropic Fermi surface, but remember that BCS is looking for the simplest Hamiltonian that exhibits superconductivity, in an attempt to capture its essence, free of all superfluous baroque. For our standard treatment $\xi_{k} = (\hbar k)^{2}/2m - \mu$ so this is OK. The eigenvalues represent the Bogoliubov spectrum for superconductors:

$$
E_{k} = \sqrt{\left[\frac{(\hbar k)^{2}}{2m} - \mu \right]^{2} + |\Delta|^{2}} \qquad (3.132)
$$

There are two branches, $\lambda = \pm E_{k}$, that correspond to particle-like (+) and hole-like (-) excitations. Then, from the corresponding (normalized) eigenvectors we find the unitary matrices $B_{\mathbf{k}}$:

$$
B_{\mathbf{k}} = \frac{1}{\sqrt{2E_{k}}} \left(\begin{matrix} \sqrt{E_{k} + \xi_{k}} & \sqrt{E_{k} - \xi_{k}} \\ -\sqrt{E_{k} - \xi_{k}} & \sqrt{E_{k} + \xi_{k}} \end{matrix} \right). \qquad (3.133)
$$

This transformation is called the Bogoliubov. Simple matrix multiplication and

$$|\Delta| = \sqrt{(E_k + \xi_k)(E_k - \xi_k)} \qquad (3.134)$$

allows to show that this matrix is unitary, and that she transforms the Hamiltonian into:

$$B_{\mathbf{k}} \cdot H_{\mathbf{k}} \cdot B_{\mathbf{k}}^\dagger = \begin{pmatrix} E_k & 0 \\ 0 & -E_k \end{pmatrix} \qquad (3.135)$$

This allows to rewrite the reduced Hamiltonian as

$$\sum_{\mathbf{k} \in \mathcal{D}} \bar{c}_{\mathbf{k}}^\dagger \cdot H_{\mathbf{k}} \cdot \bar{c}_{\mathbf{k}} \;=\; \sum_{\mathbf{k} \in \mathcal{D}} \bar{c}_{\mathbf{k}}^\dagger \cdot (B_{\mathbf{k}}^\dagger B_{\mathbf{k}}) \cdot H_{\mathbf{k}} \cdot (B_{\mathbf{k}}^\dagger B_{\mathbf{k}}) \cdot \bar{c}_{\mathbf{k}} \qquad (3.136)$$

$$= \sum_{\mathbf{k} \in \mathcal{D}} \left(\bar{c}_{\mathbf{k}}^\dagger B_{\mathbf{k}}^\dagger \right) \cdot \left(B_{\mathbf{k}} H_{\mathbf{k}} B_{\mathbf{k}}^\dagger \right) \cdot (B_{\mathbf{k}} \bar{c}_{\mathbf{k}})$$

$$= \sum_{\mathbf{k} \in \mathcal{D}} \begin{pmatrix} \hat{\alpha}_{\mathbf{k},\uparrow}^\dagger & \hat{\alpha}_{-\mathbf{k},\downarrow} \end{pmatrix} \cdot \begin{pmatrix} E_k & 0 \\ 0 & -E_k \end{pmatrix} \cdot \begin{pmatrix} \hat{\alpha}_{\mathbf{k},\uparrow} \\ \hat{\alpha}_{-\mathbf{k},\downarrow}^\dagger \end{pmatrix}$$

Here we used (3.135) and introduced the transformed (Bogoliubov) operators:

$$\begin{pmatrix} \hat{\alpha}_{\mathbf{k},\uparrow} \\ \hat{\alpha}_{-\mathbf{k},\downarrow}^\dagger \end{pmatrix} \;=\; B_{\mathbf{k}} \bar{c}_{\mathbf{k}} \qquad (3.137)$$

$$= \frac{1}{\sqrt{2E_k}} \begin{pmatrix} \sqrt{E_k + \xi_k} & \sqrt{E_k - \xi_k} \\ -\sqrt{E_k - \xi_k} & \sqrt{E_k + \xi_k} \end{pmatrix} \begin{pmatrix} \hat{c}_{\mathbf{k},\uparrow} \\ \hat{c}_{-\mathbf{k},\downarrow}^\dagger \end{pmatrix}$$

Traditionally these are written as

$$\hat{\alpha}_{\mathbf{k},\uparrow} \;=\; u_k^* \hat{c}_{\mathbf{k},\uparrow} + v_k \hat{c}_{-\mathbf{k},\downarrow}^\dagger \qquad (3.138)$$

$$\hat{\alpha}_{-\mathbf{k},\downarrow}^\dagger \;=\; -v_k^* \hat{c}_{\mathbf{k},\uparrow} + u_k \hat{c}_{-\mathbf{k},\downarrow}^\dagger \qquad (3.139)$$

with

$$u_k \;=\; \sqrt{\frac{E_k + \xi_k}{2E_k}} \qquad (3.140)$$

$$v_k \;=\; \sqrt{\frac{E_k - \xi_k}{2E_k}} \qquad (3.141)$$

You're encouraged to investigate the analogy with (1.175)-(1.176) for the bosonic case. These notations are found in many handbooks following a different derivation of the BCS theory (the derivation also followed in our advanced solid state physics course). Although derived after BCS found their solution, the matrix formulation is very insightful and lends itself for generalizations, and we keep using it here. With the Bogoliubov operators, the BCS Hamiltonian is given:

$$\sum_{\mathbf{k} \in \mathcal{D}} \bar{c}_{\mathbf{k}}^\dagger \cdot H_{\mathbf{k}} \cdot \bar{c}_{\mathbf{k}} = \sum_{\mathbf{k} \in \mathcal{D}} \left(E_k \hat{\alpha}_{\mathbf{k},\uparrow}^\dagger \hat{\alpha}_{\mathbf{k},\uparrow} - E_k \hat{\alpha}_{-\mathbf{k},\downarrow} \hat{\alpha}_{-\mathbf{k},\downarrow}^\dagger \right) \qquad (3.142)$$

Direct substitution allows you to check that the new operators, the α's, also obey fermionic anticommutation relations, so that

$$\sum_{\mathbf{k} \in \mathcal{D}} \bar{c}_{\mathbf{k}}^\dagger \cdot H_{\mathbf{k}} \cdot \bar{c}_{\mathbf{k}} = \sum_{\mathbf{k} \in \mathcal{D},\sigma} E_k \hat{\alpha}_{\mathbf{k},\sigma}^\dagger \hat{\alpha}_{\mathbf{k},\sigma} - \sum_{\mathbf{k} \in \mathcal{D}} E_k \qquad (3.143)$$

The last sum no longer has operator character, and can be added into our growing list of jetsam that consitutes the ground state energy level. What is left, is a diagonalized Hamiltonian, describing fermionic quasi particles, created and annihilated by $\hat{\alpha}^{\dagger}_{\mathbf{k},\sigma}$ and $\hat{\alpha}_{\mathbf{k},\sigma}$ respectively. These quasi particle excitations contribute an energy $E_k > 0$, so the ground state of the system is the vacuum of the quasi-particles. The final, diagonalized mean-field Hamiltonian is

$$\hat{H}^{\mathrm{mf}}_{\mathrm{BCS}} = \left[E_{deap\ sea} + \sum_{\mathbf{k}\in\mathcal{D}} (\xi_k - E_k) + \frac{|\Delta|^2}{U} \right] + \sum_{\mathbf{k}\in\mathcal{D},\sigma} E_k \hat{\alpha}^{\dagger}_{\mathbf{k},\sigma} \hat{\alpha}_{\mathbf{k},\sigma} \qquad (3.144)$$

The terms between square brackets in (3.144) represent the energy of the α-vacuum, i.e. the ground state energy of the superconducting system, measured from the Fermi level. The next term, with the α-operators, describes the Bogoliubov excitations. This is analogous to the microscopic picture that we developed for superfluids, where we have a superfluid condensate and a gas of normal-state excitations carrying entropy and viscosity. The excitations of this normal-state are no longer free particles, they have a new dispersion spectrum E_k, that can lead to frictionless flow if the Landau criterion is satisfied. This is what we explore next.

3.6.3 BCS ground state, gap and excitation spectrum

The central result of the BCS theory is summarized in the mean-field result (3.144). We see that for $\mathbf{k} \notin \mathcal{D}$, in the Fermi deep sea, nothing is changed. In a thin "Debye" window around the Fermi surface, $\mathbf{k} \in \mathcal{D}$, the dispersion is changed into a new dispersion relation $E_{\mathbf{k}}$. Only if we take the limit $|\Delta| \to 0$ we retrieve the Fermi sphere, since

$$\lim_{\Delta\to 0} E_k = |\xi_k| \qquad (3.145)$$

We have $\xi_k = (\hbar k)^2/(2m) - \mu$, so that ξ_k is positive for $k > k_F$, and negative for $k < k_F$. So, from (3.140) and (3.141) we find:

$$\lim_{\Delta\to 0} u_k = \begin{cases} 0 \text{ voor } k < k_F \\ 1 \text{ voor } k > k_F \end{cases} \qquad (3.146)$$

$$\lim_{\Delta\to 0} v_k = \begin{cases} 1 \text{ voor } k < k_F \\ 0 \text{ voor } k > k_F \end{cases} \qquad (3.147)$$

This means that in the limit $\Delta \to 0$ the α-operators just become the creation and annihilation operators for the electrons when $k > k_F$, and for holes when $k < k_F$. For $\Delta \neq 0$ these operators will no longer create electrons (or holes) in plane wave states, but they result in quasiparticles. For helium we the Bogoliubov quasiparticles forming the normal fluid on top of the superfluid condensate were interpreted as phonons and rotons. In the BCS model these quasi-particles are interpreted as **broken cooper pairs.** The smallest possible excitation energy (at $k = k_F$) is $\min(E_k) = |\Delta|$. Hence we can interpret that gap $|\Delta|$ as a binding energy for a Cooper pair. Moreover, we can interpret $|\Delta|/(\hbar k_F)$ as the superfluid critical velocity according to the Landau criterion. **As long as $\Delta \neq 0$ there is a nonzero Landau critical velocity** and hence a nonzero critical current!
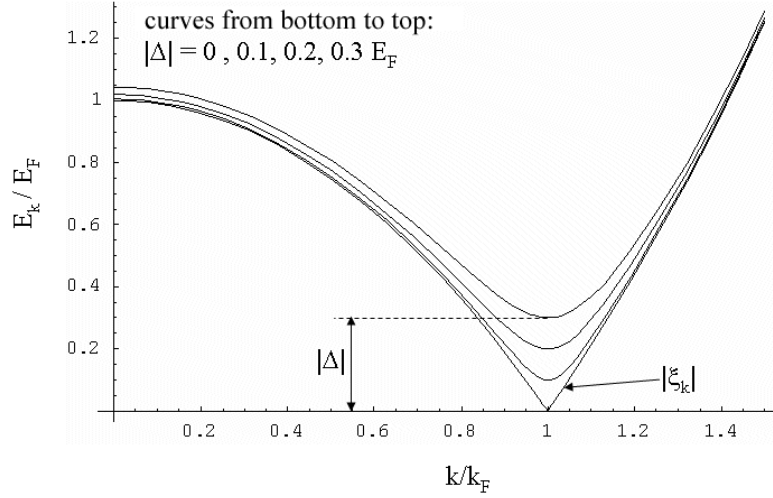
Figure 3.17: The Bogoliubov spectrum for a BCS superconductor.

In figure 3.17 Bogoliubov spectra are plotted for different values of $|\Delta|$. In practice $|\Delta| \ll \hbar\omega_D \ll E_F$, so the values of $|\Delta|$ are exaggerated for the sake of clarity in this figure. For wave vectors larger than the Fermi wave vector, the excitations are particle like, whereas for wave vectors below k_F we have hole-like excitations, with energy $\mu - (\hbar k)^2/(2m) = |\xi_k|$. Right at the fermi surface, in the normal state we can create excitations with no cost in energy at all. However, when $|\Delta|$ differs from zero, a bandgap appears! A strictly positive minimum energy needs to be invested in order to make an excitation. In the key experiments we have seen that the spectroscopic band gap is of the order of a few $100\,\mu$eV (so $|\Delta|/E_F$ is of the order $10^{-4} - 10^{-5}$). Note that the **spectroscopic band gap** equals $2|\Delta|$ rather than $|\Delta|$, since we need a photon that bridges the gap between the $+E_k$ and $-E_k$ branches, and at k_F the distance between these two branches is $2|\Delta|$. Note also that since $|\Delta|/(\hbar\omega_D)$ is of the order of $10^{-2} - 10^{-3}$, the dispersion relation is only changed in a very small piece of the Debye window – although all the electrons in the Debye window can potentially contribute to the superconducting energy, in practice only a small fraction of them actually do.

3.6.4   Critical magnetic field and density of states

The α-vacuum (=the BCS ground state=the pair condensate), has a lower energy than the normal state (=the Fermi sphere). We can calculate this energy from (3.144) by using that in the α-vacuum

$$\left\langle \alpha\text{-vac} \left| \sum_{\mathbf{k}\in\mathcal{D},\sigma} E_k \hat{\alpha}^\dagger_{\mathbf{k},\sigma} \hat{\alpha}_{\mathbf{k},\sigma} \right| \alpha\text{-vac} \right\rangle = 0 \qquad (3.148)$$

so that

$E_{BCS}(\Delta)$-$E_{BCS}(\Delta=0)$
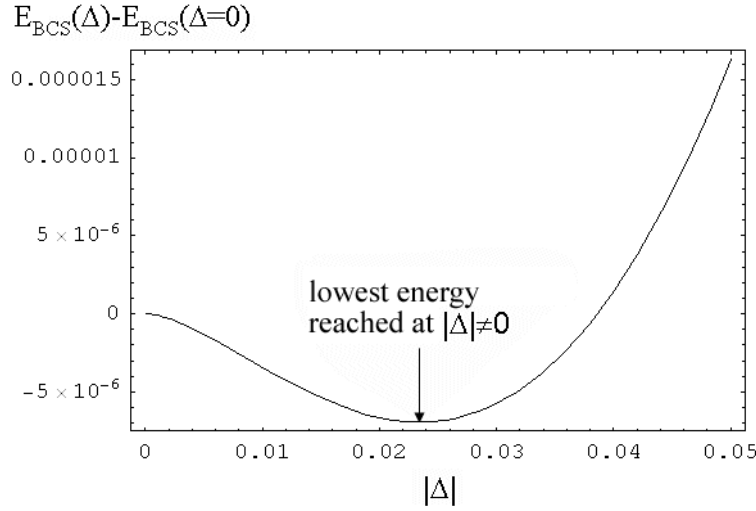
Figure 3.18: The energy difference between the superconducting state (with $\Delta \neq 0$) and the normal state ($\Delta = 0$) is shown, relative to the Fermi energy and in units of the Fermi energy. The parameters for this plot are $U = 10\ E_F$ and $\hbar\omega_D = 0.3\ E_F$, bot quite unrealistically large for the sake of clarity.

$$E_{\mathrm{BCS}}(\Delta) = E_{deap\ sea} + \sum_{\mathbf{k}\in\mathcal{D}} (\xi_k - E_k) + \frac{|\Delta|^2}{U}. \qquad (3.149)$$

Let's check again that the limit $|\Delta| \to 0$ is indeed the energy of the filled Fermi sphere:

$$
\begin{aligned}
E_{\mathrm{BCS}}(|\Delta| \to 0) &= E_{deap\ sea} + \sum_{\mathbf{k}\in\mathcal{D}} (\xi_k - |\xi_k|) \\
&= E_{deap\ sea} + 2 \sum_{\mathbf{k}\in\mathcal{D},\ k<k_F} \xi_k \\
&= 2 \sum_{\mathbf{k}<k_F} \xi_k \\
&= E_{\mathrm{fermi\ sphere}}
\end{aligned}
$$

Note that we measure the energies from E_F, i.e. we put the zero of energy for individual particles at E_F and for the collective N-particle system at NE_F. So with this choice of the zero of energy, we have $E_{\mathrm{fermi\ sphere}} = (3/5)NE_F - NE_F = -(2/5)NE_F$. We plot

$$\delta E = E_{\mathrm{BCS}}(\Delta) - E_{\mathrm{fermi\ sphere}}$$

in figure **??**, using equation (3.149). From this plot, it is clear that the minimum in energy is not reached at $|\Delta| = 0$ but in a state with $|\Delta| > 0$. The superconducting state has the lowest energy, and below T_c the Fermi sphere is unstable with respect to the superconducting state.

To find the value of this minimum, we plug in the Bogoliubov spectrum:

$$\delta E = \sum_{\mathbf{k} \in \mathcal{D}} \left(\xi_k - \sqrt{\xi_k^2 + |\Delta|^2} \right) + \frac{|\Delta|^2}{U} - 2 \sum_{\mathbf{k} \in \mathcal{D}, \; k < k_F} \xi_k \tag{3.150}$$

and replace the sums by integrals over the energy

$$\sum_{\mathbf{k} \in \mathcal{D}} F(\xi_k) = \int_{-\hbar \omega_D}^{+\hbar \omega_D} d\xi \; \mathcal{N}(\xi) F(\xi) \tag{3.151}$$

introducing the density of (normal) states $\mathcal{N}(\xi)$, calculated from the (normal) dispersion $\xi_k = (\hbar k)^2 / (2m) - \mu$. Near the Fermi surface, it is nearly constant, and we can replace it by the density of (normal) states at the Fermi surface

$$\mathcal{N}(0) = \frac{3}{2} \frac{N}{E_F}$$

so we get

$$\begin{aligned}
\delta E &= \mathcal{N}(0) \int_{-\hbar \omega_D}^{+\hbar \omega_D} \left(\xi - \sqrt{\xi^2 + |\Delta|^2} \right) d\xi + \frac{|\Delta|^2}{U} - 2\mathcal{N}(0) \int_{-\hbar \omega_D}^{0} \xi d\xi \\
&= 2\mathcal{N}(0) \int_{0}^{+\hbar \omega_D} \left(\xi - \sqrt{\xi^2 + |\Delta|^2} \right) d\xi + \frac{|\Delta|^2}{U}
\end{aligned} \tag{3.152}$$

Let's introduce

$$x = |\Delta| / (\hbar \omega_D) \tag{3.153}$$

and substitute $u = \xi / |\Delta|$ in the integral so we get

$$\frac{\delta E}{(\hbar \omega_D)^2 \mathcal{N}(0)} = \frac{x^2}{\mathcal{N}(0)U} - 2x^2 \int_{0}^{1/x} \left(\sqrt{u^2 + 1} - u \right) du \tag{3.154}$$

This simplifies to

$$\frac{\delta E}{(\hbar \omega_D)^2 \mathcal{N}(0)} = \frac{x^2}{\mathcal{N}(0)U} - x^2 \operatorname{arcsinh}(1/x) - \sqrt{x^2 + 1} + 1 \int_{0}^{1/x} \left(\sqrt{u^2 + 1} - u \right) du \tag{3.155}$$

This is actually the function plotted in figure **??**. It has extrema at

$$\frac{\partial (\delta E)}{\partial x} = 0 \Leftrightarrow \begin{cases} x = 0 \\ x = \dfrac{1}{\sinh \left[1 / (\mathcal{N}(0)U) \right]} \end{cases} \tag{3.156}$$

The $x = 0$ solution is the normal state, and the other solution is the normal state. The other solution depends on the combination $\lambda = \mathcal{N}(0)U$ which characterizes

the electron-phonon coupling strength. Since we know $|\Delta| / (\hbar \omega_D) \ll 1$ in practice, we obtain approximately

$$\boxed{|\Delta| = 2 \hbar \omega_D \exp \left\{ -\frac{1}{\mathcal{N}(0) U} \right\}} \tag{3.157}$$

This beautiful result explains two things: firstly, the isotope effect is present since the gap scales with the phonon frequency (we'll later see that the gap and the critical temperature are proportional), and secondly, all perturbation expansions for small U fail. Indeed, $|\Delta|$ has an essential singularity at $U = 0$. So, treating the interactions perturbatively and setting up a series for small U is bound to fail, and this is why it took such a long time to find a theory for superconductivity!

Plugging the result for $|\Delta|$ back into the energy, we get

$$\delta E = -\frac{1}{2} \left(\hbar \omega_D \right)^2 \mathcal{N}(0) \frac{1}{\sinh^2 \left[1 / \left(\mathcal{N}(0) U \right) \right]} = -\frac{1}{2} \mathcal{N}(0) |\Delta|^2 \tag{3.158}$$

The superfluid state is lower in energy, by an amount $-\mathcal{N}(0) |\Delta|^2 / 2$. This immediately gives us access to the critical magnetic field at zero temperature since we can equate the magnetic energy of expelling the critical field to the available energy from forming superconducting pairs:

$$\frac{\mu H_c^2}{2} = \frac{1}{2} \frac{\mathcal{N}(0)}{V} |\Delta|^2 \tag{3.159}$$

where V is the volume of the system so that $\mathcal{N}(0)/V = (3n)/(2 E_F)$ with n the (normal state) density of electrons in the metal.

We can get this result in a more intuitive way by studying the density of states (DOS) in the superconducting state, $\mathcal{N}_s(E)$. This will be different from the normal state DOS that we used before, $\mathcal{N}(\xi)$. The DOS will only be changed in a region very near to E_F, since for energies more than a few $|\Delta|$ away from E_F, the Bogoliubov spectrum reverts to ξ_k. To find the DOS, we use the fact that in **k**-space the density of states is fixed, $V/(2\pi)^3$, so that

$$\mathcal{N}_s(E) dE = \mathcal{N}(0) d\xi \tag{3.160}$$

Here we again replaced $\mathcal{N}(\xi)$ by $\mathcal{N}(0)$, the density of states at the Fermi surface. The Bogoliobov spectrum leads to $d\xi/dE = E/\sqrt{E^2 - |\Delta|^2}$ so that we get

$$\mathcal{N}_s(E) = \mathcal{N}(0) \frac{E}{\sqrt{E^2 - |\Delta|^2}} \quad \text{for } |E| > |\Delta| \tag{3.161}$$

and $\mathcal{N}_s(E) = 0$ for $|E| < |\Delta|$. This is shown in figure 3.19. In the band gap there are no states, as is obvious from the dispersion relation. Where the dispersion relation has a horizontal tangent, we have a Van Hove singularity. This occurs at $|E| = |\Delta|$. To excite a particle from the occupied bottom piece of the DOS to above the bandgap, we need to provide enough energy to cross the spectroscopic band gap $2|\Delta|$. These are the values measured by the AC conductivity key experiment mentioned before. The theoretical DOS, obtained
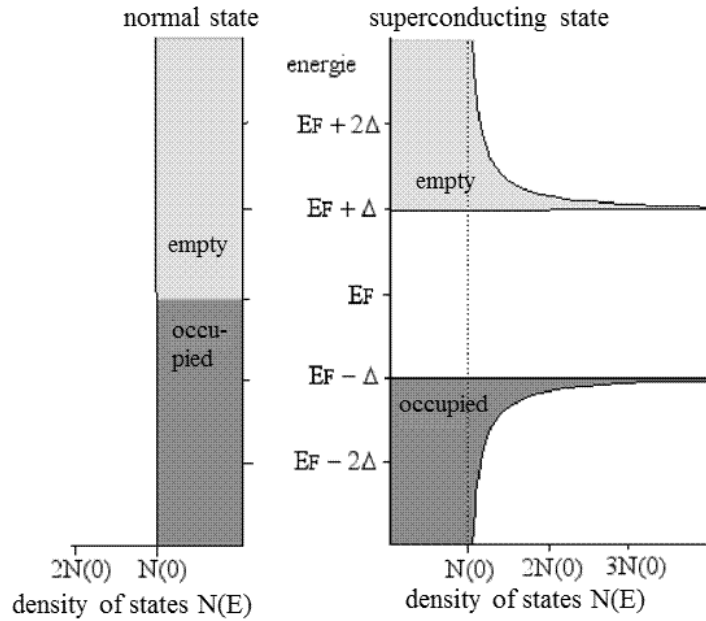
Figure 3.19: The density of states is shown (in units of the normal density of states at the Fermi surface), for both the normal state (left) and the superconducting state (right). Occupied states are shaded dark, unoccupied are light gray. Note the band gap in the superconducting DOS.
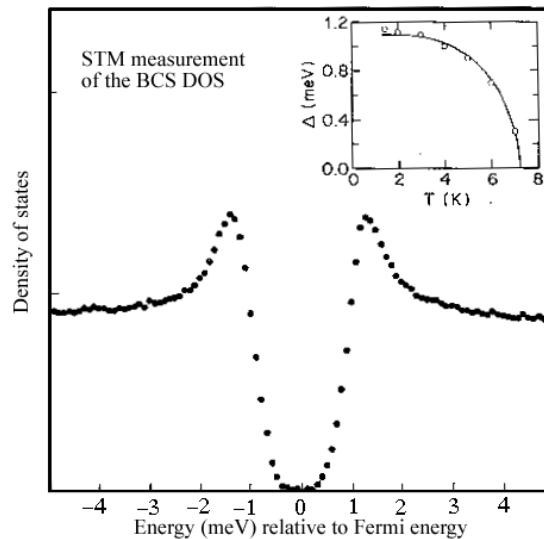

Figure 3.20: The signal from a scanning tunneling microscope is proportional to the density of states. This figure shows the measured superconducting DOS in which a (fairly large) gap is clearly visible. The gap closes down as the temperature increases, as shown in the inset.

from the BCS model, agrees very nicely with the experimentally determined DOS, as can be seen in figure 3.20. The Van Hove singularities in this figure are smoothed by the experimental energy resolution.

Finally, note that an amount $\mathcal{N}(0) |\Delta|$ of occupied states has been lowered in energy. These occupied states have dropped down to the Van Hove singularity, representing on average a lowering in energy of $|\Delta| / 2$. From this we can estimate the energy difference between superconducting and normal states as $\mathcal{N}(0) |\Delta| \times |\Delta| / 2$, in agreement with our result (3.158).

3.6.5 Gap equation

Remember that we introduced Δ as a mean field, through equation (3.122). Subsequently we forgot about that definition and we treated Δ as a variable that could take on any value, and obtained the value that minimizes the energy. Now we need to check the self-consistency of our approach: if we are succesfull, we should obtain the same value of Δ when we calculate it through

$$\Delta = -U \sum_{\mathbf{k}' \in \mathcal{D}} \langle \hat{c}_{-\mathbf{k}',\downarrow} \hat{c}_{\mathbf{k}',\uparrow} \rangle .$$

This comes down to calculating the expectation value $\langle \hat{c}_{-\mathbf{k},\downarrow} \hat{c}_{\mathbf{k},\uparrow} \rangle$ with respect to the superconducting state, i.e. the α-vacuum. To do this, we first rewrite this as a product of Nambu spinors:

$$
\begin{aligned}
\Delta &= -U \sum_{\mathbf{k} \in \mathcal{D}} \left\langle \left(\begin{array}{cc} \hat{c}_{\mathbf{k},\uparrow}^{\dagger} & \hat{c}_{-\mathbf{k},\downarrow} \end{array} \right) \cdot \left(\begin{array}{cc} 0 & 0 \\ 1 & 0 \end{array} \right) \cdot \left(\begin{array}{c} \hat{c}_{\mathbf{k},\uparrow} \\ \hat{c}_{-\mathbf{k},\downarrow}^{\dagger} \end{array} \right) \right\rangle \\
&= -U \sum_{\mathbf{k} \in \mathcal{D}} \left\langle \bar{c}_{\mathbf{k}}^{\dagger} \cdot \left(\begin{array}{cc} 0 & 0 \\ 1 & 0 \end{array} \right) \cdot \bar{c}_{\mathbf{k}} \right\rangle .
\end{aligned}
\tag{3.162}
$$

Then we apply the Bogoliubov transformation, using its unitarity:

$$
\begin{aligned}
\Delta &= -U \sum_{\mathbf{k} \in \mathcal{D}} \left\langle \bar{c}_{\mathbf{k}}^{\dagger} \cdot (B_{\mathbf{k}}^{\dagger} B_{\mathbf{k}}) \cdot \left(\begin{array}{cc} 0 & 0 \\ 1 & 0 \end{array} \right) \cdot (B_{\mathbf{k}}^{\dagger} B_{\mathbf{k}}) \cdot \bar{c}_{\mathbf{k}} \right\rangle \\
&= -U \sum_{\mathbf{k} \in \mathcal{D}} \left\langle (\bar{c}_{\mathbf{k}}^{\dagger} B_{\mathbf{k}}^{\dagger}) \cdot B_{\mathbf{k}} \left(\begin{array}{cc} 0 & 0 \\ 1 & 0 \end{array} \right) B_{\mathbf{k}}^{\dagger} \cdot (B_{\mathbf{k}} \bar{c}_{\mathbf{k}}) \right\rangle .
\end{aligned}
$$

Here $B_{\mathbf{k}}$ is still given by (3.133), and matrix multiplication results in

$$B_{\mathbf{k}} \left(\begin{array}{cc} 0 & 0 \\ 1 & 0 \end{array} \right) B_{\mathbf{k}}^{\dagger} = \frac{1}{2E_k} \left(\begin{array}{cc} |\Delta| & \xi_k - E_k \\ \xi_k + E_k & -|\Delta| \end{array} \right) ,
\tag{3.163}$$

so that

$$
\begin{aligned}
\Delta &= -U \sum_{\mathbf{k} \in \mathcal{D}} \left\langle \frac{1}{2E_k} \left(\begin{array}{cc} \hat{\alpha}_{\mathbf{k},\uparrow}^{\dagger} & \hat{\alpha}_{-\mathbf{k},\downarrow} \end{array} \right) \right. \\
&\qquad \left. \cdot \left(\begin{array}{cc} |\Delta| & \xi_k - E_k \\ \xi_k + E_k & -|\Delta| \end{array} \right) \cdot \left(\begin{array}{c} \hat{\alpha}_{\mathbf{k},\uparrow} \\ \hat{\alpha}_{-\mathbf{k},\downarrow}^{\dagger} \end{array} \right) \right\rangle .
\end{aligned}
\tag{3.164}
$$

At temperature zero the superconductor is in its ground state, and we know that this is the α-vacuum Therefore the only non-zero expectation is $\left\langle \hat{\alpha}_{-\mathbf{k},\downarrow} \hat{\alpha}^{\dagger}_{-\mathbf{k},\downarrow} \right\rangle = 1$ and we obtain

$$\Delta = U \sum_{\mathbf{k} \in \mathcal{D}} \frac{|\Delta|}{2E_k} \tag{3.165}$$

Since the right-hand side is real, the left hand side will be real too and we can drop the absolute value in $|\Delta|$. We get

$$\Delta = U \sum_{\mathbf{k} \in \mathcal{D}} \frac{\Delta}{2\sqrt{\Delta^2 + \xi_k^2}} \tag{3.166}$$

This is the temperature zero **gap equation**. There is always a solution with $\Delta = 0$, being the normal state. A solution representing the superconducting state ($\Delta \neq 0$) exists when the following equation can be satisfied:

$$1 = U \sum_{\mathbf{k} \in \mathcal{D}} \frac{1}{2\sqrt{\Delta^2 + \xi_k^2}} \tag{3.167}$$

As we did before, expression (3.151), we replace the sum over $\mathbf{k}$-states by an integral over the (normal) energy ξ times the (normal) density of states:

$$\frac{1}{U} = \mathcal{N}(0) \int_{-\hbar\omega_D}^{+\hbar\omega_D} \frac{1}{2\sqrt{\Delta^2 + \xi^2}} d\xi \tag{3.168}$$

The (normal) density of states is nearly constant in the small window $\xi \in [-\hbar\omega_D, +\hbar\omega_D]$ and we can set it equal to $\mathcal{N}(0)$, the density of states at the Fermi surface. The integral is a textbook one, for the hyperbolic arc sine:

$$\frac{1}{\mathcal{N}(0)U} = \operatorname{arcsinh}\left(\frac{\hbar\omega_D}{\Delta}\right) \tag{3.169}$$

$$\Leftrightarrow \quad \Delta = \frac{\hbar\omega_D}{\sinh\left(1/[\mathcal{N}(0)U]\right)} \approx 2\hbar\omega_D \exp\left\{-\frac{1}{\mathcal{N}(0)U}\right\} \tag{3.170}$$

This is indeed the result that we had before, expression (3.157).

3.6.6   Critical temperature

To find the critical temperature, we return to the gap equation (3.164). We know that the α-operators satisfy fermionic anti-commutation rules, so at thermal equilibrium the (particle-and hole-like) quasiparticles created by them will satisfy Fermi-Dirac statistics:

$$\left\langle \hat{\alpha}^{\dagger}_{\mathbf{k},\uparrow} \hat{\alpha}_{\mathbf{k},\uparrow} \right\rangle = n_p(\mathbf{k}) = \frac{1}{1 + \exp\{-E_k/(k_B T)\}} \tag{3.171}$$

$$\left\langle \hat{\alpha}_{-\mathbf{k},\downarrow} \hat{\alpha}^{\dagger}_{-\mathbf{k},\downarrow} \right\rangle = n_h(\mathbf{k}) = 1 - \frac{1}{1 + \exp\{-E_k/(k_B T)\}} \tag{3.172}$$
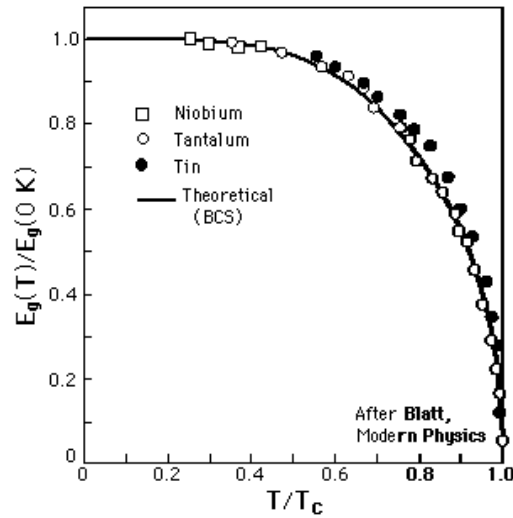
Figure 3.21: Temperature dependence of the gap, as calculated with the BCS theory (full line) and compared to experimental results for niobium, tantalum and tin. The gap $\Delta(T)$ is scaled to the zero-temperature gap $\Delta(0)$ on the y-axis.

We still find $\left\langle \hat{\alpha}^\dagger_{\mathbf{k},\uparrow} \hat{\alpha}^\dagger_{-\mathbf{k},\downarrow} \right\rangle = 0 = \langle \hat{\alpha}_{-\mathbf{k},\downarrow} \hat{\alpha}_{\mathbf{k},\uparrow} \rangle$, since the Hamiltonian (3.130) commutes with the number operator for the quasiparticles. As the temperature increases, more and more Cooper pairs are broken up: the number of excitations increases. Note that we treat the Cooper pair condensate as an inexhaustible reservoir for thermal excitations, since we do not fix the number of electrons. This feature is common to the Bogoliubov treatment of helium and of bosonic condensates. Here, we can extend the results to T_c since the pair-breaking excitations are protected by a gap. As long as the gap is not much smaller than $k_B T_c$, the number of excitations will remain suppressed until very close to T_c.

We can use the expectation values (3.171),(3.172) to simplify the gap equation (??) to

$$
\begin{aligned}
\Delta &= U \sum_{\mathbf{k} \in \mathcal{D}} \frac{|\Delta|}{2E_k} \left(\frac{2}{1 + \exp\{-E_k/(k_B T)\}} - 1 \right) \\
&= U \sum_{\mathbf{k} \in \mathcal{D}} \frac{|\Delta|}{2E_k} \tanh\left[E_k/(2k_B T) \right],
\end{aligned}
\tag{3.173}
$$

This yields the finite-temperature gap equation

$$
1 = U \sum_{\mathbf{k} \in \mathcal{D}} \frac{\tanh\left[E_k/(2k_B T) \right]}{2E_k}.
\tag{3.174}
$$

from which $\Delta(T)$ can be calculated numerically. The result is shown in figure 3.21 and it is seen to compare very well to the experimental measurements. It also allows to calculate the critical temperature, as the temperature for which $\Delta \to 0_+$. Taking the limit for Δ going to zero we find that the critical
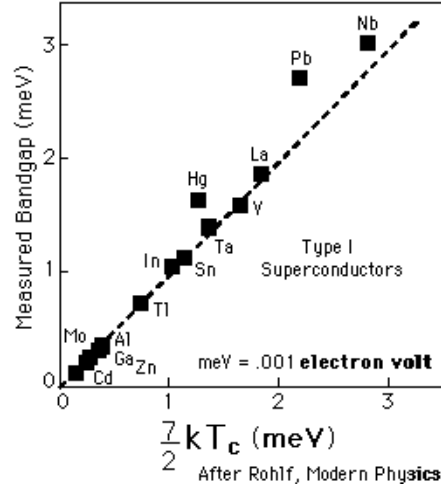
Figure 3.22: BCS theory predicts that the ratio of the spectroscopic band gap (2Δ) and the critical temperature ($k_B T_c$) is nearly 7/2. The conventional superconductors obey this relation well.

temperature has to satisfy

$$1 = U \sum_{\mathbf{k} \in \mathcal{D}} \frac{\tanh\left[\left|\xi_k\right| / (2k_B T_c)\right]}{2\left|\xi_k\right|}. \tag{3.175}$$

Indeed, we have already seen that $\lim_{\Delta \to 0_+} E_k = |\xi_k|$. This expression of course only holds when approaching the BCS-normal phase transition from within the superconducing phase. Again we transform the sum over wavenumbers into an integral over the (normal) density of energy states:

$$
\begin{aligned}
\frac{1}{\mathcal{N}(0)U} &= -\int_0^{+\hbar\omega_D} \frac{\tanh[\xi/(2k_B T_c)]}{\xi} d\xi \\
&= -\int_0^{\hbar\omega_D/(2k_B T_c)} \frac{\tanh(x)}{x} dx \tag{3.176} \\
&\approx -\log\left[\frac{\hbar\omega_D}{2k_B T_c}\right]. \tag{3.177}
\end{aligned}
$$

Here we have used $\hbar\omega_D/(2k_B T_c) \gg 1$. Working with more precision we find

$$k_B T_c \approx 1.13\hbar\omega_D \exp\left\{-\frac{1}{\mathcal{N}(0)U}\right\}. \tag{3.178}$$

Both the expression for the band gap and for the critical temperature depend on the combination $\lambda = \mathcal{N}(0)U$ representing the electron-phonon coupling strength at the Fermi surface. However, if we take the ratio of the two numbers, we get a constant:

$$\frac{2\Delta}{k_B T_c} \approx 3.52. \tag{3.179}$$

This no longer contains any adaptable model parameters, and can be directly compared to experiment. As can be seen from figure 3.22 and from the table below, the comparison is amazingly good for such a crude model:

Supergeleider	$2\Delta/(k_B T_c)$
Aluminium	3.37 ± 0.1
Cadmium	3.20 ± 0.1
Mercury	4.60 ± 0.1
Indium	3.63 ± 0.1
Niobium	3.83 ± 0.06
Lead	4.29 ± 0.04
Tin	3.46 ± 0.1

Note that the critical temperature is also proportional to $\hbar\omega_D$, so the theory predicts the isotope effect.

3.6.7 Results and challenges for BCS theory

With their "minimal model" for superconductivity, Bardeen, Cooper and Schrieffer managed to explain a wide array of superconducting phenomena well! Their theory has a single fitting parameter $\lambda = \mathcal{N}(0)U$. Let's put the main results together:

$$\Delta(T=0) = 2\hbar\omega_D e^{-1/\lambda}, \tag{3.180}$$

$$H_c(T=0) = \sqrt{\mu_v \frac{3n}{2E_F}}\Delta(T=0), \tag{3.181}$$

$$T_c = 1.13\hbar\omega_D e^{-1/\lambda}. \tag{3.182}$$

This links the isotope effect, the spectroscopic gap from AC conductivity, and the Meissner effect. Frictionless (=zero resistance) flow follows from the Landau criterion applied to the Bogoliubov spectrum $E(k) = \sqrt{\xi_k^2 + \Delta^2}$, with a critical current proportional to the Landau critical velocity:

$$J_c \approx \mathcal{N}(0)\,|\Delta| \times e \times \frac{|\Delta|}{\hbar k_F} \tag{3.183}$$

The temperature dependence $\Delta(T)$ is given by the solution of

$$1/\lambda = \int_0^{\hbar\omega_D} \frac{1}{\sqrt{\xi^2 + \Delta^2(T)}} \tanh\left(\frac{\sqrt{\xi^2 + \Delta^2(T)}}{2k_B T}\right) d\xi. \tag{3.184}$$

The energy is given by

$$\frac{\delta E}{\mathcal{N}(0)} = 2\int_0^{+\hbar\omega_D} \left(\xi - \sqrt{\xi^2 + |\Delta|^2}\right) d\xi + \lambda\,|\Delta|^2. \tag{3.185}$$

Finally, note that also the peak in the specific heat is explained in the BCS model. Indeed, we can estimate the (Shannon) entropy from the particle-like
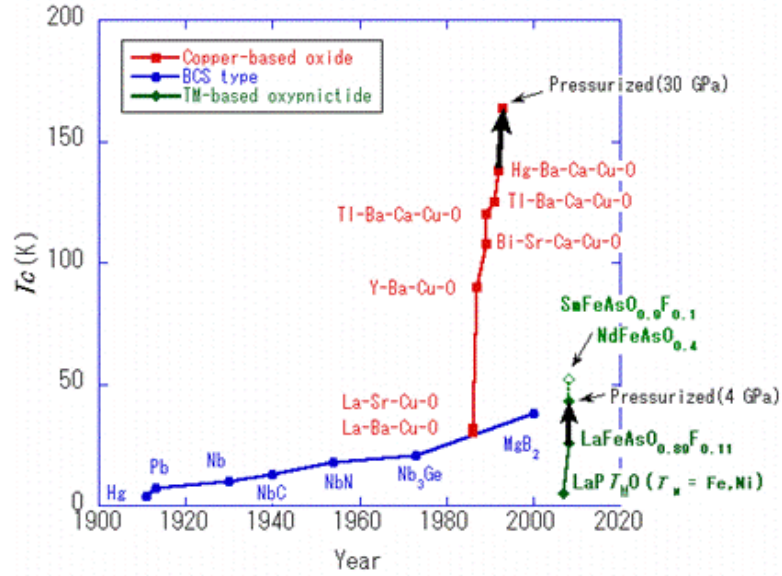
Figure 3.23: Timeline of superconducting materials (source: Hiroki Takahashi).

and hole-like quasiparticle occupations (3.171)-(3.172) as

$$S = k_B \sum_{\mathbf{k} \in \mathcal{D}} \left\{ n_p(\mathbf{k}) \log \left[n_p(\mathbf{k}) \right] + n_h(\mathbf{k}) \log \left[n_h(\mathbf{k}) \right] \right\} . \qquad (3.186)$$

The specific heat follows straightforwardly from the entropy.

It seems the BCS model explains it all! The impressive list of results following from the BCS Hamiltonian gave it immediate recognition, and its creators were awarded the Nobel prize in 1972. The minimal Hamiltonian goes a long way, and improvements thought up by the theorists like Migdal, Eliashberg, Kirghnitz,... can give the final touch to remove even the small discrepancies. But the story is not over. In figure 3.23 different superconducting materials are plotted according to the year in which their superconducting nature was discovered, and their critical temperature. The blue circles, roughly on a (blue) line that starts with mercury and ending in MgB$_2$, represent the "conventional" superconductors for which BCS theory holds. In the normal state, most are metals. The maximum temperature for these BCS superconductors is until now about 40 K, with magnesium diboride holding the record. In the late '80s however, it was found that copper oxide perovskites could also exhibit superconductivity. These are indicated with red squared in figure 3.23. Other families of superconductors were discovered before, such as the organics based on doped fullerenes, and the heavy-fermion family of metals. But the copper oxides were much more remarkable.

Not only was it remarkable that these materials are non-metallic in the undoped state (they are insulating ceramics, like porcelain), but even more impressive is that they quickly held the record critical temperatures and even broke through the liquid nitrogen barrier (77 K). Electron-phonon interaction

as the glue cannot explain these high critical temperatures, and other key experiments give very different results. For example, the isotope effect, while present for some of the atom species in the compound, is not scaling with the phonon frequency... Up till this day, we do not know the glue that binds the electrons in pairs (pairs are present, as seen by flux quantization), and BCS theory fails to explain these materials completely. We're back to using the Ginzburg-Landau theory with experimentally determined parameters. Recently, yet another family of superconducting materials have been discovered. The story becomes even weirder: these marials are iron based (iron with arsenic or selenium), and iron is magnetic! Nobody foresaw iron based superconductivity, as magnetism was believed to be always antagonistic to superconductivity. Also these materials still represent a mystery.

As long as these alternative glues for electron pairs are not understood, we will not be able to design a room temperature superconductor. This is the "holy grail" of superconductivity research, as it would greatly facilitate technological application of superconductivity to make lossless powerlines and to story energy in persistent current loops. Both of these applications are crucial in order to implement solar power or wind power on a large scale: typically these renewables cannot generate electricity continuously or in any location. Lossless storage and transport of electricity are then a requirement for these types of energy source to take over non-renewable sources. I hope that this course has provided you with the means and to pursue research and to understand the future developments in the fascinating field of superfluidity and superconductivity.

Appendix A

Thermodynamics of magnetism

You're used to thinking of the first law of thermodynamics as $dU = TdS - pdV$. Including magnetic energy in this picture may not be familiar to you, and since we need this to get a deeper understanding of superconductors I included this appendix to clarify the link between thermodynamic potentials and magnetism.

A.1 Gibbs versus Helmholtz

The first law tells us how the energy changes when there is a small (infinitesimal) change in entropy or volume. However, it will also change when there is a small change in magnetic field, for example by cranking up the current through some external coil. We know from classical electromagnetism (see for example Jackson's book) that the change in magnetic energy density is given by

$$\mathbf{H} \cdot d\mathbf{B} \tag{A.1}$$

where $\mathbf{H}$ is the magnetic field, and $\mathbf{B}$ is the flux density. In vacuum, we have $\mathbf{B} = \mu\mathbf{H}$ with μ the vacuum permeability. In a material the situation is more complicated: microscopic currents can be induced by the external magnetic field and lead to a magnetization $\mathbf{M}$ of the sample. We take this into account through $\mathbf{B} = \mu(\mathbf{H} + \mathbf{M})$. With this we can rewrite the change in magnetic energy density in the presence of a magnetizable sample as

$$\mu\mathbf{H} \cdot d\mathbf{M} + \mu\mathbf{H} \cdot d\mathbf{H} \tag{A.2}$$

The first term, $\mu\mathbf{H} \cdot d\mathbf{M}$ is the magnetic work done on the sample, and the second term $\mu\mathbf{H} \cdot d\mathbf{H}$, is the work per unit volume that would have been done even if there is no sample. This is usually not taken into account, since we are interested in the internal energy change of the subsystem. So, the first law of thermodynamics, including magnetics, becomes

$$dU = TdS - pdV + \mu V\,\mathbf{H} \cdot d\mathbf{M} \tag{A.3}$$

The internal energy $U(S, V, \mathbf{M})$ is a function of the magnetization – an extensive variable. Indeed the internal energy, being itself extensive, should be a

homogeneous function of extensive variables. The magnetic field $\mathbf{H}$ is an intensive variable. Of course, we can construct other thermodynamic potentials, such as the usual free energy

$$F(T, V, \mathbf{M}) = U(S, V, \mathbf{M}) - TS \tag{A.4}$$

where we have used a Legendre transform to replace the S-dependence by a T-dependence. Why am I stressing all these thermodynamiccy details? Because very often we don't want to work with a thermodynamic potential that is a function of the magnetization, we want to work out properties at a given external magnetic field!

Consider the following example: you want to find the specific heat

$$c = T \frac{\partial S}{\partial T} = -T \frac{\partial^2 F}{\partial T^2}, \tag{A.5}$$

so you need to take derivatives of the temperature. It is important to know what you keep constant while taking the partial derivative. For example, you have to specify whether your experiment takes place at constant volume (c_V) or at constant pressure ($c_P \neq c_V$). Similarly, you need to specify whether you want the specific heat at constant magnetization or at constant external magnetic field! Now, most experiments on superconductors happen with a constant volume of superconducting material, and in a constant external magnetic field, so you want

$$c_{V,\mathbf{H}} = -T \frac{\partial^2 F}{\partial T^2} \bigg|_{V,\mathbf{H}} \tag{A.6}$$

If you stick to $F(T, V, \mathbf{M})$ calculating this quantity is too complicated: how will you keep $\mathbf{H}$ constant while the temperature changes? This constraint is difficult to express using a function $F_s(T, V, \mathbf{M})$ that is not an explicit function of $\mathbf{H}$.

To find a function that makes the constraint easier to take into account, we perform a Legendre transform that brings us from the $\mathbf{M}$ dependence to the $\mathbf{H}$ dependence. This introduces yet another thermodynamic potential,

$$G(T, V, \mathbf{H}) = F(T, V, \mathbf{M}) - \mu V \, \mathbf{H} \cdot \mathbf{M} \tag{A.7}$$

so that

$$dG = -SdT - pdV - \mu V \mathbf{M} \cdot d\mathbf{H} \tag{A.8}$$

This is sometimes called the Gibbs free energy (where F is the Helmholtz free energy). But this is confusing, since other textbooks call $F + pV$ the Gibbs free energy! It is less confusing when you remember that we are looking for particular energy differences, such as the total change in energy as the external *magnetic field* is ramped up from 0 to its final value H_a, while *temperature* and *volume* are kept constant. The words in italic make it clear that we need a function of T, V and $\mathbf{H}$, i.e. the $G(T, V, \mathbf{H})$ introduced above:

$$\Delta G = G(T, V, \mathbf{H}) - G(T, V, \mathbf{0}) = -\mu V \int_0^{H_a} \mathbf{M} \cdot d\mathbf{H} \tag{A.9}$$

For the Meissner effect, we know that $\mathbf{M}(\mathbf{H}) = -\mathbf{H}$, and from this then we immediately get $\mu H_c^2 / 2$ as before.

A.2 Ginzburg-Landau Gibbs energy

Let's now move on to the next difficulty. We set up the GL free energy

$$F_s(T, V, \mathbf{M}) = F_n(T, V) + \int d\mathbf{r} \, \frac{1}{2\mu} \mathbf{B}^2 \tag{A.10}$$

$$+ \int d\mathbf{r} \left\{ \Psi^*(\mathbf{r}) \frac{[-i\hbar \boldsymbol{\nabla}_{\mathbf{r}} - Q\mathbf{A}(\mathbf{r})]^2}{2M} \Psi(\mathbf{r}) + a(T) \left| \Psi(\mathbf{r}) \right|^2 + \frac{b(T)}{2} \left| \Psi(\mathbf{r}) \right|^4 \right\}.$$

by adding $\mathbf{B}^2/(2\mu)$ to the free energy, as prescribed by Maxwell's theory, and in accordance with $\mathbf{J} = -\delta F/\delta \mathbf{A}$. But if we look for the energy change as we switch on an *external field* $\mathbf{H}$ from 0 to $\mathbf{H}_a$ at fixed *temperature* and *volume*, we again prefer working with the Gibbs free energy, so we need to perform the $-\mu V \mathbf{M} \cdot \mathbf{H}$ Legendre transform as above

$$G_s(T, V, \mathbf{H}) = G_n(T, V) + \int d\mathbf{r} \left\{ \frac{1}{2\mu} \mathbf{B}^2 - \mu \mathbf{M} \cdot \mathbf{H} \right\} \tag{A.11}$$

$$+ \int d\mathbf{r} \left\{ \Psi^*(\mathbf{r}) \frac{[-i\hbar \boldsymbol{\nabla}_{\mathbf{r}} - Q\mathbf{A}(\mathbf{r})]^2}{2M} \Psi(\mathbf{r}) + a(T) \left| \Psi(\mathbf{r}) \right|^2 + \frac{b(T)}{2} \left| \Psi(\mathbf{r}) \right|^4 \right\}.$$

Note that we didn't take any of the magnetic effects into acount in the normal state, where $\mathbf{M} = 0$, so $F_n(T, V) = G_n(T, V)$. We assume that if the material is in the normal state it has vacuum permittivity, so it is as if there is no sample at all as far as the magnetic field is concerned. But this does not mean that the energy won't change when $\mathbf{H}$ is switched on! Even without sample, the magnetic energy will increase as $\mu H^2/2$. Let's take this part out of the magnetic field energy, and place it into $G_n(T, V, \mathbf{H}) = G_n(T, V) + \mu H^2/2$. Then we get

$$G_s(T, V, \mathbf{H}) = G_n(T, V, \mathbf{H}) + \int d\mathbf{r} \left\{ \frac{1}{2\mu} \mathbf{B}^2 - \mu \mathbf{M} \cdot \mathbf{H} - \frac{\mu \mathbf{H}^2}{2} \right\} \tag{A.12}$$

$$+ \int d\mathbf{r} \left\{ \Psi^*(\mathbf{r}) \frac{[-i\hbar \boldsymbol{\nabla}_{\mathbf{r}} - Q\mathbf{A}(\mathbf{r})]^2}{2M} \Psi(\mathbf{r}) + a(T) \left| \Psi(\mathbf{r}) \right|^2 + \frac{b(T)}{2} \left| \Psi(\mathbf{r}) \right|^4 \right\}.$$

This is just a reshuffling of terms. Now use $\mu \mathbf{M} = \mathbf{B} - \mu \mathbf{H}$ to rewrite

$$\frac{1}{2\mu} \mathbf{B}^2 - \mu \mathbf{M} \cdot \mathbf{H} - \frac{\mu \mathbf{H}^2}{2} = \frac{1}{2\mu} \mathbf{B}^2 - \mu \mathbf{B} \cdot \mathbf{H} + \frac{\mu \mathbf{H}^2}{2}$$

$$= \frac{1}{2\mu} \left(\nabla \times \mathbf{A} - \mu \mathbf{H} \right)^2 \tag{A.13}$$

Hence, we find that the Gibbs free energy, at an externally applied field $\mathbf{H}_a$ is given by

$$G_s(T, V, \mathbf{H}_a) = G_n(T, V, \mathbf{H}_a) + \int d\mathbf{r} \left\{ \Psi^*(\mathbf{r}) \frac{[-i\hbar \boldsymbol{\nabla}_{\mathbf{r}} - Q\mathbf{A}(\mathbf{r})]^2}{2M} \Psi(\mathbf{r}) \right.$$

$$\left. + a(T) \left| \Psi(\mathbf{r}) \right|^2 + \frac{b(T)}{2} \left| \Psi(\mathbf{r}) \right|^4 + \frac{1}{2\mu} \left[\boldsymbol{\nabla} \times \mathbf{A}(\mathbf{r}) - \mu \mathbf{H}_a \right]^2 \right\}.$$

Tinkham writes the last term as $\mu(\mathbf{h} - \mathbf{H})^2/2$ – actually, he also writes this in CGS, so you replace μ by 4π to obtain the result from his book.

A.3   Vortex energy and potential

As mentioned before, it's not always the case that we really want to work at
fixed external magnetic field. An example is the calculation of the energy of a
singly quantized London vortex inside an infinitely large type II superconductor.
There, we want to work for a fixed magnetization of the bulk sample, keeping
it everywhere fixed except in near the vortex core (which is an infinitesimal
fraction of the infinite block of bulk superconductor). Indeed, we compare the
free energy with and without vortex, but with the magnetization kept the same
everywhere in the bulk away from the vortex.

In the extreme type II case we put $\Psi(\mathbf{r}) \to |\Psi_{bulk}|$ almost everywhere, since
$\xi \ll \lambda_L$. To be more careful, we put

$$\Psi(\mathbf{r}) \to \begin{cases} |\Psi_{bulk}| & \text{for } r > \xi, \\ 0 & \text{for } r < \xi, \end{cases}$$

where r is the distance to the vortex line.   Substituting this in the
Ginzburg-Landau free energy functional (3.62) , and we find

$$\begin{aligned} F_s(T,V,\mathbf{M}) &= G_n(T,V,\mathbf{M}) + V\left(a|\Psi_{bulk}|^2 + \frac{b}{2}|\Psi_{bulk}|^4 \right) \\ &+ |\Psi_{bulk}|^2 \int_{r>\xi} d\mathbf{r} \left[\frac{Q^2}{2M}\mathbf{A}^2 + \frac{1}{2\mu}(\boldsymbol{\nabla}\times\mathbf{A})^2 \right] \end{aligned} \quad (A.14)$$

Remember that M is the *total* magnetization. The first line just gives us the
energy lowering due to pair formation in the superconductor (neglecting the fact
that the pair condensate is reduced inside the tiny cores in the extreme type
II limit). The second line is the magnetic energy contribution that we're after.
We set The difference in free energy with a vortex ($\mathbf{A} \neq 0$) and without vortex
($\mathbf{A} = 0$) at fixed temperature, volume, and bulk sample magnetization, is

$$\Delta F_{magn} = \frac{1}{2\mu}\int_{r>\xi} d\mathbf{r} \left[\frac{1}{\lambda_L^2}\mathbf{A}^2 + (\boldsymbol{\nabla}\times\mathbf{A})^2 \right] \quad (A.15)$$

We have used $\lambda_L^{-2} = \mu Q^2 |\Psi_{bulk}|^2 /M$. This can be rewritten in another way
using $\mu\mathbf{J} = -\lambda_L^{-2}\mathbf{A}$:

$$\Delta F_{magn} = \frac{1}{2\mu}\int_{r>\xi} d\mathbf{r} \left[\lambda_L^2(\mu\mathbf{J})^2 + (\boldsymbol{\nabla}\times\mathbf{A})^2 \right] \quad (A.16)$$

Finally, we use $\boldsymbol{\nabla}\times\mathbf{B} = \mu\mathbf{J}$ and $\boldsymbol{\nabla}\times\mathbf{A} = \mathbf{B}$ to get

$$\Delta F_{magn} = \frac{1}{2\mu}\int_{r>\xi} d\mathbf{r} \left[\lambda_L^2(\boldsymbol{\nabla}\times\mathbf{B})^2 + (\mathbf{B})^2 \right] \quad (A.17)$$

Yet anoter expression of the same result is obtained by using $\mu\mathbf{J} = -\lambda_L^{-2}\mathbf{A}$ in
the rotor part of (A.16):

$$\Delta F_{magn} = \frac{\mu\lambda_L^2}{2}\int_{r>\xi} d\mathbf{r} \left[\mathbf{J}^2 + \lambda_L^2(\boldsymbol{\nabla}\times\mathbf{J})^2 \right] \quad (A.18)$$

For an isolated, singly quantized London vortex along the z-axis, we can use our result (3.110):

$$\mathbf{B}(\mathbf{r}) \ = \ \frac{\phi}{2\pi\lambda_L^2} K_0(r/\lambda_L)\mathbf{e}_z \tag{A.19}$$

$$\boldsymbol{\nabla} \times \mathbf{B} \ = \ -\frac{\partial B_z}{\partial r}\mathbf{e}_\varphi = -\frac{\phi}{2\pi\lambda_L^3} K_1(r/\lambda_L) \tag{A.20}$$

expressed in cylindrical coordinates $\{r, \varphi, z\}$, and get

$$\Delta F_{magn} = \frac{1}{2\mu} \left(\frac{\phi}{2\pi\lambda_L^2} \right)^2 \int_{r>\xi} d\mathbf{r} \ \left[K_1^2(r/\lambda_L) + K_0^2(r/\lambda_L) \right] \tag{A.21}$$

Per unit length L of vortex line, we get

$$\frac{\Delta F_{magn}}{L} = \frac{\phi^2}{4\pi\mu\lambda_L^2} \int\limits_{\xi/\lambda_L}^{\infty} x \left[K_1^2(x) + K_0^2(x) \right] dx \tag{A.22}$$

The integral can be evaluated analytically and written with Meijer functions, which for small ξ/λ_L is well approximated by $\ln(\lambda_L/\xi)$ such that

$$\frac{\Delta F_{magn}}{L} = \frac{\phi^2}{4\pi\mu\lambda_L^2} \ln(\lambda_L/\xi) \tag{A.23}$$

This is the free energy cost to make the vortex. To have N singly quantized vortices in the sample of volume V (and area A), the total cost in free energy per unit volume is

$$\frac{\Delta F_{magn}}{V} = \frac{N}{A} \frac{\phi_0^2}{4\pi\mu\lambda_L^2} \ln(\lambda_L/\xi) \tag{A.24}$$

However, when N vortices enters the sample, we must also gain some free energy, since there is an infinitesimal change in magnetization, and

$$\frac{\Delta F}{V} = \mu\mathbf{H} \cdot \Delta\mathbf{M} = H \ \frac{N\phi_0}{A} \tag{A.25}$$

For the first equality it is again important that we use the Helmholtz free energy, and not the Gibbs free energy. Balancing the cost and the gain of free energy allows to derive the value of the first critical magnetic field,

$$H_{c_1} = \frac{\phi_0}{4\pi\mu\lambda_L^2} \ln(\lambda_L/\xi) \tag{A.26}$$

For two singly-quantized London vortices at a distance $\mathbf{a}$, we simply add up their individual contributions,

$$\mathbf{B}(\mathbf{r} - \mathbf{a}/2) + \mathbf{B}(\mathbf{r} + \mathbf{a}/2) \tag{A.27}$$

and plug this into the formula. This gives us the "interaction potential" $U_{int}(\mathbf{a})$. It is defined such that the change in interaction potential equals the change in free energy of the two-vortex state as a function of intervortex distance, while

keeping temperature, volume, and bulk magnetization constant. After a bit of work and integrations, approximating $a \gg \lambda_L \gg \xi$, this gives

$$\frac{U_{int}(\mathbf{a})}{L} = \frac{\phi_0^2}{2\pi\mu\lambda_L^2} K_0(a/\lambda_L) \tag{A.28}$$

The repulsion will keep vortices at a maximum distance from eachother, but in order to match a flux density B, there must be a $B/(A\phi_0)$ vortices where A is the area of the sample. Hence the intervortex distance at triangular close packing is $a_v = \sqrt{2\phi_0/(\sqrt{3}B)}$. The second critical field is reached when this distance becomes compareable to ξ, so for $H_{c_2} \approx 2\phi_0/(\sqrt{3}\xi^2)$. The ratio

$$\frac{H_{c_2}}{H_{c_1}} \propto \frac{\kappa^2}{\ln(\kappa)} \tag{A.29}$$

can be very large in the extreme type II limit that we studied here.

Appendix B

Superfluidity in Helium-3

All the order parameters that we introduced to describe the superfluid or superconducting state were complex scalars. However, nature is not confined to scalars, and some systems reveal superfluid or superconducting order parameters that are higher-order tensors. In this appendix I outline the most famous example: superfluid helium-3. This example also provides you with a system where the glue between the fermions is not the electron-phonon interaction: here it is simply the interatomic potential.

B.1 BCS description of helium-3

The helium-3 atom is one neutron short of its bosonic brother, helium-4. Having two electrons in the 1s orbital, its orbital angular momentum is $J = 0$. The nucleus contains two protons and a single neutron, accounting for nuclear angular momentum $I = 1/2$, and resulting in total angular momentum $F = 1/2$. Thus, the helium-3 atom is a spin 1/2 fermion. The only way that this is going to be superfluid is if these atoms pair up.

The pair wavefunctions

$$\chi_0(\mathbf{r}_1\sigma_1, \mathbf{r}_2\sigma_2) = \langle \mathbf{r}_1\sigma_1, \mathbf{r}_2\sigma_2 | \chi_0 \rangle \tag{B.1}$$

will consist out of a spatial part and a spin part that we factorize:

$$\langle \mathbf{r}_1\sigma_1, \mathbf{r}_2\sigma_2 | = \langle \mathbf{r}_1, \mathbf{r}_2 | \otimes \langle \sigma_1\sigma_2 |, \tag{B.2}$$

$$|\chi_0\rangle = |\chi_{space}\rangle \otimes |\eta_{spin}\rangle, \tag{B.3}$$

$$\Rightarrow \chi_0(\mathbf{r}_1\sigma_1, \mathbf{r}_2\sigma_2) = \chi_{space}(\mathbf{r}_1, \mathbf{r}_2) \langle \sigma_1\sigma_2 | \eta_{spin} \rangle. \tag{B.4}$$

When the atoms are far apart, the spin basis $|\sigma_1\sigma_2\rangle \in \{|\uparrow\uparrow\rangle, |\uparrow\downarrow\rangle, |\downarrow\uparrow\rangle, |\downarrow\downarrow\rangle\}$ is appropriate. However, when the atoms are close together, the system's Hamiltonian is likely to commute with the total spin having triplet eigenstates

$$|1, 1\rangle = |\uparrow\uparrow\rangle \tag{B.5}$$

$$|1, 0\rangle = \frac{1}{\sqrt{2}} (|\uparrow\downarrow\rangle + |\downarrow\uparrow\rangle) \tag{B.6}$$

$$|1, -1\rangle = |\downarrow\downarrow\rangle \tag{B.7}$$

and a singlet eigenstate

$$|0,0\rangle = \frac{1}{\sqrt{2}} \left(|\uparrow\downarrow\rangle - |\downarrow\uparrow\rangle \right) \tag{B.8}$$

Note that the triplet eigenstates are even with respect to interchanging the two fermions and the singlet eigenstate is odd. So, if $\left|\eta_{spin}\right\rangle$ belongs to a triplet state, the spatial part of the wavefunction, $\chi_{space}(\mathbf{r}_1, \mathbf{r}_2)$ must be odd in order to satisfy the overall symmetry of the fermionic pair wavefunction. If $\left|\eta_{spin}\right\rangle$ is the singlet state, then $\chi_{space}(\mathbf{r}_1, \mathbf{r}_2)$ must be even. The potential energy, calculated as an expectation value of the interatomic interaction potential with respect to $\chi_{space}(\mathbf{r}_1, \mathbf{r}_2)$ will therefore depend on whether we have a triplet or a singlet state. Indeed, we note for the interaction part $\hat{V}$ of the Hamiltonian

$$\hat{V}\left(|\mathbf{r}_1, \mathbf{r}_2\rangle \otimes |0,0\rangle\right) = V_s(\mathbf{r}_1 - \mathbf{r}_2) \, |\mathbf{r}_1, \mathbf{r}_2\rangle \otimes |0,0\rangle \tag{B.9}$$

$$\hat{V}\left(|\mathbf{r}_1, \mathbf{r}_2\rangle \otimes |1,m\rangle\right) = V_t(\mathbf{r}_1 - \mathbf{r}_2) \, |\mathbf{r}_1, \mathbf{r}_2\rangle \otimes |1,m\rangle \tag{B.10}$$

where V_s represents the singlet potential, and V_t represents the triplet potential and is assumed independent of $m = +1, 0, -1$.

This distinction between singlet and triplet is important when setting up a BCS-type model for Helium-3:

$$\hat{H}_{BCS} = \sum_{\mathbf{k},\sigma} \xi_{\mathbf{k}} \hat{c}_{\mathbf{k},\sigma}^\dagger \hat{c}_{\mathbf{k},\sigma} \tag{B.11}$$

$$- \sum_{\mathbf{k},\mathbf{k}' \in \mathcal{D}} \sum_{\sigma_1 \sigma_2; \sigma_1' \sigma_2'} U_{\sigma_1 \sigma_2; \sigma_1' \sigma_2'}(\mathbf{k} - \mathbf{k}') \hat{c}_{\mathbf{k},\sigma_1}^\dagger \hat{c}_{-\mathbf{k},\sigma_2}^\dagger \hat{c}_{-\mathbf{k}',\sigma_1'} \hat{c}_{\mathbf{k}',\sigma_2'}.$$

In the original BCS treatment of superconductors, we assumed that the pairs had opposite spin. This was necessary in order to avoid exchange contributions weakening the phonon-mediated electron-electron interaction, but in the case of helium we are working with interatomic potentials and pairs do not necessarily have opposite spin! We need to take all the spin combinations into account à priori.

It is also important to note that in our Hamiltonian we have to keep a $\mathbf{k}$-dependence in U. We didn't do that in the BCS treatment, but at least for the triplet potential $V_t(\mathbf{k} - \mathbf{k}')$ we are forced to take the wave vector dependence into account. That is because the triplet potential depends on the direction of $\mathbf{k} - \mathbf{k}'$ with respect to the (z-axis of the) intrinsic angular momentum $\ell = 1$ of the triplet pair! Indeed, if plan to throw a spinning Ninja star at an enemy, it makes a big difference whether the axis of spinning of the blades is parallel to the face of your enemy, or perpendicular to it.

The matrix elements can be related to the triplet and singlet potentials. For example,

$$\begin{aligned}
U_{\uparrow\downarrow;\downarrow\uparrow} &= \langle\uparrow\downarrow| \hat{V} |\downarrow\uparrow\rangle \\
&= \frac{1}{2} \left(\langle 1,0| + \langle 0,0| \right) \hat{V} \left(|1,0\rangle - |0,0\rangle \right) \\
&= \frac{1}{2} \left(V_t - V_s \right) \tag{B.12}
\end{aligned}$$

We can calculate all matrix elements of U in this way, resulting in

$$U_{\sigma_1\sigma_2;\sigma_1'\sigma_2'} = \begin{pmatrix} V_t & 0 & 0 & 0 \\ 0 & \frac{1}{2}(V_t + V_s) & \frac{1}{2}(V_t - V_s) & 0 \\ 0 & \frac{1}{2}(V_t - V_s) & \frac{1}{2}(V_t + V_s) & 0 \\ 0 & 0 & 0 & V_t \end{pmatrix} \qquad \text{(B.13)}$$

We've used the ordering $\{|\uparrow\uparrow\rangle, |\uparrow\downarrow\rangle, |\downarrow\uparrow\rangle, |\downarrow\downarrow\rangle\} = \{1, 2, 3, 4\}$ of the basis states to determine row and column numbers $1, 2, 3, 4$ in this matrix.

B.2 Singlet and triplet order parameter

Now we get a nice exercise going through the steps of our mean-field BCS treatment, as outlined in chapter 3, sections 3.6.1-3.6.2. Steps 1 and 2 consist in making a mean field approximation and introducing the self-consistent auxiliary variables

$$\Delta_{\alpha\beta}(\mathbf{k}) = -\sum_{\mathbf{k}'\in\mathcal{D}}\sum_{\gamma,\delta} U_{\alpha\beta;\gamma\delta}(\mathbf{k} - \mathbf{k}') \langle \hat{c}_{-\mathbf{k}',\gamma}\hat{c}_{\mathbf{k}',\delta}\rangle. \qquad \text{(B.14)}$$

This transforms the Hamiltonian into

$$\hat{H}_{BCS}^{mf} = \sum_{\mathbf{k},\sigma} \xi_{\mathbf{k}} \hat{c}_{\mathbf{k},\sigma}^\dagger \hat{c}_{\mathbf{k},\sigma} + \sum_{\mathbf{k},\alpha\beta} \left[\hat{c}_{\mathbf{k},\alpha}^\dagger \hat{c}_{-\mathbf{k},\beta}^\dagger \Delta_{\alpha\beta}(\mathbf{k}) + \Delta_{\alpha\beta}^*(\mathbf{k}) \hat{c}_{-\mathbf{k},\alpha}\hat{c}_{\mathbf{k},\beta} \right]$$

$$- \sum_{\mathbf{k},\alpha\beta}\sum_{\mathbf{k}',\gamma\delta} \Delta_{\alpha\beta}^*(\mathbf{k}) U_{\alpha\beta;\gamma\delta}^{-1}(\mathbf{k} - \mathbf{k}')\Delta_{\gamma\delta}(\mathbf{k}'). \qquad \text{(B.15)}$$

This is the generalization of expression (3.124). Note that the order parameter now carries two spin indices, as we can in principle make pairs of fermions of any spin combination. It also inherits the $\mathbf{k}$-dependence from the interaction potential.

The next step is rewriting the second term in Nambu spinor notation, so we get

$$\hat{H}_{BCS}^{mf} = \sum_{\mathbf{k},\sigma} \xi_{\mathbf{k}} \hat{c}_{\mathbf{k},\sigma}^\dagger \hat{c}_{\mathbf{k},\sigma} - \sum_{\mathbf{k},\alpha\beta}\sum_{\mathbf{k}',\gamma\delta} \Delta_{\alpha\beta}^*(\mathbf{k}) U_{\alpha\beta;\gamma\delta}^{-1}(\mathbf{k} - \mathbf{k}')\Delta_{\gamma\delta}(\mathbf{k}')$$

$$+ \sum_{\mathbf{k}} \bar{c}_{\mathbf{k}}^\dagger \cdot H_{\mathbf{k}} \cdot \bar{c}_{\mathbf{k}} + 2\sum_{\mathbf{k},\sigma} \xi_{\mathbf{k}} \qquad \text{(B.16)}$$

This is the analogue of expression (3.127). However, this time we need a 4-component spinor since we cannot use the spin symmetry:

$$\bar{c}_{\mathbf{k}} = \begin{pmatrix} \hat{c}_{\mathbf{k},\uparrow} \\ \hat{c}_{-\mathbf{k},\downarrow} \\ \hat{c}_{-\mathbf{k},\downarrow}^\dagger \\ \hat{c}_{\mathbf{k},\uparrow}^\dagger \end{pmatrix} \qquad \text{(B.17)}$$

We get for the Hamiltonian matrix

$$H_{\mathbf{k}} = \left(\begin{array}{cc|cc} \xi_{\mathbf{k}} & 0 & \Delta_{\uparrow\uparrow}(\mathbf{k}) & \Delta_{\uparrow\downarrow}(\mathbf{k}) \\ 0 & \xi_{\mathbf{k}} & \Delta_{\downarrow\uparrow}(\mathbf{k}) & \Delta_{\downarrow\downarrow}(\mathbf{k}) \\ \hline \Delta_{\uparrow\uparrow}^*(\mathbf{k}) & \Delta_{\downarrow\uparrow}^*(\mathbf{k}) & -\xi_{\mathbf{k}} & 0 \\ \Delta_{\uparrow\downarrow}^*(\mathbf{k}) & \Delta_{\downarrow\downarrow}^*(\mathbf{k}) & 0 & -\xi_{\mathbf{k}} \end{array} \right) \qquad \text{(B.18)}$$

This is similar to expression (3.128), where each entry has been replaced by a 2 by 2 matrix, taking into account the 4 possible spin combinations. Hermitean 2 by 2 matrices can be decomposed in Pauli matrices and the unit matrix, so let's see where that brings us if we apply it to the Δ-matrix. We simply rewrite the four unknown functions $\Delta_{\alpha\beta}(\mathbf{k})$ by linear combinations of four other unknown functions $\Delta, d_x(\mathbf{k}), d_y(\mathbf{k}), d_z(\mathbf{k})$. You can always find four of these functions so that

$$\left(\begin{array}{cc} \Delta_{\uparrow\uparrow}(\mathbf{k}) & \Delta_{\uparrow\downarrow}(\mathbf{k}) \\ \Delta_{\downarrow\uparrow}(\mathbf{k}) & \Delta_{\downarrow\downarrow}(\mathbf{k}) \end{array} \right) = \left(\begin{array}{cc} -d_x(\mathbf{k}) + id_y(\mathbf{k}) & \Delta + d_z(\mathbf{k}) \\ -\Delta + d_z(\mathbf{k}) & d_x(\mathbf{k}) + id_y(\mathbf{k}) \end{array} \right) \quad \text{(B.19)}$$

exactly holds. From the notation you can already suspect that we intend to associate Δ with the unit matrix and singlet pairing, and $\mathbf{d}(\mathbf{k})$ with the pauli matrices and triplet pairing. This becomes more clear if we decompose the matrix as follows

$$\left(\begin{array}{cc} \Delta_{\uparrow\uparrow}(\mathbf{k}) & \Delta_{\uparrow\downarrow}(\mathbf{k}) \\ \Delta_{\downarrow\uparrow}(\mathbf{k}) & \Delta_{\downarrow\downarrow}(\mathbf{k}) \end{array} \right) = \left[\Delta \left(\begin{array}{cc} 1 & 0 \\ 0 & 1 \end{array} \right) + \mathbf{d}(\mathbf{k}) \cdot \boldsymbol{\sigma} \right] \cdot i\sigma_y \quad \text{(B.20)}$$

where $\boldsymbol{\sigma} = \sigma_x \mathbf{e}_x + \sigma_y \mathbf{e}_x + \sigma_z \mathbf{e}_x$ with $\sigma_x, \sigma_y, \sigma_z$ the Pauli matrices.

From the definition (B.14) it's not hard to show that for potentials with inversion symmetry

$$\Delta_{\alpha\beta}(\mathbf{k}) = -\Delta_{\beta\alpha}(-\mathbf{k}) \quad \text{(B.21)}$$

From (B.19) it follows that

$$\left(\begin{array}{cc} -\Delta_{\uparrow\uparrow}(-\mathbf{k}) & -\Delta_{\downarrow\uparrow}(-\mathbf{k}) \\ -\Delta_{\uparrow\downarrow}(-\mathbf{k}) & -\Delta_{\downarrow\downarrow}(-\mathbf{k}) \end{array} \right) = \left(\begin{array}{cc} d_x(-\mathbf{k}) - id_y(-\mathbf{k}) & \Delta - d_z(-\mathbf{k}) \\ -\Delta - d_z(-\mathbf{k}) & -d_x(-\mathbf{k}) - id_y(-\mathbf{k}) \end{array} \right)$$
$$\text{(B.22)}$$

Since (B.21) holds, the matrices on the right hand sides of (B.19) and (B.22) must be the equal. Hence we find that upon swapping $\mathbf{k}$ to $-\mathbf{k}$, Δ is not affected (even if we'd kept a $\mathbf{k}$-dependence) whereas

$$\mathbf{d}(\mathbf{k}) = -\mathbf{d}(-\mathbf{k}) \quad \text{(B.23)}$$

This means that Δ is even when two particles are swapped (in momentum space, and hence in position space). Thus, the spin part associated with this order parameter must be odd, it must be the singlet. Indeed, Δ **is the order parameter of singlet pairing**. This is the same Δ as the one we found in the BCS theory of metals. However, $\mathbf{d}(\mathbf{k})$ acquires a minus sign when swapping the two particles in momentum space – it is odd in the spatial sector of the pair wavefunction and thus it must be even in the spin sector. **The vectorial order parameter $\mathbf{d}(\mathbf{k})$ is associated with triplet pairing**.

In ^{3}He, it turns out that the triplet potential is more strongly attractive than the singlet potential! So, in stead of having singlet Cooper pairs of helium-3 atoms, we obtain the more complicated triplet pairing as the ground state.

B.3   A and B phases of superfluid helium-3

Even though we can see from the interatomic potential that the triplet pairing is the ground state, this does completely fix the superfluid order! We now have a vectorial order parameter, and this offers more possibilities and hence more
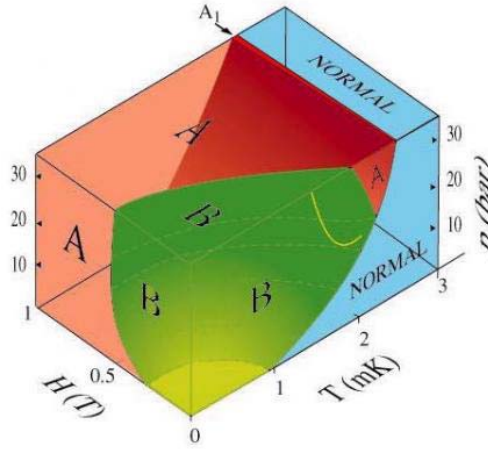
Figure B.1: Phase diagram of ^{3}He. The superfluid phase is related to triplet pairing of helium atoms, and characterized by a vectorial order parameter $\mathbf{d}(\mathbf{k})$. The vectorial character allows for many different phases, of which two can be the ground state at given temperatures, pressues and magnetic fields. These are denoted by the A and B phases. Image source: Lounasmaa laboratory, Aalto University, Finland.

possible phases than a scalar order parameter. Not only can we play with the magnitude of $\mathbf{d}(\mathbf{k})$, but also with its direction relative to $\mathbf{k}$.

Just as for the usual BCS case, let's fix the magnitude of k to be the Fermi wave vector. This means that we consider only helium-3 atoms at or very near to the Fermi surface as contributing to pairing. That will be in line with the experiment, showing that the critical temperature for superfluidity in helium-3 is very low ($T_c \ll T_F$, just like for superconductors. In 1970, David Lee, Doug Osheroff and Bob Richardson found this transition to be at about 2.5 mK, and this earned them the 1996

So the only thing we still need to worry about is the relative direction of $\mathbf{d}$ with respect to $\mathbf{k}$. Decomposing $\mathbf{k}$ in spherical coordinates, with $\mathbf{k} = \{k_F, \theta_\mathbf{k}, \phi_\mathbf{k}\}$, we can write

$$\begin{pmatrix} d_x \\ d_y \\ d_z \end{pmatrix} = \sqrt{\frac{3}{4\pi}} \begin{pmatrix} \eta_{xx} & \eta_{xy} & \eta_{xz} \\ \eta_{yx} & \eta_{yy} & \eta_{yz} \\ \eta_{zx} & \eta_{zy} & \eta_{zz} \end{pmatrix} \cdot \begin{pmatrix} \sin(\theta_\mathbf{k})\cos(\phi_\mathbf{k}) \\ \sin(\theta_\mathbf{k})\sin(\phi_\mathbf{k}) \\ \cos(\theta_\mathbf{k}) \end{pmatrix} \quad \text{(B.24)}$$

The only unknowns that we have to find now are the η's, and these are independent of $\mathbf{k}$. We'll be able to set up gap equations to determine these constants if we plug in these solutions into (B.19), and this into (B.18), and then diagonalize that matrix, and use the diagonalisation to calculate the expectation value for the self-consistent variables (B.14). That's a heck of a long calculation, and we won't do it here. Tony Legget did it, and got the Nobel prize for it in 2003.

To complete this appendix, I'll just list the two phases of helium-3 that make
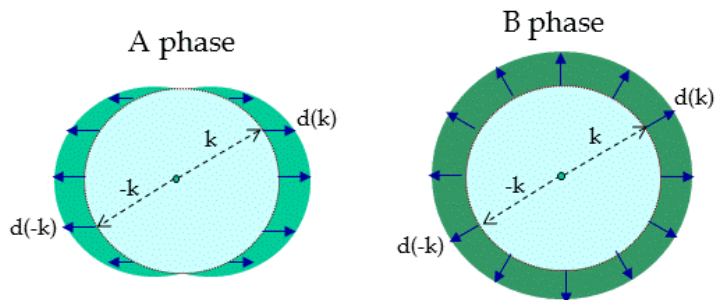
Figure B.2: The vectorial order parameter $\mathbf{d(k)}$ in the A and B phase is shown by the full arrows starting on the Fermi sphere.

it as a ground state in bulk. These are both solutions of the gap equations. Already in the very first experiments, it was found that helium-3 had two different phases when cooled down, and these were called the A phase and the B phase. Not very poetic, but accidentally these were described first by **A**nderson, Brinkman and Morel (for the A phase) and by **B**alain and Werthamer (for the B phase). The phase diagram for these A and B phases is shown in figure B.1.

The A phase is characterized by

$$\eta_{ij} \propto \begin{pmatrix} 1 & i & 0 \\ 0 & 0 & 0 \\ 0 & 0 & 0 \end{pmatrix} \tag{B.25}$$

and an excitation spectrum

$$E_{\mathbf{k}} = \sqrt{\xi_{\mathbf{k}}^2 + \|\mathbf{d(k)}\|^2 \pm \|\mathbf{d(k)} \times \mathbf{d^*(k)}\|} \tag{B.26}$$

The form of η means that $\mathbf{d}$ only has an x-component, so the direction of $\mathbf{d}$ is locked and independent of $\mathbf{k}$. It's magnitude varies as $\sin(\theta_{\mathbf{k}})$ so that the gap will vanish at the north and south poles of the Fermi spheres, as shown in the left panel of figure B.2. This phase will be favoured when there is an external magnetic field. Indeed $d_x = (\Delta_{\uparrow\uparrow} - \Delta_{\downarrow\downarrow})/2$, which tells us that the triplet pairs will align their spins, and this reduced the energy in an external magnetic field. So, the direction of the vectorial order parameter here is locked to the external field.

In the B phase we have

$$\eta_{ij} \propto \begin{pmatrix} 1 & 0 & 0 \\ 0 & 1 & 0 \\ 0 & 0 & 1 \end{pmatrix} \tag{B.27}$$

and

$$E_{\mathbf{k}} = \sqrt{\xi_{\mathbf{k}}^2 + \|\mathbf{d(k)}\|^2} \tag{B.28}$$

Now the direction of $\mathbf{d}$ is locked to $\mathbf{k}$. This means that the angle between $\mathbf{d}$ and the angular momentum $\mathbf{L}$ of the pair is fixed. Above the critical temperature,

both the total spin of any two atoms and their total angular momentum are independent, but below the critical temperature, the directions of the spin and the angular momentum are locked to eachother. This is the nature of the superfluid phase transition as conceived by Leggett. It is illustrated in the right hand side of figure B.2. The excitation spectrum is not gapped. When no magnetic field is present, this phase dominates the superfluid part of the phase diagram (apart from a small region at high pressure).

It turns out that we have way more solutions that just these two (and the normal state with $\mathbf{d} = 0$ everywhere). There exist many different superfluid phases that may become the ground state under some exotic conditions such as strong confinement. The zoo of solutions are catalogued in a book by Dieter Vollhardt and Peter Wölfle, *The Superfluid Phases of Helium 3* (Dover Publications, 2013). This zoo itself generates an even bigger zoo of quasiparticles and excitations and types of vortices, half-vortices, skyrmions, ...

Bibliography

Many great textbooks on superfluidity and superconductivity have appeared, and it is an impossible task to list them all. Therefore I restrict myself to those books I consulted most in order to select the material covered in this course, listed in alphabetical order of the first author:

- James F. Annett, *Superconductivity, superfluids and condensates*, Oxford Master Series in Condensed Matter Physics, Oxford University Press, 2004.

- Pierre G. de Gennes, *Superconductivity of Metals and Alloys*, Advanced Book Classics, Westview Press, 1999.

- Anthony J. Leggett, *Quantum Liquids: Bose-Einstein condensation and Cooper pairing in condensed matter systems*, Oxford Graduate Texts, Oxford University Press, 2006.

- Chris J. Pethick and Smith, *Bose-Einstein condensation in Dilute Gases*, Cambridge University Press, 2008.

- Sandro Stringari and Lev P. Pitaevskii, *Bose-Einstein condensation*, Oxford University Press, 2003.

- David R. Tilley and John Tilley, *Superfluidity and Superconductivity*, Graduate Student Series in Physics, Institute of Physics Publishing, 1990.

- Michael Tinkham, *Introduction to superconductivity: second edition*, Dover Publications, 2004.